MATHEMATICAL MODELLING AND SIMULATION OF HARD AND SOFT NIP CALENDERS USED IN TEXTILE INDUSTRY

Thesis submitted in fulfillment of the requirements for the Degree of

DOCTOR OF PHILOSOPHY

By

NEELAM GUPTA

DEPARTMENT OF MATHEMATICS

JAYPEE UNIVERSITY OF INFORMATION TECHNOLOGY

WAKNAGHAT, DISTRICT SOLAN, H.P., INDIA

NOVEMBER, 2021

Table of Contents

DECLARATION BY THE SCHOLAR

I hereby declare that the work reported in Ph.D. thesis entitled **"Mathematical Modelling and Simulation of Hard and Soft Nip Calenders used in Textile Industry "** submitted at **Jaypee University of Information Technology, Waknaghat, Solan (H.P.), India** is an authentic record of my work carried out under the supervision of **Dr. Neel Kanth**. I have not submitted this work elsewhere for any other degree or diploma. I am fully responsible for the content of my Ph.D. thesis.

Neelam Gupta
(Enrollment No.: 176853)
Department of Mathematics
Jaypee University of Information Technology,
Waknaghat, Solan, H.P., INDIA
Date:

SUPERVISOR's CERTIFICATE

This is to certify that the work reported in Ph.D. thesis entitled **"Mathematical Modelling and Simulation of Hard and Soft Nip Calenders used in Textile Industry "** submitted by **Neelam Gupta**, at **Jaypee University of Information Technology, Waknaghat, Solan (H.P.), India** is a bonafide record of her original work carried out under my supervision. This work has not been submitted elsewhere for any other degree or diploma.

Dr. Neel Kanth
(Supervisor)
Department of Mathematics
Jaypee University of Information Technology,
Waknaghat, Solan (H.P.), INDIA
Date:

Acknoledgement

Words are often too weak to express one's inner feeling of indebtedness to one's benefactors. The same difficulty haunts me in penning down the deep sense of gratitude. I thank the **ALMIGHTY**, whose blessings have enabled me to accomplish my Ph.D. work successfully. I humbly bow my head in gratitude for all **HIS MERCY**.

"A teacher is a pious gift of God, whose precious guidance enables one to select the right path. "

It is my privilege to express my respect and a deep sense of gratitude to my supervisor **Dr. Neel Kanth**, Assistant Professor, Department of Mathematics, Jaypee University of Information Technology, Waknaghat, Solan, India for his valuable advice, magnificent supervision, conscientious guidance, endless efforts and constant patience throughout my Ph.D. work, due to which this work was able to take the shape in which it has been presented. It was his valuable discussions and deep knowledge through which I have gained a lot. His constant encouragement and confidence imbibing attitude have always been moral support for me. I feel very indebted to his keen interest, constant encouragement and for teaching me various valuable lessons in professional and personal life.

With profound sense of gratitude, I express my highest respect and whole hearted regards from inner core of my heart to my ever loved Parents, **Smt. Meena Gupta** and **Late Sh. Brij Bhushan Gupta** who have given me the life and taught the concepts of life and their silent sacrifices and dedicated efforts to educate me to this level and without whose valuable moral support the thesis would not have seen the light of the day. Their good wishes always stood by me every moment throughout my research work. My efforts will remain incomplete if I do not express my gratitude and indebtedness to my Grandfather **Late Sh. Bhagat Ram Gupta**, my Grandmaa **Late Smt. Kala Gupta** for providing me continuous support. Let me add colors to this acknowledgement by thanking my loving brother **Mr. Umang Gupta** for his encouragement and everlasting affection at every stage of my studies.

I will give credit to my achievements and heartfelt thanks to my dearest husband

Mr. Gaurav Sharma, who was always with me during my Ph.D. work and play a role of backbone to me. I also would like to thank to my son **Mr. Gauransh Sharma**, who joined us during my PhD, for giving me unlimited happiness and pleasure. I am expressing my humble gratitude to my dear in-laws **Sh. Prem Chand Sharma & Smt. Suman Sharma** and brother-in-law **Mr. Saurabh Sharma** for their affectionate encouragement, immense love and support.

I express my thanks to the Honourable Vice-chancellor **Prof. (Dr.) Rajendra Kumar Sharma**, **Prof. (Dr.) Ashok Kumar Gupta** (Dean Academics & research) and **Maj Gen Rakesh Bassi (Retd.)** (Registrar and Dean of Students) for their constant support with all the academic and infrastructure facilities required in the research work.

I would like to express my gratitude to **Prof. (Dr.) Karanjeet Singh** (Head of the Department), **Dr. Rakesh Kumar Bajaj**, **Dr. R.S. Durai**, **Dr. Bhupender Kumar Pathak**, **Dr. Pradeep Kumar Pandey**, **Dr. Saurabh Srivastava**, **Dr. Mandeep Singh**, **Dr. Rajesh Sharma** and **Dr. Dheeraj Sharma** for their valuable suggestions, encouragement time to time during my research work. I am very much thankful to all my colleague research scholars for providing me constant courage and cooperation.

I would like my sincere thanks to **Mrs. Riti Dang** for their continuous support, inspiration and blessings throughout my research work. I would also like to express my heartfelt gratitude and regards to Library Officials of JUIT Waknaghat for providing me all the required resources whenever needed during my research work.

Words perhaps would fail to express my deep sense of gratitude and esteemed regards to all the distinguished teachers, who taught me from the beginning of my studies till now. Last but not least, I am highly thankful to those who helped me directly or indirectly during the course of research and who are unnamed. Still I hope, they shall understand and accept my sincere thanks.

Neelam Gupta

Abstract

Calendering is mechanical finishing process used in many industries such as polymer, paper, leather, printing and textile, implemented at the final stage when thin sheet of material is exposed to combine effect of moisture, heat and pressure between two or more rotating rolls (Nips) of same or different composition pressed against each other. In simple words, it is the high speed ironing process that primarily imparts luster. These rolls may be hard or soft, heated at different temperatures and vary in number from 3 to 11 depending upon the type of calender.

In dynamic process of calendering, it is extremely difficult to evaluate the interaction of design and process parameters such as load applied, bulk modulus, speed and radius of rolls, number of nips, temperature of the rolls and fabric temperature under local external and internal conditions. Thus there is need of development of various mathematical models like models for nip mechanics, steady and unsteady state heat transfer models for complete analysis of the problem. The forecast investigation aims at identifying the relative effect of each parameter on the quality of fabric in different types of calenders such as machine calender, soft calender, temperature gradient calender used in textile industry. In this thesis, a comprehensive description of finishing process, mathematical modelling and simulation of nip mechanics and heat transfer in calendering process has been done. Methodology of systematic investigation for simulation of calendering models, namely models for nip mechanics and conduction heat transfer under different initial and boundary conditions has been developed.The above objectives are achieved with the help of MATLAB software.

The nip mechanics model developed is generalized model which can overcome the difficulties poised by the models of Hertz and Meijers. The nip mechanics model for machine calender (NMMM) and nip mechanics model for rolling calender (NMMR) developed are extension of Hertz and modification of Meijers which can be suitably used for textile calenders of any design depending upon composition of material. The developed models are simulated to investigated the impact of load applied, equivalent diameter, equivalent bulk modulus and cover thickness on nip width. The obtained results of the developed models are compared with the data obtained from textile mill

and with the results obtained by Hertz model. The data obtained from textile mill matches more closely with the NMMM and NMMR solution as compared with the Hertz solution. From NMMM and NMMR, it is found that nip width increases with increase in line load, equivalent diameter, cover thickness and decrease in equivalent bulk modulus. With increase in nip width, dwell time increases which has direct on gloss and smoothness of the fabric. Average pressure remains same in case of Hertz solution, while developed models shows that average pressure decreases with increase in cover thickness. With the help of model developed, rolling and machine calenders can be designed according to the nature of fabric required, as nip width acts as an imperative part in influencing eminence of the fabric.

Calendering enhances the surface properties of the fabric by making it more glossy and smooth with the help of mechanical and thermal energy. Simultaneous heat transfer has an important impact on the calendering process and on the functioning of calender stack. Heat transfer to the fabric in calendering system used in textile industry occurs in different situations. Heat is mainly transferred by conduction to fibers in contact with the heated rolls under two conditions (a) when fabric is inside the calender nip (b) when fabric is outside the nip. Heat is generated during compression in the nip or may be supplied externally from hot roll heated by supplying pressurized hot water or oil or steam/hot air showering to the fabric to raise temperature of the fabric.

In the present investigation, heat transfer model has been developed for machine and rolling calenders under both the conditions. Simulation of the heat transfer model when fabric is inside the calender nip having same and different roll temperature for machine and rolling calender gives an evolutionary advantage that helps in predicting the fabric temperature at various depths in thickness direction inside the nip which is not possible using temperature measuring instruments as they can only measure temperature on the surface of the fabric. The impact of roll temperature on fabric temperature in thickness direction at various depths, dwell time, thermal diffusivity, roll temperature on average fabric temperature has also been investigated. It is found that the middle part of fabric remains at initial temperature and temperature of the fabric decreases from outer part to mid part of the fabric from both sides in thickness

direction. Also it is found that with increase in roll temperature, dwell time and thermal diffusivity, average fabric temperature increases as more heat is conducted at different layers of the fabric. The heat transfer model developed has been solved using homotopy perturbation method and finite difference methods namely explicit forward time central space method (FTCS), implicit backward time central space method (BTCS), Crank Nicolson (CN) method. The results obtained using homotopy perturbation method are similar with the exact results while there is a negligible error in the results obtained using finite difference methods. It is found that results obtained using BTCS method are very close to results obtained using HPM. Comparison of results obtained using explicit FTCS, implicit BTCS and Crank Nicolson methods with results obtained from HPM reflects the remarkable applicability of numerical methods in analyzing the temperature profile of the fabric inside the calender nip for same and different roll temperatures. From the simulation of the heat transfer model, it is clear that with increase in roll temperature (and/or) decrease in calender speed, more heat penetrates inside the fabric from both sides in thickness direction which results in increase of average fabric temperature.

With increase in pressure and temperature in calendering system beyond a certain limit can cause damage to the fibre bond resulting in reduction in the mechanical strength of the fabric. To overcome these undesirable effects, the process of temperature gradient calendering is employed. Temperature gradient calender (TGC) consist of alternating hard and soft rolls in which soft roll at room temperature and hard roll at higher temperature. The mathematical model for TGC has also been developed considering incompressible and compressible medium and simulated to anticipate the temperature profile of the fabric in thickness direction.

The impact of roll temperature on fabric temperature in thickness direction at various depths, impact of dwell time, thermal diffusivity, roll temperature on average fabric temperature has been investigated when fabric is inside the temperature gradient calender nip. It is found that the side of fabric which is in touch with the heated roll is at higher temperature as compared to the side which is in contact with the non heated roll. With increase in heated roll temperature, dwell time and thermal diffusivity, more heat is conducted to the fabric which increases the average temperature

of the fabric. In case of TGC, heat is not transformed upto the center of the fabric in thickness direction, thus the fibres which are in direct contact with the heated roll get deformed permanently, while the fibres on the other side and upto the middle of the fabric do not get deformed due to which the surface properties of the fabric are developed while maintaining the bulk and strength properties. Subsequently better gloss and smoothness of the fabric can be accomplished in case of TGC with more than one nip without affecting the bulk and strength properties. Also, neglecting the effect of volume change results, difference in amount of heat conducted at distinct depths and on the average fabric temperature, so volume change during the heat transfer inside the calender nip cannot be neglected.

When fabric comes out from the calender nip, one side of the fabric is in contact with the heated roll and other side is exposed to air having convective heat loss. During subsequent contact with the roll, fabric assumes a temperature gradient which diminishes as the fabric heats upto the roll temperature. Mathematical model for heat transfer when one side of fabric is in contact with the roll and other side is in contact with air have been developed and simulation of the model has been done for machine and rolling calender used in textile industry. From the results, it is found that the side of fabric which is in touch with the hot roll gets heated and temperature decreases as depth increases. The other side of fabric which is in contact with air remains nearly at the same temperature. Also, there is remarkable increase in average fabric temperature before entering into the second nip of calendering machine. The comparison of results obtained using explicit FTCS method with results obtained from analytical method reflects the remarkable applicability of numerical methods in analyzing the temperature profile of the fabric when fabric comes out from the calender nip.

Nomenclature

Q	Heat transfer rate
Q_v	Energy generated per unit volume
κ_p	Thermal conductivity
ρ	Density of material
c_p	Specific heat of material
α	Thermal diffusivity
H	Separation between bodies before deformation
$R_1^{'}, R_1^{''}$	Principal radii of curvature of first body
$R_2^{'}, R_2^{''}$	Principal radii of second body
A, B, C, D	Arbitrary constants
B_1, B_2	Two different bodies in contact
x, y, z	Spatial coordinates
G	Line load
G(Z)	Pressure distribution
N_w	Nip width
R_1, R_2	Roll radius
R	Equivalent radius
D_1, D_2	Diameter of rolls
D_E	Equivalent diameter
E_1, E_2	Bulk modulus of two rolls
E^*	Equivalent bulk modulus
b	Cover thickness of roll
K(x)	Kernel of integral equation
v(x)	Vertical displacement under load
Z, ξ, θ	Non dimensional variables
g_0^*	Vertical displacement at center of contact area
ν_1, ν_2	Poisson's ratio
T	Temperature

$\alpha_0, \alpha_1, \alpha_2$	Constants determined by numerical integration for different values of Poisson's ratio
T_0	Initial temperature of fabric
T_r	Same roll temperature
T_h	Heated roll temperature
T_1, T_2	Different roll temperature
L	Fabric thickness
p	Embedding parameter
$\mathbb{A}$	General differential operator (linear or nonlinear)
f(r)	Known analytic function
$\mathbb{B}$	Boundary operator
$\mathbb{L}$	Linear operator
$\mathbb{N}$	Nonlinear operator
Γ	Boundary of the domain
Ω	Domain
C_m	Fourier coefficient
d	Dimensionless diffusion number
Δt	Time step
V	Velocity vector
u_1, v_1	Velocities in x and y direction
$x_h(y)$	Functions describing the surface of the hot roll
$x_c(y)$	Functions describing the surface of the cold roll
$\delta(t)$	Heat penetration depth
η	Similarity variable
t	Dwell time
ρ_0	Density of the uncalendered fabric
b_0	Thickness of the uncalendered fabric
b_{min}	Minimum fabric thickness
h	Convection heat transfer coefficient
h_s	Contact resistance

h_f	Film resistance
Bi	Biot number
Bi_s	Biot number for contact resistance
E_p	Exponent
W_b	Basis weight of fabric
ϑ	The difference between fabric temperature and initial temperature of fabric
R_T	Roll temperature
T_R	The difference between the roll temperature and the initial temperature

List of Tables

List of Figures

Research Publications

The subject matter of the thesis is based on the following research papers published/under publication in the various national and international journals/conference proceedings co-authored with the supervisor.

List of Journal Publications:

1. Neelam Gupta and Neel Kanth, "Analysis of Nip Mechanics Model for Rolling Calender used in Textile Industry,"Journal of the Serbian Society for Computational Mechanics, Vol. 12(2), pp.39-52, 2018. ISSN: 1820-6530 (print), 2620-1941 (online). DOI: 10.24874/jsscm.2018.12.02.03. **Indexed: Scopus, ESCI(Web of Science)**

2. Neelam Gupta and Neel Kanth, "Study of Heat Conduction inside Rolling Calender Nip for Different Roll Temperatures,"Journal of Physics Conference Series, Vol. 1276, pp.012044 (1-9), 2019. ISSN: 1742-6588(print), 1742-6596(online). DOI:10.1088/1742-6596/1276/1/012044. **Indexed: Scopus, ESCI(Web of Science)**

3. Neelam Gupta and Neel Kanth, "Analytical approximate solution of heat conduction equation using new homotopy perturbation method,"Matrix science Mathematic, Vol. 3(2), pp.1-7, 2019. ISSN:2521-0831(print), 2521-084X(online). **(Indexed: Copernicus)**

4. Neelam Gupta and Neel Kanth, "A Comparative Study of NHPM and FDM for Solving Unsteady Heat Conduction Equation."(**Under Review**)

5. Neelam Gupta and Neel Kanth, "Mathematical Modelling and Simulation of Transient Heat transfer in Temperature Gradient Calendering."(**Communicated**)

6. Neelam Gupta and Neel Kanth, "Analytical Approximation Analysis of Heat Conduction Inside the Calender Nip."(**Communicated**)

List of Conference Paper Publications:

1. Neelam Gupta and Neel Kanth, "Study of Heat Flow in a Rod using Homotopy Analysis Method and Homotopy Perturbation Method," AIP conference proceedings, Vol. 2061(1), pp.020013(1-8), 2019. ISSN: 0094-243X(print), 1551-7616(online). **Indexed: Scopus, Web of Science**

2. Neelam Gupta and Neel Kanth, "Analysis of Heat Conduction inside the Calender Nip Used in Textile Industry," AIP conference proceedings, Vol. 2214(1), pp. 020008, 2020. DOI: 10.1063/5.0003343. **Indexed: Scopus, Web of Science**

Book Chapter Published:

1. Neelam Gupta and Neel Kanth, "Application of Perturbation Theory in Heat Flow Analysis," A Collection of Papers on Chaos Theory and Its Applications, 173, 2021. ISBN:978-1-83962-858-0 (print), 978-1-83962-875-7 (online). DOI: 10.5772/intechopen.91599. **Indexed: Web of Science**

Chapter 1

Introduction

1.1 Status of Indian Textile Industry

The textile industry is second-largest employment generating sector for both skilled and unskilled labour in India. Textile industry is one of the oldest industries and has a formidable presence in the national economy. The textile sector also has a direct link with the rural economy and performance of major fibre crops and crafts such as cotton, wool, silk, handicrafts and handlooms, which employ millions of farmers and craft persons in rural and semi-urban areas. India's textiles industry has a capacity to produce wide variety of products suitable for different market segments, both within India and across the world. The industry uses a wide variety of fibres ranging from natural fibres like cotton, jute, silk and wool to man made fibres like polyester, viscose, acrylic and multiple blends of such fibres and filament yarn. India is the second largest producer of fibre in the world and the major fibre produced is cotton [1–6]. Textile industry contributes to about 14% of manufacturing value-addition, accounts for around one-third of our gross export in our economy. India's spinning sector consisted of about $1,146$ small-scale independent firms and $1,599$ larger scale independent units. Weaving sector consists of about 3.9 millions handlooms and 3.8 millions powerloom enterprises. India is second in global textile manufacturing and also second in silk and cotton production. The Indian textiles and apparel industry

contributed 7% to the GDP, 12% to export earnings and held 5% of the global trade in textiles and apparel. The industry (including dyed and printed) attracted Foreign Direct Investment (FDI) worth US $3.75 billion from April 2000 to March 2021.
India is working on major initiatives, to boost its technical textile industry. Owing to the pandemic, the demand for technical textiles in the form of PPE suits and equipment is on rise. Top textile industries in the sector are attaining sustainability in their products by manufacturing textiles that use natural recyclable materials. The future for the Indian textiles industry looks promising by strong domestic consumption as well as export demand.

1.2 Role of Modelling and Simulation in Industry

In process industry, optimization and control with the help of mathematical models are extremely essential in today's scenario when the globalization has taken place with liberalized economy. Global market with quality product at competitive prices, public awareness regarding environmental degradation, acute shortages of raw material and energy, and high prices of all basic inputs have forced the engineers to adopt design of process, plant and system in a most quantized and deterministic way which is possible through interaction of mathematics, engineering and physical sciences [7–9].
Mathematical modelling essentially consists of translating real word problem into mathematical problem, solving the mathematical problem and interpreting these solution in the language of the real world. It is an abstract model that uses mathematical language to describe the behavior of a system. It is used to describe, analyse, correlate, simulate, optimize and finally control an existing or contemplated process. It helps to convert a physical problem into mathematical formulations whose theoretical and numerical analysis provides insight, answers, and guidance useful for study the behavior of the system. The model must be simple, coherent, less time consuming and must include most pertinent parameters influencing the system. It prepares the way for better design or control of a system and allows the efficient use of modern computing capabilities. Mathematical models may be classified according to their na-

ture. Thus mathematical models may be linear or non linear according as the basic equations describing them are linear or non linear. These may be static or dynamic according as the time variations in the system are not or are taken into account. Also, these may be discrete or continuous according as the variables involved are discrete or continuous [10–14].

The structure configuration of mathematical modelling is shown in figure 1.1. Before converting real world situation to a mathematical model, all its essential characteristics relevant to the situation and those aspects which are irrelevant or whose relevance is minimal and related data is collected to get some initial insight of the problem. Next step is to formulate the mathematical model using algebraic, transcendental, differential, difference, integral, integro-differential equations etc., with the help of physical, chemical, biological, social, economic laws which are relevant to the situation and to solve these equations using mathematical techniques. Then the final solution is translated into real world language and is compared with the available observations or data. If agreement is good, then model is accepted. If agreement is not good, examine the assumptions and approximations and change them in the light of discrepancies observed and follow the same procedure. Continue the same process till a satisfactory model is obtained which explains all earlier data and observations [11–15].

After mathematical modelling, simulation of the process is performed. Simulation is a powerful tool that can be used to study the behavior of the system. Any process which is to be simulated is considered as a system which may also be defined as a group of objects interacting in order to produce some result. It is a process of forming an abstract model of a real world situation in order to understand the effects of modifications and introducing various strategies on the situation. The major advantage of simulation is that it permits experimentation with real and proposed situation without modifying the real solution and without actually observing its occurrence [16,17].

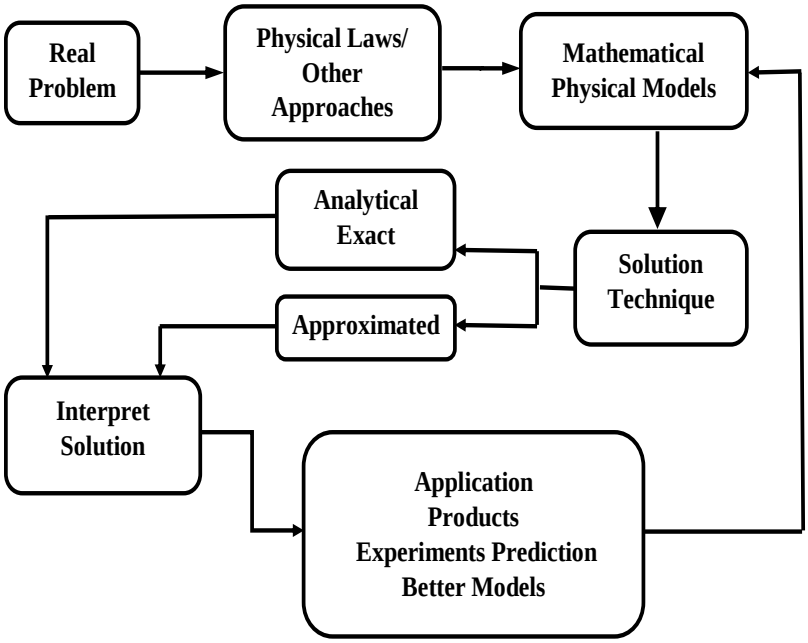

Figure 1.1: Structural configuration of mathematical modelling

1.3 Mathematical Modelling of Calendering Process

Most real processes are dynamic in nature which means that they are time dependent. This kind of process is too complicated, to be modelled precisely. Calendering process is also dynamical in nature. A interactive model for calendering system is the requirement for today's scenerio. Calendering is derived from Greek word "Kylindros" which means, "to press web (thin sheet)" between rolls or plates. Calendering is a mechanical finishing process in many industries like textile, paper, leather and many more where a thin web (thin sheet) is pressed inside the nip formed by two or more rolls in contact arranged in the form of vertical stack shown in Figure 1.2 and 1.3.

These rolls may be hard or soft and vary in number from 3 to 11 depending upon the type of calender. The rolls of calender are heated at different temperatures. Heat is generated during compression in the nip or may be supplied externally from hot roll heated by supplying pressurized hot water or oil or steam/hot air showering to the

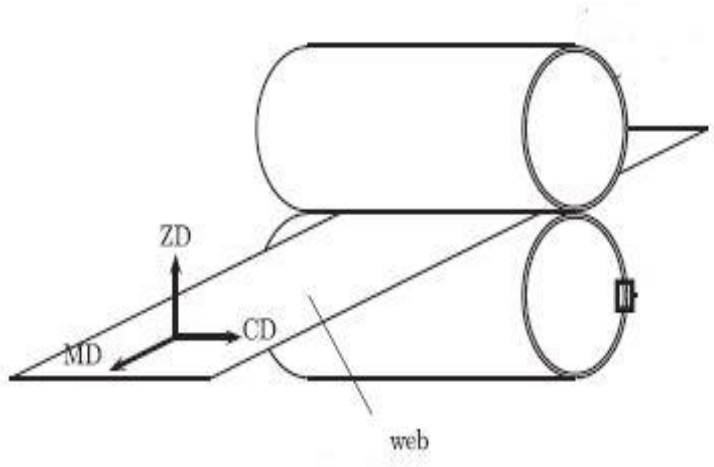

Figure 1.2: Calendering process

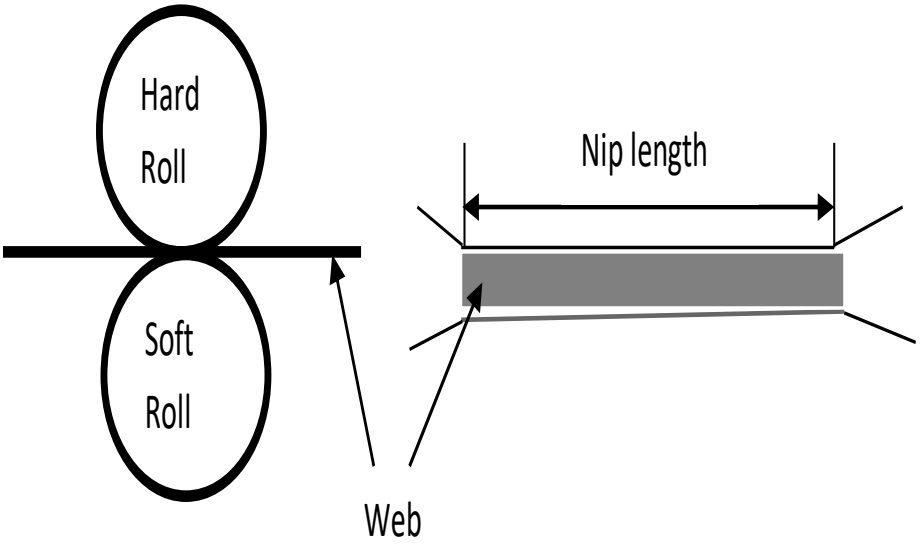

Figure 1.3: Calender nip

web to raise temperature of the web. When the required roll surface temperature is 150°C or less, circulating water or steam may be used for heating. By using heated oil, roll temperature up to 200°C may be obtained. The design and process parameters such as time, temperature, number of nips, nip width, machine speed, roll diameter, roll hardness and total load to the rolls affects the output quality of web. Properties of the roll material such as the modulus of elasticity and the Poisson ratio are also the important factors in the calendering action. The effects of various parameters discussed above are subject to scrutiny and interactions among these variables has to be analysed [17, 18].

The changes occur in web during calendering are mostly permanent, affecting the quality of web. The surface properties of web like gloss and smoothness improve while other properties like bulk, strength and bending stiffness decrease during and after calendering process. Thus calendering operation is an optimization of above properties. Although the qualitative effects of various mechanisms in calendering have been known quite a long time, the process knowledge has remained largely superficial and empirical in nature. The observations and studies have been mainly focused on final web quality and not directly to the process itself.

The main point is how the process parameters need to be set in order to optimize the process and how to obtain the best final product quality. Direct answers to all these questions are not readily available but it is realized that there has been a growing need of modelling with the increase in speed of machine or productivity. Mechanisms in calendering, particularly the nip mechanics and heat transport can be studied by mathematical modelling since the direct observations here are difficult or impossible. The nip mechanics model is useful to evaluate the nip width, maximum nip pressure, and pressure distribution inside the nip. Since nip width plays an important role to analyse heat conduction inside the calender roll nips, therefore nip mechanics model is interlinked with the heat transfer model. Heat transfer model describes how temperature is being distributed inside the web during the calendering process using heat conduction equation under different initial and boundary conditions according to the type of calender [17–21].

1.4 Heat Transfer in Calendering Process

Simultaneous heat transfer has an important impact on the calendering process and on the functioning of calender stack [22–31].

Considering the general three dimensional energy balance equation [29]

Energy conducted in left face + heat generated with in element = change in internal energy + energy conducted out right face.

Hence

$$Q_x + Q_y + Q_z + Q_{gen} = Q_{x+dx} + Q_{y+dy} + Q_{z+dz} + \frac{dE}{dt} \tag{1.4.1}$$

where

$$Q_x = -\kappa_p dxdy\frac{\partial T}{\partial x} \tag{1.4.2}$$

$$Q_{x+dx} = -\kappa_p dxdy\frac{\partial T}{\partial x}\rfloor_{x+dx} = -dxdy\Big[\kappa_p\frac{\partial T}{\partial x} + \frac{\partial}{\partial x}\big(\kappa_p\frac{\partial T}{\partial x}\big)dx\Big] \tag{1.4.3}$$

$$Q_y = -\kappa_p dxdy\frac{\partial T}{\partial y} \tag{1.4.4}$$

$$Q_{y+dy} = \kappa_p dxdy\frac{\partial T}{\partial y}\rfloor_{y+dy} = -dxdy\Big[\kappa_p\frac{\partial T}{\partial y} + \frac{\partial}{\partial y}\big(\kappa_p\frac{\partial T}{\partial y}\big)dx\Big] \tag{1.4.5}$$

$$Q_z = -\kappa_p dxdy\frac{\partial T}{\partial z} \tag{1.4.6}$$

$$Q_{z+dz} = \kappa_p dxdy\frac{\partial T}{\partial z}\rfloor_{z+dz} = -dxdy\Big[\kappa_p\frac{\partial T}{\partial z} + \frac{\partial}{\partial z}\big(\kappa_p\frac{\partial T}{\partial z}\big)dx\Big] \tag{1.4.7}$$

$$Q_{gen} = Q_v dxdydz \tag{1.4.8}$$

$$\frac{dE}{dt} = \rho c_p dxdy\frac{\partial T}{\partial t}dx \tag{1.4.9}$$

$$\frac{\partial}{\partial x}\left(\kappa_p\frac{\partial T}{\partial x}\right) + \frac{\partial}{\partial y}\left(\kappa_p\frac{\partial T}{\partial y}\right) + \frac{\partial}{\partial z}\left(\kappa_p\frac{\partial T}{\partial z}\right) + Q_v = \rho c_p\frac{\partial T}{\partial t} \tag{1.4.10}$$

The first three terms on left hand side of equation (1.4.10) represents the rate of net energy transport due to conduction. The last term on left hand side of equation (1.4.10) represents the rate of generation of energy. The term on right hand side of equation (1.4.10) represents the rate of change of stored energy.

Equation (1.4.10) can be rewritten as

$$\frac{\partial^2 T}{\partial x^2} + \frac{\partial^2 T}{\partial y^2} + \frac{\partial^2 T}{\partial z^2} + \frac{Q_v}{\kappa_p} = \frac{1}{\alpha}\frac{\partial T}{\partial t} \tag{1.4.11}$$

where

$$\alpha = \frac{\kappa_p}{\rho c_p}$$

where T is the temperature, t is time, Q_v is the energy generated per unit volume, ρ is the density, κ_p is thermal conductivity and c_p is the specific heat of material. Equation (1.4.11) represents the unsteady state heat transfer in three dimensions. Using equation (1.4.11), the one dimensional heat conduction equation can be rewritten as

$$\frac{\partial T}{\partial t} = \alpha \frac{\partial^2 T}{\partial x^2} \tag{1.4.12}$$

Equation (1.4.12) is partial differential equation which is parabolic in nature and can be solved analytically and numerically by different methods. The problem can be solved in the case of calender using various kinds of initial and boundary conditions which in turn depend on design and process parameters of various calenders.

1.5 Present Objectives

Nip mechanics and heat transfer models developed earlier fit to a certain situation of specific calender type. Therefore, the existing models are not enough to cover the entire spectrum of modelling of calenders used in textile industry. The present objectives of this thesis are as follows:

- To analyse the existing models of nip mechanics and develop nip mechanics model which is suitable for hard and soft nip calenders used in textile industry.
- To develop heat transfer model when fabric is inside the calender nip under the following conditions
  - Nip rolls are having same temperature.
  - Nip rolls are having different temperatures.
  - When one roll of the nip is at very high temperature and other roll is at room temperature (Temperature Gradient).

- To develop heat transfer model when fabric comes out of the calender nip having one side in touch with the heated roll and other side in contact with air.
- To simulate the developed models based on the published data and data obtained from textile industry.

1.6 Background and Motivation

Calendering is a mechanical finishing process used in textile industry to obtain smooth fabric surface. Both hard nip and soft nip calenders are used in textile industry which are divided into different types according to the design and process parameters. All calender rolls are made of iron, the only difference is in the composition of covering material. Hard rolls are having covering of chilled cast iron while soft rolls are having covering of soft material such as cotton, wool, Nylon 610 etc. Soft calenders are having less pressure inside the calender nip as compared to hard nip calender due to the covering of soft material on one of the nip roll. Due to this reason soft calenders are commonly used in textile industry [17–21]. The surface properties of fabric during soft calendering process are enhanced by pressure and temperature between the web and heated roll. Sometimes, fabric may also get damaged during calendering process due to excess rise in temperature and pressure. To overcome these undesirable factors, temperature gradient calendering is used. Temperature gradient calender is having alternate hard and soft rolls in which soft roll is kept at room temperature and hard roll is kept at very high temperature ranging from 250-350°C. Temperature gradient calendering selectively plasticize only the outer surface of the fabric, leading to better smoothness for given thickness. During this process, heat is not transformed upto the center of the fabric in thickness direction inside the calender nip. Thus the fibres which are in direct contact with the heated roll get deformed permanently, while the fibres on the other side and upto the middle of the fabric do not get deformed due to which the surface properties of the fabric are developed while maintaining the bulk and strength properties. Heat conduction to the fabric inside the calender nip depends upon compression area (nip width) generated by rolls in contact [32–38].

Many researchers have worked on modeling of solid-solid contact problems. Out of these, most important models are given by Hertz(1881) and Meijers(1965). Hertz developed the nip mechanics model dealing with contact between two solids which for mathematical purposes can be considered infinite. Hertz analysis applies to two elastic, isotropic and homogenous cylinders in contact, with their axis parallel, under applied load G for calculating the nip width. Hertz solution does not hold true if the contacting bodies are heterogeneous or having layered structure(Non-hertzian contact). Hertz had not considered the thickness of the material covering the rolls such as chilled cast iron in case of hard calender and soft covering material in case of soft calender. So this model cannot be applied in case of calendering process because of the layered structure of calendering rolls [38, 39]. P Meijers dealt with the contact problem of a rigid cylinder pressed on an elastic layer connected rigidly to a rigid base. It is assumed that there is no friction between cylinder and layer and that the cylinder is long enough to ensure a plane deformation [40].

N.V. Deshpande dealt with the calculation of nip width, penetration and pressure for contact between cylinders with elastomeric covering for printing press. He showed that the expressions derived by Meijers can be used to determine the nip width and nip pressure when an incompressible elastomeric layer is squeezed between cylinders [41]. Ahmadi et. al. dealt with the non-Hertzian contact stress analysis for an elastic half space- normal and sliding contact. A general method of numerical solution in the non Hertzian elastic contact problem is developed using rectangular subdivisions [42]. Liu Shuangbiao et.al. extended the Hertz theory for circular and elliptical point contact problems involving coated bodies to express maximum contact pressure, contact radius and contact approach in terms of applied load, equivalent radius and an extended equivalent modulus that properly considers the presence of a coating [43, 44]. Khedkar et.al. has done the case study on calendering process used in textile industry. During this study, they found the problems in textile industry and proceeding for solution [45].

R.J.Kerekes dealt with various aspects due to heat transfer in calendering. Equations to predict the temperature distribution in a web has been solved using analytical method when web passes through a high speed calender stack. Predicted surface

temperature of web were compared to temperature measured at several locations in the stack using infra red thermometers [28]. M.F.Gratton et. al. dealt with the temperature gradient calendering of foodboard. It is shown that temperature gradient calendering produces smooth, glossy surfaces with less bulk reduction than conventional machine calendering [36]. Wikstrom et. al. carried out finite element modeling for calendering and dealt with some aspects of the effects of temperature gradients and structure in homogeneities [46]. Lehtinen et. al. developed an analytical solution for heat transfer in temperature gradient calendering process and derived for the temperature field of the web. The solution also takes in to account the change in volume of the web being calendered [34].

Hamel et. al. studied convective heat transfer in calendering process. The convective heat transfer to air from a heated roll in a calender stack was measured on a pilot calender for a wide range of speeds, surface temperatures and configurations representative of commercial operating conditions [47]. Kawka et. al. measured the effect of temperature and moisture content on the behavior of web in a nip using an environmentally controlled calendering facility reproducing all industrially relevant calendering conditions except width. Kawka et. al. also dealt with the effect of geometry and thermal boundary conditions on calender roll thermal deformation [48]. Guerin et. al. studied the impact of some parameters on heat transfer during calendering for wood free coated thin sheets. The purpose of this work was to furnish certain result validating the theory of heat transfer and to observe the effect of temperature of heated roll, dwell time and nip pressure [49]. Vyse Bob et.al. carried out investigation for achieving the same level of smoothness, gloss and caliper using the different type of calenders ,i.e. multiple hard nip, single soft nip or supercalender [50].

Though the above models are available in literature, there are some limitations of the models. Thus these models cannot be applied directly to textile industry. The nip mechanics model developed in this research work is generalized model which can overcome the difficulties poised by the models of Hertz and Meijers. The developed models are extension of Hertz and modification of Meijers which can be suitable for calenders of any design used in textile industry. Also heat transfer model for most

commonly used calenders used in textile industry under different initial and boundary conditions have been developed using analytical approximate and numerical methods. Simulation is carried out for the developed models using the published data and data obtained from textile industry.

Chapter 2

A Brief Review of Mechanical Finishing Process in Textile Industry

Mechanical finishing is an important process used in textile industry which is done with the help of calenders. Knowledge of process, design and operational parameters and their limitations is an imperative necessity to analyse the process of various types of calenders such as hard nip calenders, soft nip calenders and temperature gradient calenders used in textile industry. In this chapter, a brief description of fabric manufacturing process and operation of various type of calenders used in textile industry is discussed.

2.1 Manufacturing Process of Fabric in Textile Industry

Fibre is the basic component in making of a fabric. A fibre is a thin long hair like substance which has the suitable properties to spin it into a yarn. Yarn is the combination of several fibres twisted together to weave or knit a fabric. Fabric is the

output of weaving or knitting several yarns together. The fabric obtained from yarn is termed as raw fabric. The whole manufacturing process of fabric in textile industry is shown in Figure 2.1.

Raw fabric after leaving the knitting machine cannot be used directly as it contains various kind of impurities. Next step during textile manufacturing is singeing. The main objective of this process is to eliminate shapeless messy fibres coming out from fabric surface and to provide unwrinkled, shiny and polished fibres [1–6].

After Singeing, desizing is done which is used to eliminate various kind of sizing materials used at yarn stage which becomes unusable when yarn is converted to fabric. Also, if desizing has been done in inappropriate way, it may cause malfunctioning of dyeing process, non uniform printing and dissimilar patterns on fabric. After this bleaching of fabric is done which removes the inherited and already acquired natural coloring components from the raw fabric to obtain desired whiteness. For this, tanks are filled with sodium hydroxide, high density materials (weighting agents), esters and stabilizers. Fabric is dipped into these tanks and heated at near about 100°C for half an hour. After this fabric is washed in tanks containing fresh water.

Sometimes during the bleaching process, fabric may get damaged and can also compresses across the width. So to set the fabric, stenter machine is used. The setting of fabric implies the width setting in such a way that printing/dyeing takes place as per the requirement. Next step is to color the fabric i.e. dyeing process. A liquid consisting of dyes and specific chemicals is used for dyeing process. Temperature and time management are the two crucial elements in dyeing process. After dyeing, fabric undergo through the washing pads where steam is used to eliminate the dye which is not still permanently incorporated on the fabric [51–56, 56–58].

Printing designs can also incorporated on dyed fabrics, if required. Dyeing process and printing process are connected to each other. In printing process, one or more colors can be used to color specific area of fabric whereas in dyeing process single color has to be used on the entire fabric. Textile printing can be done using different kind of material such as silkscreen, engraved plates, woodcut, rolls or stencils. After printing fabric undergoes through curing process which is done to strengthen the fabric color so that color becomes permanent on fabric. At last, finishing of fabric

takes place which is done to upgrade the quality, reliability, aesthetic and functional properties of the fabric [57].

Textile finishing consists a series of processes which converts the dyed, printed fabric

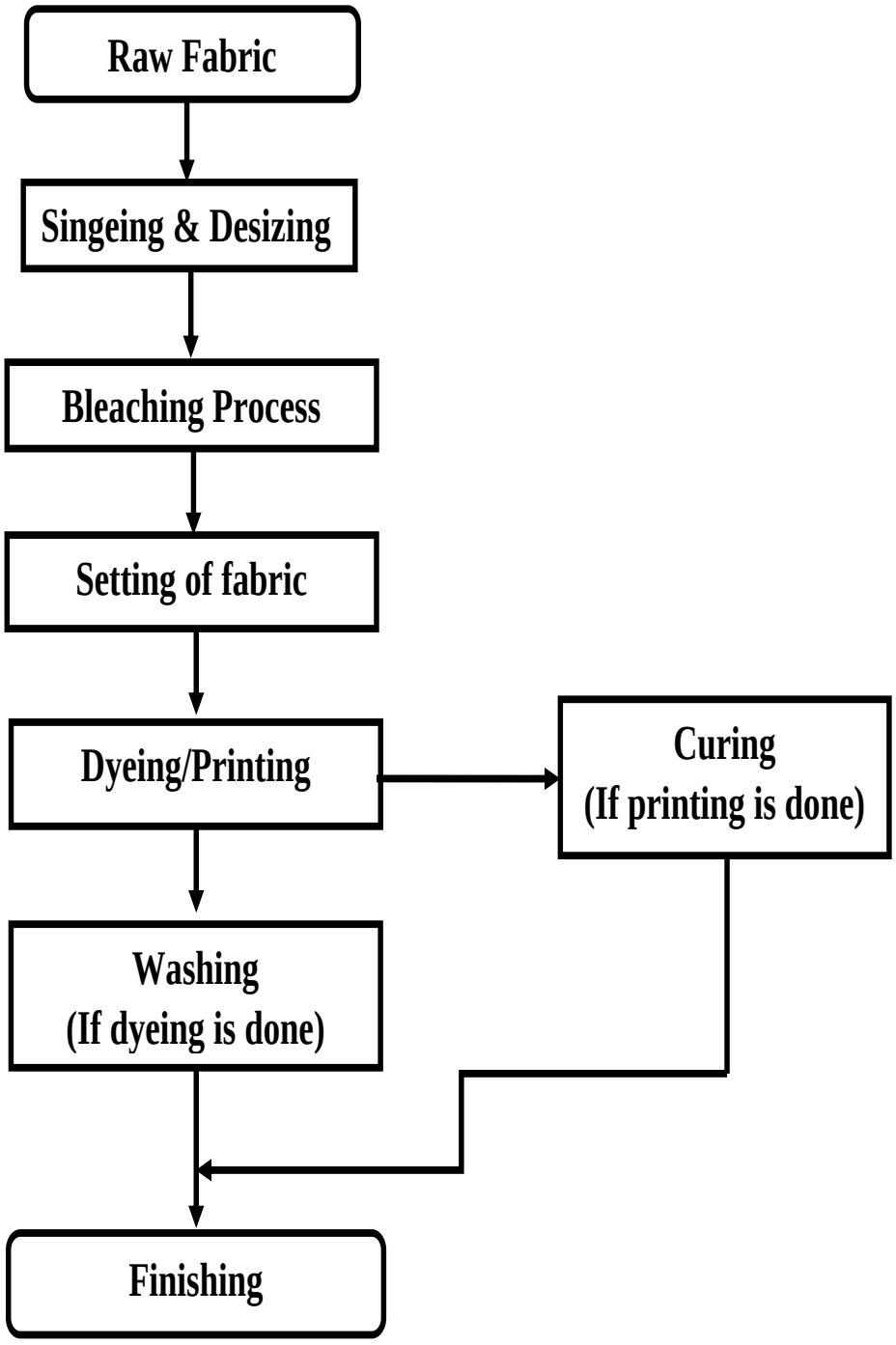

Figure 2.1: Manufacturing process in textile industry

into finished fabric having desired end use properties. Finishing can be temporary or permanent depending upon the fabric required. During finishing process, fabric undergoes through various chemical and mechanical treatments which makes fabric more receptive, attractive and useful.

Chemical finishing involves the addition of chemicals to fabric to achieve the desired results. A series of techniques such as mercerizing, easy care finish etc. are applied during this finishing process which involves chemicals reactions and softening treatments. Chemical finishing process can be used to modify fabric appearance, handle, control fabric dimension, improve fabric performance, protect the fibre or impart easy care properties [58]. Mechanical finishing involves calenders for better finish of fabric and explained in detail in next section.

2.2 Mechanical Finishing Process in Textile Industry

Mechanical finish is performed to enhance the desired smoothness and gloss to the fabric using calenders. It is a continuous shaping process in which fibre acquire its final shape to get the desired finish such as flattening, luster, compressing, glazing, moire, schreiner, smoothing, texturing and other embossed patterns on the fabric. Calendering makes one or both surfaces of the fabric thin, smooth, glossy and shiny. Calendering upgrade the transparency and lucidity of the fabric as shown in Figure 2.2. Finishing can be varied to desired degree by increasing/decreasing number of rolls, by loading or relieving the weight of roll to create higher/lower nip pressure and by heating/cooling of rolls. High temperature and pressure is required for squeezing the fabric between the calender rolls [59].

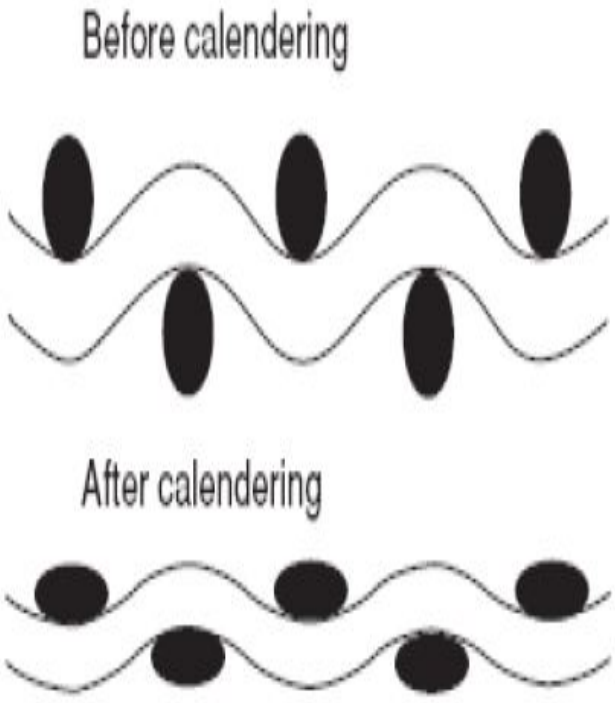

Figure 2.2: Calendering effect of fabric

2.2.1 Calender Roll Construction

Cylindrical rolls are working elements of the calender and the means by which the calender functions are accomplished. The metal used in calender rolls must be hard for better finishing. Hard rolls formed by iron carbon alloys i.e. chilled cast iron rolls and which may also contain manganese, phosphorus, sulphur, small amounts of silicon and sometimes chromium and nickel has been used. The term chilled comes out from the rapid removal of heat from the surface of the roll when it is cast. This causes carbon in that section to be bound to the iron as iron carbides, which are very hard and durable. In the usual method of manufacture, these rolls are cast from a single melt in a vertical pit, where heavy metal rings, called chills, are stacked to a depth sufficient to produce the full roll width. The thermal mass of these chills takes away the heat of the molten cast iron to produce a chill depth of white iron of $10 - 15$mm in the calender roll. The actual surface hardness ranges from about $70 - 78$ Shore C.

Steel rolls are used when high durability is required with extraordinary high surface hardness [60–66].

By providing a compressible covering on a roll, the intensity of a iron-iron nip is reduced and the nip width is widened. Soft rolls have an external cover or soft material made of rings die cut from sheets of fabric, cloth fibers or non woven mats which have been assembled over the steel core of the roll. The soft material is then pressed axially in huge machines capable of exerting thousands of tones of force to densify the covering to almost rock like hardness. Surface of soft roll can then be finished using metal working techniques until it has a high degree of surface finish and a precise diameter. Many different types of soft materials are available for these rolls including long- fiber cotton, wool, blue denim, nylon 610 and specialty blends. These soft rolls can not work at high temperature and high loading. For operating at high temperature and high loading composite material roll covering are used. In general these are material roll with a strong synthetic fiber embedded in a polymeric material, capable of withstanding hundreds of kilo Newton's per meter of nip force and operating at temperatures in the same range as ordinary soft rolls, that is up to about 80°C [30].

2.3 Types of Calenders used in Textile Industry

There are basically three types of calenders on the basic of desired surface properties i.e. hard nip calender, soft nip calender and temperature gradient calender as shown in Figure 2.3. The basic difference in these types of calenders is the type of material used for making the rolls and temperature of heated roll. The design and process variables of three different principal types of calenders are given in table 2.1 of APPENDIX.

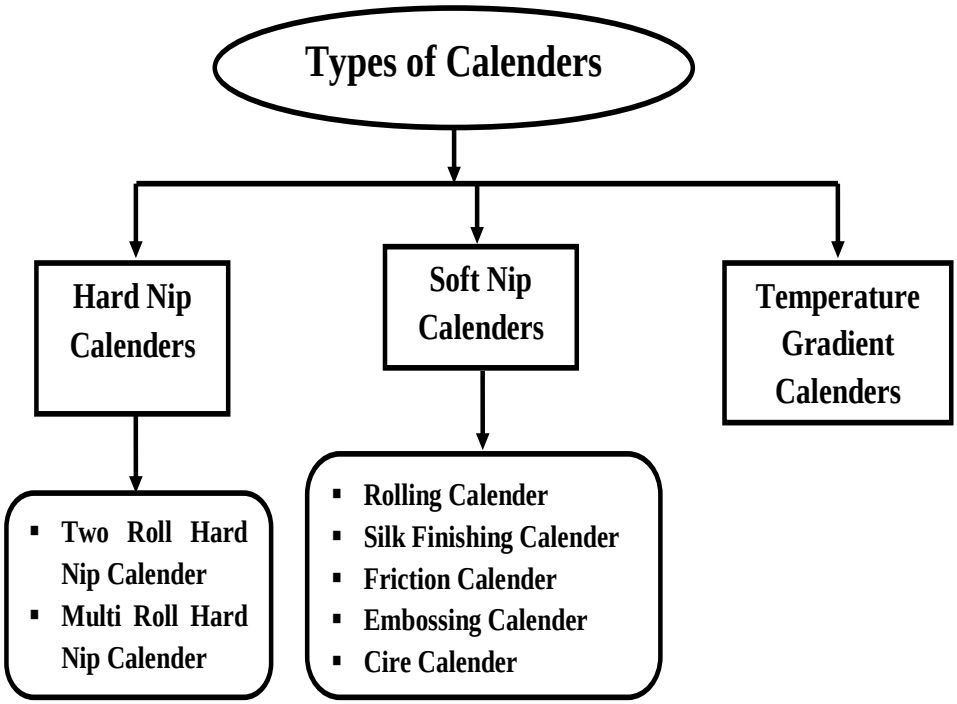

Figure 2.3: Types of calenders

2.3.1 Hard Nip Calender

In hard nip calender, the fabric is squeezed between two or more hard nip rolls. The control parameters are linear pressure between the rolls, numbers of nips and the roll surface temperatures. The basic principle of hard nip calendering is to densifying the fabric with pressure/temperature and copying the surface of the rolls to the fabric [22, 30, 66]. The main disadvantage of hard nip calendering is that the nip that is formed between the hard rolls is short and the actual contact pressure in the nip is high, even with a low linear load. As fabric has uneven structure, this kind of high pressure can cause blackening of the fabric. High pressure densifies the fabric and crushes some of the fibers and breaks the fiber bonding. Hard nip calenders are described in two main categories which are discussed below in detail.

- Two roll hard nip calender
- Multi roll hard nip calender

2.3.1.1 Two Roll Hard Nip Calender

This kind of calender is mainly used for pre calendering or for those fabric which don't require massive calendering. In two roll hard nip calender, one roll is a heated roll and other is deflection compensated roll. Rolls are usually vertically arranged with one above the other as shown in figure 2.4. Heated roll is either double walled rolls or peripherally drilled roll. The surface of roll is heated using hot water to obtain temperature of 100°C to 210°C. In slower machines, only one drive is used, normally for the heated roll. High speed machines require drives for both nip rolls to prevent speed differences in the nip. Web spreading rolls are used before the nip to ensure that the fabric enters the nip evenly without wrinkles.

Figure 2.4: Two roll hard nip calender

2.3.1.2 Multi Roll Hard Nip Calender

Multi roll hard nip calender consists of more than three hard rolls, most commonly it is having five to eight hard rolls. In multi nip calender, a typical arrangement of roll stack is having king roll, queen roll and intermediate rolls. Bottom roll is known as king roll and having largest diameter among all the rolls, next to king roll is queen roll which is having diameter less than king roll but equal to top roll. The other remaining rolls are known as intermediate rolls which are having diameter less than queen roll. These rolls are relatively smaller in diameter and the linear load is achieved by the weight of the rolls as shown in Figure 2.5. In multi roll hard nip calender, the rolls are heated in the range of 100 °C to 250 °C with the help of induction heating or through percolation of hot water or hot oil. Having more intermediate rolls in the stack increases the linear load in the bottom nips. This method of creating linear load is simple and rather precise because the linear load generated by the weight of the rolls is naturally generated along the whole width of the roll face, because of this fact, multi roll hard nip calenders are widely used in textile industry. Multi roll hard nip calenders normally have only one main drive. The driven roll is either the bottom roll or the second roll from the bottom. In some calenders, more driven rolls are used to ensure draw control at high speeds. The main problem on multi roll hard nip calenders are the runnability problems caused by widening and elongation of the web in the process. The nip pressure compresses the fabric, simultaneously the fabric is getting wider but as the web is transferred to the next nip, it has no chance to widen out. This can cause wrinkles at the next nip and might cause web breaks. Another problem in multi roll calenders is barring. This is a vibration behavior of the calender roll stack that begins due to unevenness of the fabric entering the calender or mechanical vibration induced by the calender, drives and surrounding machinery. Because all rolls in the calender work together in the calender stack, the vibration pattern is transferred from one roll to another, causing excessive vibration and a howling noise, resulting in machine direction (MD) thickness variations in the calendered fabric.

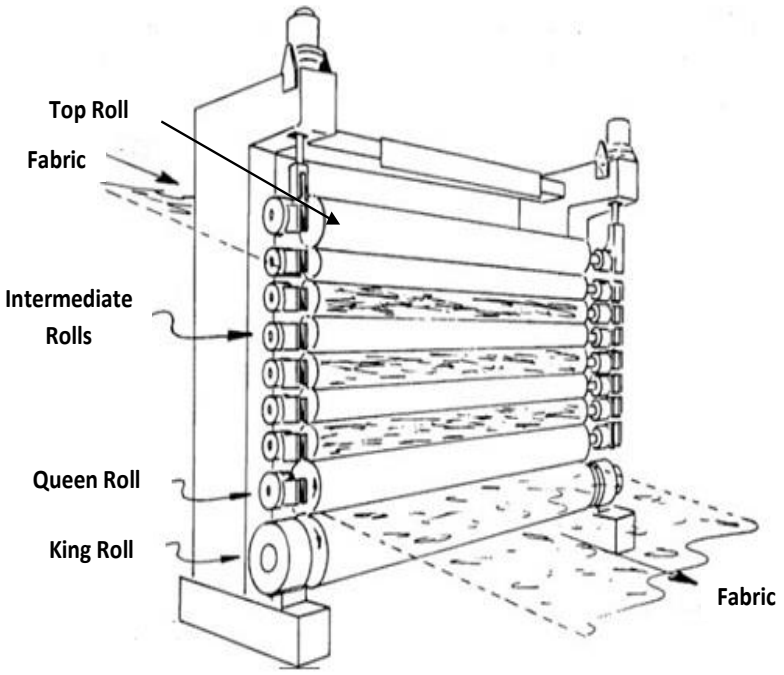

Figure 2.5: Multi roll hard nip calender

2.3.2 Soft Calender

Soft calenders are made up of alternate hard and soft rolls. Hard roll can be heated upto 250 °C with the help of induction heating or through percolation of hot water or hot oil. These rolls vary in number from 3 to 11 depending upon the type of finishing required and type of fabric to be calendered. The most commonly used calender consist of three rolls as shown figure 2.6. The key difference between hard nip and soft nip calendering is the time of contact between fabric and calender rolls or equivalently the nip length. In soft nip calender, pressure in the nip is low as compared to pressure in hard nip calenders. Heat transfer between the soft calender roll and the fabric is better because the nip is longer in case of soft calendering process. The surface and strength properties of the fabric are preserved better as compared to hard nip calendering [17, 19, 20, 30]. The types of soft nip calenders used in textile industry for getting various types of finishing according to fabric are rolling calender, silk finishing calender, friction calender, embossing calender and cire calender. The

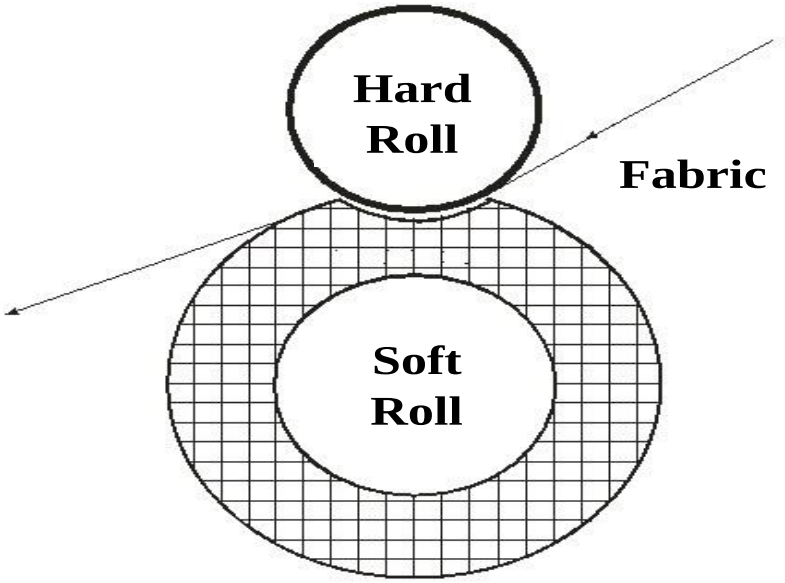

Figure 2.6: Soft calendering process

design and process parameters of these calenders are given in table 2.2 of APPENDIX. The most commonly used soft calender in textile industry is rolling calender.

2.3.2.1 Rolling Calender

Rolling calender imparts shiny, lustrous smooth fabric surface to the fabric. The basic mechanical action of this type of calender is to cause the fibers and webs to not only reshape but to also possibly flatten or deform around one another as it also causes the fibers to more tightly stack around one another. In rolling calendering, 3 to 11 alternate hard and soft rolls may be used depending on the type of finish required. Three roll and seven roll calenders with alternate hard and filled rolls are most popular. The main top hard roll is driven by a variable speed motor, either directly or through a roller chain drive while the intermediate filled roll can be driven with off nip drive. When required the hard roll can be heated by gas, hot oil, electric or steam up to 210 °C. The hard roll is made of chilled cast iron and soft rolls are having covering of soft materials like cotton, wool or mixture of these two. This is an open frame type calender with bottom loading and a bearing type of double row

spherical rollers. Among the special features of rolling calender is an oil circulating system for bearing boxes that is required for roll heating systems over 150 °C. In rolling calender of three rolls, the two rolls are run together at the same peripheral speeds so that there is no slippage between them as shown in figure 2.7. Under these conditions, the surface of fabric is simply flattened to the extent which is required. This process can be applied to all types of fabrics including high content cotton woven/non or impregnated fabrics and knitted cloths [22, 30, 66].

Figure 2.7: Rolling calender

2.3.3 Temperature Gradient Calender

The essential elements for enhancing the surface properties of the web inside the calender nip are pressure and temperature between the web and heated roll. Excess rise in temperature and pressure, sometimes leads to unacceptable consequences like damage and strength reduction of the web. Temperature gradient calendering, which is a combination of hard and soft rolls, having soft roll at room temperature and hard roll at higher temperature is used to overcome these undesirable factors. Hard roll (heated roll) is having layer of chilled cast iron whereas soft roll is having layer of soft

material like cotton, elastic material, polymers etc [32–34].

In temperature gradient calendering, the temperature of the soft roll has no contribution in temperature distribution because the contact time between heated roll and fabric is less, so heat transfer during temperature gradient calendering can be treated as transient heat conduction into a semi-infinite medium. The heated roll surface temperature can be up to 150°C-350°C. This is normally done with proculation of heated oil inside the calender roll. High temperature produces better web surface quality, uniformity and smoothness and preserve bulk and strength properties [36, 37].

Temperature gradient calendering selectively plasticize only the outer surface of the fabric, leading to better smoothness for given thickness. In case of temperature gradient calendering, heat is not transformed upto the center of the fabric in thickness direction, thus the fibres which are in direct contact with the heated roll get deformed permanently, while the fibres on the other side and upto the middle of the fabric do not get deformed due to which the surface properties of the fabric are developed while maintaining the bulk and strength properties as shown in figure 2.8.

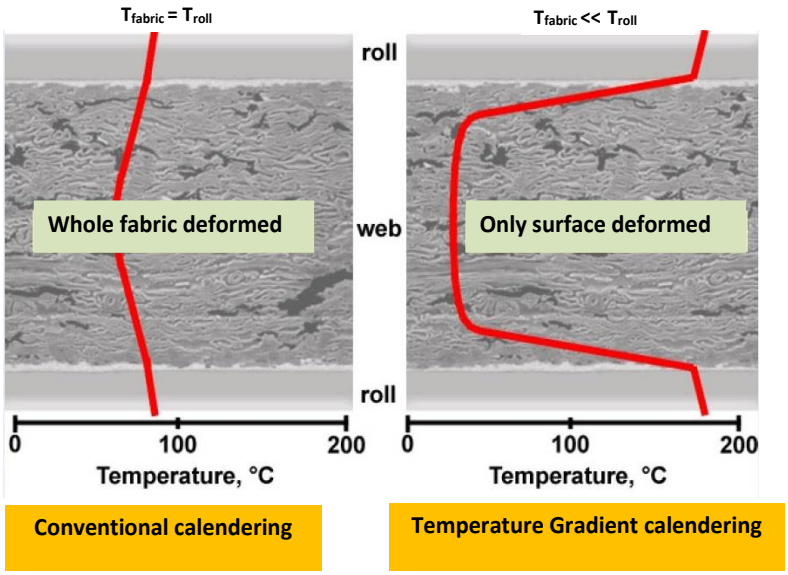

Figure 2.8: Temperature gradient calender

2.4 Effect of Calendering on Fabric Properties

Fabric properties like thickness, roughness, gloss and porosity properties subsequently changes during calendering process, but cannot change independently. These properties correlate strongly with each other. A change in one influences the other. Calendering improves the surface properties which is accompanied with thickness reduction. Improvement of surface properties of fabric is the prime requirement of calendering. The strength properties will be reduced by excessive calendering.

2.4.1 Gloss and Smoothness

Gloss and smoothness are developed differently in calendering process. Gloss is obtained mainly by friction, whereas smoothness is produced mainly by high pressure per unit area. Thus at high temperature, gloss will develop more rapidly than smoothness whereas at high pressure, smoothness will develop more rapidly than gloss.

2.4.2 Opacity

If the fabric is calendered at high moisture content, the number of optical contact is increased and there is a decrease in opacity. The opacity of the fabric is minimized when the fibers are squeezed with each other, consequently destroying air-fiber linkage.

2.4.3 Tensile Strength

Tensile strength is the amount of load or stress that can be handled by fabric before it stretches or breaks. When fabric undergoes calendering process, its tensile properties increases. The tensile strength will be higher in machine direction (MD) than in cross direction (CD) due to better fiber orientation in the fabric along machine direction.

2.4.4 Tear Strength

Tear strength is measure of how well a fabric can withstand the effect of tearing. Tear properties of fabric increases in machine direction during calendering process.

2.4.5 Air Permeability

Air permeability measures how easily air is passed through fabric. Air permeability of fabric increases when fabric undergoes calendering process.

2.5 Calendering Parameters Affecting Fabric Quality

The various design and process parameters affecting the final quality of the fabric are linear load, number of nips, calender speed, roll material and roll temperature which are explained in detail below.

2.5.1 Linear Load

Linear load is process variable that describes the applied force divided by calendering width. The nip pressure i.e. the pressure compressing the fabric in the nip is mostly affected by linear load. In hard nip calendering, the nip pressure is higher at constant load than in soft nip calendering because of narrow nip. Linear load affects fabric thickness and smoothness by compressing the fabric structure. Higher nip load/nip pressure improves the surface properties such as roughness and gloss by increasing the replication of the roll surface patterns on the fabric.

2.5.2 Number of Nips

With increase in number of nips fabric passes more time inside the nips which enhances the surface properties of fabric. Hence the fabric surface properties like smoothness and gloss increases while thickness decreases when more nips are used at same or different roll temperatures.

2.5.3 Calender Speed

Calender speed is a key parameter for maximizing productivity and also for developing final fabric properties. Calender speed determines dwell time in the nip and consequently the extent of deformation. Increasing calendering speed and reducing calender roll diameter will reduce the dwell time.

2.5.4 Roll Material

In case of soft calendering, the fabric gets more equal densification due to elasticity of the roll cover while passing through the nip as compared with the fabric calendered in hard nip. This means that soft cover distributes the compressive stress in the nip. Roughness of roll surface has large effect on fabric surface properties. A typical surface roughness level for a heated hard roll is $0.2 - 0.4$ Ra. Surface roughness of soft roll must be at a level where it does not have a harmful effect on the fabric. A typical surface roughness for a soft roll is $0.3 - 0.6$ Ra.

2.5.5 Roll Temperature

Roll temperature has prominent effect on the smoothness and gloss of the fabric, as compared to the pressure and number of nips. Fabric temperature can be increased most effectively by increasing the temperature of the heated roll during calendering process. With increase in temperature of the fabric, fabric smoothness can be improved. The surface fibers are selectively heated, plasticized and compressed, while

the middle of the web remains cool, resilient and bulky when fabric temperature is lower than the heated roll temperature.

2.6 Conclusion

In this chapter, a comprehensive description of the manufacturing process of fabric in textile industry along with the various unit operations, finishing process in textile industry and design and process parameters of various types of textile calenders are described. The material of construction of various calenders, hardness, temperature level, nip load, surface roughness and other important calendering parameters which effects the quality of fabric are discussed. Effect of calendering on fabric properties are also outlined.

Chapter 3

Nip Mechanics Models for Textile Calenders

The solid to solid contact may be combination of different geometrical shapes such as roll to roll, roll to plate, plate to plate, plate to sphere and many more. These contacts may be homogeneous or can be heterogeneous also. These contacting solids can be rigid, elastic, plastic, elasto-plastic in nature and can also have a layered structure of these type of materials. All these combinations have practical application in textile calendering, offset printing press, leather calendering and many more process industries. Based on geometrical shapes, governing equations will be different from each other. In textile industry, roll to roll contact problems are of prime importance. In this chapter, generalized nip mechanics model has been developed which can be used for different types of calender used in textile industry, as the available nip mechanics model cannot be applied directly to calendering of fabric due to their limitations.

3.1 Development of Nip Mechanics Model

The problem of two non conforming contact of two elastic solids was first solved by Hertz under several restrictive assumptions. The non conforming bodies when brought in contact without deformation will touch at a point or along a line. In case

of cylindrical elastic bodies which are in contact with each other having their axis parallel give rise to line contact. The contact area is small as compared with the size of cylindrical bodies in contact [66–71].

The undeformed shapes of these cylindrical bodies considering x axis to lie in plane of cross section and y axis parallel to the axes of cylinders are given by

$$Z_1 = F_1(x, y) \tag{3.1.1}$$

$$Z_2 = F_2(x, y) \tag{3.1.2}$$

Thus separation between them before applying load is given by

$$H = Z_1 + Z_2 = F(x, y) \tag{3.1.3}$$

According to Hertz theory the equation od undeformed surface near the region of contact, can be defined accurately by the function

$$H = Ax^2 + 2Bxy + Cy^2 \tag{3.1.4}$$

where B can be made zero by suitable choice of axes, hence

$$H = Ax^2 + Cy^2 = \frac{1}{2R'}x^2 + \frac{1}{2R''}y^2 \tag{3.1.5}$$

where A and C are positive constants and R' and R'' are defined as the principal relative radii of curvature.

When load G is applied to two non conforming bodies in contact, the contact region must extend at equal distance. During the compression distant points of two bodies B_1 and B_2 move towards point O, parallel to z axis by displacements δ_1 and δ_2 respectively. If the two solids do not deform their profiles would overlap as shown by dotted lines in Figure 3.1. Due to contact pressure, the surface of each body is displaced parallel to Oz by an amount u_{z1} and u_{z2} (measured positive into each body) relative to the distant points B_1 and B_2. If after deformation, the points S_1 and S_2 are coincident with in the contact surface then

$$u_{z1} + u_{z2} + H = \delta_1 + \delta_2 \tag{3.1.6}$$

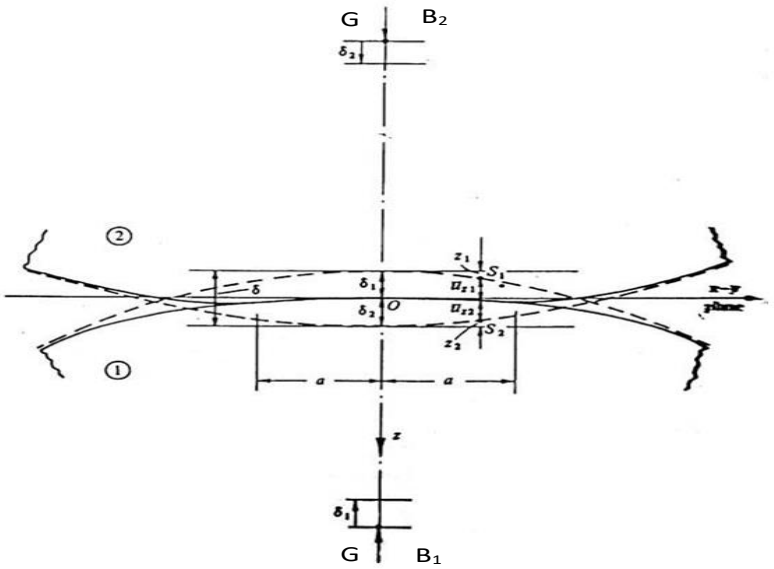

Figure 3.1: Geometry of two rolls when load G is applied

Taking $\delta = \delta_1 + \delta_2$ and using equation (3.1.5),

$$u_{z1} + u_{z2} = \delta - Ax^2 + By^2 \tag{3.1.7}$$

where x and y are the common coordinates of S_1 and S_2 projected on to the xy plane. If S_1 and S_2 lie outside the contact area then

$$u_{z1} + u_{z2} < \delta - Ax^2 + By^2 \tag{3.1.8}$$

3.2 Hertz Nip Mechanics Model

The first satisfactory analysis of the stresses at the contact of two elastic solids is due to Hertz. Hertz formulated the conditions expressed by equations (3.1.7) and (3.1.8) which must be satisfied by the normal displacements on the surface of the solids. He introduced the simplification that, for the purpose of calculating the local deformation, each body can be regarded as an elastic half-space loaded over a small elliptical region of its plane surface [72–75].

Hertz model provided the expression for the radius of the contact surface and contact pressure at the interface of the two non confirming elastic spheres under normal force

based on following assumptions [38, 39]:

1. Material properties of contacting bodies are same and identical in all directions.
2. Seismic dissipation of energy due to vibration or sound wave during contact of two bodies is not considered.
3. Elastic bodies in contact follows Hooke's law.
4. The radii of curvature of the contacting bodies are much larger than the contact radius, which implies the bodies are experiencing traction only at the contacting surface.
5. Friction effects are neglected i.e. contacting bodies are considered smooth.
6. Geometrical nonlinearities arising due to large deformations are not considered.

When two cylindrical bodies with their axis both lying parallel to the y axis are pressed by a force, they make contact over a long strip of width lying parallel to y axis.
The Hertzian nip pressure, which is exerted between two frictionless elastic solids in contact is given by

$$G(x) = \frac{2G}{\pi(N_w/2)}\left(1 - \left(\frac{x}{N_w/2}\right)^2\right)^{1/2} \tag{3.2.1}$$

where G is the force per unit length of the cylinder and N_w is the nip width.
For the case of cylinders of radius R_1 and R_2, the equation for separation between corresponding points on the unloaded surfaces becomes

$$H = Ax^2 = \frac{1}{2}\left(\frac{1}{R_1} + \frac{1}{R_2}\right)x^2 = \frac{1}{2}\left(\frac{1}{R}\right)x^2 \tag{3.2.2}$$

For points lying within the contact area after applying load G, equation (3.1.7) becomes

$$u_{z1} + u_{z2} = \delta - Ax^2 = \delta - \frac{1}{2}\left(\frac{1}{R}\right)x^2 \tag{3.2.3}$$

For points lying outside the contact area after applying load G,

$$u_{z1} + u_{z2} > \delta - \frac{1}{2}\left(\frac{1}{R}\right)x^2 \tag{3.2.4}$$

On differentiating equation (3.2.3) w.r.t. x,

$$\frac{\partial u_{z1}}{\partial x} + \frac{\partial u_{z2}}{\partial x} = -\left(\frac{1}{R}\right)x \tag{3.2.5}$$

The surface gradient due to a pressure $G(x)$ acting on a strip $-\frac{N_w}{2} \leq x \leq \frac{N_w}{2}$ is given by

$$\frac{\partial u_{z1}}{\partial x} + \frac{\partial u_{z2}}{\partial x} = -\frac{2}{\pi E^*}\int_{-a}^{a}\frac{G(s)}{x-s}ds \tag{3.2.6}$$

Substituting equation (3.2.6) in equation (3.2.5),

$$\int_{-\frac{N_w}{2}}^{\frac{N_w}{2}}\frac{G(s)}{x-s}ds = \frac{\pi E^*}{2R}x \tag{3.2.7}$$

which is an integral equation and its solution is given by

$$G(x) = -\frac{\pi E^*}{2R}\left(\frac{x^2 - \frac{(N_w/2)^2}{2}}{\pi((N_w/2)^2 - x^2)^{1/2}}\right) + \frac{N_w}{\pi((N_w/2)^2 - x^2)^{1/2}} \tag{3.2.8}$$

The load G must be positive throughout the contact for which

$$G \geq \frac{\pi(N_w/2)^2 E^*}{4R} \tag{3.2.9}$$

If G exceeds the value given by the right hand side of equation (3.2.9) then the pressure rises to an infinite value at $x = \pm a$.

So

$$G = \frac{\pi(N_w/2)^2 E^*}{4R} \tag{3.2.10}$$

i.e.

$$\left(\frac{N_w}{2}\right)^2 = \frac{4GR}{\pi E^*} \tag{3.2.11}$$

So nip width $N_w = 2a$ is

$$N_w = 2\sqrt{(\frac{2GD_E}{\pi E^*})} \tag{3.2.12}$$

where N_w is the nip width, G is the load applied, D_E is the equivalent diameter and E^* is the equivalent bulk modulus.

The equivalent diameter D_E for two cylindrical bodies in contact is given by

$$\frac{1}{D_E} = \frac{1}{D_1} + \frac{1}{D_2} \tag{3.2.13}$$

where D_1 and D_2 are the diameters of two cylindrical rolls in contact with each other. Also, the equivalent bulk modulus E^* of two cylindrical rolls in contact is give by

$$\frac{1}{E^*} = \frac{1-\nu_1^2}{E_1} + \frac{1-\nu_2^2}{E_2} \tag{3.2.14}$$

where E_1, E_2 are the bulk modulus and ν_1, ν_2 are Poisson's proportion of two cylindrical rolls in contact respectively.

3.3 Models for Mechanics for Non Hertzian Normal Contact of Elastic Bodies

Hertz model accuracy is a matter of concern when the material of the contacting bodies deviates from the basic Hertz assumptions, as in case of calendering process used in many industries in which harder material will dome into the softer one, known as non hertzian contact. Therefore use of Hertz model can result in erroneous predictions of normal contact forces for situations which deviate significantly from the Hertz problem. When the material being deformed is a relatively thin layer, the finite thickness of the deformable material should be taken in to account. Meijers modified the Hertz equation for contact problem of a steel cylinder pressed on a soft elastic layer of thickness b. Figure 3.11 shows the geometry of the problem.

The basic integral equation of Fredholm type of the second kind has been proposed for the pressure distribution under the cylinder in the case of plane strain when ratio of half nip width $(N_w/2)$ and cover thickness b is less than one is

$$\frac{1-\nu^2}{\pi E} \int_{-N_w/2}^{N_w/2} G(\xi) K(x-\xi) b\xi = v(x) \tag{3.3.1}$$

Where E is the bulk modulus, $G(x)$ is the pressure distribution and $v(x)$ is the vertical displacement along the upper edge of the layer and $K(x)$ is given by

$$K(x) = \frac{1-\nu^2}{\pi E} \int_{-\infty}^{\infty} \frac{[(3-4\nu)\sinh 2\omega - 2\omega] e^{-i\omega x/b}}{\omega[(3-4\nu)\cosh 2\omega + 2\omega^2 + 5 - 12\nu + 8\nu^2]} b\omega \tag{3.3.2}$$

The plane strain equation is based on the assumption that the classical linear theory of elasticity applies to the contact problem. This assumption implies that the ratio

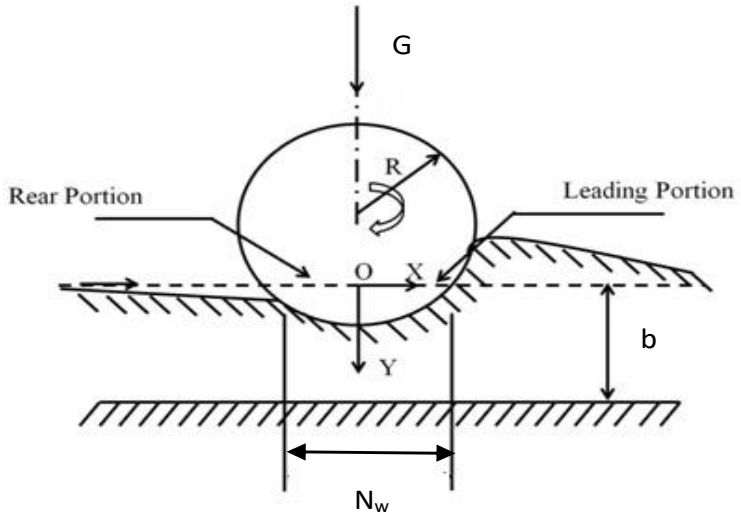

Figure 3.2: Geometry of the problem

of half nip width $(N_w/2)$ and radius of the roll R must be small in comparison with unity. The kernel has logarithm singularity at $x = 0$. Splitting off the singularity one may expand the regular remainder in a uniformly convergent power series for $|x/2b| < 1$.

$$K(x) = -2ln|\frac{x}{2b}| + \sum_{k=0}^{k=\infty} \alpha_k (\frac{x}{2b})^{2k} \tag{3.3.3}$$

Introducing non-dimensional variables $Z = \frac{x}{N_w/2}$ and $\xi = \frac{\xi}{N_w/2}$ in equation (3.3.1). For small values of $\frac{N_w/2}{b}$ the logarithmic term in the kernel given by equation (3.3.3) is the principal term, so equation (3.3.1) can be written in the form

$$\frac{(1-\nu^2)(N_w/2)}{\pi E} \int_{-1}^{1} G(\xi)[-2ln|\frac{Z-\xi}{2}| - 2ln\frac{N_w}{2b}]b\xi = g_0^* - \frac{(N_w/2)^2}{2R} Z^2 - \frac{(1-\nu^2)(N_w/2)}{\pi E} \int_{-1}^{1} G(\xi) \sum_{k=0}^{\infty} \alpha_k (\frac{N_w/2}{b})^{2k} (\frac{Z-\xi}{2})^{2k} b\xi \tag{3.3.4}$$

$$\int_{-1}^{1} \frac{G(\xi)}{Z-\xi} b\xi = \frac{\pi E}{2(1-\nu^2)} \frac{N_w/2}{R} Z + \frac{1}{2} \sum_{k=1}^{\infty} k\alpha_k (\frac{N_w/2}{h})^{2k} \int_{-1}^{1} G(\xi) (\frac{Z-k}{2})^{2k-1} b\xi \tag{3.3.5}$$

$\frac{N_w/2}{h} = 0$ the above equation reduces to the equation for a circular disk on half plane. For small values of $(\frac{N_w}{2})$ assuming that solution is in the form of power series with

respect to small parameter $(\frac{N_w/2}{b})^2$.

$$G(Z) = \sum_{j=0}^{\infty} G_j(Z)(\frac{N_w}{2b})^{2j} \tag{3.3.6}$$

The equation (3.3.6) can be expanded as

$$G(Z) = G_0(Z) + G_1(Z)(\frac{N_w}{2b})^2 + G_2(Z)(\frac{N_w}{2b})^4 + G_3(Z)(\frac{N_w}{2b})^6 + ... \tag{3.3.7}$$

Where $G_0(Z)$ is the Hertzian pressure distribution. $G_i(Z)$ satisfies the integral equation relating the contact pressure and the displacement in the contact region where $i = 0, 1, 2, 3....$

Substituting equation (3.3.5) in (3.3.7) and equating like powers of $\frac{N_w}{2h}$ in both members gives recurrent system of integral equations

$$\int_{-1}^{1} \frac{G_0(\xi)}{Z-\xi} b\xi = \frac{\pi E}{2(1-\nu^2)} \frac{N_w/2}{R} Z \tag{3.3.8}$$

$$\int_{-1}^{1} \frac{G_j(\xi)}{Z-\xi} b\xi = \frac{1}{2} \sum_{k=1}^{j} k\alpha_k \int_{-1}^{1} G_{j-k}(\xi)(\frac{Z-\xi}{2})^{2k-1} b\xi \quad j = 1, 2, 3... \tag{3.3.9}$$

The equations (3.3.8) and (3.3.9) are singular integral equations of type Cauchy principal value equation on a finite interval. Solution of equation (3.3.8) and (3.3.9), restricting up to $j = 3$ is given by,

Hence

$$G_0(Z) = \frac{\pi E N_w \sqrt{1-Z^2}}{4(1-\nu^2)R} \tag{3.3.10}$$

$$G_1(Z) = \frac{\pi E N_w \sqrt{1-Z^2}}{4(1-\nu^2)R} (\frac{1}{8})\alpha_1 \tag{3.3.11}$$

$$G_2(Z) = \frac{\pi E N_w \sqrt{1-Z^2}}{4(1-\nu^2)R} \left(\frac{1}{64}\right)(\alpha_1^2 + 5\alpha_2 + 4\alpha_2 Z^2) \tag{3.3.12}$$

The requirement that the pressure remains bounded at the ends of the contact area ensures that the equation have unique solution. The total load G on the cylinder per unit length is obtained by integrating the pressure distribution is

$$G = \int_{-\frac{N_w}{2}}^{\frac{N_w}{2}} G(Z) dZ \tag{3.3.13}$$

Substituting equations (3.3.10), (3.3.11) and (3.3.12) in equation (3.3.7),

$$\begin{aligned} G(Z) = & \frac{\pi E N_w \sqrt{1-Z^2}}{4(1-\nu^2)R} + \frac{\pi E N_w \sqrt{1-Z^2}}{4(1-\nu^2)R}(\frac{1}{8})\alpha_1(\frac{N_w}{2b})^2 \\ & + \frac{\pi E N_w \sqrt{1-Z^2}}{4(1-\nu^2)R}(\frac{1}{64})(\alpha_1^2 + 5\alpha_2 + 4\alpha_2 Z^2)(\frac{N_w}{2b})^4 \end{aligned} \tag{3.3.14}$$

$$G = \frac{\pi E}{4(1-\nu^2)} \frac{N_w^2}{4R}[1 + \frac{1}{8}\alpha_1(\frac{N_w}{2b})^2 + \frac{1}{64}(\alpha_1^2 + 6\alpha_2)(\frac{N_w}{2b})^4] \tag{3.3.15}$$

where α_0, α_1, α_2, are determined by numerical integration for different values of Poisson's ratio.

When there are two cylinders having Poisson's ratio ν_1 and ν_2 and bulk modulus E_1 and E_2 and their axis parallel the above equation can be modified as

$$G = \frac{\pi E^*}{4} \frac{N_w^2}{2D_E}[1 + \frac{1}{8}\alpha_1(\frac{N_w}{2b})^2 + \frac{1}{64}(\alpha_1^2 + 6\alpha_2)(\frac{N_w}{2b})^4] \tag{3.3.16}$$

where E^* and D_E can be found out from equations (3.2.13) and (3.2.14). The equation (3.3.16) is a general model for all kinds of solid-solid contact. This equation is used to calculate nip width of calenders used in various process industries such as paper, leather, textile and rubber etc.

3.3.1 Special Cases of the Generalized Model

3.3.1.1 Nip Mechanics Model for Hard Nip Calender

In case of hard calender (machine calender), the Poissons ratio is taken as 0.3 for the hard rolls having covering of chilled cast iron. For this value of Poissons ratio, α_1 and α_2 are taken as 5.7278 and -7.8479 respectively.

Thus using equation (3.2.13) and (3.2.14), equation (3.3.16) becomes

$$E^* = 2.545\frac{GD_E}{N_w^2}[1 + 0.179(\frac{N_w}{b})^2 - 0.0139(\frac{N_w}{b})^4]^{-1} \tag{3.3.17}$$

Equation (3.3.17) works as nip mechanics model for machine calenders (NMMM) used in textile industry.

3.3.1.2 Nip Mechanics Model for Soft Nip Calender

In case of soft calender, as $E_1 \gg E_2$, equation (3.2.14) becomes

$$\frac{1}{E^*} = \frac{1-\nu_2^2}{E_2} \tag{3.3.18}$$

Thus using equation (3.3.19) in equation (3.3.16),

$$G = \frac{\pi E_2}{4(1-\nu^2)} \frac{N_w^2}{2D_E}[1 + \frac{1}{8}\alpha_1(\frac{N_w}{2b})^2 + \frac{1}{64}(\alpha_1^2 + 6\alpha_2)(\frac{N_w}{2b})^4] \tag{3.3.19}$$

In this case, the Poissons ratio is taken as 0.48 for the soft rolls. For this value of Poissons ratio, α_1 and α_2 are taken as 7.7938 and -11.7696 respectively. Thus

$$E^* = 1.959\frac{GD_E}{A^2}[1 + 0.2436(\frac{N_w}{b})^2 - 0.0096(\frac{N_w}{b})^4]^{-1} \tag{3.3.20}$$

Equation (3.3.20) works as nip mechanics model for soft calenders such as rolling calender used in textile industry.

3.4 Simulation of Nip Mechanics Model

The parameters affecting nip width are line load, roll diameter, bulk modulus and poisson ratio of material used. The design and process parameters given in table 3.1 of APPENDIX are taken into consideration for simulation of a single nip machine and rolling calender. The equivalent diameter and equivalent bulk modulus are computed using equation (3.2.13) and equation (3.2.14). The computed equivalent diameters for machine calender and rolling calender are $240mm$ and $210.01mm$ respectively. The computed equivalent bulk modulus for machine calender and rolling calender are $76.923kN/mm^2$ and $3.132kN/mm^2$ respectively. The impact of a variety of design and process parameters has been examined by nip mechanics models given by equation (3.3.17) and (3.3.20). Results obtained by NMMM and NMMR are then compared with Hertz solution given by equation (3.2.12).

3.5 Results and Discussion

3.5.1 Impact of Various Design and Process Parameters on Machine Calender

Impact of load applied, equivalent diameter, equivalent bulk modulus and cover thickness on nip width has been investigated for machine calender. Also impact of cover thickness on average pressure has been investigated for machine calender.

3.5.1.1 Impact of Load Applied on Nip Width for Machine Calender

The nip width N_w is computed for different values of the load applied G by utilizing equation (3.3.17) on keeping other parameters constants. The calculated values are given in table 3.2 of APPENDIX. The graphs are plotted for different values of the load applied as shown in Figure 3.3. The results obtained from the Hertz model is compared with the results obtained by nip mechanics model for machine calender (NMMM) and textile mill data. Figures clearly shows that nip width increases with increase in line load. Also, it is found that nip mechanics model for machine calender provides better results as compared to the Hertz model and obtained results matches more closely with the data obtained from textile mill.

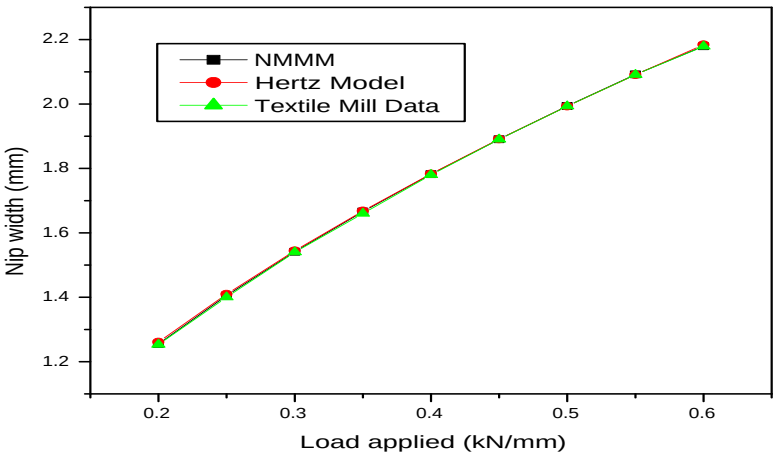

Figure 3.3: Impact of load applied on nip width for machine calender

3.5.1.2 Impact of Equivalent Diameter on Nip Width for Machine Calender

The nip width N_w is computed for different values of the equivalent diameter D_E with the constant load applied $0.263kN/mm$ by utilizing equation (3.3.17) on keeping other parameters constants. The calculated values are given in table 3.3 of APPENDIX. The graphs are plotted for different values of the load applied as shown in Figure 3.4 . It shows that with increase in equivalent diameter and assuming other parameters constant, nip width increases. The results obtained from the Hertz model is compared with the results obtained by nip mechanics model for machine calender (NMMM). It is found that there is a difference in the values of nip width obtained from nip mechanics model for machine calender and Hertz model because of the cover thickness factor which cannot be neglected.

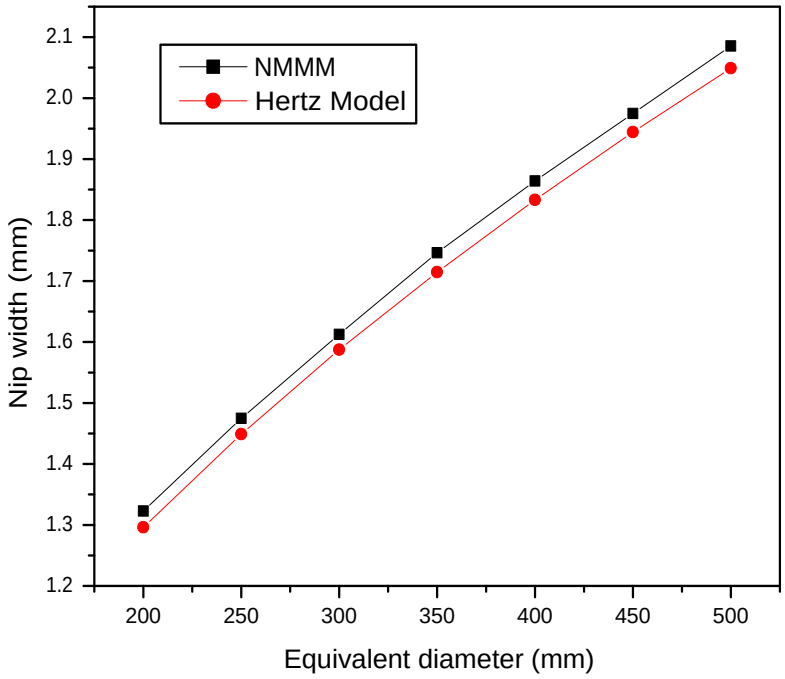

Figure 3.4: Impact of equivalent roll diameter on nip width for machine calender

3.5.1.3 Impact of Equivalent Bulk Modulus on Nip Width for Machine Calender

The nip width N_w is computed for different values of the equivalent bulk modulus E^* with the constant load applied $0.263kN/mm$ by utilizing equation (3.3.17) on keeping other parameters constants. The calculated values are given in table 3.4 of APPENDIX. The graphs are plotted for different values of the load applied as shown in Figure 3.5. It demonstrates that with increase in equivalent bulk modulus and assuming other parameters constant, nip width decreases. The results obtained from the Hertz model is compared with the results obtained by nip mechanics model for machine calender (NMMM). It is found that there is a difference in the values of nip width obtained from nip mechanics model for machine calender and Hertz model because of the cover thickness factor which cannot be neglected.

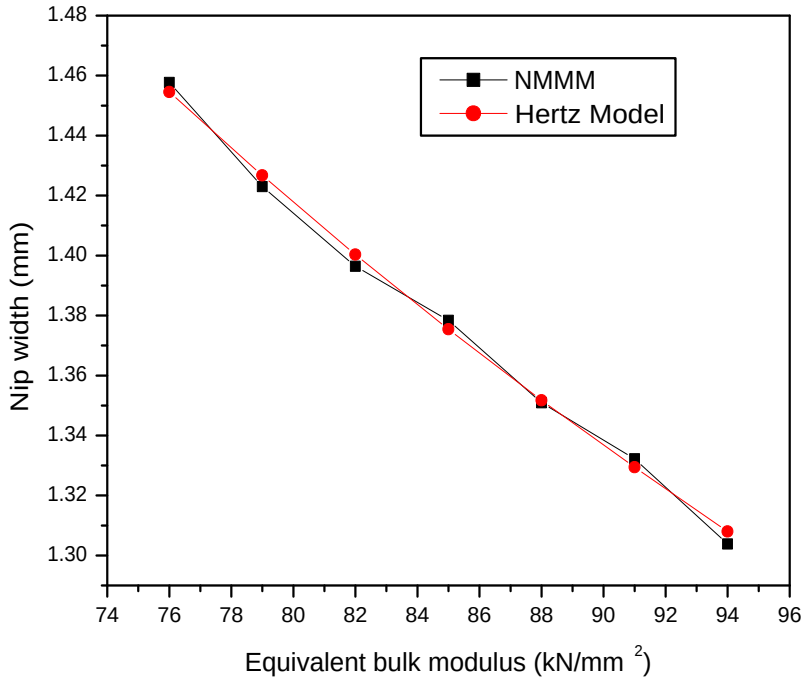

Figure 3.5: Impact of equivalent bulk modulus on nip width for machine calender

3.5.1.4 Impact of Cover Thickness on Nip Width for Machine Calender

The nip width N_w is computed for different values of the cover thickness b with the constant load applied $0.263kN/mm$ by utilizing equation (3.3.17) on keeping other parameters constants. The calculated values are given in table 3.5 of APPENDIX. The graphs are plotted for different values of the load applied as shown in Figure 3.6. It demonstrates that with increase in cover thickness and assuming other parameters constant, nip width increases. The results obtained from the Hertz model is compared with the results obtained by nip mechanics model for machine calender (NMMM). It is found that there is a significant difference between the results obtained from nip mechanics model for machine calender and Hertz model because NMMM considered the cover thickness of hard roll while Hertz Model does not take it into account.

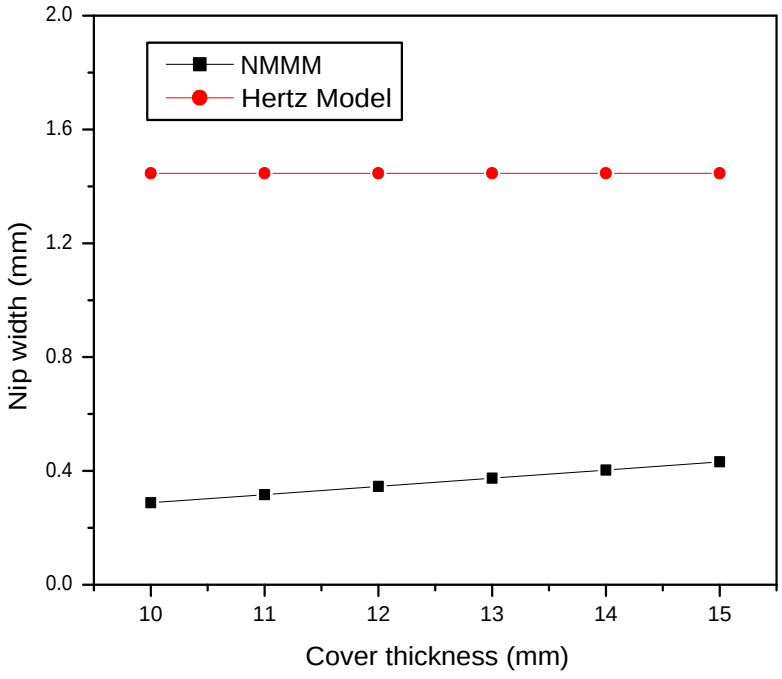

Figure 3.6: Impact of cover thickness on nip width for machine calender

3.5.1.5 Impact of Cover Thickness on Average Pressure for Machine Calender

Average pressure is computed by dividing nip load by nip width for different values of the cover thickness b with the constant load applied $0.263kN/mm$ by utilizing equation (3.3.17) on keeping other parameters constants. The calculated values are given in table 3.6 of APPENDIX. The graphs are plotted for different values of the load applied as shown in Figure 3.7. The results obtained from the Hertz model is compared with the results obtained by nip mechanics model for machine calender (NMMM). It demonstrates that with increase in cover thickness and assuming other parameters constant, average pressure remains same in case of Hertz solution. Average pressure decreases with increase in cover thickness in case of nip mechanics model for machine calender (NMMM). It is found that there is a huge difference between the results obtained from the nip mechanics model for machine calender and Hertz model because NMMM considered the cover thickness of hard roll while Hertz Model does not take it into account.

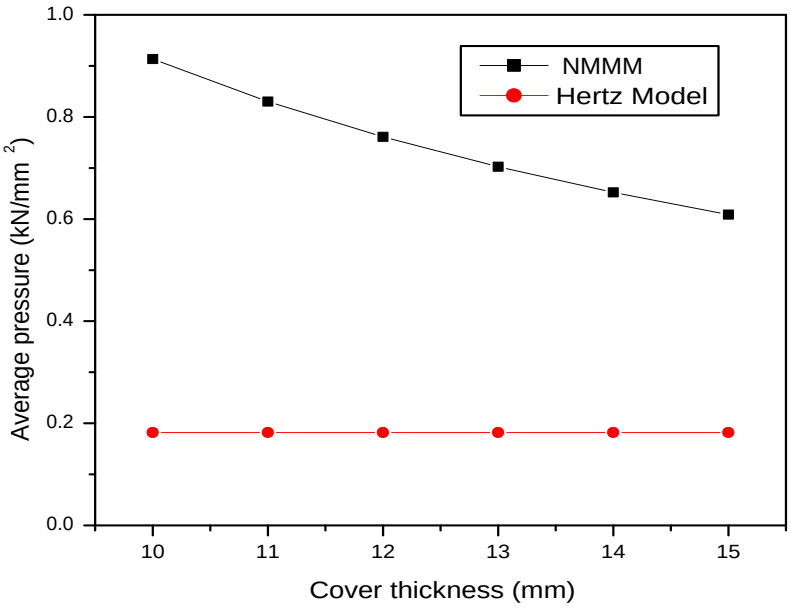

Figure 3.7: Impact of cover thickness on average pressure for machine calender

3.5.2 Impact of Various Design and Process Parameters on Rolling Calender

Impact of load applied, equivalent diameter, equivalent bulk modulus and cover thickness on nip width has been investigated for rolling calender. Also impact of cover thickness on average pressure has been investigated for rolling calender.

3.5.2.1 Impact of Load Applied on Nip Width for Rolling Calender

The nip width N_w is computed for different values of the load applied G by utilizing equation (3.3.20) on keeping other parameters constants. The calculated values are given in table 3.7 of APPENDIX. The graphs are plotted for different values of the load applied as shown in Figure 3.8. The results obtained from the Hertz model is compared with the results obtained by nip mechanics model for rolling calender (NMMR) and textile mill data. Figures clearly shows that nip width increases with increase in line load. Also, it is found that nip mechanics model for rolling calender provides better results as compared to the Hertz model and obtained results matches more closely with the data obtained from textile mill.

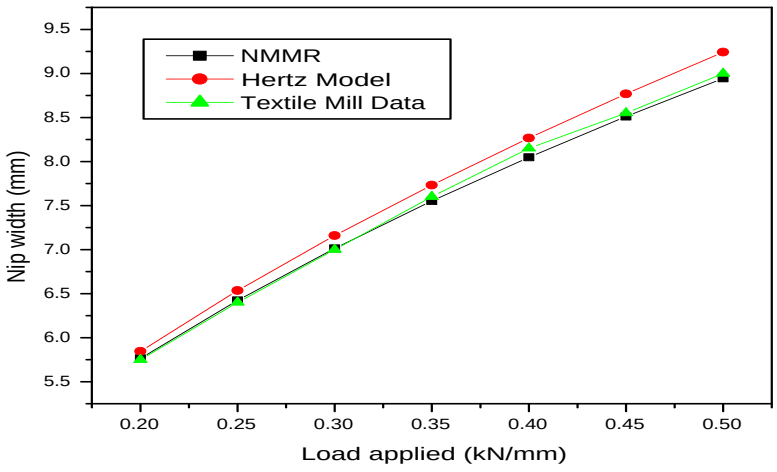

Figure 3.8: Impact of load applied on nip width for rolling calender

3.5.2.2 Impact of Equivalent Diameter on Nip Width for Rolling Calender

The nip width N_w is computed for different values of the equivalent diameter D_E with the constant load applied $0.263kN/mm$ by utilizing equation (3.3.20) on keeping other parameters constants. The calculated values are given in table 3.8 of APPENDIX. The graphs are plotted for different values of the load applied as shown in Figure 3.9 . It shows that with increase in equivalent diameter and assuming other parameters constant, nip width increases. The results obtained from the Hertz model is compared with the results obtained by nip mechanics model for rolling calender (NMMR). It is found that there is a difference in the values of nip width obtained from nip mechanics model for rolling calender and Hertz model because of the cover thickness factor which cannot be neglected.

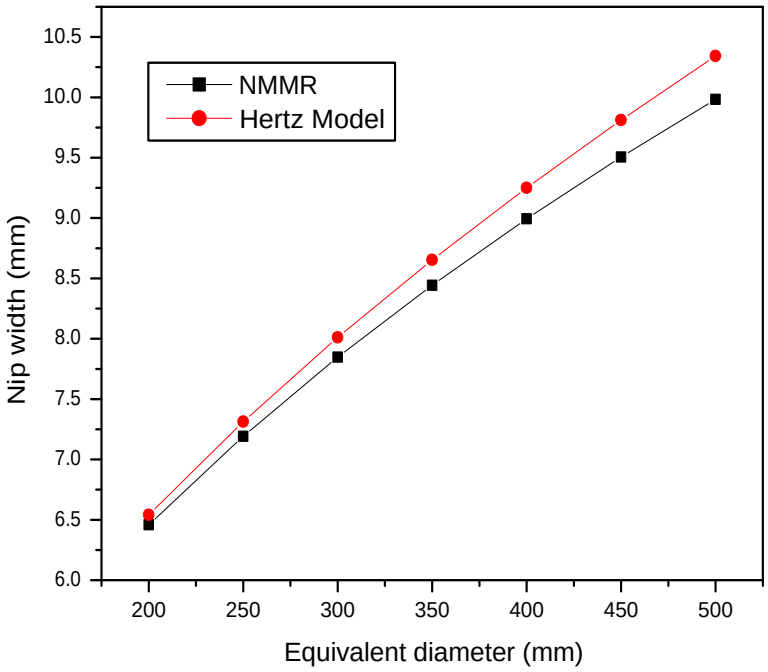

Figure 3.9: Impact of equivalent roll diameter on nip width for rolling calender

3.5.2.3 Impact of Equivalent Bulk Modulus on Nip Width for Rolling Calender

The nip width N_w is computed for different values of the equivalent bulk modulus E^* with the constant load applied $0.263kN/mm$ by utilizing equation (3.3.20) on keeping other parameters constants. The calculated values are given in table 3.9 of APPENDIX. The graphs are plotted for different values of the load applied as shown in Figure 3.10. It demonstrates that with increase in equivalent bulk modulus and assuming other parameters constant, nip width decreases. The results obtained from the Hertz model is compared with the results obtained by nip mechanics model for rolling calender (NMMR). It is found that there is a difference in the values of nip width obtained from nip mechanics model for rolling calender and Hertz model because of the cover thickness factor which cannot be neglected.

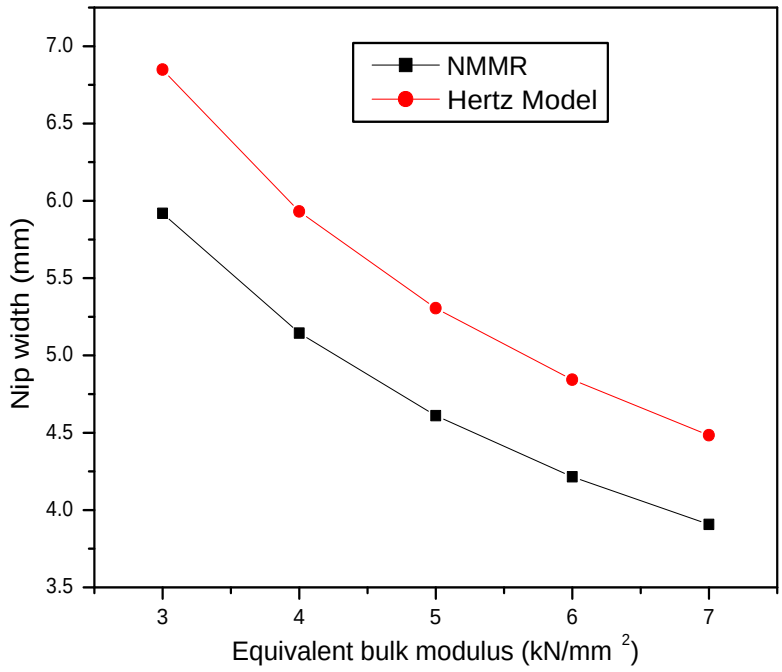

Figure 3.10: Impact of equivalent bulk modulus on nip width for rolling calender

3.5.2.4 Impact of Cover Thickness on Nip Width for Rolling Calender

The nip width N_w is computed for different values of the cover thickness b with the constant load applied $0.263kN/mm$ by utilizing equation (3.3.20) on keeping other parameters constants. The calculated values are given in table 3.10 of APPENDIX. The graphs are plotted for different values of the load applied as shown in Figure 3.11. It demonstrates that with increase in cover thickness and assuming other parameters constant, nip width increases. The results obtained from the Hertz model is compared with the results obtained by nip mechanics model for rolling calender (NMMR). It is found that there is a huge difference between the results obtained from nip mechanics model for rolling calender and Hertz model because NMMR considered the cover thickness of soft roll while Hertz Model does not take it into account.

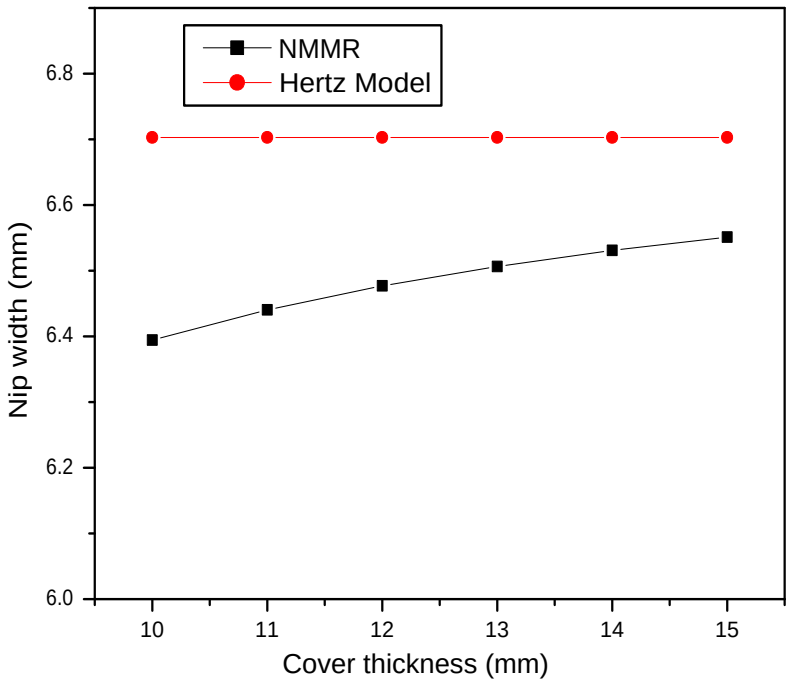

Figure 3.11: Impact of cover thickness on nip width for rolling calender

3.5.2.5 Impact of Cover Thickness on Average Pressure for Rolling Calender

Average pressure is computed by dividing nip load by nip width for different values of the cover thickness b with the constant load applied $0.263kN/mm$ by utilizing equation (3.3.20) on keeping other parameters constants. The calculated values are given in table 3.11 of APPENDIX. The graphs are plotted for different values of the load applied as shown in Figure 3.12. The results obtained from the Hertz model is compared with the results obtained by nip mechanics model for rolling calender (NMMR). It demonstrates that with increase in cover thickness and assuming other parameters constant, average pressure remains same in case of Hertz solution. Average pressure decreases with increase in cover thickness in case of nip mechanics model for rolling calender (NMMR). It is found that there is a huge difference between the results obtained from nip mechanics model for rolling calender and Hertz model because NMMR considered the cover thickness of soft roll while Hertz Model does not take it into account.

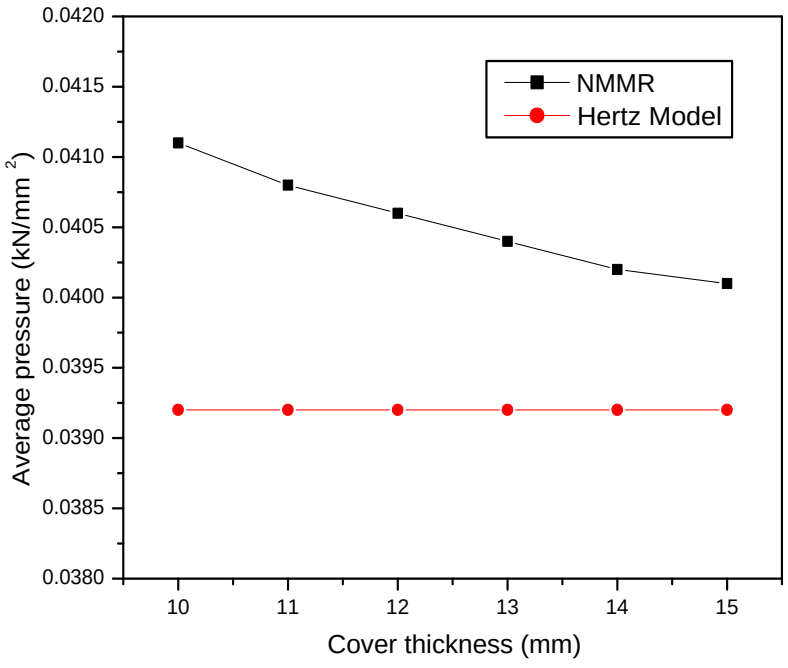

Figure 3.12: Impact of cover thickness on average pressure for rolling calender

3.6 Conclusion

The models created in this analysis are comprehensive models which are significant to textile manufacturing. These are generalized models which can overcome the difficulties poised by the models of Hertz and Meijers. Hertz had not considered the elastic cover thickness on the cylinder, so this model cannot be applied to textile calenders. The solution given by Meijers cannot be applied directly for the calendering process because of the results presented by him are in non dimensional form which making it difficult to extract the needed information. The NMMM and NMMR models developed in this present investigation are extension of Hertz and modification of Meijers which can be suitably used for textile calenders of any design. With the help of model developed, rolling and machine calender can be designed according to the nature of fabric required, as nip width acts as an imperative part in influencing eminence of fabric. The Hertz model and modified Meijers model (NMMM/NMMR) are used subsequently for simulation to analyze the Impact of design and process parameters on nip width and the obtained results of the present models are compared with the results obtained by Hertz model. From the analysis of the model it is found that the both the models give better results as compared to conventional models. These models help to obtain a fabric with better gloss and smoothness because cover thickness plays crucial role in calendering process which is not considered by the Hertz model.

Chapter 4

Heat Transfer Model when Fabric is Inside the Textile Calender Nip

Calendering enhances the surface properties of the fabric by making it more glossy and smooth with the help of mechanical and thermal energy. Simultaneous heat transfer has an important impact on the calendering process and on the functioning of calender stack. Heat is mainly transferred by conduction to fibers in contact with the heated rolls under two conditions (a) when fabric is inside the calender nip (b) when fabric is outside the nip, as shown in figure 4.1. Calender rolls are heated to a certain extent using different heat transfer processes such as percolation of hot water, hot oil, steam application or due to induction heating to the calender rolls. Heat can also be generated either due to friction especially if there one steel roll and one soft roll are in action or due to compression in the nip. Applying higher temperature, the smoothness and gloss of the fabric will be enhanced. When fabric is inside the calender nip, heated rolls may or may not have same temperature. Therefore, variations in temperature may occur across the face of calender due to temperature variations across the fabric. When fabric passes through the nip there is very short time for which heat is transferred. Thus the fabric is neither heated nor cooled to an equilibrium state. It is always in a transient state wherein the temperature distribution through its thickness is changing with time. So the nip width calculation is an important factor

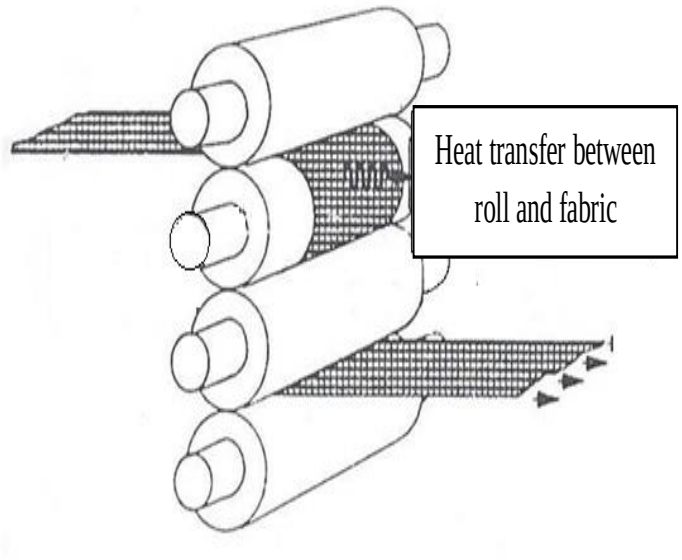

Figure 4.1: Heat transfer in calendering process

for calculation of heat transfer in the nip. In this chapter, mathematical model for conduction heat transfer have been developed when fabric is inside the textile calender nip having same and different roll temperature. The developed mathematical models have been solved for machine calender and rolling calender using analytical, analytical approximate and numerical methods under different initial and boundary conditions.

4.1 Heat Conduction Model

The one dimensional unsteady state heat conduction equation is given by

$$\frac{\partial T}{\partial t} = \alpha \frac{\partial^2 T}{\partial x^2} \tag{4.1.1}$$

Solution of equation (4.1.1) is used for finding temperature distribution when fabric is inside the calender nip under different initial and boundary conditions depending upon the type of calender.

When fabric is inside the textile calender nip, heated rolls may or may not have the same temperature and heat is mainly transferred by conduction to the fibers in contact with the heated rolls from both sides of the fabric which give rise to following cases.

Case1: Both the rolls of the nip are having same temperature

Initial and boundary conditions when fabric thickness of L units is in between the two rolls of same temperature T_r are

$$T(x,0) = T_0,\ T(0,t) = T_r = T(L,t) \tag{4.1.2}$$

Case2: Both the rolls of the nip are having different temperature

Initial and boundary conditions when fabric thickness of L units is in between the two rolls of different temperature T_1 and T_2 are

$$T(x,0) = T_0,\ T(0,t) = T_1, T(L,t) = T_2 \tag{4.1.3}$$

Case 1 and case 2 both are applicable in case of machine calender because in machine calendering process, calender rolls can be at same or different roll temperatures whereas only case 2 is applicable in case of rolling calender because calender rolls are at different temperatures in rolling calender.

4.2 Method used for Solving Heat Conduction Model

Analytical Approximate Methods

Various kind of physical problems can be solved using perturbation methods. Perturbation methods provide the most versatile tool available in analysis of engineering problems but these methods have their own drawbacks. All perturbation methods are based on some perturbation quantity to obtain approximate solutions. Various non-linear problems do not have small parameters therefore inappropriate choice of small parameter leads to wrong results [76–86].

In 1999, Ji huan He introduced a new method known as homotopy perturbation method (HPM). This method has eliminated the limitations of traditional perturbation methods. It is a combination of homotopy in topology and classical perturbation method which provides a convenient way to obtain analytical approximate solution for wide variety of differential equation problems arising in various field. In this method, a homotopy with a small embedding parameter $p \in [0,1]$ is constructed. The result

obtained using HPM are in series form which are convergent in nature and very close to exact results [87–98].

For outline the general procedure of the homotopy perturbation method, consider the differential equation

$$\mathbb{A}(u) - f(r) = 0 \quad r \in \Omega \tag{4.2.1}$$

$$\mathbb{B}(u, \frac{\partial u}{\partial x}) = 0 \quad r \in \Gamma \tag{4.2.2}$$

where $\mathbb{A}$ is a general differential operator (linear or nonlinear), $f(r)$ is a known analytic function, $\mathbb{B}$ is a boundary operator and Γ is the boundary of the domain Ω. The operator $\mathbb{A}$ can be generally divided into two operators, $\mathbb{L}$ and $\mathbb{N}$, where $\mathbb{L}$ is linear and $\mathbb{N}$ is a nonlinear operator. Equation (4.2.1) can be written as

$$\mathbb{L}(u) + \mathbb{N}(u) - f(r) = 0 \tag{4.2.3}$$

Now, construct a homotopy $v(r, p) : \Omega \times [0, 1] \to R$ which satisfies the relation

$$H(v, p) = (1 - p)[\mathbb{L}(v) - \mathbb{L}(u_0)] + p[\mathbb{A}(v) - f(r)] = 0, \quad r \in \Omega \tag{4.2.4}$$

Here $p \in [0, 1]$ is called the homotopy parameter and u_0 is an initial approximation for the solution of equation (4.2.1), which satisfies the boundary conditions. Clearly, from equation (4.2.4),

$$H(v, 0) = \mathbb{L}(v) - \mathbb{L}(u_0) \tag{4.2.5}$$

$$H(v, 1) = \mathbb{A}(v) - f(r) \tag{4.2.6}$$

Assuming that the solution of equation (4.2.4) can be expressed as a series in p,

$$v = v_0 + pv_1 + p_2v_2 + p_3v_3 + \tag{4.2.7}$$

On setting $p = 1$, the approximate solution of Equation (4.2.7) is

$$u = \lim_{p \to 1} v = v_0 + pv_1 + p_2v_2 + p_3v_3 + \tag{4.2.8}$$

Finite Difference Methods

Various numerical solution techniques are available for solving different kind of partial differential equations (PDE). However due to ease of application, finite difference methods (FDM) are still a valuable means of solving PDE. FDM has been used for

solving wide range of PDE problems which can be linear, nonlinear, time dependent or time independent by approximating derivatives with finite differences, as shown in figure 4.2. Discrete indicates that the numerical solution is known only at a finite

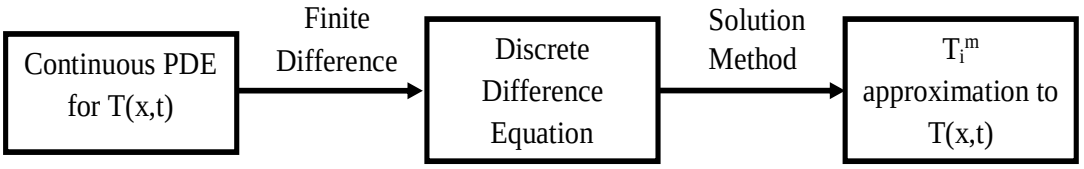

Figure 4.2: Schematic representation of numerical solution using finite difference

number of points in the physical domain. However, increment in the number of discrete points increases not only the resolution but also the accuracy of the numerical solution [99–110].

The process of discretization leads to a set of algebraic equations, these algebraic equations are evaluated so as to obtain values for the unknown quantities of the discretization. For one dimensional heat equation, the coordinate axes are divided into steps of uniform lengths Δx and Δt along x and t axis respectively. The mesh is obtained by drawing horizontal and vertical lines along the step points. The intersection points of this mesh are called nodes, where discrete solutions are obtained [111–122]. Use of different combinations of mesh points in the difference formulas results in different methods. However, the rate at which the numerical solution converges to the true solution varies with the scheme. In this chapter, three finite difference methods i.e. forward time central space (FTCS) method, backward time central space (BTCS) method and Crank Nicolson (CN) method are used for finding numerical solution of heat transfer models under different initial and boundary conditions.

4.3 Solution of Heat Transfer Model

In this section, heat transfer model for same and different roll temperature has been solved using homotopy perturbation method, forward time central space (FTCS)

method, backward time central space (BTCS) method and Crank Nicolson (CN) method.

4.3.1 Solution of Heat Transfer Model using Homotopy Perturbation Method

For case 1

Let

$$\psi = T - T_r \tag{4.3.1}$$

Therefore equation (4.1.1) can be rewritten as

$$\frac{\partial \psi}{\partial t} = \alpha \frac{\partial^2 \psi}{\partial x^2} \tag{4.3.2}$$

The homotopy for heat conduction equation given by equation (4.3.2) is

$$\left(\frac{\partial \nu}{\partial t} - \frac{\partial \psi_0}{\partial t}\right) + p\left(\frac{\partial \psi_0}{\partial t} - \alpha \frac{\partial^2 \nu}{\partial x^2}\right) = 0 \tag{4.3.3}$$

Then I.C. and B.C. changes to

$$\psi(x,0) = \psi_0,\ \psi(0,t) = 0 = \psi(L,t) \tag{4.3.4}$$

Let the initial approximation be $\psi_0 = C_n \sin \frac{\pi x}{L} \cos \pi^2 t$.
Suppose the solution of equation (4.3.2) is given by

$$\nu = \nu_0 + p\nu_1 + p^2\nu_2 + p^3\nu_3 + p^4\nu_4 + ... \tag{4.3.5}$$

Using equation (4.3.5) in equation (4.3.3) and comparing the coefficients of same powers of p,

$$
\begin{aligned}
p^0 &: \frac{\partial \nu_0}{\partial t} = \frac{\partial \psi_0}{\partial t} \\
p^1 &: \frac{\partial \nu_1}{\partial t} = \alpha \frac{\partial^2 \nu_0}{\partial x^2}, \nu_1(0,t) = 0 = \nu_1(L,t) \\
p^2 &: \frac{\partial \nu_2}{\partial t} = \alpha \frac{\partial^2 \nu_1}{\partial x^2}, \nu_2(0,t) = 0 = \nu_2(L,t) \\
p^3 &: \frac{\partial \nu_3}{\partial t} = \alpha \frac{\partial^2 \nu_2}{\partial x^2}, \nu_3(0,t) = 0 = \nu_3(L,t)
\end{aligned}
$$

-
-
-

$$
p^n : \frac{\partial \nu_n}{\partial t} = \alpha \frac{\partial^2 \nu_{n-1}}{\partial x^2}, \nu_n(0,t) = 0 = \nu_n(L,t) \tag{4.3.6}
$$

Solving the above system of equation (4.3.6),

$$
\begin{aligned}
\nu_0 &= C_n \sin\left[\frac{\pi x}{L}\right] \cos\left[\pi^2 t\right] \\
\nu_1 &= -C_n \frac{\alpha \sin\left[\frac{\pi x}{L}\right] \sin\left[\pi^2 t\right]}{L^2} + \sin\left[\frac{\pi x}{L}\right] \\
\nu_2 &= -C_n \frac{\alpha \left(L^2 \pi^2 t + \alpha \cos\left[\pi^2 t\right]\right) \sin\left[\frac{\pi x}{L}\right]}{L^4} + \frac{L^4 \sin\left[\frac{\pi x}{L}\right] + \alpha^2 \sin\left[\frac{\pi x}{L}\right]}{L^4} \\
\nu_3 &= -C_n \frac{\alpha \left(\pi^2 t \left(-2L^4 + L^2 \pi^2 \alpha t - 2\alpha^2\right) + 2\alpha^2 \sin\left[\pi^2 t\right]\right) \sin\left[\frac{\pi x}{L}\right]}{2L^6} + \sin\left[\frac{\pi x}{L}\right]
\end{aligned}
$$

-
-
-

and so on... (4.3.7)

Taking $p = 1$ in equation (4.3.5),

$$
\psi = \lim_{p \to 1} \nu = \nu_0 + \nu_1 + \nu_2 + \nu_3 + \nu_4 + \nu_5 + \nu_6 + \nu_7 + ... \tag{4.3.8}
$$

Using equation (4.3.7) in equation (4.3.8),

$$
\psi(x,t) = \sum_{m=1}^{\infty} C_m \left[sin \frac{m\pi}{L} x \right] e^{-m^2 \pi^2 \alpha t / L^2} \tag{4.3.9}
$$

Using I.C. $\psi(x,0) = \psi_0$ in equation (4.3.9)

$$\psi_0 = \sum_{m=1}^{\infty} C_m \left[sin \frac{m\pi}{L} x \right] \tag{4.3.10}$$

Equation (4.3.10) represents Fourier sine series where the constant C_m is the Fourier coefficient.

Thus equation (4.3.9) becomes

$$\psi\,(x,t) = \sum_{m=1}^{\infty} B_m e^{-m^2\pi^2\alpha t/L^2} \left[sin \frac{m\pi}{L} x \right] \tag{4.3.11}$$

where

$$B_m = \frac{2}{L} \int_0^L \psi_0 sin \frac{m\pi}{L} x^{'} dx^{'} \tag{4.3.12}$$

when m is even, $B_m = 0$;

when m is odd, $B_m = \frac{4\psi_0}{m\pi}$.

Therefore equation (4.3.11) becomes

$$\psi(x,t) = \frac{4\psi_0}{\pi} \sum_{m=1,3,5}^{\infty} \frac{1}{m} sin \frac{m\pi}{L} x e^{-m^2\pi^2\alpha t/L^2} \tag{4.3.13}$$

$$\frac{\psi}{\psi_0} = \frac{4}{\pi} \sum_{m=1,3,5}^{\infty} \frac{1}{m} sin \frac{m\pi}{L} x e^{-m^2\pi^2\alpha t/L^2} \tag{4.3.14}$$

Using equation (4.3.1), equation (4.3.14) becomes

$$\frac{T - T_r}{T_0 - T_r} = \frac{4}{\pi} \sum_{m=1,3,5}^{\infty} \frac{1}{m} sin \frac{m\pi}{L} x e^{-m^2\pi^2\alpha t/L^2} \tag{4.3.15}$$

Equation (4.3.15) can be simplified as

$$T(x,t) = T_r + (T_0 - T_r) \frac{4}{\pi} \sum_{m=1,3,5}^{\infty} \frac{1}{m} sin \frac{m\pi}{L} x e^{-m^2\pi^2\alpha t/L^2} \tag{4.3.16}$$

For case 2

Suppose

$$T = q + w \tag{4.3.17}$$

where q satisfies the equation

$$\frac{\partial^2 q}{\partial x^2} = 0 \tag{4.3.18}$$

along with $q = T_1$ at $x = 0$, $q = T_2$ at $x = L$

w satisfies the equation

$$\frac{\partial w}{\partial t} = \alpha \frac{\partial^2 w}{\partial x^2} \tag{4.3.19}$$

along with $w = 0$ at $x = 0$ and $x = L$, $w = T_0 - q$ at $t = 0$.

From equation (4.3.18),

$$q = T_1 + (T_2 - T_1)\frac{x}{L} \tag{4.3.20}$$

Using (4.3.9), equation (4.3.19) changes to

$$w = \sum_{m=1}^{\infty} C_m \left[sin \frac{m\pi}{L} x \right] e^{-m^2\pi^2\alpha t/L^2} \tag{4.3.21}$$

Now applying the I.C. $w = T_0 - q$ in equation (4.3.21),

$$T_0 - q = \sum_{m=1}^{\infty} C_m \left[sin \frac{m\pi}{L} x \right] \tag{4.3.22}$$

$$T_0 - (T_1 + (T_2 - T_1)\frac{x}{L}) = \sum_{m=1}^{\infty} C_m \left[sin \frac{m\pi}{L} x \right] \tag{4.3.23}$$

Equation (4.3.23) represents Fourier sine series where the constant C_m is the Fourier coefficient.

Equation (4.3.21) can be rewritten as

$$w = \sum_{m=1}^{\infty} B_m \left[sin \frac{m\pi}{L} x \right] e^{-m^2\pi^2\alpha t/L^2} \tag{4.3.24}$$

where

$$B_m = \frac{2}{d} \int_0^L [T_0 - (T_1 + (T_2 - T_1)\frac{x^{'}}{L})] \sin \frac{m\pi}{L} x^{'} dx^{'} \tag{4.3.25}$$

$$B_m = \frac{2}{m\pi}(T_2 \cos m\pi - T_1) + \frac{2}{L} \int_0^L T_0 \sin \frac{m\pi}{L} x^{'} dx^{'} \tag{4.3.26}$$

Substituting equation (4.3.20) and equation (4.3.24) in equation (4.3.17),

$$T = T_1 + (T_2 - T_1)\frac{x}{L} + \sum_{m=1}^{\infty} B_m \left[sin \frac{m\pi}{L} x \right] e^{-m^2\pi^2\alpha t/L^2} \tag{4.3.27}$$

Substituting the value of B_m from equation (4.3.26) in (4.3.27),

$$\begin{aligned} T = T_1 + (T_2 - T_1)\frac{x}{L} + \sum_{m=1}^{\infty} \sin \frac{m\pi}{L} x e^{-m^2\pi^2\alpha t/L^2} [\frac{2}{m\pi}(T_2 \cos m\pi \\ - T_1) + \frac{2}{L} \int_0^d T_0 \sin \frac{m\pi}{L} x^{'} dx^{'}] \end{aligned} \tag{4.3.28}$$

$$T = T_1 + (T_2 - T_1)\frac{x}{L} + \sum_{m=1}^{\infty} \sin\frac{m\pi}{L} x e^{-m^2\pi^2\alpha t/L^2} [\frac{2}{m\pi}(T_2(-1)^n - T_1) + \frac{2}{L}\int_0^L T_0 \sin\frac{m\pi}{L} x' dx'] \tag{4.3.29}$$

On solving equation (4.3.29),

$$T(x,t) = T_1 + (T_2 - T_1)\frac{x}{L} + [e^{-\pi^2\alpha t/L^2} \sin\frac{\pi}{L} x\{\frac{2}{\pi}(-T_2 - T_1) + \frac{4T_0}{\pi}\} + e^{-4\pi^2\alpha t/L^2} \sin\frac{2\pi}{L} x\{\frac{1}{\pi}(T_2 - T_1)\}] \tag{4.3.30}$$

4.3.2 Solution of Heat Transfer Model using Forward Time Central Space Method (FTCS)

Explicit FTCS method is Ist order method in time and is conditionally stable. In FTCS method, the difference formula for time derivative is

$$\frac{\partial T}{\partial t} = \frac{T_{i,j+1} - T_{i,j}}{\Delta t} + O(\Delta t) \tag{4.3.31}$$

And the difference formula for spatial derivative is

$$\frac{\partial^2 T}{\partial x^2} = \frac{T_{i+1,j} - 2T_{i,j} + T_{i-1,j}}{(\Delta x)^2} + O(\Delta x) \tag{4.3.32}$$

Using equation (4.3.31) and (4.3.32), equation (4.1.1) becomes

$$\frac{T_{i,j+1} - T_{i,j}}{\Delta t} = \alpha\left(\frac{T_{i+1,j} - 2T_{i,j} + T_{i-1,j}}{\Delta x^2}\right) \tag{4.3.33}$$

On rearranging,

$$T_{i,j+1} = T_{i,j} + \alpha\frac{\Delta t}{(\Delta x)^2}(T_{i+1,j} - 2T_{i,j} + T_{i-1,j}) \tag{4.3.34}$$

Therefore,

$$T_{i,j+1} = T_{i,j} + d(T_{i+1,j} - 2T_{i,j} + T_{i-1,j}) \tag{4.3.35}$$

Here d is the dimensionless diffusion number, given by

$$d = \alpha\frac{\Delta t}{(\Delta x)^2} \tag{4.3.36}$$

The order of accuracy of the explicit FTCS method is $O(\Delta t, \Delta x^2)$. This method is conditionally stable for $d \leq 0.5$. Equation (4.3.35) is solved using MATLAB for Case 1 and Case 2.

4.3.3 Solution of Heat Transfer Model using Backward Time Central Space Method (BTCS)

BTCS method is Ist order in time, IInd order in space and is unconditionally stable. Implicit BTCS method results in simultaneous linear equations for the temperature at all nodes for a particular time, instead of the temperature being found one node at a time.

In BTCS method, the difference formula for time derivative is

$$\frac{\partial T}{\partial t} = \frac{T_{i,j+1} - T_{i,j}}{\Delta t} + O(\Delta t) \tag{4.3.37}$$

And the difference formula for spatial derivative is

$$\frac{\partial^2 T}{\partial x^2} = \frac{T_{i-1,j+1} - 2T_{i,j+1} + T_{i+1,j+1}}{(\Delta x)^2} + O(\Delta x) \tag{4.3.38}$$

Using equations (4.3.37) and (4.3.38), equation (4.1.1) can be rewritten as

$$\frac{T_{i,j+1} - T_{i,j}}{\Delta t} = \alpha\left(\frac{T_{i-1,j+1} - 2T_{i,j+1} + T_{i+1,j+1}}{\Delta x^2}\right) \tag{4.3.39}$$

On rearranging,

$$T_{i,j+1} = T_{i,j} + \alpha\frac{\Delta t}{(\Delta x)^2}(T_{i-1,j+1} - 2T_{i,j+1} + T_{i+1,j+1}) \tag{4.3.40}$$

Using equation (4.3.36),

$$-dT_{i-1,j+1} + (1+2d)T_{i,j+1} - d(T_{i+1,j+1}) = T_{i,j} \tag{4.3.41}$$

The time step Δt should be taken small to obtain the acceptable accuracy. Equation (4.3.41) is solved using MATLAB for Case 1 and case 2.

4.3.4 Solution of Heat Transfer Model using Crank Nicolson (CN) method

CN method is IInd order in time and is unconditionally stable. CN method is having a IInd order accuracy in time for one dimensional heat conduction equation. The

accuracy of this method is same in both space and time. This method has significant advantages when time accurate solutions are important. Also, this method is unconditional stable and has higher order of accuracy.

In CN method, the difference formula for time derivative is

$$\frac{\partial T}{\partial t} = \frac{T_{i,j+1} - T_{i,j}}{\Delta t} + O(\Delta t) \tag{4.3.42}$$

And the central difference formula at time $t_{j+1/2}$ for spatial derivative is

$$\begin{aligned} \frac{\partial^2 T}{\partial x^2} = \frac{1}{2}\Bigg(& \frac{T_{i-1,j+1} - 2T_{i,j+1} + T_{i+1,j+1}}{\Delta x^2} \\ & + \frac{T_{i-1,j} - 2T_{i,j} + T_{i+1,j}}{\Delta x^2}\Bigg) + O(\Delta x) \end{aligned} \tag{4.3.43}$$

Using equations (4.3.42) and (4.3.43), equation (4.1.1) can be rewritten as

$$\begin{aligned} \frac{T_{i,j+1} - T_{i,j}}{\Delta t} = \frac{1}{2}\alpha\Bigg(& \frac{T_{i-1,j+1} - 2T_{i,j+1} + T_{i+1,j+1}}{\Delta x^2} \\ & + \frac{T_{i-1,j} - 2T_{i,j} + T_{i+1,j}}{\Delta x^2}\Bigg) \end{aligned} \tag{4.3.44}$$

On rearranging,

$$\begin{aligned} T_{i,j+1} - T_{i,j} = \frac{1}{2}\alpha\frac{\Delta t}{(\Delta x)^2}(& T_{i-1,j+1} - 2T_{i,j+1} \\ & + T_{i+1,j+1} + T_{i+1,j} - 2T_{i,j} + T_{i+1,j}) \end{aligned} \tag{4.3.45}$$

Using equation (4.3.36),

$$-dT_{i-1,j+1} + 2(1+d)T_{i,j+1} - d(T_{i+1,j+1}) = dT_{i-1,j} + 2(1-d)T_{i,j} + dT_{i+1,j} \tag{4.3.46}$$

Equation (4.3.46) is solved using MATLAB for Case 1 and case 2.

4.4 Simulation of Models

Simulation of heat transfer model is done for machine and rolling single nip calender using equations (4.3.16), (4.3.30), (4.3.35), (4.3.41) and (4.3.46). Roll temperature (RT) is taken in the range from 100°C to 210°C for machine calender and from 70°C to 210°C for rolling calender. The initial fabric temperature are taken as 50°C and 70°C. The range of design and process parameters and adopted values for single nip machine calender and rolling calender for simulation purpose are given in table 3.1 of APPENDIX.

4.5 Results and Discussion

4.5.1 Impact of Various Design and Process Parameters on Machine Calender having Same Roll Temperature

The impact of roll temperature on fabric temperature in thickness direction at various depths, impact of dwell time, thermal diffusivity, roll temperature on average fabric temperature has been investigated when fabric is inside the calender nip for machine calender having same roll temperature.

4.5.1.1 Impact of Roll Temperature on Fabric Temperature in Thickness Direction at Various Depths for Machine Calender having Same Roll Temperature

The impact of roll temperature on fabric temperature in thickness direction at various depths with initial temperature 50°C and 70°C has been investigated when fabric is inside the machine calender nip having same roll temperature. The calculated values are given in tables 4.1 to 4.8 of APPENDIX. The results obtained are shown in figures 4.3 and 4.4.

It clearly shows that when fabric is inside the machine calender nip having same roll temperature, the middle part of fabric remains at initial temperature and temperature of the fabric decreases from outer part to mid part of the fabric from both sides in thickness direction. The results obtained using homotopy perturbation method are similar with the exact results while there is a negligible error in the results obtained using finite difference methods.

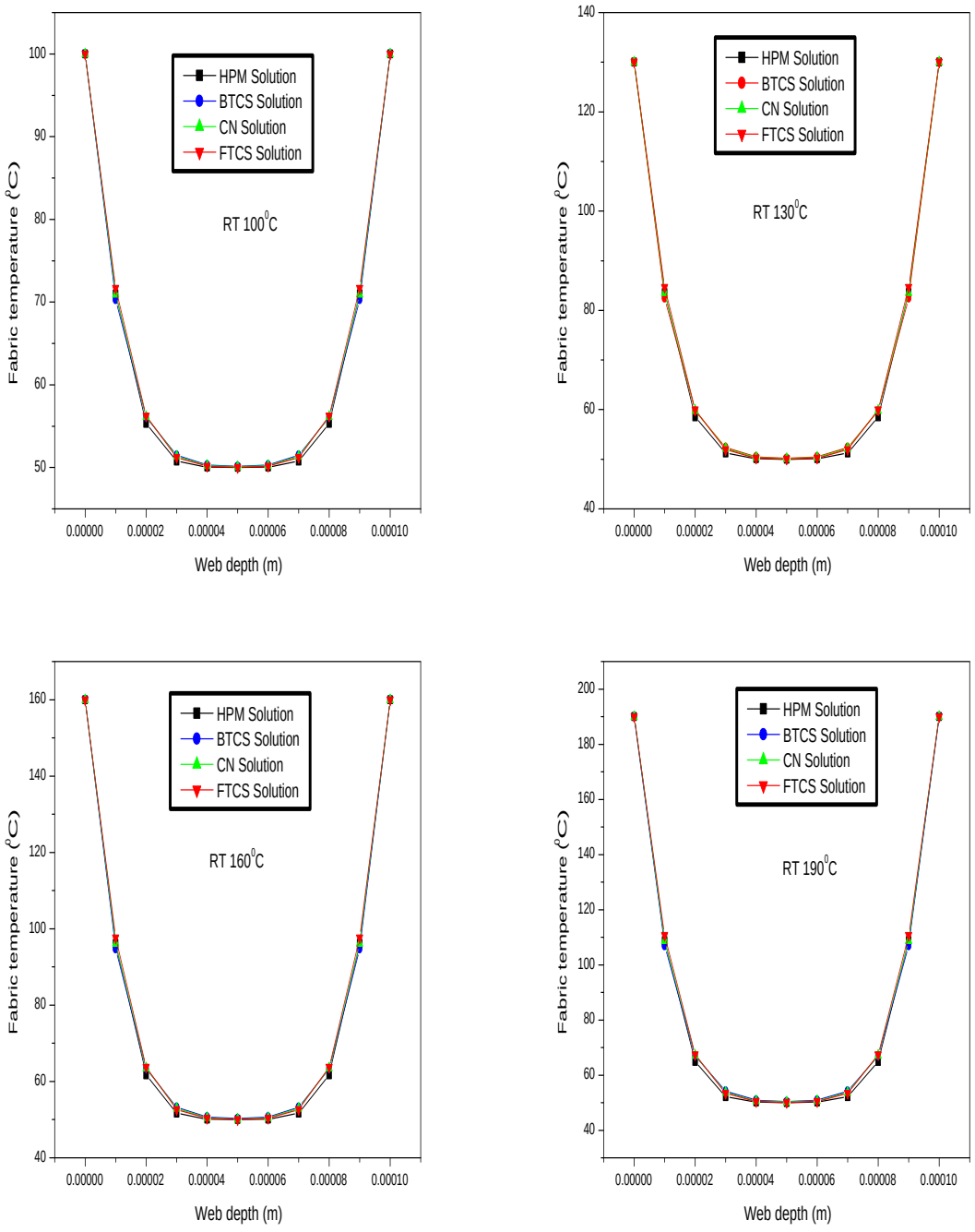

Figure 4.3: Impact of same roll temperature on fabric temperature in thickness direction at various depths with initial temperature 50°C for machine calender

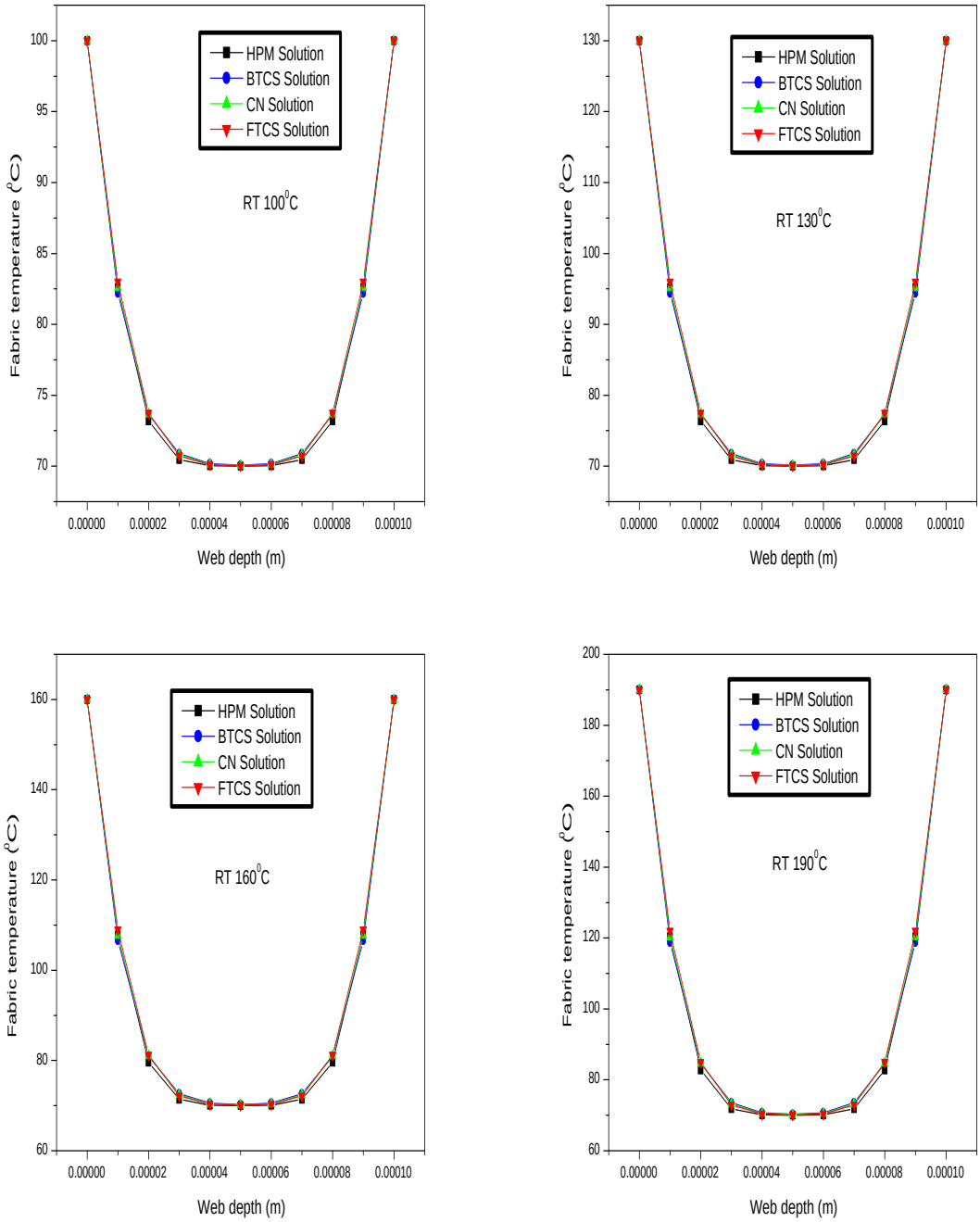

Figure 4.4: Impact of same roll temperature on fabric temperature in thickness direction at various depths with initial temperature 70°C for machine calender

4.5.1.2 Impact of Roll Temperature on Average Fabric Temperature for Machine Calender having Same Roll Temperature

The impact of roll temperature on average fabric temperature with initial temperature 50°C and 70°C has been investigated when fabric is inside the machine calender nip having same roll temperature. The calculated values are given in tables 4.1 to 4.8 of APPENDIX. The results obtained are shown in figures 4.5 and 4.6.
It clearly indicates that, with increase in roll temperature, average fabric temperature increases linearly. The results obtained using homotopy perturbation method are similar with the exact results while there is a negligible error in the results obtained using finite difference methods.

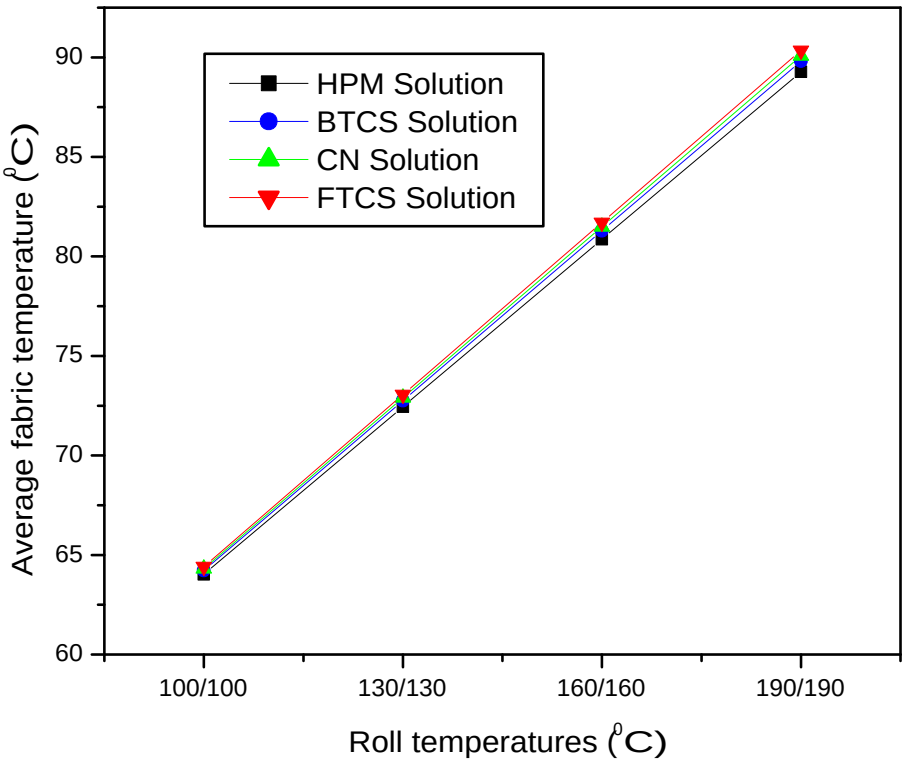

Figure 4.5: Impact of same roll temperature on average fabric temperature with initial temperature 50°C for machine calender

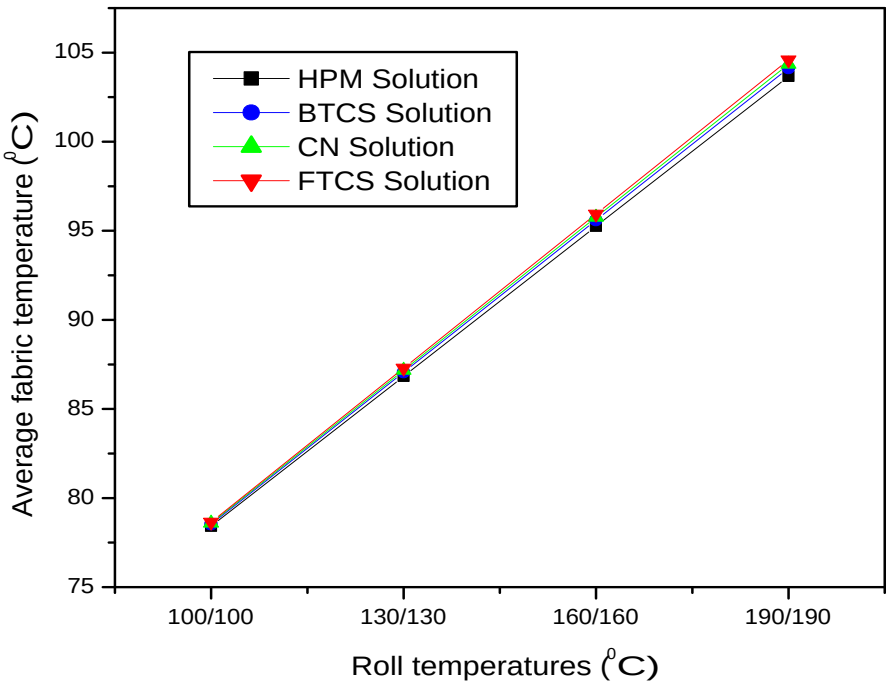

Figure 4.6: Impact of same roll temperature on average fabric temperature with initial temperature 70°C for machine calender

4.5.1.3 Impact of Dwell Time on Average Fabric Temperature for Machine Calender having Same Roll Temperature

The impact of dwell time on average fabric temperature with initial temperature 50°C and 70°C has been investigated when fabric is inside the machine calender nip having same roll temperature. The calculated values are given in tables 4.9 to 4.16 of APPENDIX. The results obtained are shown in figures 4.7 and 4.8.

It clearly indicates that, with increase in dwell time average fabric temperature increases as more heat is conducted at different layers of the fabric with increase in dwell time. The results obtained using homotopy perturbation method are similar with the exact results while there is a significant error in the results obtained using finite difference methods.

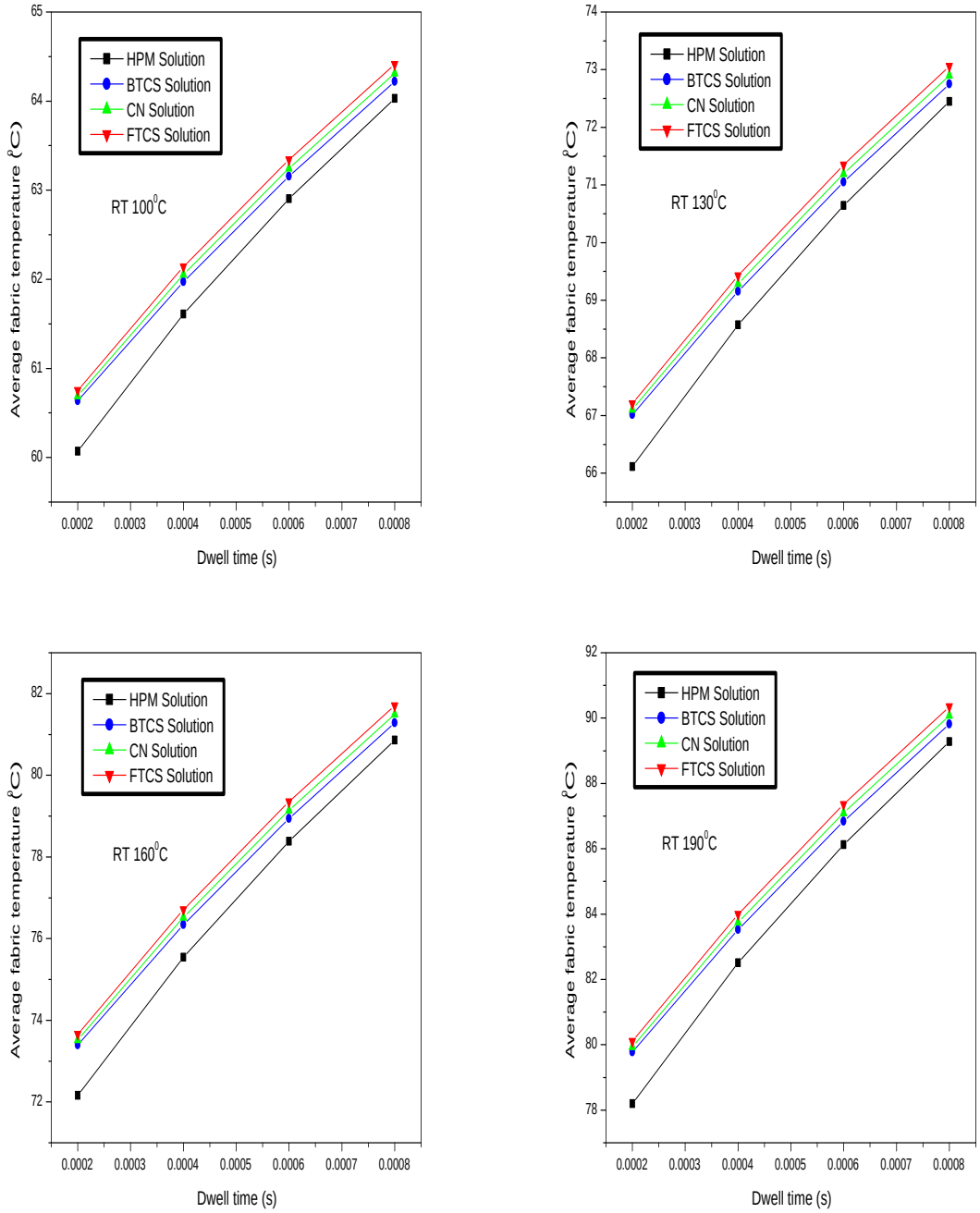

Figure 4.7: Impact of dwell time on average fabric temperature with initial temperature 50°C for machine calender having same roll temperature

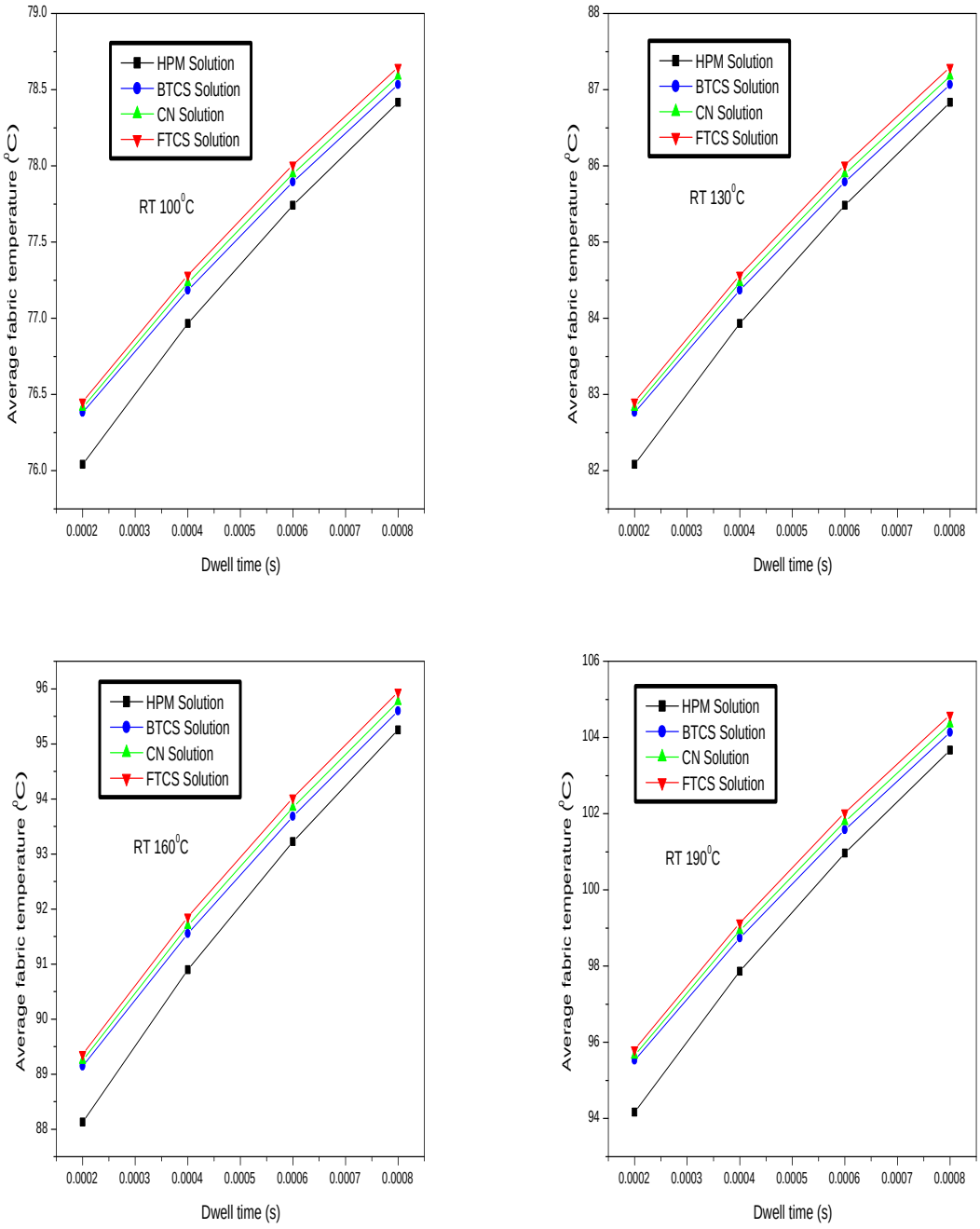

Figure 4.8: Impact of dwell time on average fabric temperature with initial temperature 70°C for machine calender having same roll temperature

4.5.1.4 Impact of Thermal Diffusivity on Average Fabric Temperature for Machine Calender having Same Roll Temperature

The impact of thermal diffusivity on average fabric temperature with initial temperature 50°C and 70°C has been investigated when fabric is inside the machine calender nip having same roll temperature. The calculated values are given in tables 4.17 to 4.24 of APPENDIX. The results obtained are shown in figures 4.9 and 4.10.
It clearly indicates that, with increase in thermal diffusivity average fabric temperature increases. The results obtained using homotopy perturbation method are similar with the exact results while there is significant error in the results obtained using finite difference methods.

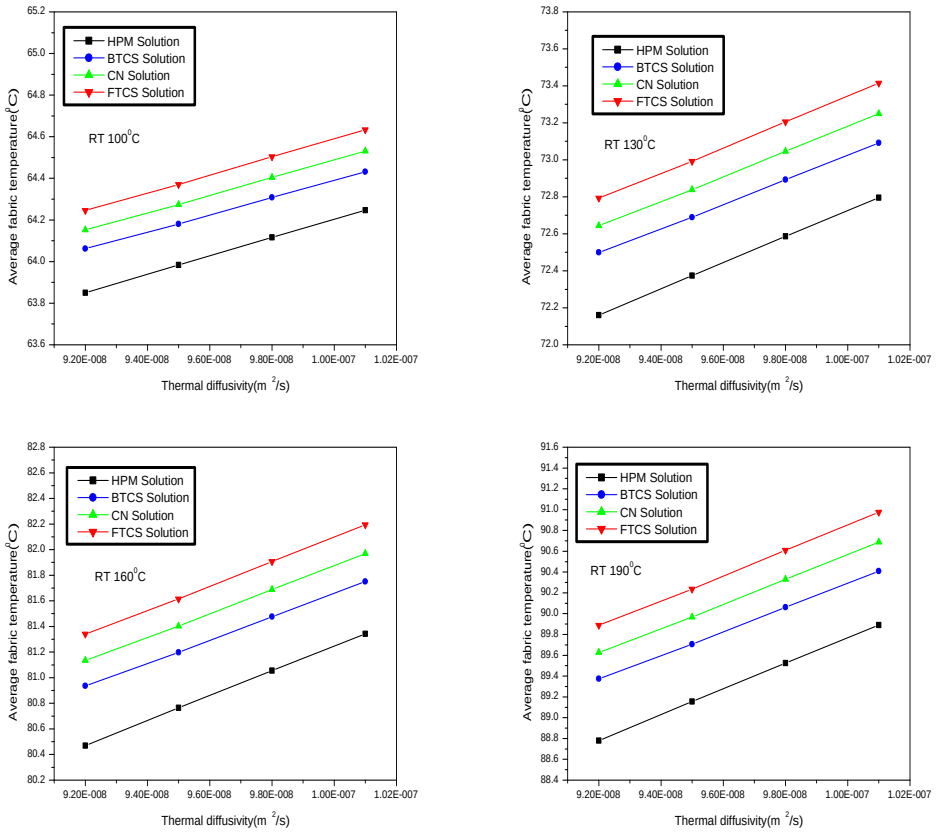

Figure 4.9: Impact of thermal diffusivity on average fabric temperature with initial temperature 50°C for machine calender having same roll temperature

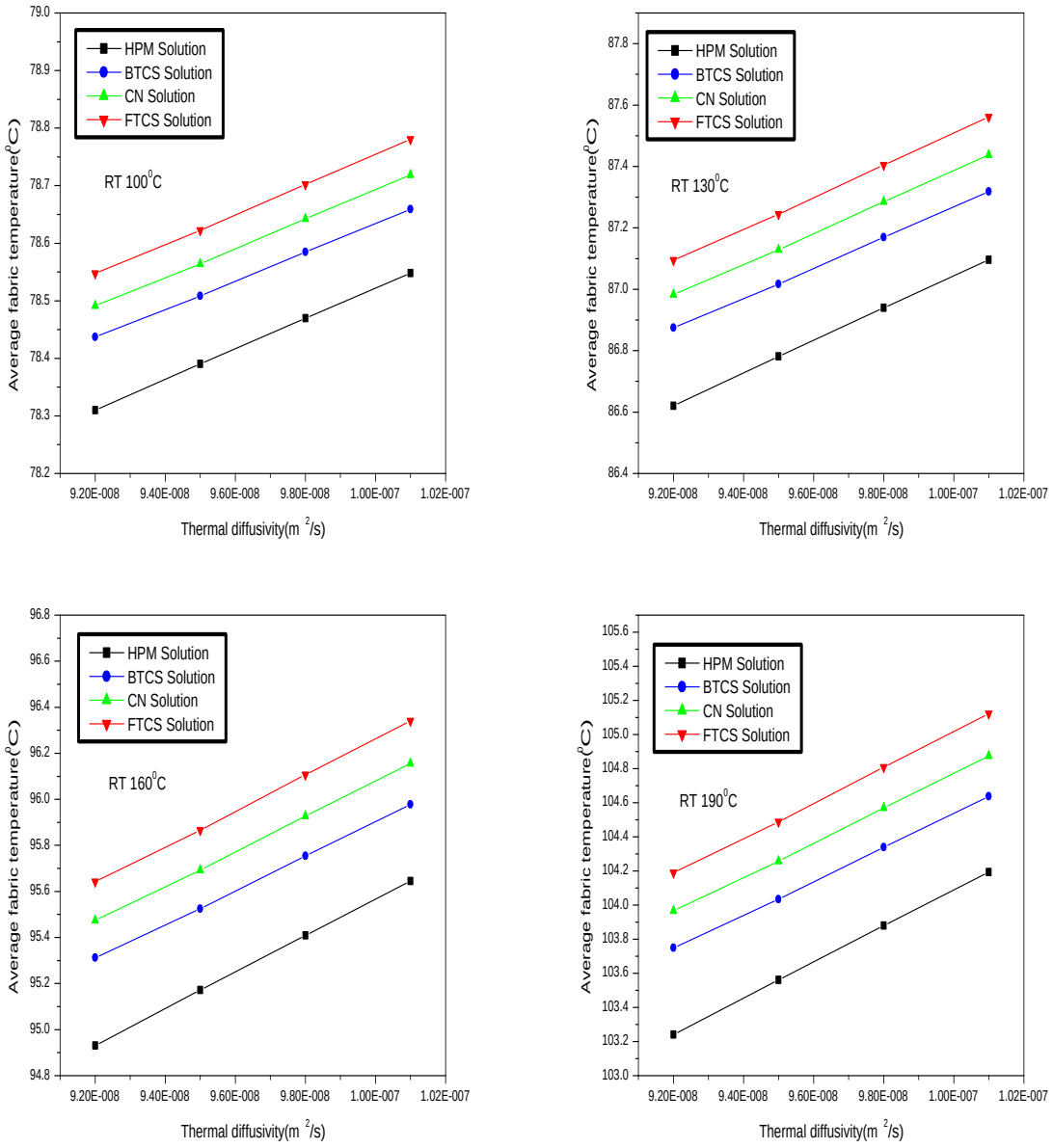

Figure 4.10: Impact of thermal diffusivity on average fabric temperature with initial temperature 70°C for machine calender having same roll temperature

4.5.2 Impact of Various Design and Process Parameters on Machine Calender having Different Roll Temperature

The Impact of roll temperature on fabric temperature in thickness direction at various depths, impact of dwell time, thermal diffusivity, roll temperature on average fabric temperature has been investigated when fabric is inside the calender nip for machine calender having different roll temperature.

4.5.2.1 Impact of Roll Temperature on Fabric Temperature for Machine Calender having Different Roll Temperature

The impact of roll temperature on fabric temperature in thickness direction at various depths with initial temperature 50°C and 70°C has been investigated when fabric is inside the machine calender nip having different roll temperature. The calculated values are given in tables 4.25 to 4.32 of APPENDIX. The results obtained are shown in figures 4.11 and 4.12.

It clearly shows that temperature of the fabric decreases from outer part to mid part of the fabric from both sides in thickness direction. When rolls are at different temperature, the side of the fabric which is in contact with the roll having higher temperature is more heated as compared to other roll at low temperature. The results obtained using homotopy perturbation method are similar with the exact results while there is a significant error in the results obtained using finite difference methods.

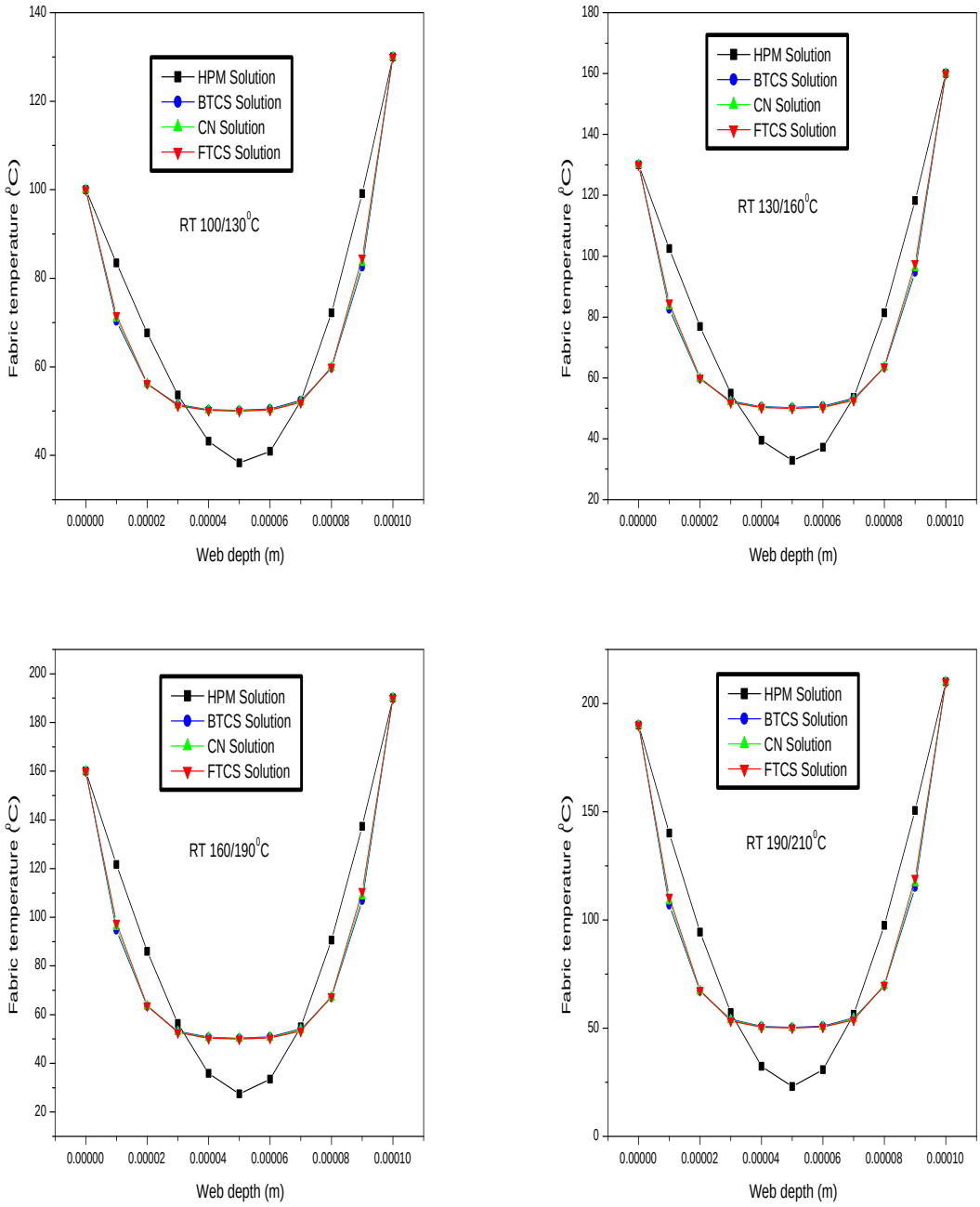

Figure 4.11: Impact of different roll temperature on fabric temperature in thickness direction at various depths with initial temperature 50°C for machine calender

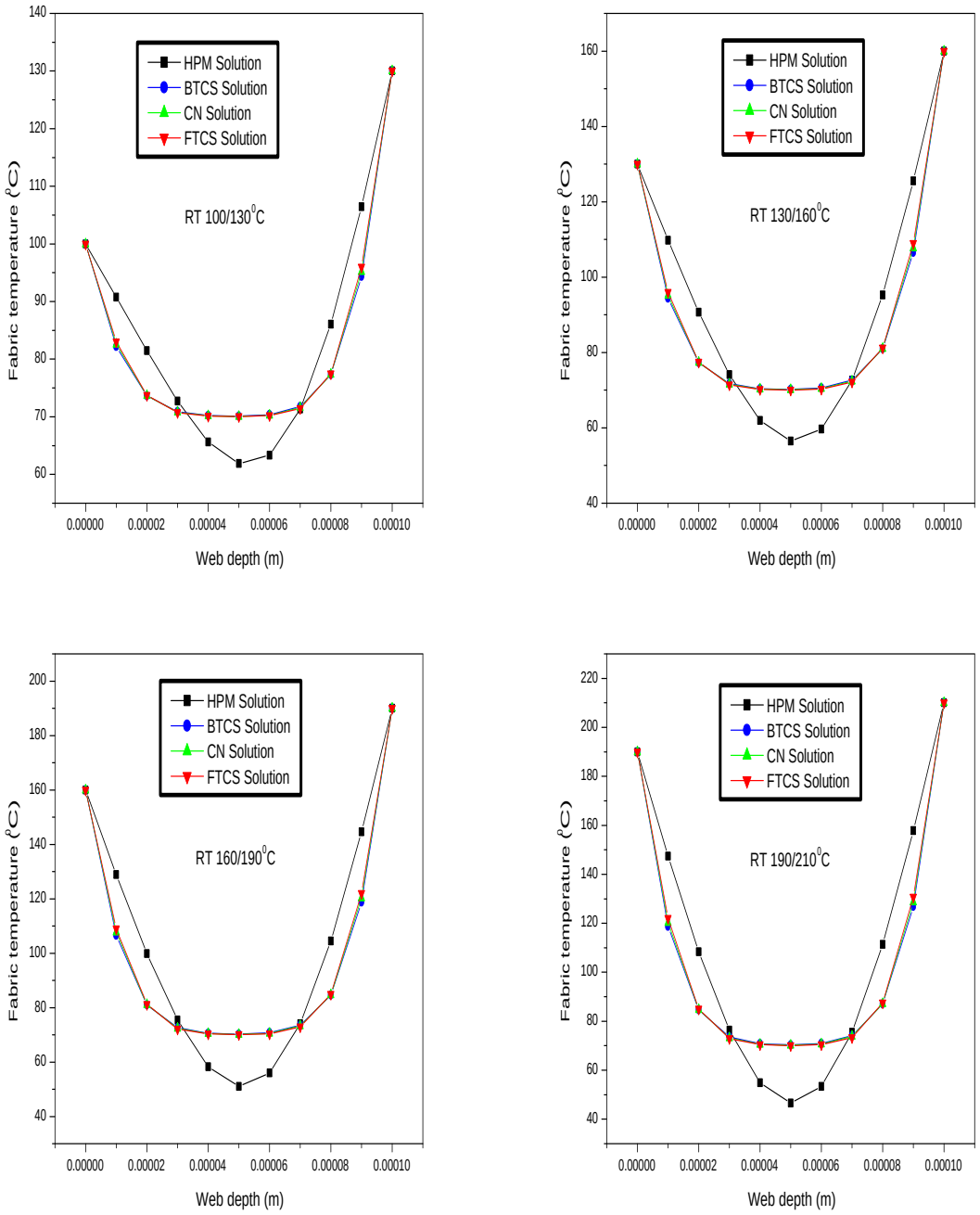

Figure 4.12: Impact of different roll temperature on fabric temperature in thickness direction at various depths with initial temperature 70°C for machine calender

4.5.2.2 Impact of Roll Temperature on Average Fabric Temperature for Machine Calender having Different Roll Temperature

The impact of roll temperature on average fabric temperature with initial temperature 50°C and 70°C has been investigated when fabric is inside the machine calender nip having different roll temperature. The calculated values are given in tables 4.25 to 4.32 of APPENDIX. The results obtained are shown in figures 4.13 and 4.14.
It clearly indicates that, with increase in roll temperature, average fabric temperature increases. The results obtained using homotopy perturbation method are similar with the exact results while there is a significant error in the results obtained using finite difference methods.

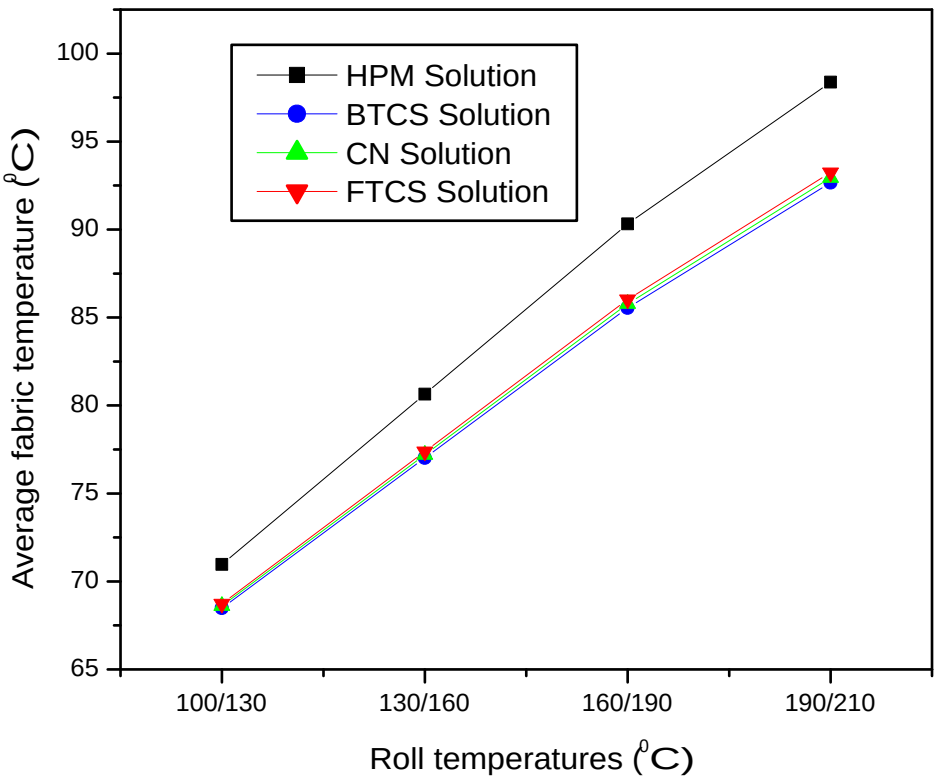

Figure 4.13: Impact of different roll temperature on average fabric temperature with initial temperature 50°C for machine calender

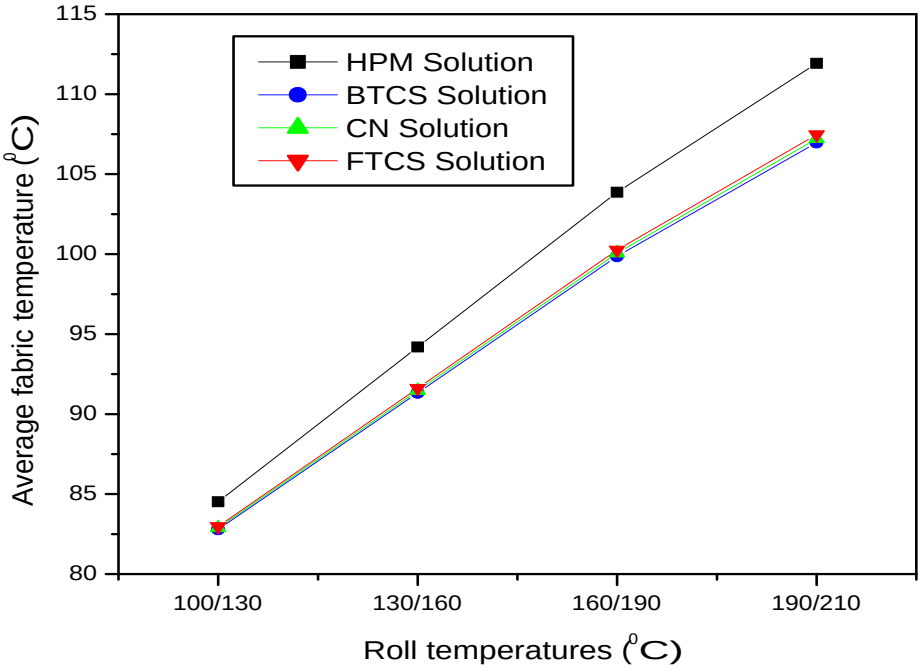

Figure 4.14: Impact of different roll temperature on average fabric temperature with initial temperature 70°C for machine calender

4.5.2.3 Impact of Dwell Time on Average Fabric Temperature for Machine Calender having Different Roll Temperature

The impact of dwell time on average fabric temperature with initial temperature 50°C and 70°C has been investigated when fabric is inside the machine calender nip having different roll temperature. The calculated values are given in tables 4.33 to 4.40 of APPENDIX. The results obtained are shown in figures 4.15 and 4.16.

It clearly indicates that, with increase in dwell time average fabric temperature increases as more heat is conducted at different layers of the fabric with increase in dwell time. The results obtained using homotopy perturbation method are similar with the exact results while there is a significant error in the results obtained using finite difference methods.

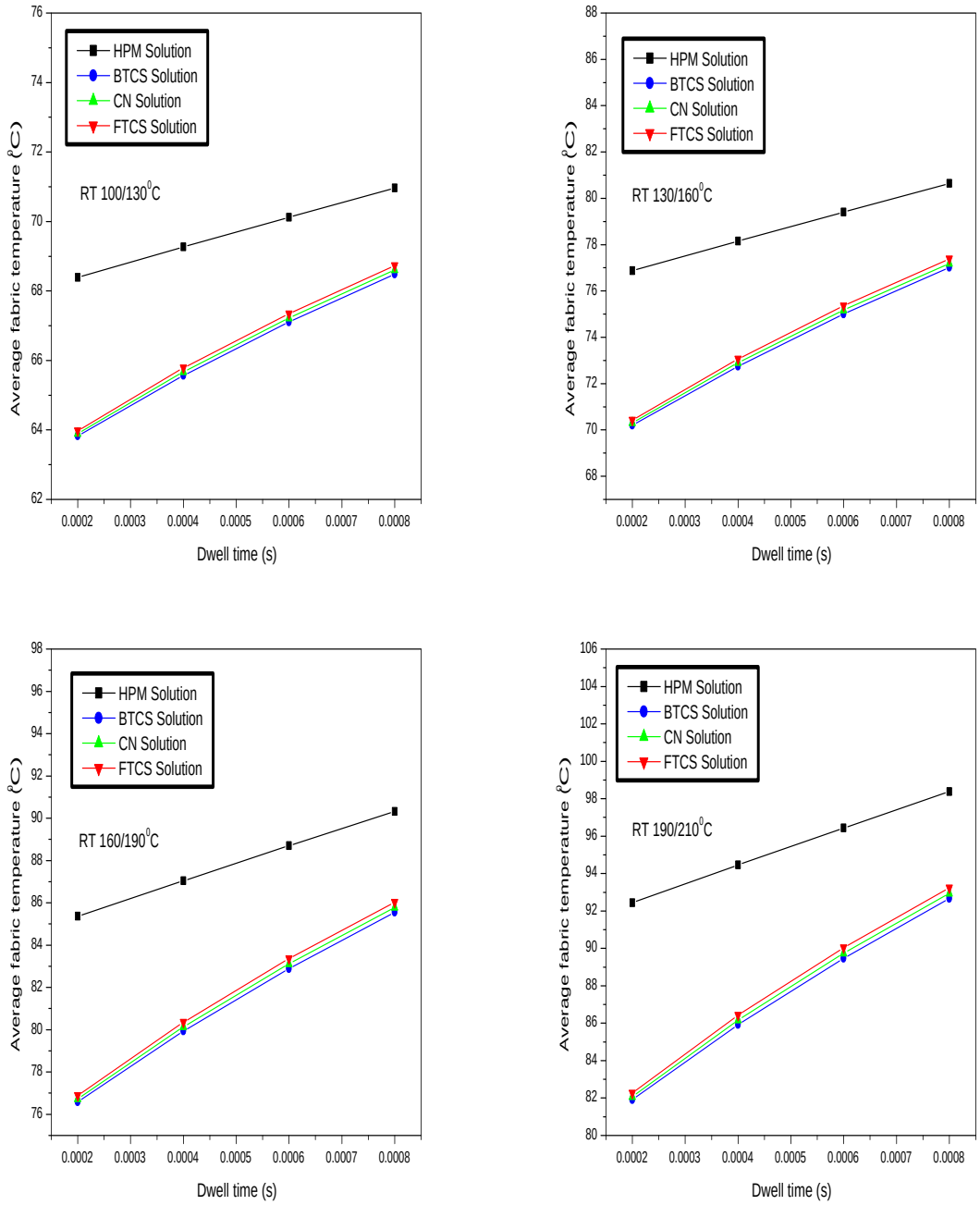

Figure 4.15: Impact of dwell time on average fabric temperature with initial temperature 50°C for machine calender having different roll temperature

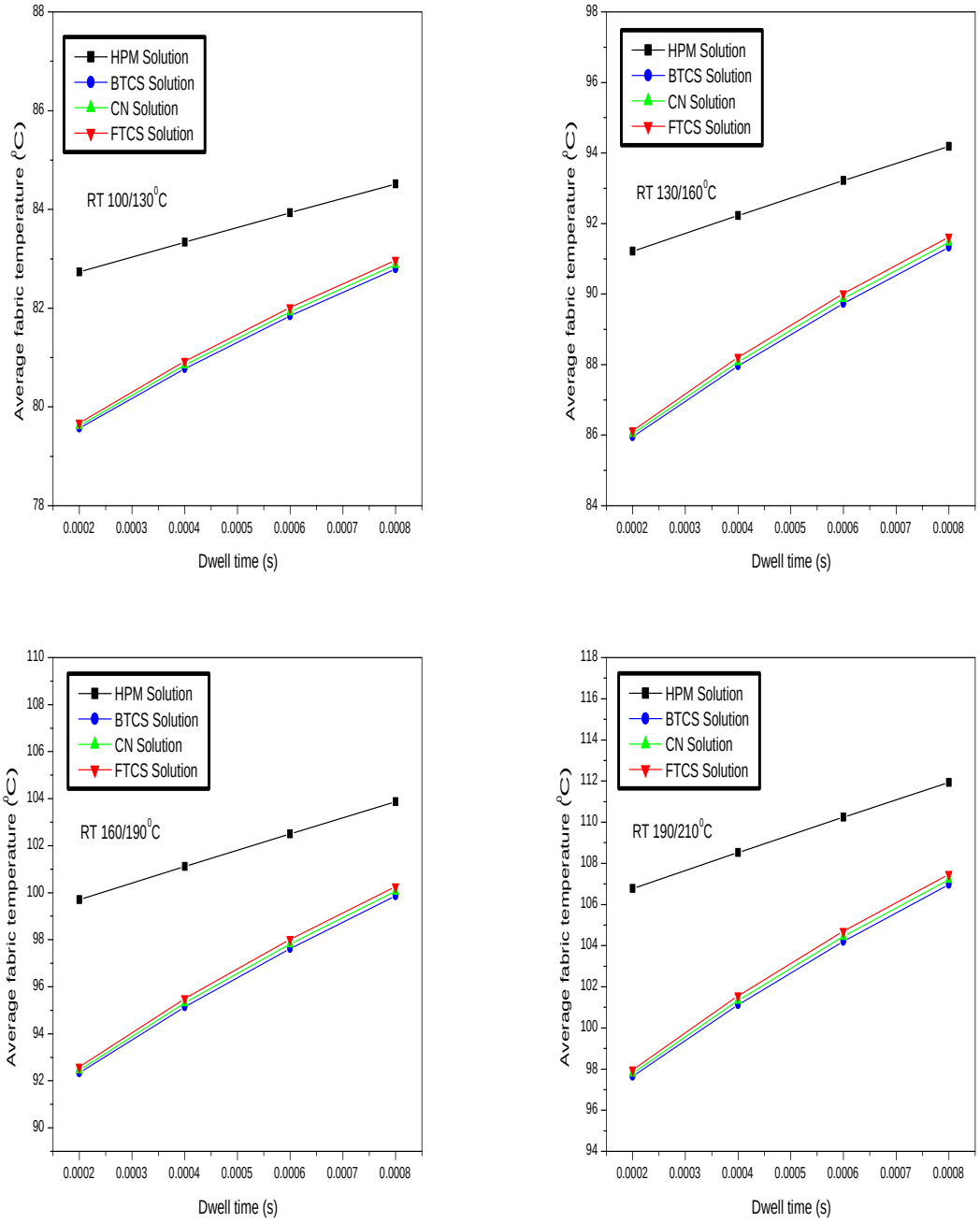

Figure 4.16: Impact of dwell time on average fabric temperature with initial temperature 70°C for machine calender having different roll temperature

4.5.2.4 Impact of Thermal Diffusivity on Average Fabric Temperature for Machine Calender having Different Roll Temperature

The impact of thermal diffusivity on average fabric temperature with initial temperature 50°C and 70°C has been investigated when fabric is inside the machine calender nip having different roll temperature. The calculated values are given in tables 4.41 to 4.48 of APPENDIX. The results obtained are shown in figures 4.17 and 4.18.
It clearly indicates that, with increase in thermal diffusivity average fabric temperature increases. The results obtained using homotopy perturbation method are similar with the exact results while there is significant error in the results obtained using finite difference methods.

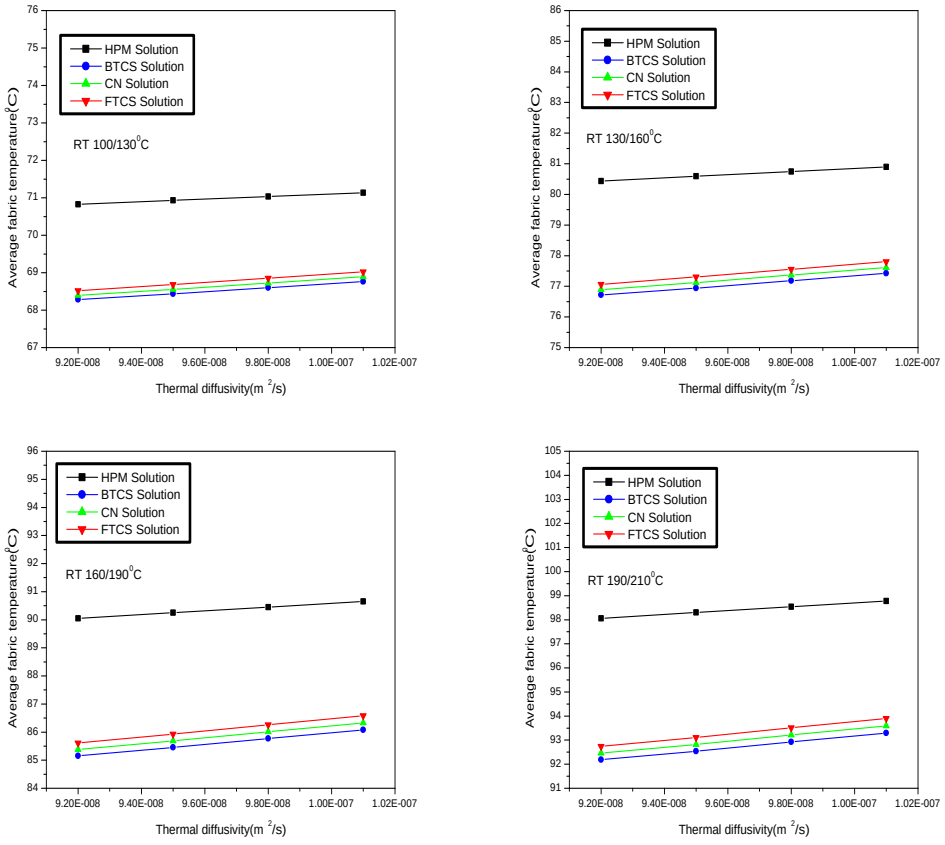

Figure 4.17: Impact of thermal diffusivity on average fabric temperature with initial temperature 50°C for machine calender having different roll temperature

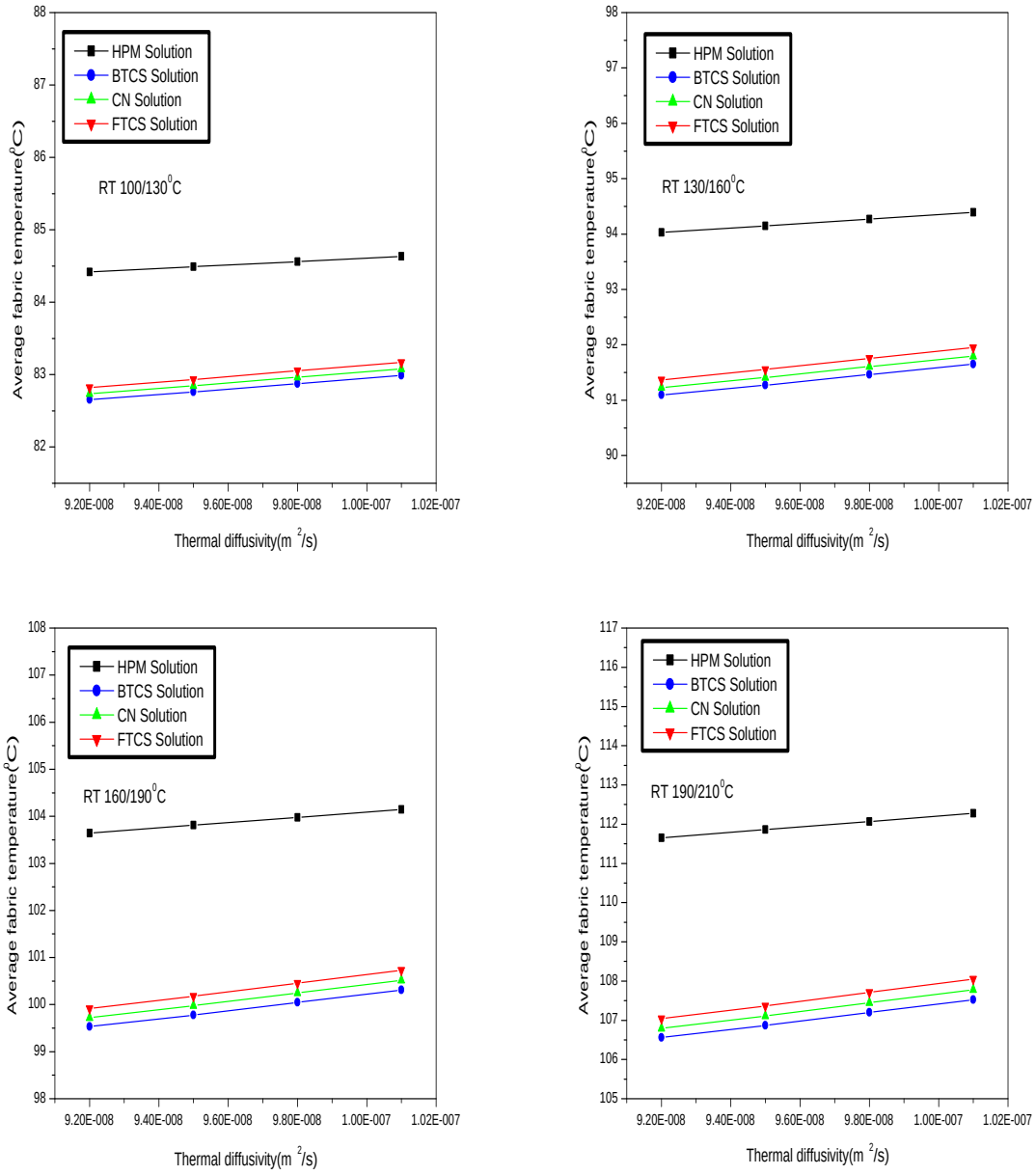

Figure 4.18: Impact of thermal diffusivity on average fabric temperature with initial temperature 70°C for machine calender having different roll temperature

4.5.3 Impact of Various Design and Process Parameters on Rolling Calender

The impact of roll temperature on fabric temperature in thickness direction at various depths, impact of dwell time, thermal diffusivity, roll temperature on average fabric temperature has been investigated when fabric is inside the calender nip for rolling calender having different roll temperature.

4.5.3.1 Impact of Roll Temperature on Fabric Temperature in Thickness Direction at Various Depths for Rolling Calender

The impact of roll temperature on fabric temperature in thickness direction at various depths with initial temperature 50°C and 70°C has been investigated when fabric is inside the rolling calender nip. The calculated values are given in tables 4.49 to 4.56 of APPENDIX. The results obtained are shown in figures 4.19 and 4.20.
It clearly shows that temperature of the fabric decreases from outer part to mid part of the fabric from both sides in thickness direction. In rolling calender, rolls are at different temperature, therefore side of the fabric which is in contact with the roll having higher temperature is more heated as compared to other roll at low temperature. The results obtained using homotopy perturbation method are similar with the exact results while there is a negligible error in the results obtained using finite difference methods.

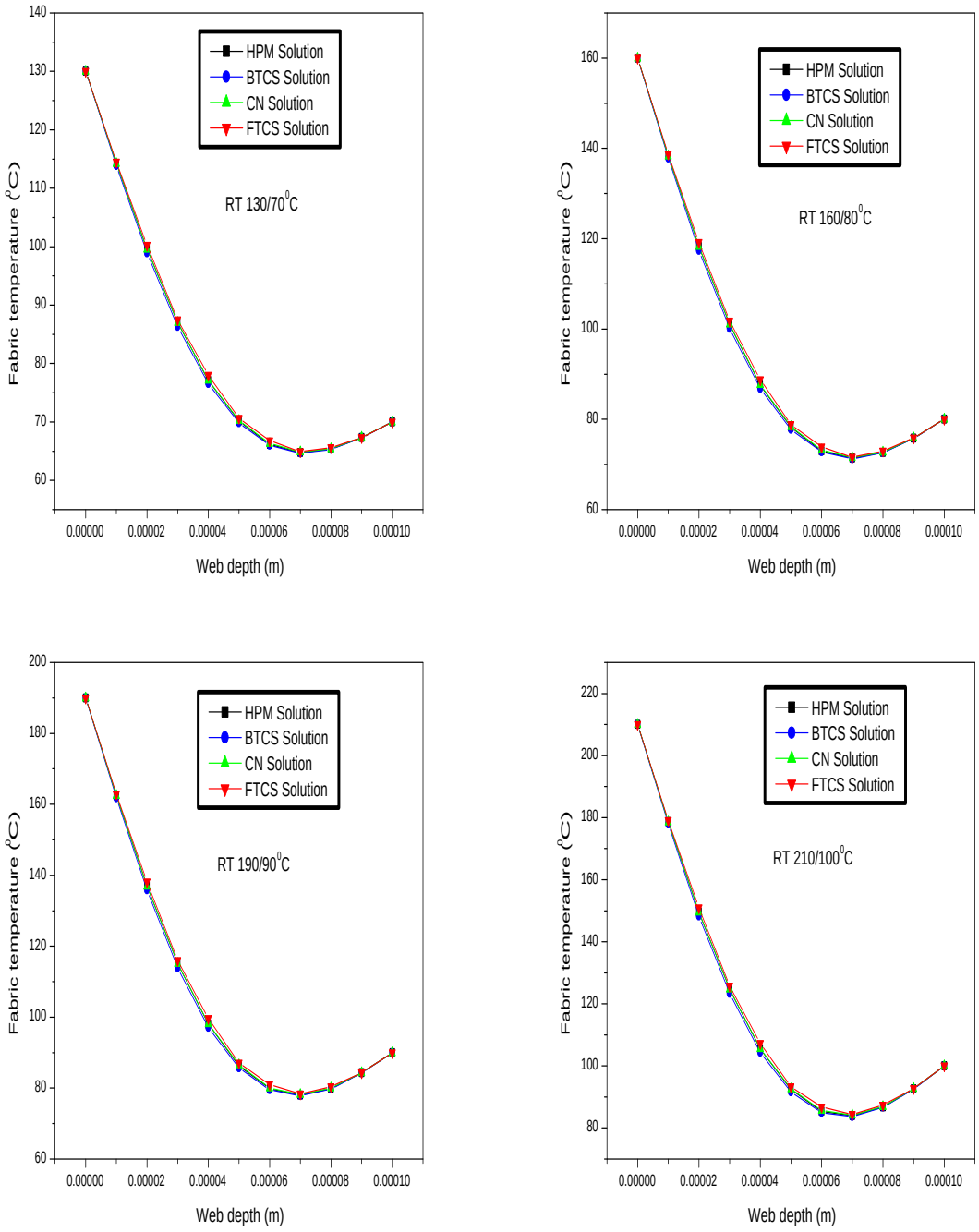

Figure 4.19: Impact of roll temperature on fabric temperature in thickness direction at various depths with initial temperature 50°C for rolling calender

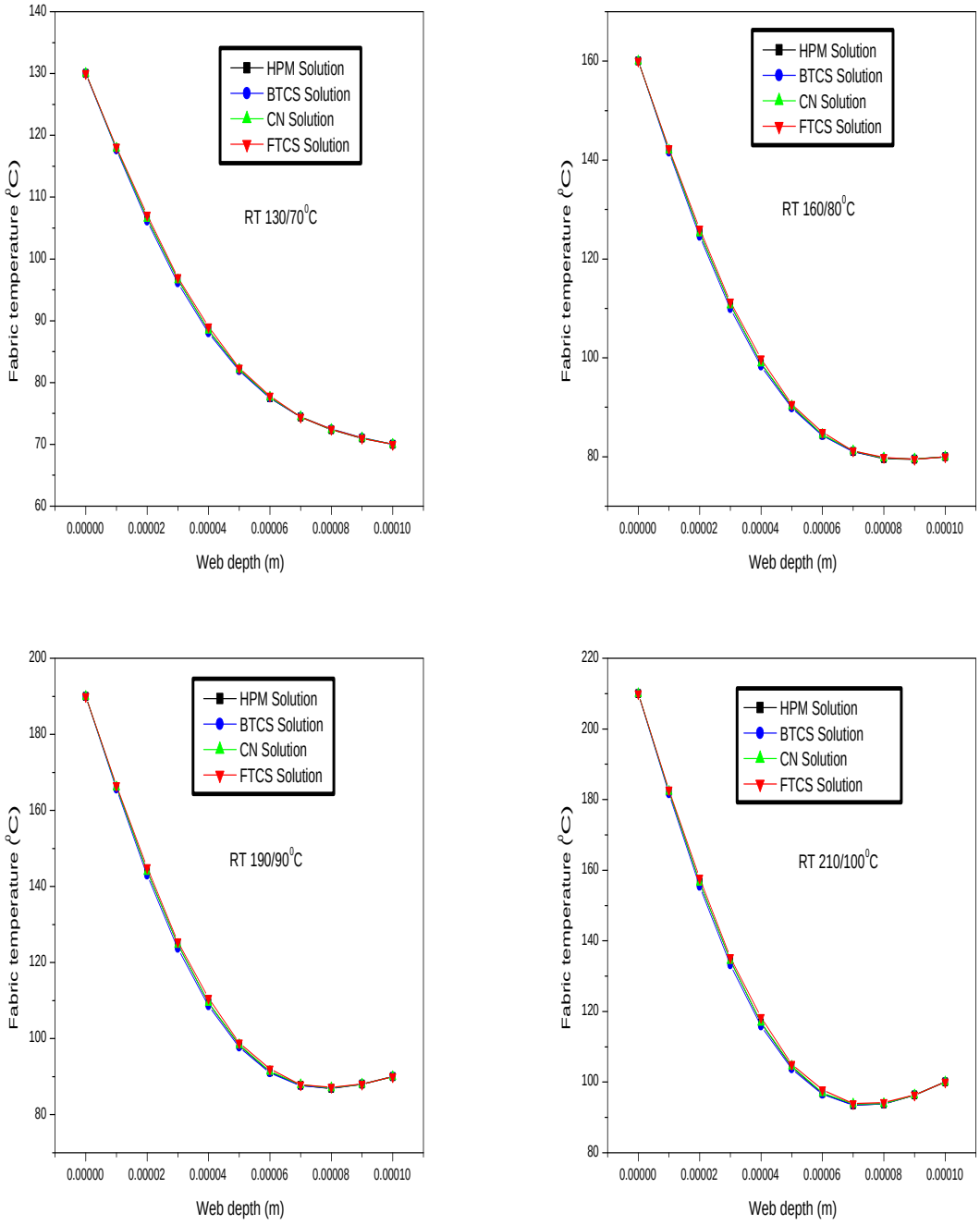

Figure 4.20: Impact of roll temperature on fabric temperature in thickness direction at various depths with initial temperature 70°C for rolling calender

4.5.3.2 Impact of Roll Temperature on Average Fabric Temperature for Rolling Calender

The impact of roll temperature on average fabric temperature with initial temperature 50°C and 70°C has been investigated when fabric is inside the rolling calender nip. The calculated values are given in tables 4.49 to 4.56 of APPENDIX. The results obtained are shown in figures 4.21 and 4.22.

It clearly indicates that, with increase in roll temperature, average fabric temperature increases. The results obtained using homotopy perturbation method are similar with the exact results while there is a negligible error in the results obtained using finite difference methods.

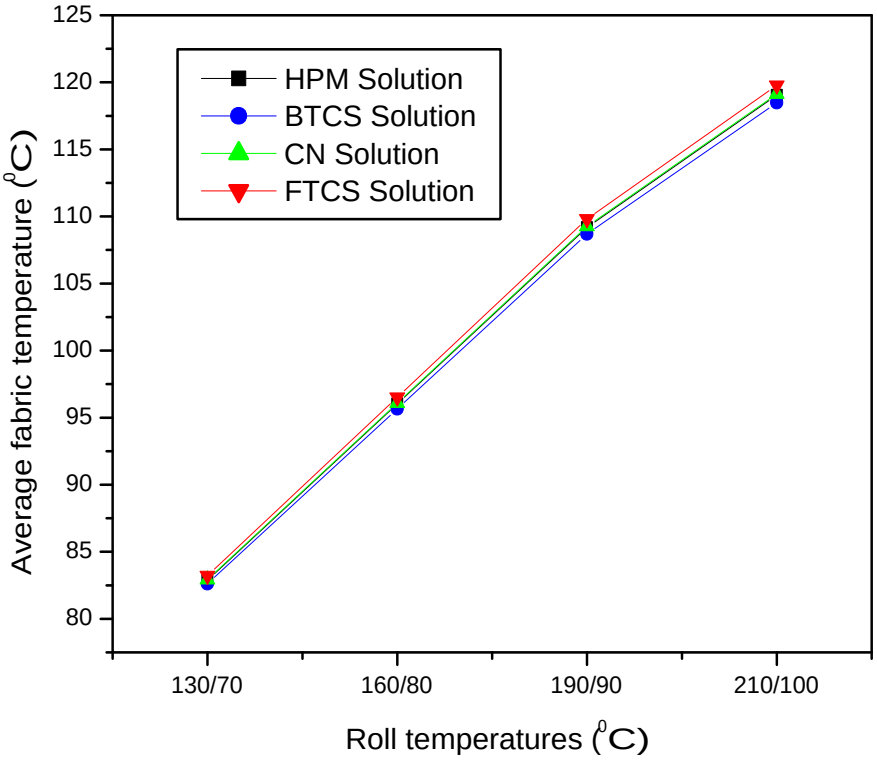

Figure 4.21: Impact of roll temperature on average fabric temperature with initial temperature 50°C for rolling calender

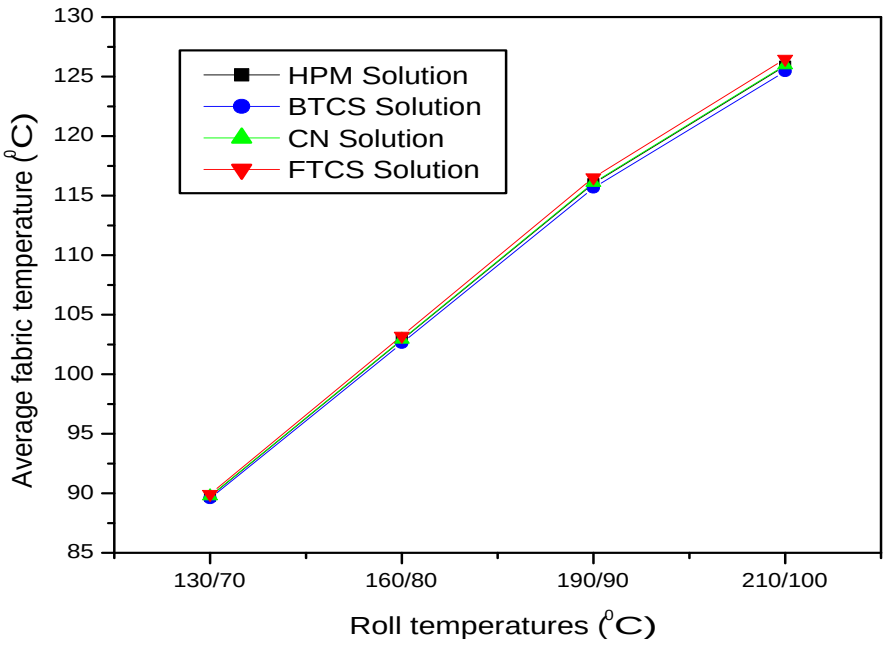

Figure 4.22: Impact of roll temperature on average fabric temperature with initial temperature 70°C for rolling calender

4.5.3.3 Impact of Dwell Time on Average Fabric Temperature for Rolling Calender

The impact of dwell time on average fabric temperature with initial temperature 50°C and 70°C has been investigated when fabric is inside the rolling calender nip. The calculated values are given in tables 4.57 to 4.64 of APPENDIX. The results obtained are shown in figures 4.23 and 4.24.

It clearly indicates that, with increase in dwell time average fabric temperature increases as more heat is conducted at different layers of the fabric with increase in dwell time. The results obtained using homotopy perturbation method are similar with the exact results while there is a negligible error in the results obtained using finite difference methods.

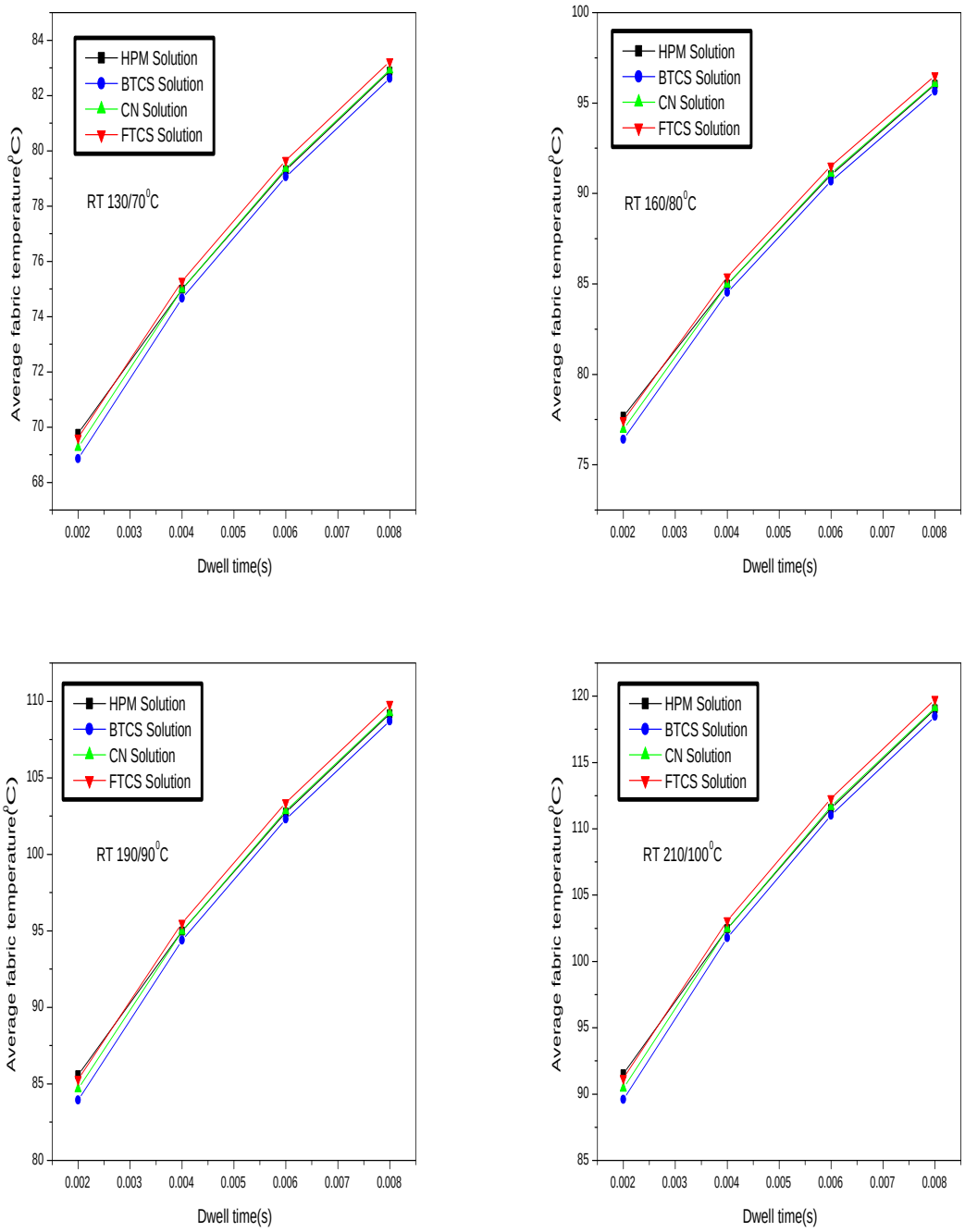

Figure 4.23: Impact of dwell time on average fabric temperature with initial temperature 50°C for rolling calender

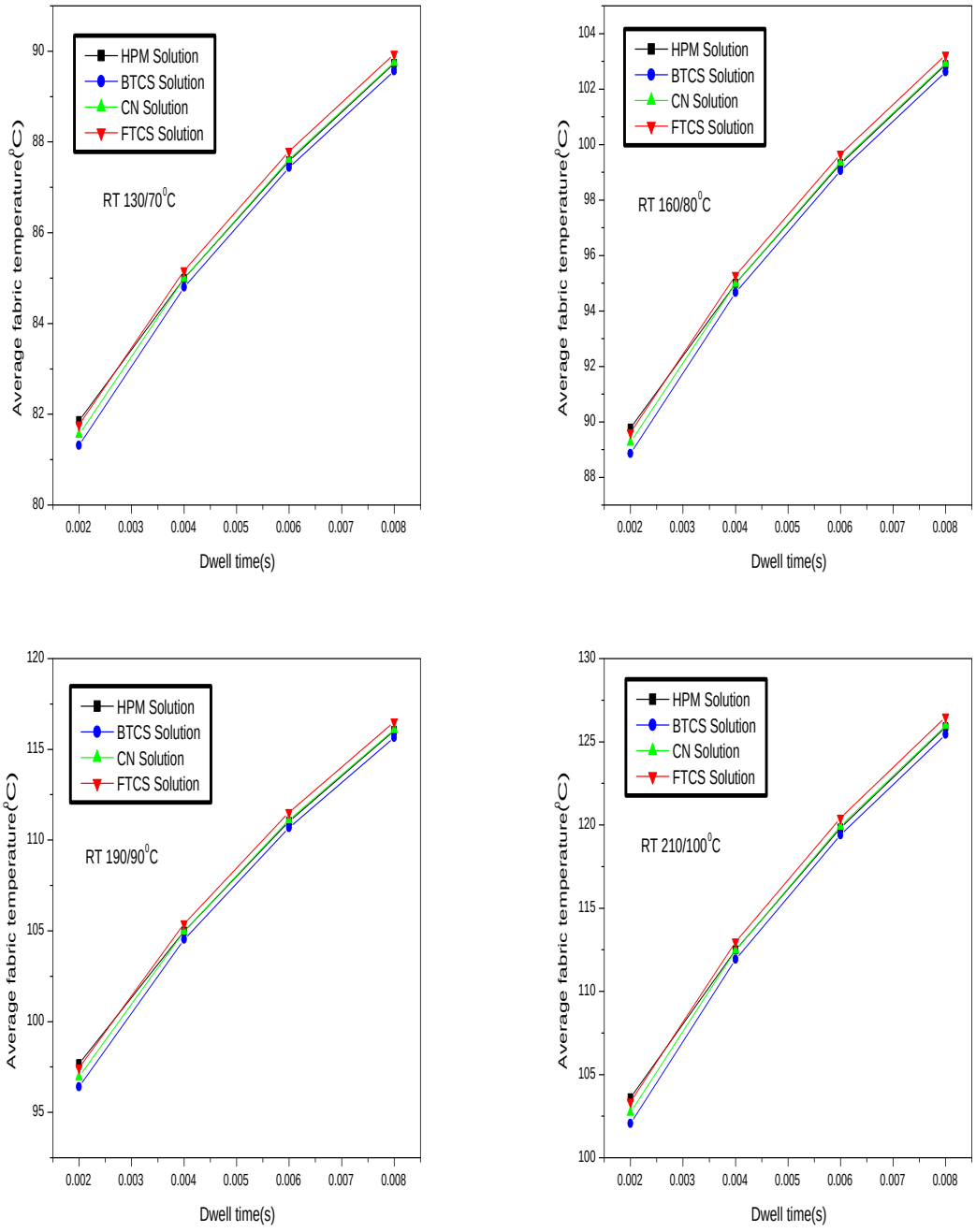

Figure 4.24: Impact of dwell time on average fabric temperature with initial temperature 70°C for rolling calender

4.5.3.4 Impact of Thermal Diffusivity on Average Fabric Temperature for Rolling Calender

The impact of thermal diffusivity on average fabric temperature with initial temperature 50°C and 70°C has been investigated when fabric is inside the rolling calender nip. The calculated values are given in tables 4.65 to 4.72 of APPENDIX. The results obtained are shown in figures 4.25 and 4.26.

It clearly indicates that, with increase in thermal diffusivity average fabric temperature increases. The results obtained using homotopy perturbation method are similar with the exact results while there is significant error in the results obtained using finite difference methods.

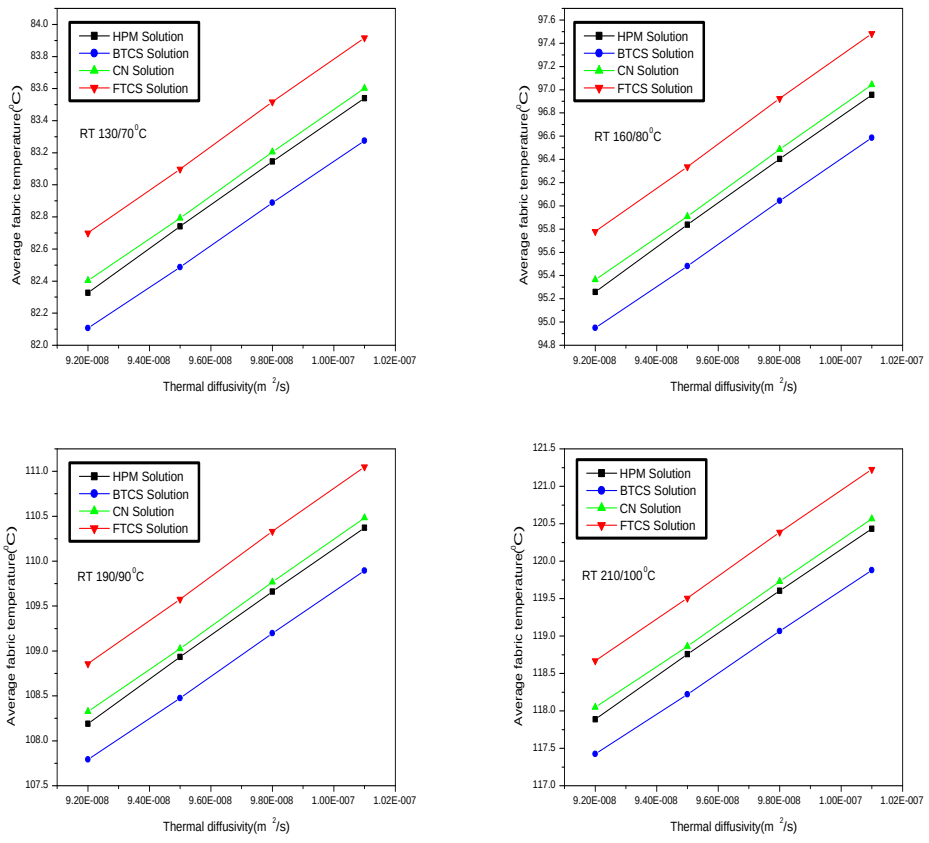

Figure 4.25: Impact of thermal diffusivity on average fabric temperature with initial temperature 50°C for rolling calender

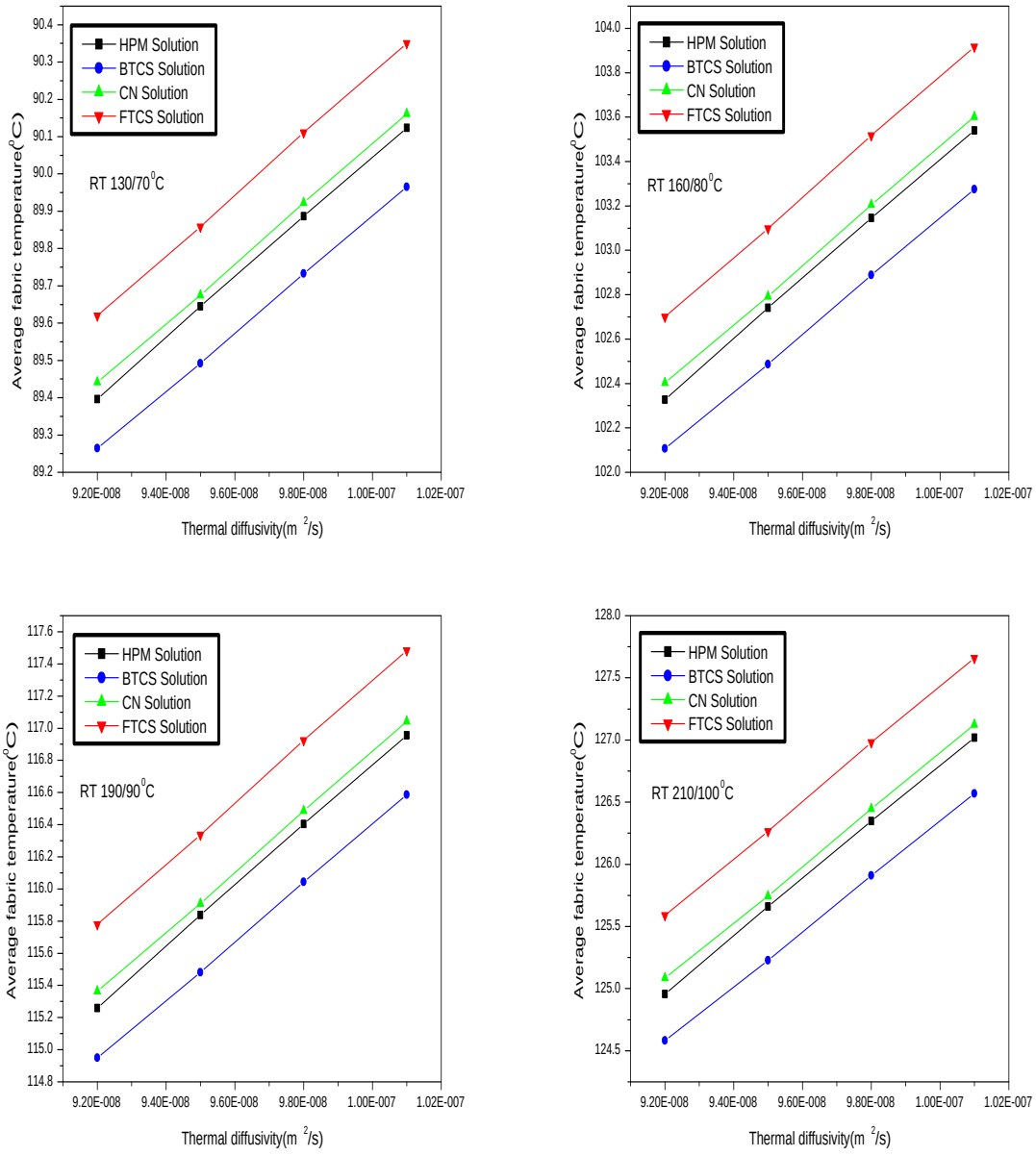

Figure 4.26: Impact of thermal diffusivity on average fabric temperature with initial temperature 70°C for rolling calender

4.6 Conclusion

This model gives an evolutionary advantage that helps in predicting the fabric temperature at various depths in thickness direction inside the nip which is not possible using temperature measuring instruments as they can only measure temperature on the surface of the fabric. From the simulation of the heat transfer model, it is clear that with increase in roll temperature (and/or) decrease in calender speed, more heat penetrates inside the fabric from both sides in thickness direction which results in increase of average fabric temperature. For machine calender when fabric comes out of the nip, there is remarkable increase in average fabric temperature in the range of 12% to 80% with increase in same roll temperature from 100°C to 190°C and in the range of 20% to 96% with increase in different roll temperature from 100°C to 210°C. For rolling calender when fabric comes out of the nip, there is remarkable increase in average fabric temperature in the range of 29% to 80% with increase in different roll temperature from 70°C to 210°C. By increasing the calendering speed beyond a certain limit will not bring any change in average temperature and also makes pressure effect less efficient which results in decrease of gloss and smoothness. Also, with increase in thermal diffusivity coefficient of the fabric, there is increase in average fabric temperature under the same process parameters. So fabric having more thermal diffusivity can be treated to get desired gloss and smoothness under less cost as compared with fabric having less thermal diffusivity coefficient. Increasing roll temperature, pressure and decreasing calendering speed are key factors for improving gloss and smoothness. Therefore for obtaining desired gloss and smoothness a balance between mechanical energy, thermal energy and dwell time is to be made. It is found that results obtained using BTCS method are very close to results obtained using HPM. Also, comparison of results obtained using explicit FTCS, implicit BTCS and Crank Nicolson CN methods with results obtained from HPM reflects the remarkable applicability of numerical and analytical approximate methods in analyzing the temperature profile of the fabric inside the calender nip for same and different roll temperatures.

Chapter 5

Heat Transfer Model when Fabric is Inside the Temperature Gradient Calender Nip

The essential elements for enhancing the surface properties of the fabric inside the calender nip are pressure and temperature between the fabric and heated roll. With increase in pressure and temperature in calendering system, surface smoothness for the fabric can be improved but with increase in both the factors beyond a certain limit can cause damage to the fibre bond resulting in reduction in the mechanical strength of the fabric. To overcome these undesirable effects, the process of temperature gradient calendering is employed. Temperature gradient calender (TGC) consist of alternating hard and soft rolls in which soft roll at room temperature and hard roll at higher temperature. Hard roll (heated roll) is having a thin layer of chilled cast iron whereas soft roll is having a thin layer of elastic material like cotton, epoxy and Nylon 610. polymers, etc. The heated roll surface temperature is between the range 150°C-350°C which is obtained by percolation of heated oil inside the calender roll. In TGC, it is possible to produce a temperature gradient in the thickness direction of the fabric at the same time as the fabric is compressed in the nip, also heat is not transformed upto the center of the fabric in thickness direction, thus the fibres

which are in direct contact with the heated roll get deformed permanently, while the fibres on the other side and upto the middle of the fabric do not get deformed. Thus desirable softening, better fabric surface quality and uniformity of the surface layers can be obtained while preserving the interior bulk and strength properties. Temperature gradient calendering selectively plasticize only the outer surface of the fabric, leading to better smoothness for given thickness.

5.1 Heat Conduction Model

In this section, mathematical models for heat transfer in temperature gradient calender considering incompressible and compressible semi infinite medium have been developed. The heat equation in one dimension considering x axis only is given by

$$\frac{\partial T}{\partial t} = \alpha \frac{\partial^2 T}{\partial x^2} \tag{5.1.1}$$

Equation (5.1.1) can be solved for finding temperature distribution when fabric is inside the calender nip under different initial and boundary conditions depending upon the type of calender.

Case1: Mathematical Model for Heat Transfer in Temperature Gradient Calender Considering Incompressible Semi Infinite Medium

In TGC, the temperature of the cold roll has no contribution in temperature distribution because the contact time between heated roll and fabric is so less. So heat transfer during this procedure can be treated as transient heat conduction into a semi-infinite medium. Semi infinite solid is bounded by the plane $x = 0$ and extends to ∞ towards x positive. So the face $x = L$, has been moved to $x \longrightarrow \infty$.

Therefore, initial and boundary conditions for equation (5.1.1) are taken as

$$T(x, 0) = T_0 \tag{5.1.2}$$

$$\left.\begin{aligned} T(0, t) &= T_h \\ \lim_{x\to\infty} T(x, t) &= T_0 \end{aligned}\right\} \tag{5.1.3}$$

where T_h is the temperature of heated roll and T_0 is the initial temperature of the fabric.

Case2: Mathematical Model for Heat Transfer in Temperature Gradient Calender Considering Compressible Semi Infinite Medium

In this case, change in volume of fabric is considered when it is compressed inside the nip of temperature gradient calender as shown in the Figure 5.1 which is bounded by the plane $x = 0$ and extends to ∞ towards x positive.

Neglecting moisture evaporation, velocity and temperature field are governed by

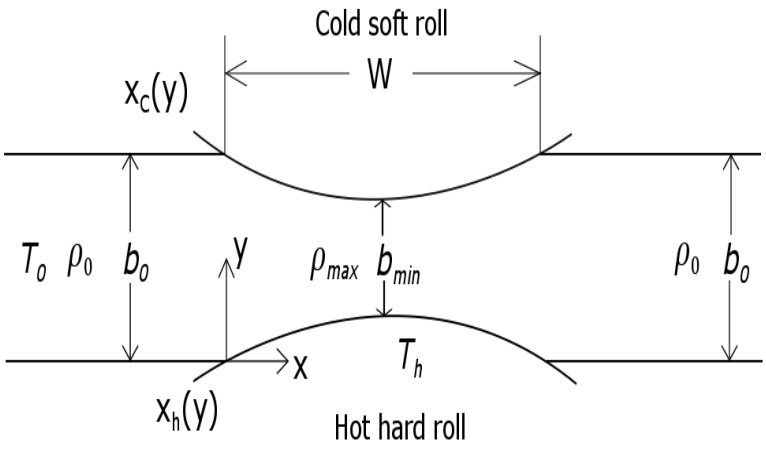

Figure 5.1: Schematic figure of calender nip

continuity and energy equations

$$\nabla \bullet (\rho V) = 0 \tag{5.1.4}$$

$$\rho(x) c_p V \bullet \nabla T = \nabla \bullet (\kappa \nabla T) = 0 \tag{5.1.5}$$

where V is the velocity vector.

Due to viscous nature of fabric, it can be assumed to have same y direction velocity component as x direction component. As density (ρ) is independent of x direction. Therefore from equation (5.1.4),

$$\rho\frac{\partial u_1(x,y)}{\partial x}+v_1\frac{\partial \rho(y)}{\partial y}=0 \tag{5.1.6}$$

where u_1 and v_1 are velocities in x and y direction respectively. Since thickness of the fabric is very small, heat conduction in y direction can be neglected. The thermal conductivity is constant in x direction.

Therefore equation (5.1.5) can be rewritten as

$$u_1(x,y)\frac{\partial T(x,y)}{\partial x}+v_1\frac{\partial T(x,y)}{\partial y}=\alpha(y)\frac{\partial^2 T(x,y)}{\partial x^2} \tag{5.1.7}$$

where α is the thermal diffusivity.

The B.C. for u_1 are

$$\left.\begin{aligned} u_1(x_h(y),y)&=v_1\tfrac{dx_h(y)}{dy}\\ u_1(x_c(y),y)&=v_1\tfrac{dx_c(y)}{dy}\end{aligned}\right\} \tag{5.1.8}$$

$x_h(y)$ and $x_c(y)$ are the functions describing the surface of the hot and cold rolls respectively as shown in Figure 5.1.

Neglecting contact resistance between the hot roll and fabric, boundary conditions for equation (5.1.7) are

$$\left.\begin{aligned} T(x_h(y),y)&=T_h\\ T(x,0)&=T_0\end{aligned}\right\} \tag{5.1.9}$$

5.2 Methodology Used

Mathematical model for heat transfer in temperature gradient calender considering semi infinite medium are solved using Lie transformation method and Heat balance integral methods.

Lie Transformation Method: Symmetry methods for differential equations was originally developed by Sophus Lie in the latter half of the ninteenth century. Sophus Lie introduced the notion of a continuous group of transformations acting on the space of independent and dependent variables of the system. He showed that the order of an ODE could be reduced by one if it is invariant under a one parametric Lie

group of point transformations and in case of PDE, the invariance under a continuous group of point transformations leads directly to the superposition of solutions in terms of transformations. If a system of PDE is invariant under a Lie group of point transformations, special solutions called similarity solutions can be obtained, that are invariant under a subgroup of the full group admitted by the system. These solutions result from solving a reduced system of differential equations with fewer independent variables. Lie group of transformations are characterized by infinitesimal generators. The function appearing in the infinitesimal generator of a Lie group of transformations satisfy an overdetermined system of linear differential equations [123, 124].
Let $x = (x_1, x_2, x_3, ..., x_n)$ lies in region $D \subset R^n$. The set of transformations

$$\tilde{x} = X(x; \epsilon) \tag{5.2.1}$$

defined for each x in D and parameter $\epsilon \in T \subset R$ with $\phi(\epsilon, \delta)$ defining a law of composition of parameters ϵ and δ in T such that

1. For every ϵ in T, the transformations are bijective on D.
2. T with the law of composition ϕ forms a group.
3. For each x in D, $\tilde{x} = x$ when $\epsilon = \epsilon_0$ corresponds to the identity element e of T, i.e.,
   $X(x; \epsilon_0) = x$
4. If $\tilde{x} = X(x; \epsilon)$, $\tilde{\tilde{x}} = X(\tilde{x}; \delta)$, then
   $\tilde{\tilde{x}} = X(x; \phi(\epsilon, \delta))$
   such family of transformation is known as the one parameter group of transformations.

A one parameter group of transformations defines a one parameter Lie group of transformations if, in addition to satisfy axioms (1)-(4) of above definition, the following holds [123, 124]:

1. ϵ is a continuous parameter, i.e., T, is an interval in R. Without loss of generality, $\epsilon = 0$ corresponds to the identity element e.

2. X is infinitely differentiable w.r.t. x in D and an analytical function of ϵ in T.

3. $\phi(\epsilon, \delta)$ is an analytic function of ϵ and δ in T.

Heat Balance Integral Method: The heat balance integral method was introduced by Goodman is a well-known approximate mathematical technique for solving heat transfer problems and particularly the location of the free boundary in heat conduction problems involving a phase of change. A number of thermal and phase change problems are solved using heat balance integral method. It is a simple approximate technique originally developed for analyzing thermal problems. The standard heat balance integral method approximates solutions to the heat equation by first introducing a heat penetration depth, $\delta(t)$, where for $x \geq \delta$ the temperature change above the initial temperature is assumed to be negligible. An approximating function is then defined for the temperature, typically a polynomial, and by applying sufficient boundary conditions, all the unknown coefficients can be determined in terms of the unknown function δ. Finally, the governing heat equation is integrated for $x \in [0, \delta]$ [125–128].

5.3 Solution of Case 1 using Lie Transformation Method

Introducing dimensionless variables

$$\theta = \frac{T - T_0}{T_h - T_0} \tag{5.3.1}$$

$$\tau = \alpha t \tag{5.3.2}$$

equations (5.1.1), (5.1.2) and (5.1.3) get transformed to

$$\frac{\partial \theta}{\partial \tau} = \frac{\partial^2 \theta}{\partial x^2} \tag{5.3.3}$$

$$\theta(x, 0) = 0 \tag{5.3.4}$$

$$\left.\begin{aligned} \theta(0,\tau) &= 1 \\ \lim_{x\to\infty}\theta(x,\tau) &= 0 \end{aligned}\right\} \tag{5.3.5}$$

The solution of equation (5.3.3) along with conditions given by equations (5.3.4) and (5.3.5) is found using invariance under Lie group of point transformation. A restricted class of one parameter transformation group is considered which is applicable to equation (5.3.3).

Considering one parameter transformation group

$$\left.\begin{aligned} x_1 &= x + \epsilon\xi(x,\tau) + O(\epsilon^2) \\ \tau_1 &= \tau + \epsilon\eta(x,\tau) + O(\epsilon^2) \\ \phi_1 &= \phi + \epsilon\zeta(x,\tau) + O(\epsilon^2) \end{aligned}\right\} \tag{5.3.6}$$

The above system of equations must hold for all values of $x, t, \phi, \phi_x, \phi_t, \phi_{xt}$. On setting the coefficients of $x, t, \phi, \phi_x, \phi_t, \phi_{xt}$ to zero,

$$\left.\begin{aligned} \tfrac{\partial\eta}{\partial x} &= 0 \\ \tfrac{\partial\zeta}{\partial\tau} - \tfrac{\partial^2\zeta}{\partial\tau^2} &= 0 \\ 2\tfrac{\partial\zeta}{\partial x} + \tfrac{\partial\xi}{\partial\tau} - \tfrac{\partial^2\xi}{\partial x^2} &= 0 \\ 2\tfrac{\partial\xi}{\partial x} - \tfrac{\partial\eta}{\partial\tau} + \tfrac{\partial^2\eta}{\partial x^2} &= 0 \end{aligned}\right\} \tag{5.3.7}$$

The solution of determining equations is given by

$$\left.\begin{aligned} \xi(x,\tau) &= \kappa_1 + \beta x + \gamma x t + \delta t \\ \eta(x,\tau) &= \alpha_1 + 2\beta t + \gamma t^2 \\ \zeta(x,\tau) &= -\gamma(\tfrac{1}{4}x^2 + \tfrac{1}{2}t) - \tfrac{1}{2}\delta x + \lambda \end{aligned}\right\} \tag{5.3.8}$$

where $\kappa, \beta, \gamma, \delta, \alpha_1, \lambda$ are six arbitrary parameters.

For parameter β, the similarity variables are given by

$$\frac{dx}{\xi} = \frac{dt}{\eta} = \frac{du}{\zeta} \tag{5.3.9}$$

where ξ, η and ζ are given by equation (5.3.8).

Using these similarity variables, equation (5.3.3) reduces to

$$\frac{d^2\theta}{d\eta^2} + 2\eta\frac{d\theta}{d\eta} = 0 \tag{5.3.10}$$

Also, equation (5.3.4) reduces to

$$\eta = \infty, \theta = 0 \tag{5.3.11}$$

and equation (5.3.5) reduces to

$$\eta = 0, \theta = 1 \tag{5.3.12}$$

The other boundary condition given by equation (5.3.5) reduces to the same form as given by equation (5.3.11).

Putting $\frac{d\theta}{d\eta} = \xi_1$ in equation (5.3.10), we get

$$\frac{d\xi_1}{d\eta} + 2\eta\xi_1 = 0 \tag{5.3.13}$$

Integrating equation (5.3.13),

$$\xi_1 = Ce^{-\eta^2} \tag{5.3.14}$$

Therefore

$$\frac{d\theta}{d\eta} = Ce^{-\eta^2} \tag{5.3.15}$$

Integrating equation (5.3.15),

$$\theta = C\int_0^\eta e^{-\eta^2}d\eta + D \tag{5.3.16}$$

where C and D are integration constants.

Using the initial and boundary conditions given by equation (5.3.11), equation (5.3.12),

$$C = \frac{-2}{\sqrt{\pi}}, D = 1 \tag{5.3.17}$$

Putting the values of C and D from equation (5.3.17) in equation (5.3.16)

$$\theta = 1 - \frac{2}{\sqrt{\pi}}\int_0^\eta e^{-\eta^2}d\eta \tag{5.3.18}$$

The integral in the above equation is known as error function. Thus

$$\theta = 1 - erf(\eta) \tag{5.3.19}$$

$$\frac{T - T_0}{T_h - T_0} = erfc(\eta) \tag{5.3.20}$$

where η is similarity variable and for the solution of given problem, Let η is given by

$$\eta = \frac{x}{2\sqrt{\alpha t}} \tag{5.3.21}$$

Therefore, equation (5.3.20) becomes

$$T(x,t) = T_0 + (T_h - T_0)erfc(\frac{x}{2\sqrt{\alpha t}}) \tag{5.3.22}$$

where t is dwell time and $erfc(\frac{x}{2\sqrt{\alpha t}})$ is the complementary error function.
The above equation is used to find the temperature distribution in fabric inside the temperature gradient calender nip considering incompressible semi infinite medium.

5.4 Solution of Case 1 using Heat Balance Integral Method

Introducing dimensionless variables

$$\theta = \frac{T - T_0}{T_h - T_0} \tag{5.4.1}$$

$$\tau = \alpha t \tag{5.4.2}$$

The heat equation, I.C. and B.C. get transformed to the following forms

$$\frac{\partial \theta}{\partial \tau} = \frac{\partial^2 \theta}{\partial x^2} \tag{5.4.3}$$

with I.C.

$$\theta(x,0) = 0 \tag{5.4.4}$$

and B.C.

$$\left.\begin{aligned} \theta(0,\tau) &= 1 \\ \lim_{x\to\infty} \theta(x,\tau) &= 0 \end{aligned}\right\} \tag{5.4.5}$$

Equation (5.4.3) is solved under initial and boundary conditions given by equations (5.4.4) and (5.4.5).

Define $\delta(t)$ i.e. distance over which the temperature changes is felt at time t. Integrate equation (5.4.3) from $x = 0$ to $x = \delta(t)$ giving

$$\left(\frac{\partial T}{\partial x}\right)_{x=\delta(t)} - \left(\frac{\partial T}{\partial x}\right)_{x=0} = \frac{1}{\alpha}\int_0^{\delta(t)} \frac{\partial T}{\partial t} dx \tag{5.4.6}$$

The right hand side integral is performed by applying rule of differentiation under the integral sign, hence

$$\left(\frac{\partial T}{\partial x}\right)_{x=\delta(t)} - \left(\frac{\partial T}{\partial x}\right)_{x=0} = \frac{1}{\alpha}\left[\frac{d}{dt}\int_0^{\delta(t)} T dx - T_{x=\delta}\frac{d\delta}{dt}\right] \tag{5.4.7}$$

But $\left(\frac{\partial T}{\partial x}\right)_{x=\delta} = 0$ and $T = T_0$ at $x = \delta$

Let

$$\phi = \int_0^{\delta(t)} T dx \tag{5.4.8}$$

Hence equation (5.4.3) becomes

$$-\alpha\left(\frac{\partial T}{\partial x}\right)_{x=0} = \frac{d}{dt}(\phi - T_0\delta) \tag{5.4.9}$$

$$-\kappa\left(\frac{\partial T}{\partial x}\right)_{x=0} = \rho C_p \frac{d}{dt}(\phi - T_0\delta) \tag{5.4.10}$$

Rate of input of energy at face $x = 0$ at any time t= Rate of energy of the sensible heat of the heated layer of thickness $\delta(t)$.

To calculate the integral method solution, the B.C. at ∞ with

$$T(\delta(t), t) = \frac{\partial \phi}{\partial x}(\delta(t), t) = 0 \tag{5.4.11}$$

where δ is sufficiently far from the boundary such that the boundary temperature has a negligible effect.

Therefore

$$\left.\begin{aligned} T &= T_h \ at \ x = 0 \\ T &= T_0 \ at \ x = \delta \\ \tfrac{\partial T}{\partial x} &= 0 \ at \ x = \delta \end{aligned}\right\} \tag{5.4.12}$$

Another condition can be obtained by evaluating the differential equation at $x = \delta(t)$, where $T = T_h$=constant.

Therefore

$$\left.\begin{array}{ll} \frac{\partial T}{\partial t} & = 0 \ at \ x = \delta \\ \frac{\partial^2 T}{\partial x^2} & = 0 \ at \ x = \delta \end{array}\right\} \tag{5.4.13}$$

Using the above conditions, The solution for $G(x,t)$ is an appropriate approximate polynomial

$$\theta(x,t) = \left(1 - \frac{x}{\delta}\right)^m \tag{5.4.14}$$

then on integrating the heat equation over $x \in [0, \delta]$, substituting for $G(x,t)$ using equation (5.4.14) and then again on integration, it leads to

$$\delta = \sqrt{2m(m+1)t} \tag{5.4.15}$$

Taking seventh order polynomial, using equation (5.4.14) and (5.4.15), the resulting solution is given by

$$T(x,t) = T_0 + (T_h - T_0)\left[1 - 7\left(\frac{x}{\delta}\right) + 21\left(\frac{x}{\delta}\right)^2 - 35\left(\frac{x}{\delta}\right)^3 + 35\left(\frac{x}{\delta}\right)^4 - 21\left(\frac{x}{\delta}\right)^5 + 7\left(\frac{x}{\delta}\right)^6 - 21\left(\frac{x}{\delta}\right)^7\right] \tag{5.4.16}$$

with

$$\delta = \sqrt{112\alpha t} \tag{5.4.17}$$

5.5 Solution of Case 2 using Lie Transformation Method

Using equation (5.1.8) in equation (5.1.6), the velocity field is given by

$$V(x,y) = v\Big[\frac{dx_h(y)}{dy} - \frac{(x - x_h)}{\rho}\frac{d\rho(y)}{dy}\Big] \tag{5.5.1}$$

Using equation (5.5.1) in equation (5.1.8),

$$\rho(y)b(y) = constant = \rho_0 b_0 \tag{5.5.2}$$

where $b(y) = x_c(y) - x_h(y)$ is the fabric thickness.

Considering non dimensional variable ϕ given by

$$\theta = \frac{T(x,y) - T_0}{T_h - T_0} \tag{5.5.3}$$

with similarity transformation

$$\eta_1(x,y) = (x - x_h(y))\rho(x)\sqrt{u}\Big[\int_0^{N_w} \alpha(s)(\rho(s)^2)ds\Big]^{\frac{1}{2}} \tag{5.5.4}$$

Using equation (5.5.3) and (5.5.4), equation (5.1.7) reduces to

$$\frac{d^2\theta}{d\eta_1^2} + \frac{\eta_1}{2}\frac{d\theta}{d\eta_1} = 0 \tag{5.5.5}$$

with the boundary conditions $\theta = 1$ at $\eta_1 = 0$ and $\theta = 0$ at $\eta_1 = \infty$

The solution of equation (5.5.5) using Lie transformation method as discussed in previous subsection is given by

$$\theta(\eta_1) = erfc\Big[\frac{\eta_1}{2}\Big] \tag{5.5.6}$$

Using equation (5.5.3,

$$\theta = \frac{T(x,y) - T_0}{T_h - T_0} = erfc\left[\frac{(x - x_h(y))\rho(x)\sqrt{u}\Big[\int_0^{N_w} \alpha(s)(\rho(s)^2)ds\Big]^{\frac{1}{2}}}{2}\right] \tag{5.5.7}$$

Since nip width is very large in comparison with fabric thickness, therefore the assumption that the compression and the expansion of the fabric during the calendering procedure are linear, leads to no great error. Furthermore it is assumed that the density of the calendered fabric equals that of the uncalendered fabric, therefore the density variation is modelled with the triangular function

$$\frac{\rho(y)}{\rho_0} = \frac{b_0}{b_{min}} + (1 - \frac{b_0}{b_{min}})\frac{y - \frac{N_w}{2}}{\frac{N_w}{2}} \tag{5.5.8}$$

where N_w is the nip width, ρ_0 the density of the uncalendered fabric, b_0 is the thickness of uncalendered fabric and b_{min} is the minimum thickness of the fabric during the

calendering procedure. Assuming α to be constant and substituting $\rho(x)$ from equation (5.5.8) and $x_h(N_w) = 0$ in to equation (5.5.7) yields the temperature distribution inside the calender nip of width N_w

$$T(x,t) = T_0 + (T_h - T_0)erfc\left(\frac{\sqrt{3}}{\sqrt{(\frac{b_0}{b_{min}})^2 + \frac{b_0}{b_{min}} + 1}}\frac{x}{2\sqrt{\alpha t}}\right) \tag{5.5.9}$$

where t is the dwell time. The above equation is used to find the temperature distribution in fabric inside the temperature gradient calender nip considering compressible semi infinite medium.

5.6 Simulation of Heat Transfer Models Considering Incompressible and Compressible Semi Infinite Medium

The solution of mathematical models for heat transfer considering incompressible and compressible semi infinite medium described in equations (5.3.22), (5.4.16) and (5.5.9) are used to investigate the impact of roll temperature, dwell time, thermal diffusivity on average fabric temperature when fabric is inside the calender nip using the data given in table 3.1 of APPENDIX. The initial fabric temperature is taken as 50°C and 70°C and heated roll temperatures are taken in the range from 200°C to 320°C. Nip width (N_w) is taken as $0.0065m$ which is calculated using nip mechanics model for rolling calender (NMMR).

5.7 Results and Discussion

5.7.1 Impact of Various Design and Process Parameters on Temperature Gradient Calender Considering Incompressible Medium

The impact of roll temperature on fabric temperature in thickness direction at various depths, impact of dwell time, thermal diffusivity, roll temperature on average fabric temperature has been investigated when fabric is inside the temperature gradient calender considering incompressible medium.

5.7.1.1 Impact of Roll Temperature on Temperature Profile of Fabric at Distinct Depths in Thickness Direction Considering Incompressible Medium

Temperature profile of fabric having initial temperature 50°C and 70°C on various depths has been calculated for incompressible semi infinite medium using equations (5.3.22) and (5.4.16). It is found that there is significant error between the results obtained using Lie and Integral method. The calculated values are given in tables 5.1 to 5.8 of APPENDIX. It is found that the side of fabric which is in touch with the heated roll is at higher temperature as compared to the side which is in contact with the non heated roll. Also, temperature of fabric decreases with increase in web depth and after the middle part, it remains at initial fabric temperature as shown in figures 5.2 and 5.3.

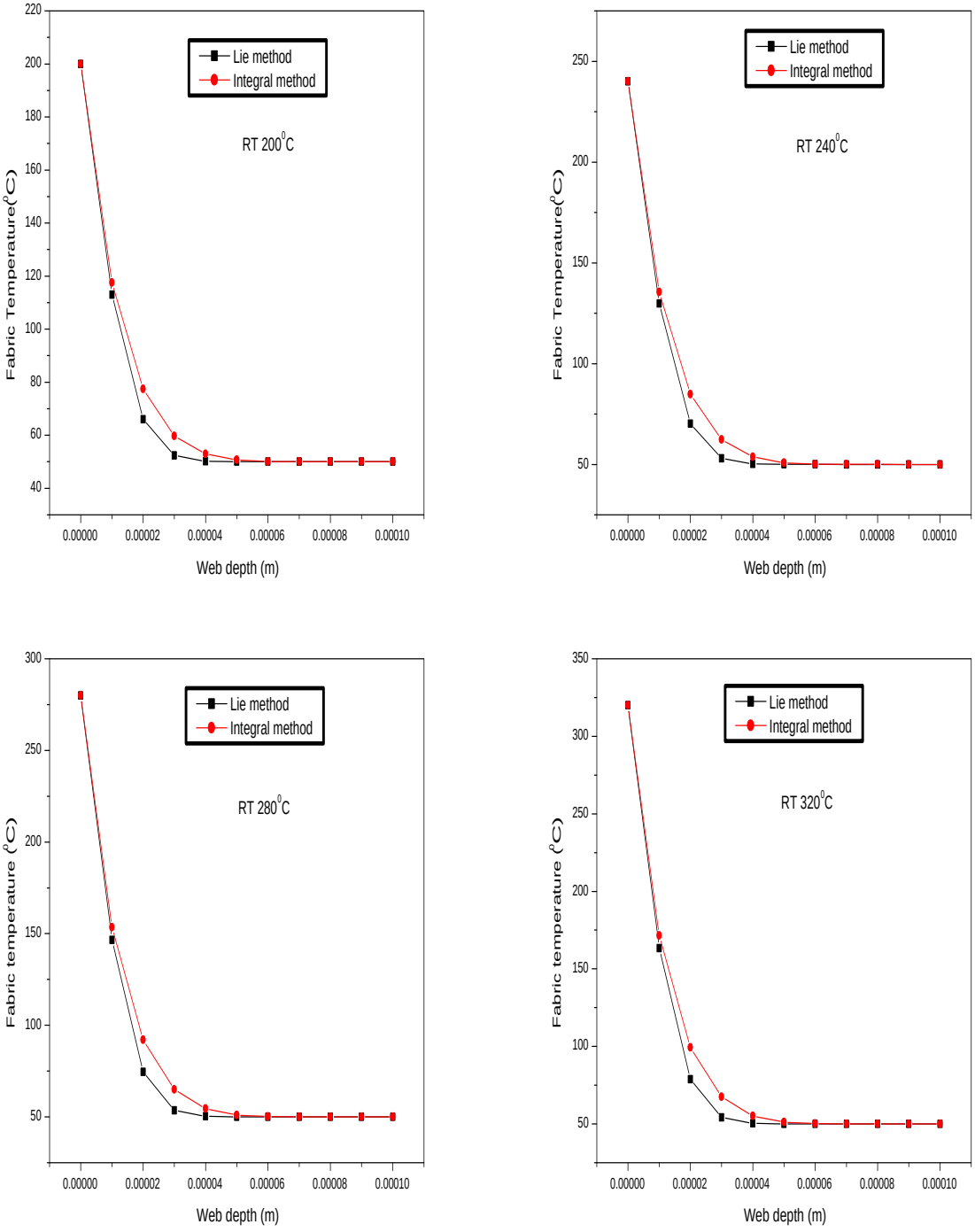

Figure 5.2: Impact of roll temperature on temperature profile of fabric at distinct depths in thickness direction at initial temperature 50°C for incompressible semi infinite medium

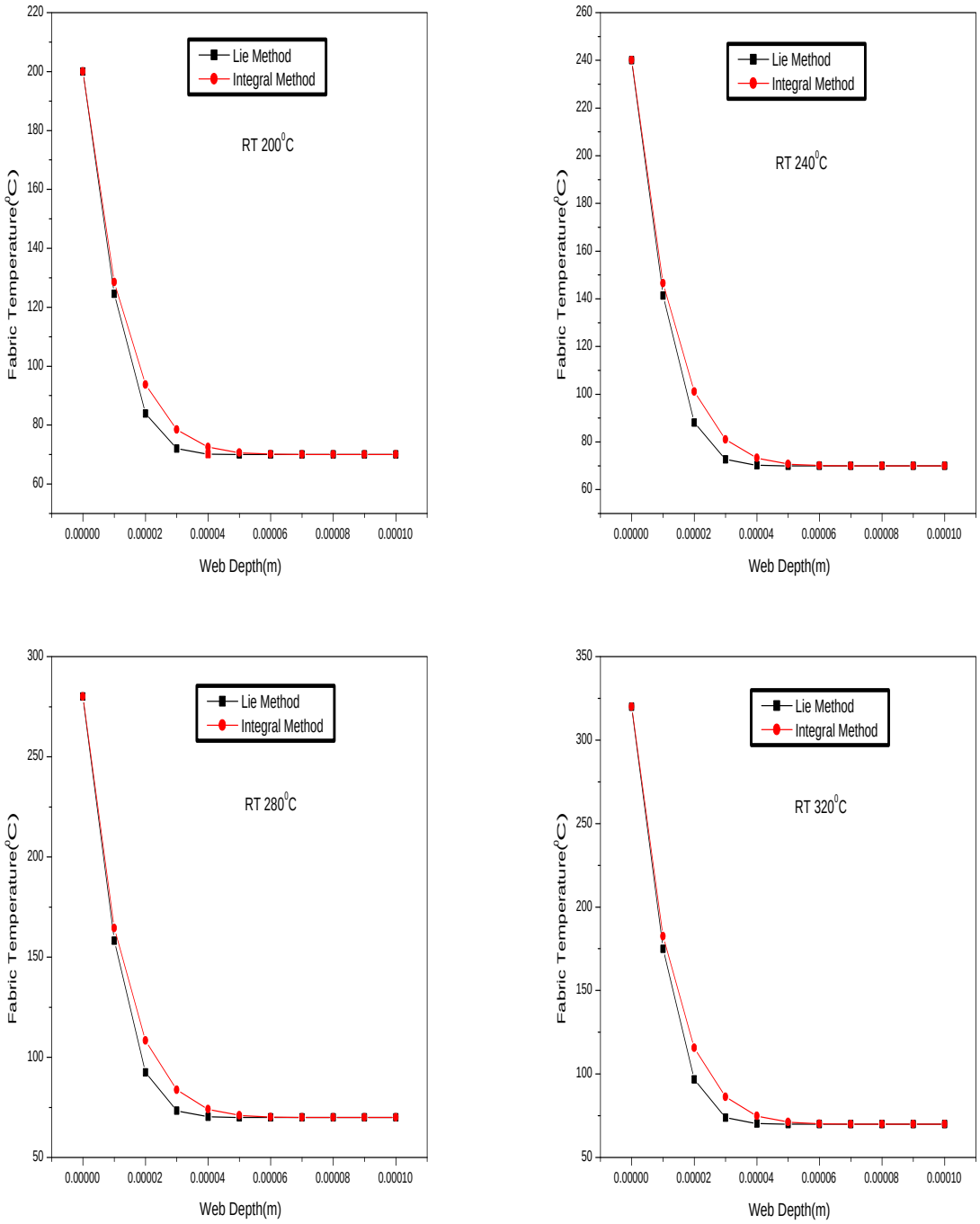

Figure 5.3: Impact of roll temperature on temperature profile of fabric at distinct depths in thickness direction at initial temperature 70°C for incompressible semi infinite medium

5.7.1.2 Impact of Heated Roll Temperature on Average Fabric Temperature Considering Incompressible Medium

The impact of heated roll temperature on average fabric temperature having initial temperature 50°C and 70°C considering incompressible medium has been calculated using equations (5.3.22) and (5.4.16). There is significant error between the results obtained using Lie and Integral method. The calculated values are given in tables 5.1 to 5.8 of APPENDIX. It is found that with increase in heated roll temperature, average temperature of the fabric increases when fabric is inside the nip as shown in figures 5.4 and 5.5.

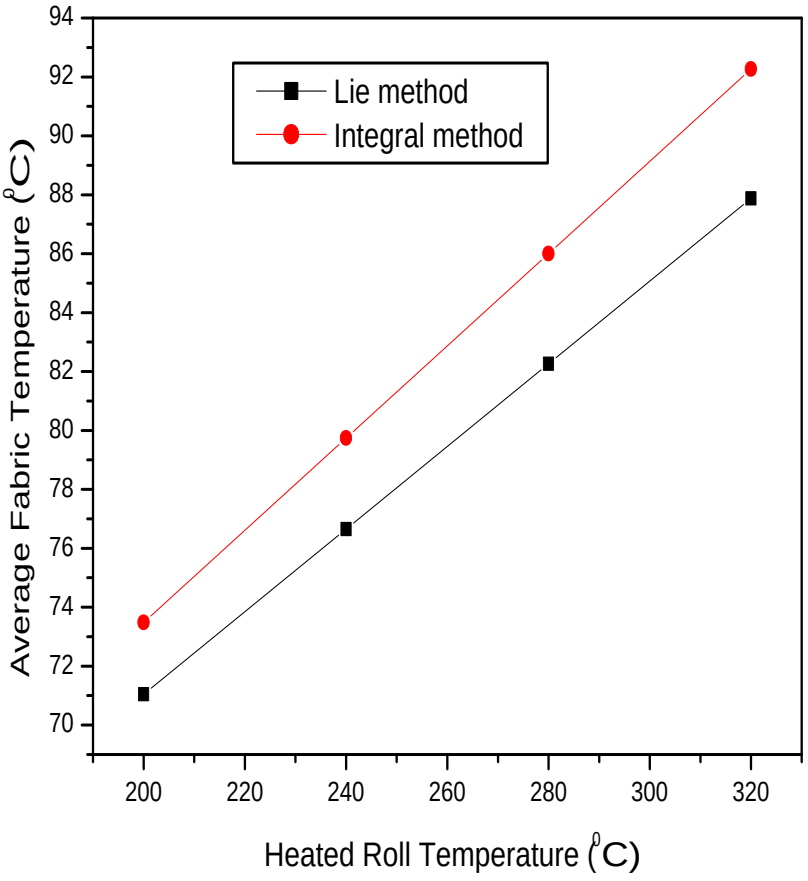

Figure 5.4: Impact of heated roll temperature on average fabric temperature at initial temperature 50°C for incompressible semi infinite medium

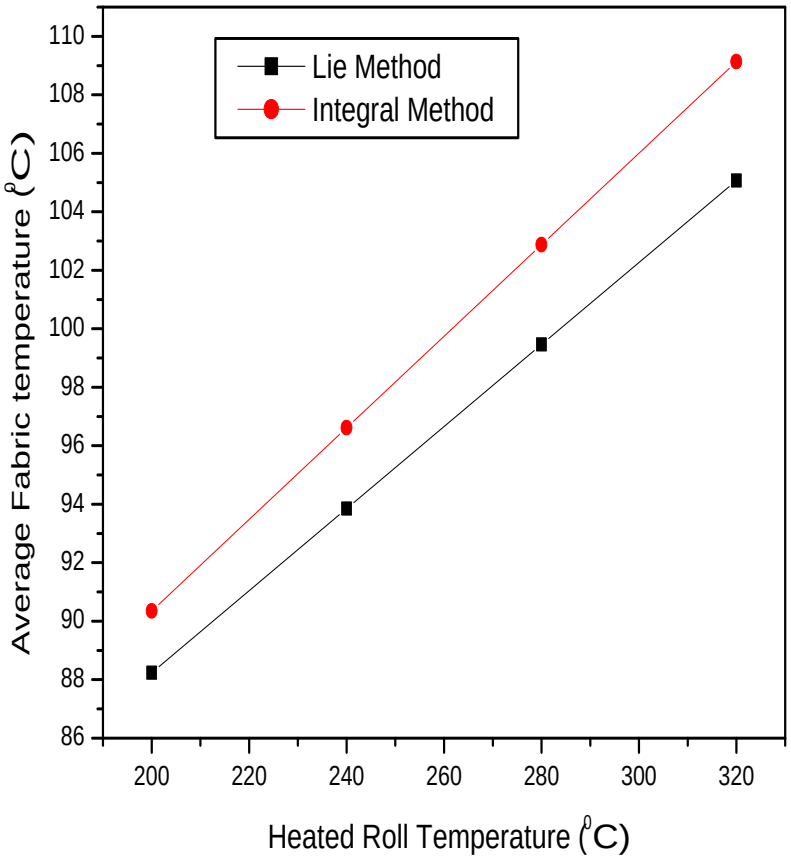

Figure 5.5: Impact of heated roll temperature on average fabric temperature at initial temperature 70°C for incompressible semi infinite medium

5.7.1.3 Impact of Dwell Time on Average Fabric Temperature Considering Incompressible Medium

The impact of dwell time on average fabric temperature having initial temperature 50°C and 70°C considering incompressible medium has been calculated using equations (5.3.22) and (5.4.16). It is found that there is significant error between the results obtained using Lie and Integral method. The calculated values are given in tables 5.9 to 5.16 of APPENDIX. With increase in dwell time, fabric spends more time inside the calender nip due to which heat penetrates upto the center of fabric from the side which is in touch with the heated roll due to which average fabric temperature increases as shown in figures 5.6 and 5.7.

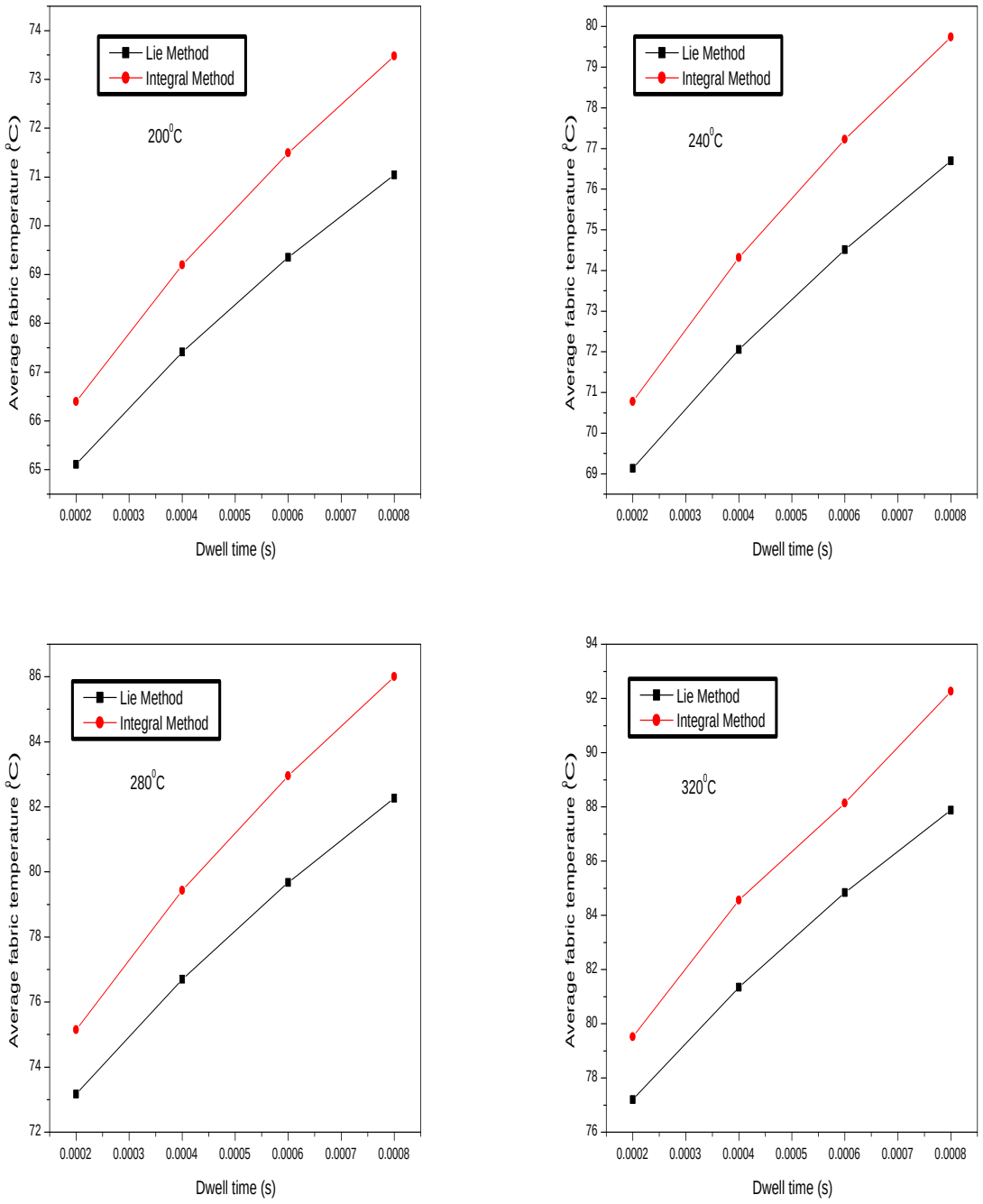

Figure 5.6: Impact of dwell time on average fabric temperature at initial temperature 50°C for incompressible semi infinite medium

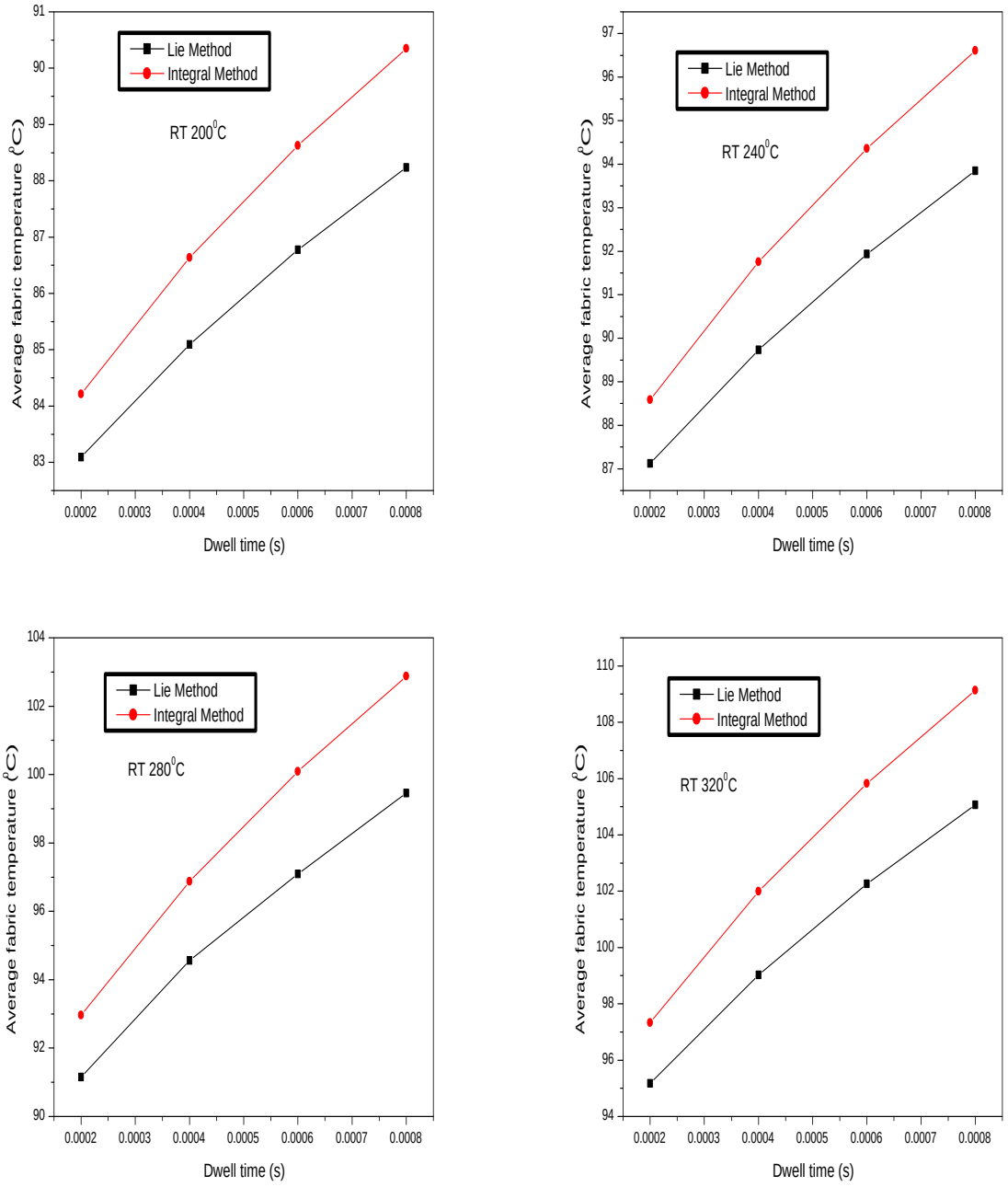

Figure 5.7: Impact of dwell time on average fabric temperature at initial temperature 70°C for incompressible semi infinite medium

5.7.1.4 Impact of Thermal Diffusivity on Average Fabric Temperature Considering Incompressible Medium

The impact of thermal diffusivity on average fabric temperature having initial temperature 50°C and 70°C considering incompressible medium has been calculated using

equations (5.3.22) and (5.4.16). It is found that there is significant error between the results obtained using Lie and Integral method. The calculated values are given in tables 5.17 to 5.24 of APPENDIX. With increase in thermal diffusivity, more heat penetrates to the fabric inside the calender nip upto the center of fabric which increases the average fabric temperature as shown in figures 5.8 and 5.9.

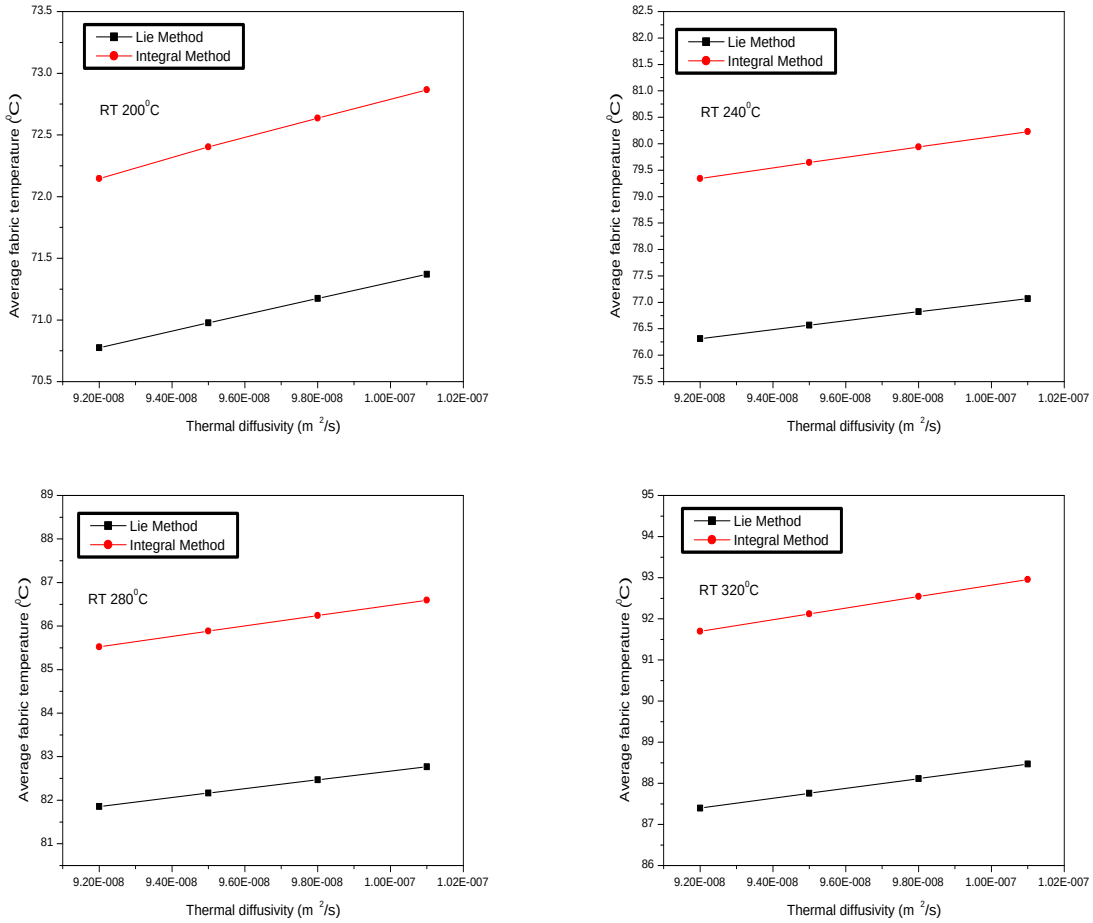

Figure 5.8: Impact of thermal diffusivity on average fabric temperature at initial temperature 50°C for incompressible semi infinite medium

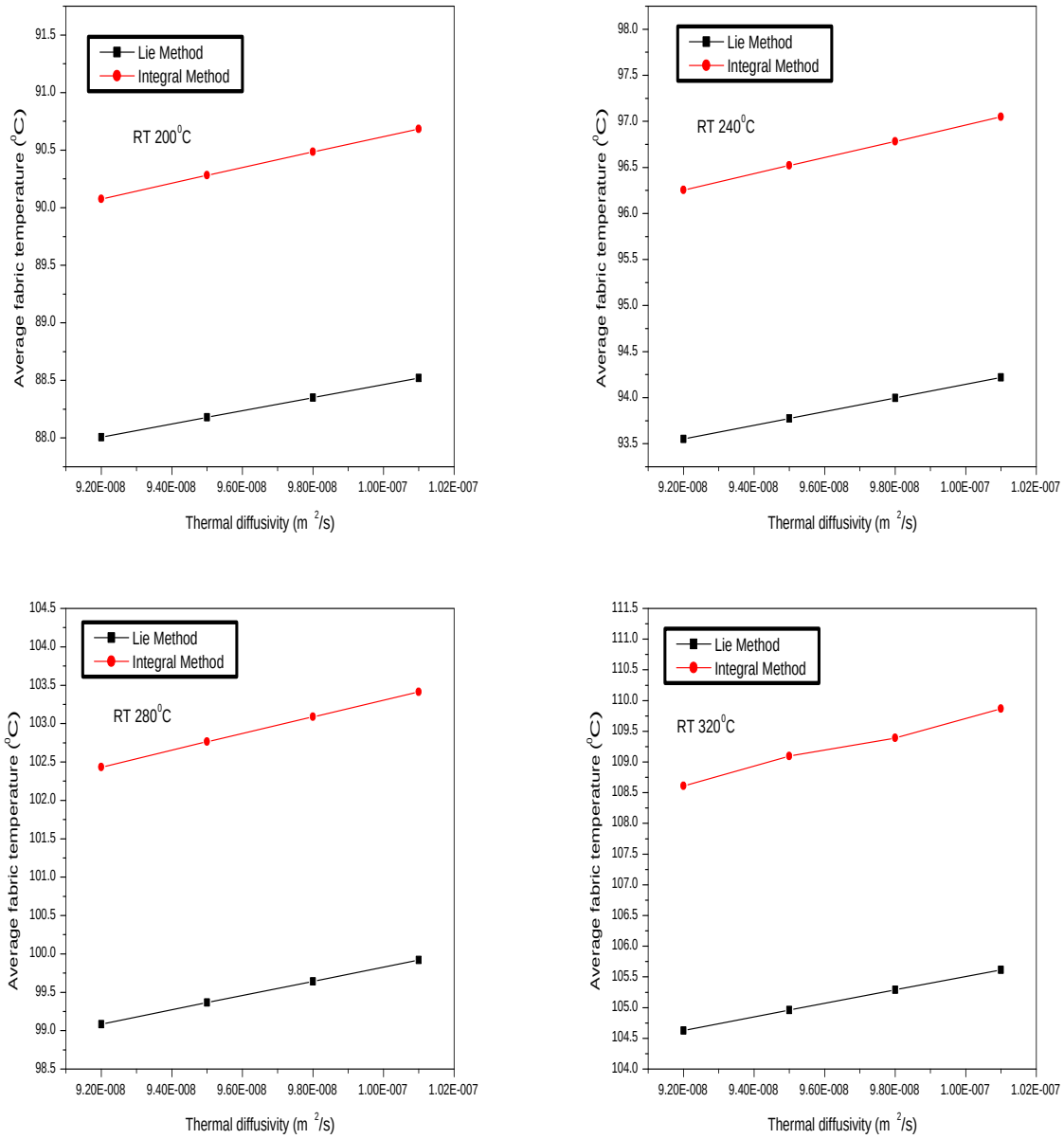

Figure 5.9: Impact of thermal diffusivity on average fabric temperature at initial temperature 70°C for incompressible semi infinite medium

5.7.2 Impact of Various Design and Process Parameters on Temperature Gradient Calender Considering Incompressible and Compressible Medium

The impact of roll temperature on fabric temperature in thickness direction at various depths, impact of dwell time, thermal diffusivity, roll temperature on average fabric temperature has been investigated when fabric is inside the temperature gradient calender considering incompressible and compressible medium.

5.7.2.1 Impact of Roll Temperature on Temperature Profile of Fabric at Distinct Depths in Thickness Direction Considering Incompressible and Compressible Medium

Temperature profile of fabric having initial temperature 50°C and 70°C on various depths has been calculated for compressible semi infinite medium using equations (5.3.22) and (5.5.9). The calculated values are given in tables 5.25 to 5.32 of APPENDIX. It is found that when impact of change in volume is taken into account, there is significant difference in temperature at the outermost surface to the middle of the fabric in thickness direction from heated roll side. The temperature difference after the middle part becomes negligible with increase in web depth as shown in figures 5.10 and 5.11.

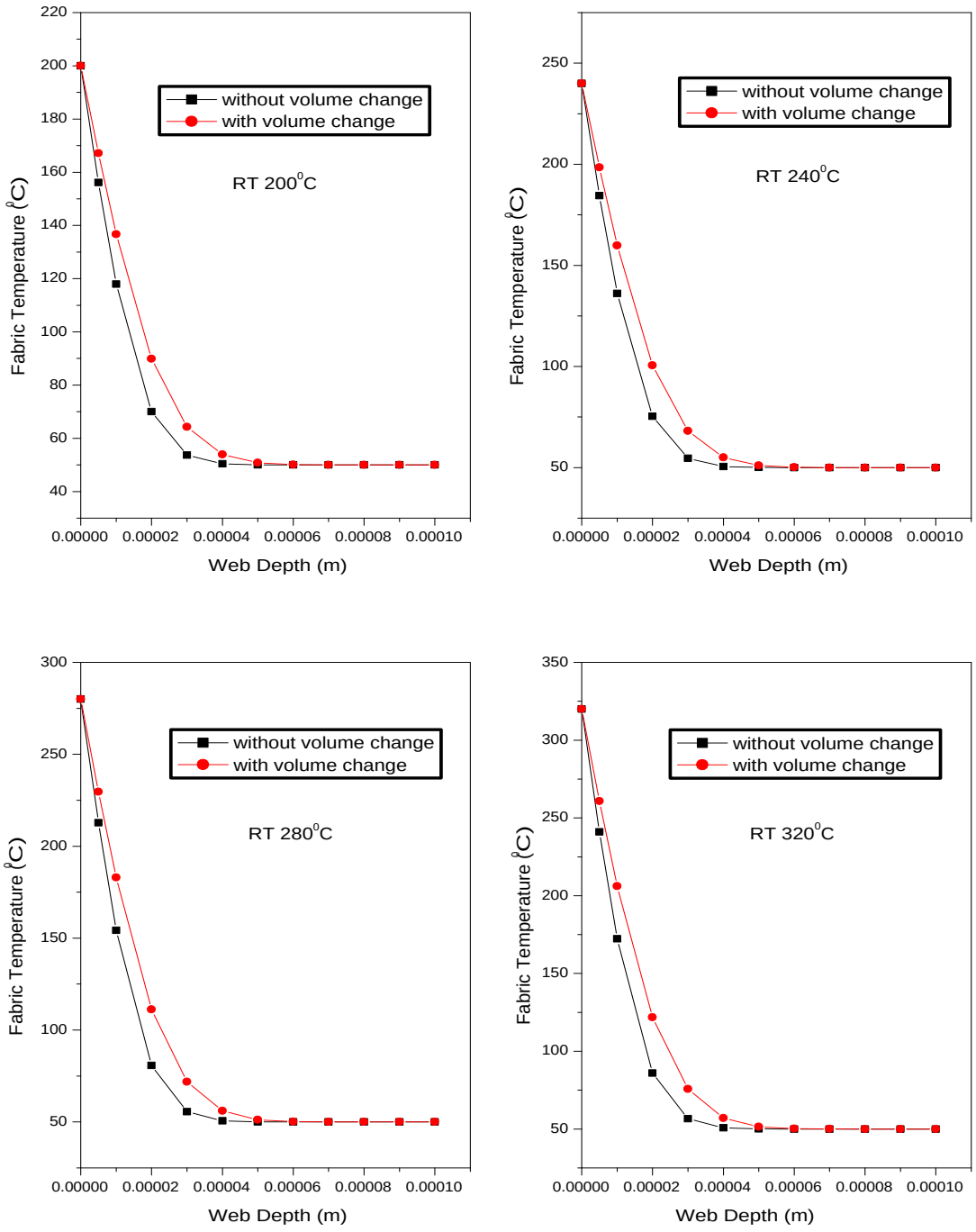

Figure 5.10: Impact of roll temperature on temperature profile of fabric at distinct depths in thickness direction at initial temperature 50°C for incompressible and compressible semi infinite medium

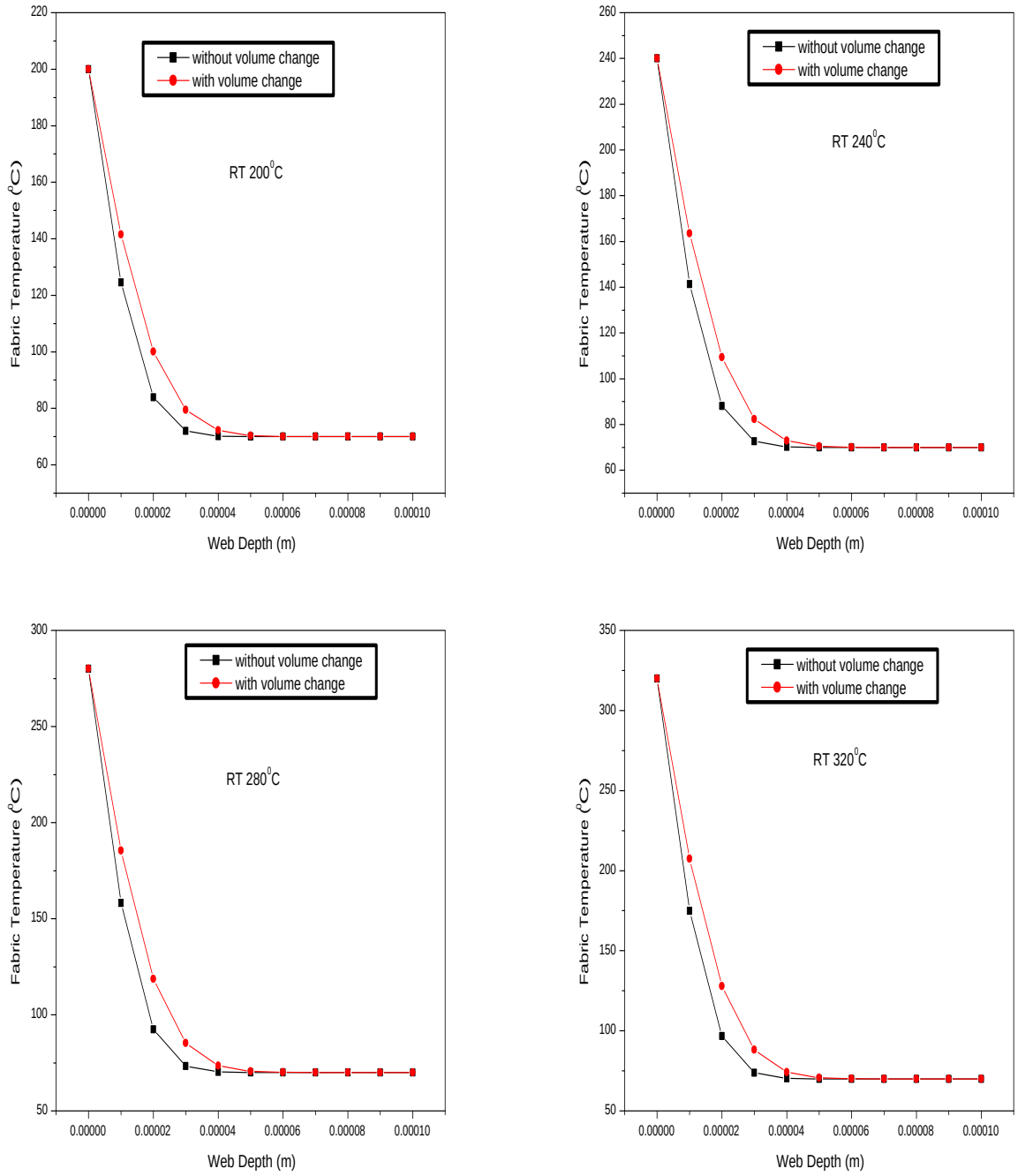

Figure 5.11: Impact of roll temperature on temperature profile of fabric at distinct depths in thickness direction at initial temperature 70°C for incompressible and compressible semi infinite medium

5.7.2.2 Impact of Heated Roll Temperature on Average Fabric Temperature Considering Incompressible and Compressible Medium

The impact of heated roll temperature on average fabric temperature having initial temperature 50°C and 70°C considering compressible medium has been calculated using equations (5.3.22) and (5.5.9). The calculated values are given in tables 5.25 to 5.32 of APPENDIX. It is found that the difference between average fabric temperature for compressible and incompressible semi infinite medium increases with increase in heated roll temperature as shown in figures 5.12 and 5.13.

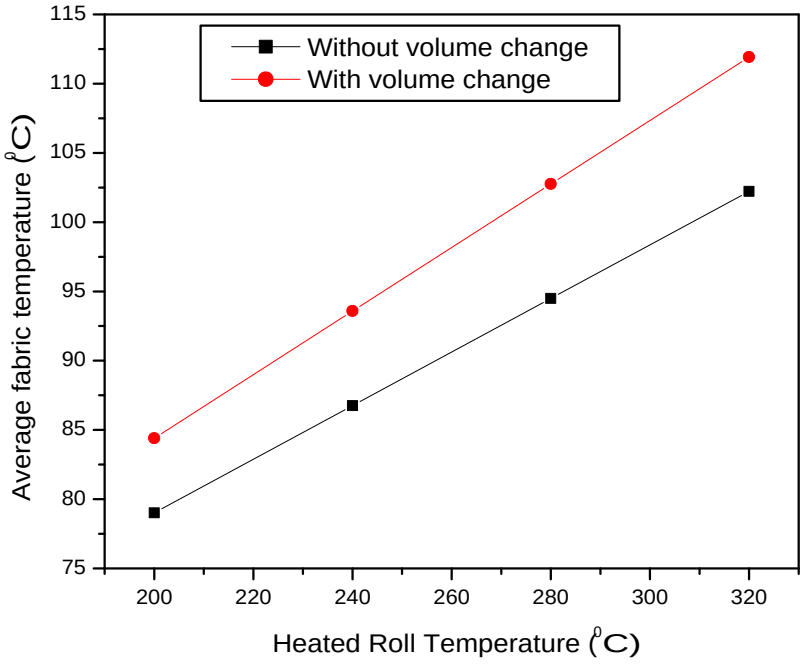

Figure 5.12: Impact of heated roll temperature on average fabric temperature at initial temperature 50°C for incompressible and compressible semi infinite medium

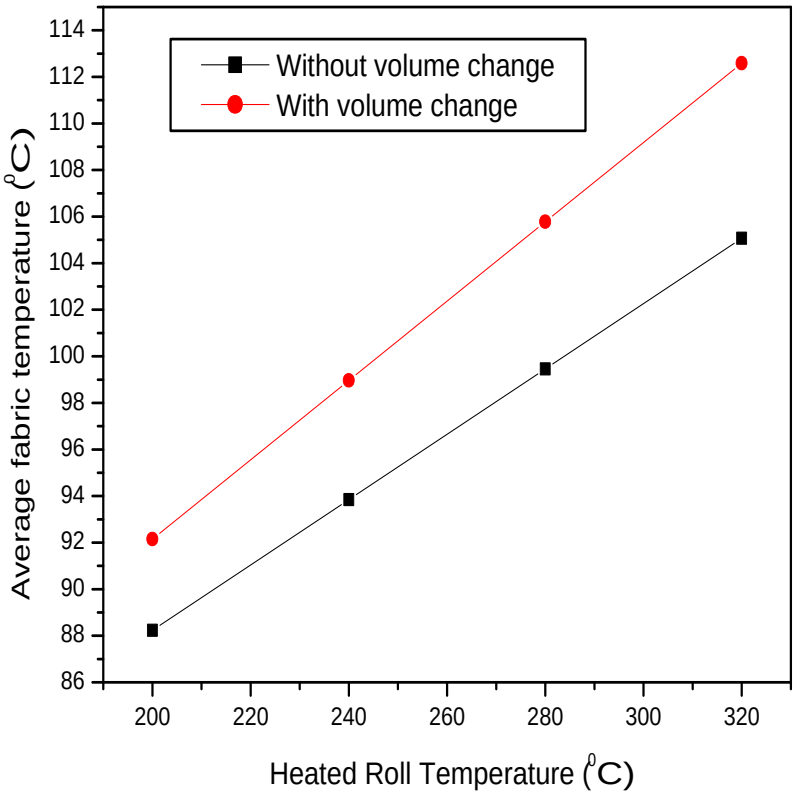

Figure 5.13: Impact of heated roll temperature on average fabric temperature at initial temperature 70°C for incompressible and compressible semi infinite medium

5.7.2.3 Impact of Dwell Time on Average Fabric Temperature Considering Incompressible and Compressible Medium

The impact of dwell time on average fabric temperature having initial temperature 50°C and 70°C considering compressible medium has been calculated using equations (5.3.22) and (5.5.9). The calculated values are given in tables 5.33 to 5.40 of APPENDIX. With increase in dwell time, fabric spends more time inside the calender nip due to which more heat penetrates upto the center of fabric from the side which is in touch with the heated roll which increases average fabric temperature as shown in figures 5.14 and 5.15. It is found that the difference between average fabric temperature for compressible and incompressible semi infinite medium increases with increase in dwell time and roll temperature.

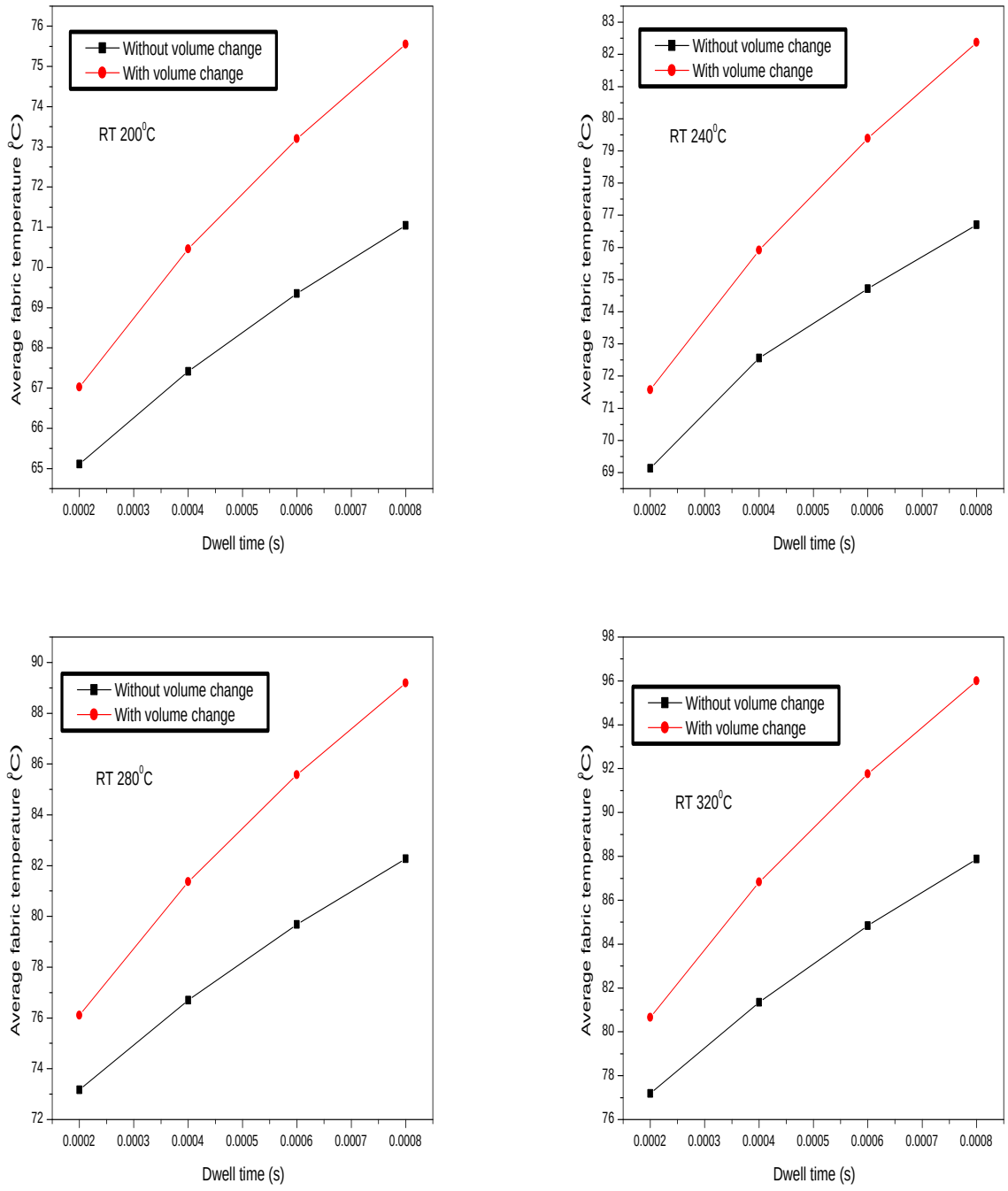

Figure 5.14: Impact of dwell time on average fabric temperature at initial temperature 50°C for incompressible and compressible semi infinite medium

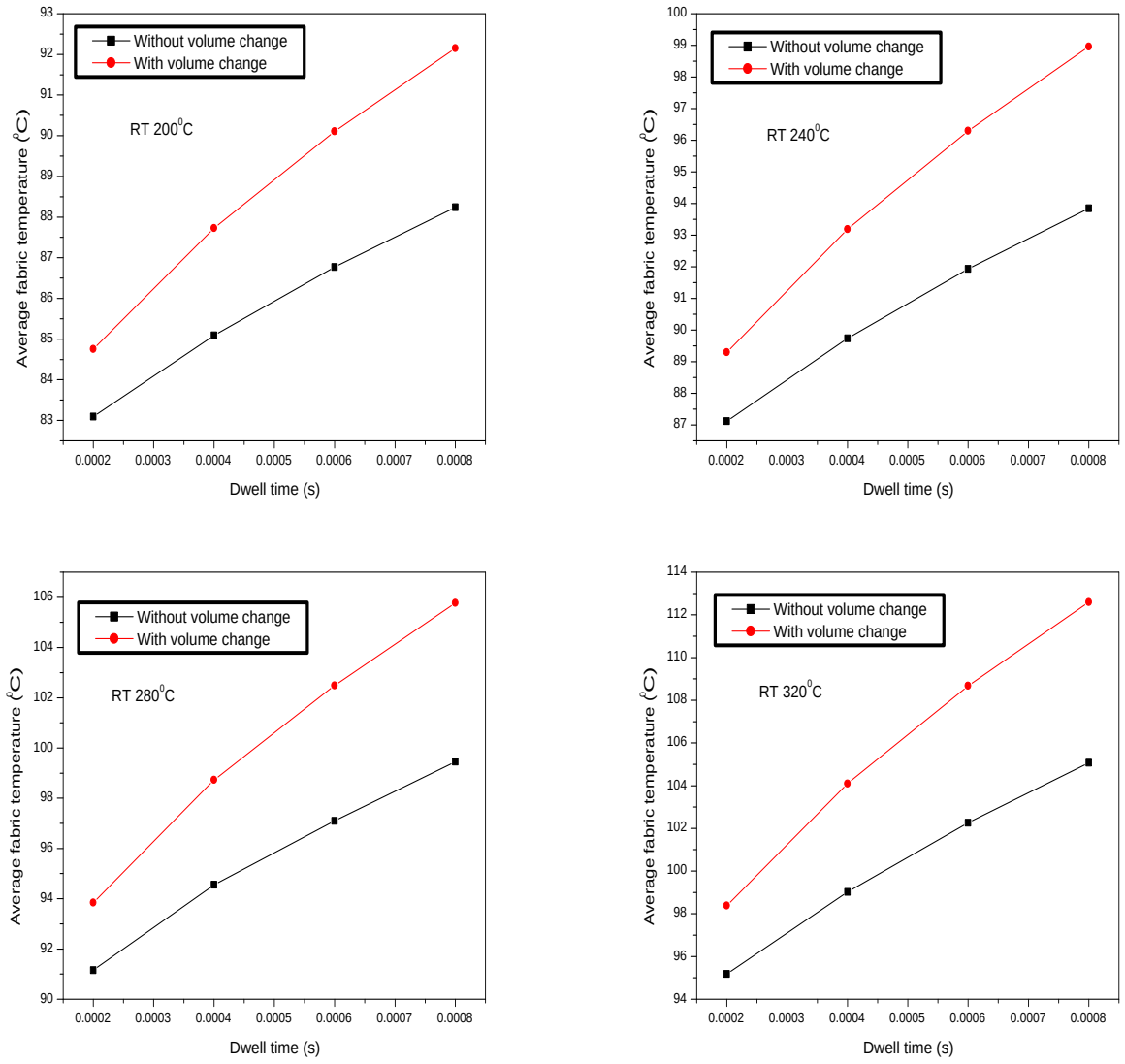

Figure 5.15: Impact of dwell time on average fabric temperature at initial temperature 70°C for incompressible and compressible semi infinite medium

5.7.2.4 Impact of Thermal Diffusivity on Average Fabric Temperature Considering Incompressible and Compressible Medium

The impact of thermal diffusivity on average fabric temperature having initial temperature 50°C and 70°C considering compressible semi infinite medium has been calculated using equations (5.3.22) and (5.5.9). Then the results obtained for incompressible semi infinite medium are compared with the results obtained for compressible semi infinite medium. The calculated values are given in tables 5.41 to 5.48 of

APPENDIX. With increase in thermal diffusivity, more heat penetrates to the fabric inside the calender nip upto the center of fabric which increases the average fabric temperature as shown in figures 5.16 and 5.17. It is found that the difference between average fabric temperature for compressible and incompressible semi infinite medium increases with increase in thermal diffusivity and roll temperature.

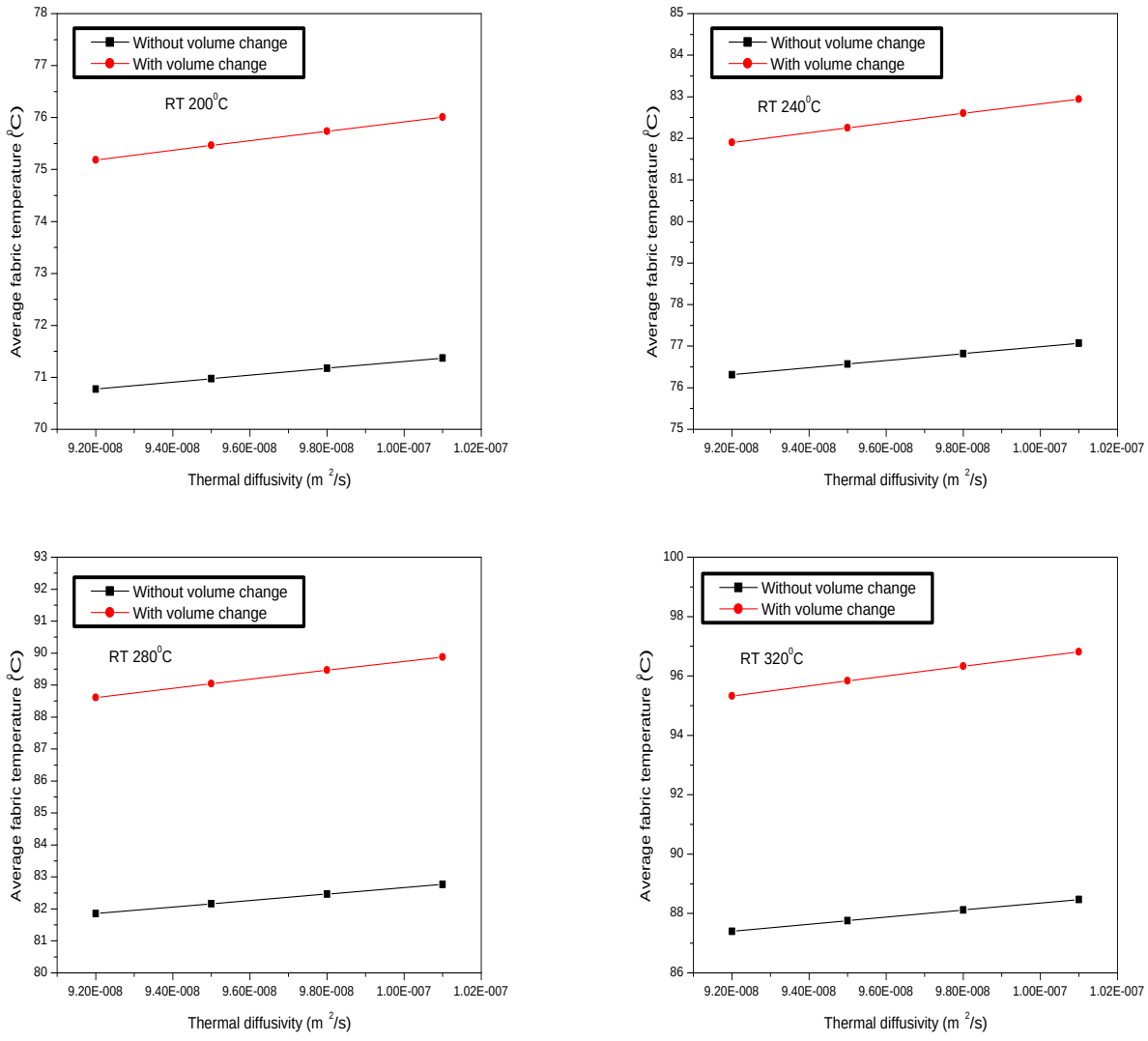

Figure 5.16: Impact of thermal diffusivity on average fabric temperature at initial temperature 50°C for incompressible and compressible semi infinite medium

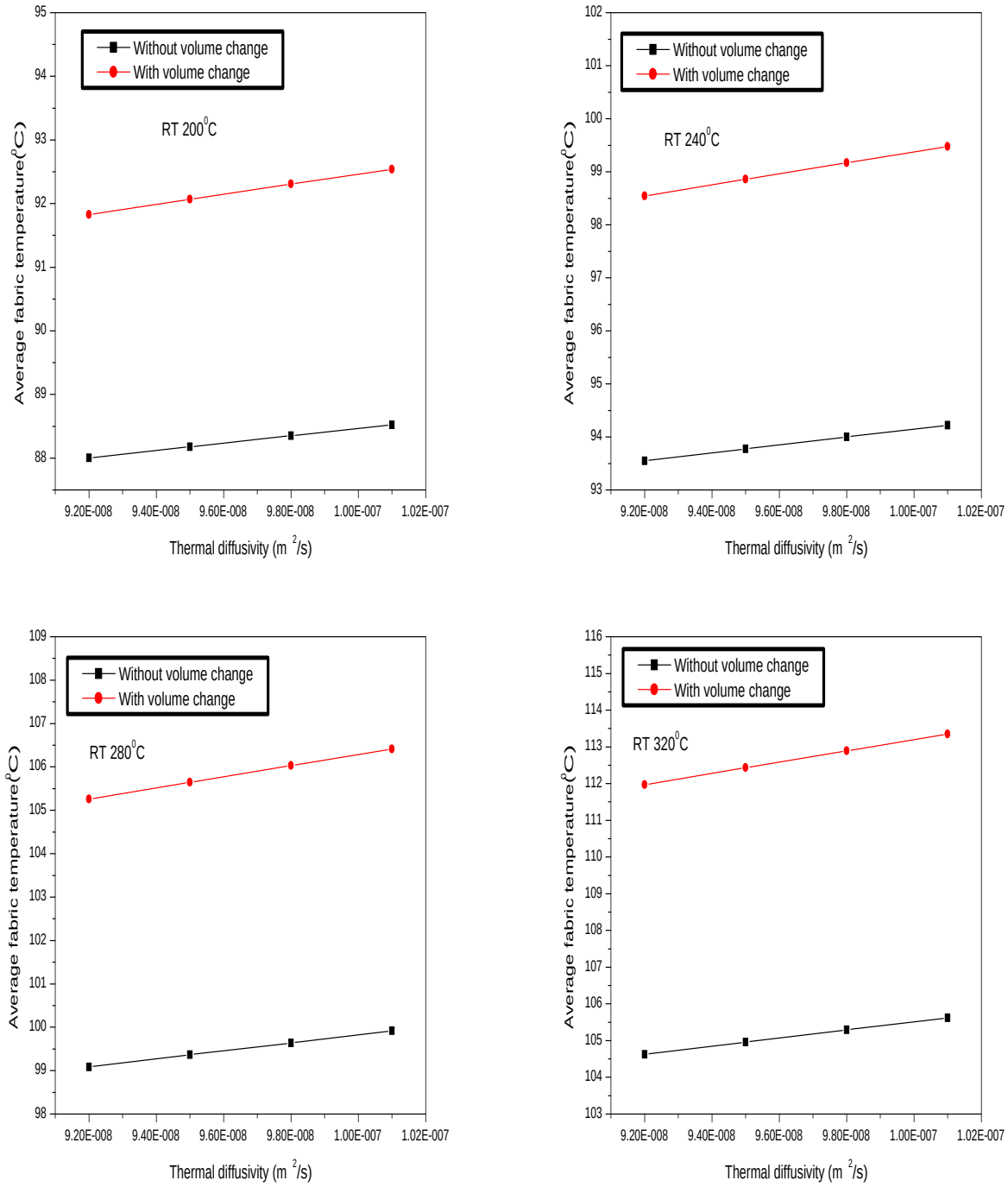

Figure 5.17: Impact of thermal diffusivity on average fabric temperature at initial temperature 70°C for incompressible and compressible semi infinite medium

5.8 Conclusion

The mathematical models developed in this chapter for incompressible and compressible medium can be utilized to anticipate the temperature profile of the fabric in thickness direction in TGC, as it is not possible to measure the temperature of the fabric at distinct depths physically. With increase in heated roll temperature (and/or) dwell time, more heat is conducted to the fabric, which increases the average temperature of the fabric. It is found that for temperature gradient calender when fabric comes out of the nip, there is remarkable increase in average fabric temperature in the range of 25% to 76% with increase in roll temperature from 200°C to 320°C. In case of TGC, heat is not transformed upto the center of the fabric in thickness direction, thus the fibres which are in direct contact with the heated roll get deformed permanently, while the fibres on the other side and upto the middle of the fabric do not get deformed due to which the surface properties of the fabric are developed while maintaining the bulk and strength properties. Subsequently better gloss and smoothness of the fabric can be accomplished in case of TGC with more than one nip without affecting the bulk and strength properties. Also, neglecting the effect of volume change results, difference in amount of heat conducted at distinct depths and on the average fabric temperature, so volume change during the heat transfer inside the calender nip cannot be neglected.

Chapter 6

Heat Transfer Model when Fabric Comes Out from the Calender Nip

The calendering process modifies the structure and surface of the fabric through simultaneous supply of pressure. The inclusion of heat conduction between the roll and the fabric enhances the effect of pressure. Heat transfer to the fabric in calendering system used in textile industry occurs in different situations. When fabric comes out from the calender nip, one side of the fabric is in contact with the heated roll and other side is exposed to air having convective heat loss. During subsequent contact with the roll, fabric assumes a temperature gradient which diminishes as the fabric heats upto the roll temperature. However even after contact over full half circumference of roll, a substantial temperature gradient exists [129–136].

Figure 2 shows the heat transfer to a web (fabric) is governed by three resistances i.e. material resistance of the fabric, contact resistance on the wall side and film resistance on the exposed side. Contact resistance and film resistance are called surface resistances. The nature of these resistances determines the boundary conditions to heat transfer. Material resistance is determined by thermal conductivity and web thickness. The combined effect of contact resistance and thermal conductivity is called apparent thermal conductivity. Contact resistance between fabric and solid surface occurs because of imperfect contact due to surface roughness. The magnitude

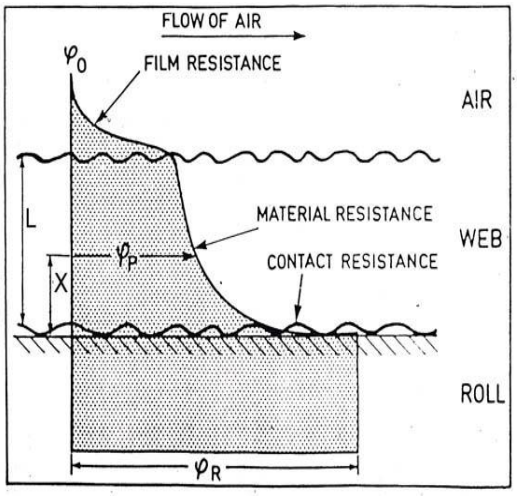

Figure 6.1: Heat transfer when fabric comes out from calender nip

of contact resistance is defined by h_s. Film resistance between the web and flowing air exists because the major resistance to heat transfer to the surroundings occurs over a very small distance in the boundary layer of fabric surface. This resistance is defined by coefficient h_f. The relative importance between the material and surface resistances may be assessed by non dimensional parameter called Biot number given by

$$Bi_s = \frac{L \times h}{k_p}$$

where L is fabric thickness, h is convection heat transfer coefficient and κ_p is thermal conductivity. If Bi is very large, the material resistance offers virtually all of the resistance to heat transfer. If it is small, all of the resistances are offered by surface resistances.

In this chapter, mathematical model for heat transfer have been solved when fabric comes out from the calender nip i.e. one side of fabric is in contact with the roll and other side is in contact with air. The developed mathematical models has been solved for machine calender and rolling calender using analytical and forward time central space finite difference method.

6.1 Mathematical Model for Heat Transfer when Fabric Comes Out of the Calender Nip

The one dimensional heat conduction equation is given by

$$\frac{\partial T}{\partial t} = \alpha \frac{\partial^2 T}{\partial x^2} \tag{6.1.1}$$

with initial and boundary conditions given by

$$T = f(x) \text{ at } t = 0 \tag{6.1.2}$$

$$-\frac{\partial T}{\partial x} + h_s T = 0 \text{ at } x = 0, t > 0 \tag{6.1.3}$$

$$\frac{\partial T}{\partial x} + h_s T = 0 \text{ at } x = L, t > 0 \tag{6.1.4}$$

where h_s is contact heat transfer coefficient. The above B.C represents the radiation at the ends in to the medium at zero temperature. These convection boundary conditions are also known as Newton boundary conditions. These boundary conditions corresponds to the existence of convection heating or cooling at the surface. This condition assumes that the heat conduction at the surface of material is equal to the heat convection at the surface in the same direction.

6.2 Solution of Heat Transfer Model having Convective Boundary Conditions

The expression $e^{-\lambda^2 \alpha t}(A \cos \lambda x + B \sin \lambda x)$ satisfies equation (6.1.1). It also satisfies equations (6.1.3) and (6.1.4) provided that

$$-\lambda B + h_s A = 0 \tag{6.2.1}$$

$$\lambda(B \cos \lambda L - A \sin \lambda L) + h_s(B \sin \lambda L + A \cos \lambda L) = 0 \tag{6.2.2}$$

From equations (6.2.1) and (6.2.2),

$$\frac{A}{B} = \frac{\lambda}{h_s} \tag{6.2.3}$$

and

$$\tan \lambda L = \frac{2\lambda h_s}{\lambda^2 - h_s^2} \tag{6.2.4}$$

where A is any arbitrary constant and λ is any root other than zero of equation (6.2.4). Hence the expression $A(\cos \lambda x + \frac{h_s}{\lambda} \sin \lambda x)e^{-\lambda^2 \alpha t}$ satisfies equations (6.1.1) ,(6.1.3) and (6.1.4).

To form an idea of the distribution of real roots of (6.2.4), the roots correspond to the abscissa of the common points of the curves

$$\eta = 2 \cot \zeta \tag{6.2.5}$$

and

$$\eta = \frac{\zeta}{h_s L} - \frac{h_s L}{\zeta} \tag{6.2.6}$$

The second of these curves is a hyperbola, whose center is at the origin, and whose asymptotes are

$$\zeta = 0 \text{ and } \eta = \frac{\zeta}{h_s L} \tag{6.2.7}$$

If this hyperbola and the cotangent curves are drawn, from that it will be clear that roots lie one in each of the intervals $(0, \pi)$, $(\pi, 2\pi)$,... and the negative roots are equal to the absolute values of the positive ones. Also there are no repeated roots and imaginary roots.

Let us assume that $f(x)$ can be developed in an infinite series

$$f(x) = A_1 X_1 + A_2 X_2 + ... \tag{6.2.8}$$

where

$$X_n = \cos \lambda_n x + \frac{h_s}{\lambda_n x} \tag{6.2.9}$$

and λ being the nth positive root of equation (6.2.4).

Then the solution becomes

$$T = \sum_{n=1}^{\infty} A_n X_n e^{-\alpha \lambda_n^2 t} \tag{6.2.10}$$

Since

$$\frac{d^2 X_m}{dx^2} + \alpha_m^2 X_m = 0 \tag{6.2.11}$$

and

$$\frac{d^2X_n}{dx^2} + \alpha_n^2 X_n = 0 \tag{6.2.12}$$

Multiply equation (6.2.11) by X_n and equation (6.2.12) by X_m and then subtracting resulting equations,

$$(\alpha_m^2 - \alpha_n^2)\int_0^L X_m X_n dx = \int_0^L \left(X_m \frac{d^2X_n}{dx^2} - X_n \frac{d^2X_m}{dx^2}\right)dx \tag{6.2.13}$$

Equation (6.2.13) can be rewritten as

$$(\alpha_m^2 - \alpha_n^2)\int_0^L X_m X_n dx = \left[X_m \frac{dX_n}{dx} - X_n \frac{dX_m}{dx}\right]_0^L \tag{6.2.14}$$

But

$$-\frac{dX_r}{dx} + h_s X_r = 0 \text{ when } x = 0 \tag{6.2.15}$$

$$\frac{dX_r}{dx} + h_s X_r = 0 \text{ when } x = L \tag{6.2.16}$$

where r is any positive integer.

Thus

$$(\alpha_m^2 - \alpha_n^2)\int_0^L X_m X_n dx = 0 \tag{6.2.17}$$

and when $m \neq n$

$$\int_0^L X_m X_n = 0 \tag{6.2.18}$$

$$\alpha_n^2 \int_0^L X_n^2 dx = -\int_0^L X_n \frac{d^2X_n}{dx^2} dx \tag{6.2.19}$$

$$\alpha_n^2 \int_0^L X_n^2 dx = -\left[X_n \frac{dX_n}{dx}\right]_0^L + \int_0^L \left(\frac{dX_n}{dx}\right)^2 dx \tag{6.2.20}$$

But

$$\alpha X_n = \alpha \cos \alpha_n x + h_s \sin \alpha_n x \tag{6.2.21}$$

$$\frac{dX_n}{dx} = -\alpha \sin \alpha_n x + h_s \cos \alpha_n x \tag{6.2.22}$$

Therefore

$$\alpha_n^2 X_n^2 + \left(\frac{dX_n}{dx}\right)^2 = \alpha_n^2 + h^2 \tag{6.2.23}$$

and

$$\alpha_n^2 \int_0^L X_n^2 dx + \int_0^L \left(\frac{dX_n}{dx}\right)^2 dx = (\alpha_n^2 + h_s^2)L \tag{6.2.24}$$

But

$$\alpha_n^2 \int_0^L X_n^2 - \int_0^L \left(\frac{dX_n}{dx}\right)^2 dx = -\left[X_n \frac{dX_n}{dx}\right]_0^L \tag{6.2.25}$$

$$2\alpha_n^2 \int_0^L X_n^2 dx = L(\alpha_n^2 + h_s^2) - \left[X_n \frac{dX_n}{dx}\right]_0^L \tag{6.2.26}$$

$$-\frac{dX_n}{dx} + h_s X_n = 0 \text{ when } x = 0 \tag{6.2.27}$$

$$\frac{dX_n}{dx} + h_s X_n = 0 \text{ when } x = L \tag{6.2.28}$$

Therefore

$$X_n \frac{dX_n}{dx} = -h_s X_n^2 \text{ when } x = L \tag{6.2.29}$$

$$X_n \frac{dX_n}{dx} = h_s X_n^2 \text{ when } x = 0 \tag{6.2.30}$$

But

$$\alpha_n^2 X_n^2 + \left(\frac{dX_n}{dx}\right)^2 = \alpha_n^2 + h_s^2 \tag{6.2.31}$$

Therefore

$$X_n^2 = 1 \text{ both when } x = 0 \text{ and } x = L \tag{6.2.32}$$

Thus

$$\left[X_n \frac{dX_n}{dx}\right]_0^L = -2h_s \tag{6.2.33}$$

and

$$\int_0^L X_n^2 dx = \frac{(\alpha_n^2 + h_s^2)L + 2h_s}{2\alpha_n^2} \tag{6.2.34}$$

Hence, by assuming possibility of expansion and integrating term by term

$$A_n \int_0^L X_n^2 dx = \int_0^L f(x) X_n dx \tag{6.2.35}$$

and

$$A_n = \frac{2\alpha_n^2}{(\alpha_n^2 + h_s^2)L + 2h_s} \int_0^L f(x) X_n dx \tag{6.2.36}$$

Thus

$$T(x,t) = 2\sum_{n=1}^{\infty} e^{-\lambda^2 \alpha t} \frac{\alpha_n \cos \alpha_n x + h_s \sin \alpha_n x}{(\alpha_n^2 + h_s^2)L + 2h_s} \int_0^L f(x)(\alpha_n \cos \alpha_n x + h_s \sin \alpha_n x) dx \tag{6.2.37}$$

If the radiation takes place at $x = 0$ and $x = L$ into media at temperature T_1 and T_2, the problem can be reduced to the above as usual by putting

$$T = u + w \tag{6.2.38}$$

where u is a function of x only, which satisfies the equation

$$\frac{d^2u}{dx^2} = 0 \tag{6.2.39}$$

$$-\frac{du}{dx} + h_s(u - T_1) = 0 \text{ at } x = 0 \tag{6.2.40}$$

$$\frac{du}{dx} + h_s(u - T_2) = 0 \text{ at } x = L \tag{6.2.41}$$

So that

$$u = \frac{(T_2 - T_1)h_s x + T_1(1 + Lh_s) + T_2}{Lh_s + 2} \tag{6.2.42}$$

and w is a function of x and t which satisfies equations

$$\frac{\partial w}{\partial t} = \alpha \frac{\partial^2 w}{\partial x^2} \tag{6.2.43}$$

$$w = f(x) - u \text{ when } t = 0 \tag{6.2.44}$$

$$-\frac{\partial w}{\partial t} + h_s w = 0 \text{ when } x = 0, t > 0 \tag{6.2.45}$$

$$\frac{\partial w}{\partial t} + h_s w = 0 \text{ when } x = L, t > 0 \tag{6.2.46}$$

So the complete solution is

$$\begin{aligned} T = {} & \frac{(T_2 - T_1)h_s x + T_1(1 + Lh_s) + T_2}{Lh_s + 2} \\ & + 2\sum_{n=1}^{\infty} e^{-\lambda^2 \alpha t} \frac{\alpha_n \cos \alpha_n x + h_s \sin \alpha_n x}{(\alpha_n^2 + h_s^2)L + 2h_s} \int_0^L (f(x) - u)(\alpha_n \cos \alpha_n x + h_s \sin \alpha_n x)dx \end{aligned} \tag{6.2.47}$$

If the thickness of slab is taken as $2L$ and origin is taken at the center, then the solution becomes

$$T = \sum_{n=1}^{\infty} e^{-\lambda^2 \alpha t} \frac{c_n \cos \alpha_n x + d_n \sin \alpha_n x}{(\alpha_n^2 + h_s^2)L + h_s} \int_{-L}^{L} f(x)(c_n \cos \alpha_n x + d_n \sin \alpha_n x)dx \tag{6.2.48}$$

where

$$c_n = h_s \sin \alpha_n L + \alpha_n \cos \alpha_n L \tag{6.2.49}$$

$$d_n = h_s \cos \alpha_n L - \alpha_n \sin \alpha_n L \tag{6.2.50}$$

and α_n are the positive roots of

$$\tan 2\alpha L = \frac{2\alpha h_s}{\alpha^2 - h_s^2} \tag{6.2.51}$$

since the above equation is equivalent to

$$(h_s \sin \alpha L + \alpha \cos \alpha L)(h_s \cos \alpha L - \alpha \sin \alpha L) = 0 \tag{6.2.52}$$

Its positive root α_n, comprise the positive roots of two equations

$$\alpha \tan \alpha L - h_s = 0 \tag{6.2.53}$$

$$\alpha \tan \alpha L + h_s = 0 \tag{6.2.54}$$

If $f(x)$ is an even function of x, equation (6.2.48) reduces to

$$T = 2 \sum_{n=1}^{\infty} e^{-\lambda^2 \alpha t} \frac{(h_s^2 + \alpha_n^2) \cos \alpha_n x}{(\alpha_n^2 + h_s^2)L + h_s} \int_0^L f(x) \cos \alpha_n x dx \tag{6.2.55}$$

where α_n is the positive root of equation (6.2.53). This is also the solution of the problem of conduction of heat in the region $0 < x < L$, with no flow of heat over the region $x = 0$, radiation into a medium at zero at $x = L$, and initial temperature $f(x)$.
If $f(x)$ is a odd function of x, equation (6.2.48) reduces to

$$T = 2 \sum_{n=1}^{\infty} e^{-\lambda^2 \alpha t} \frac{(h_s^2 + \alpha_n^2) \sin \alpha_n x}{(\alpha_n^2 + h_s^2)L + h} \int_0^L f(x) \sin \alpha_n x dx \tag{6.2.56}$$

where α_n are the positive root of equation (6.2.54). This is also the solution of the problem of conduction of heat in the region $0 < x < L$, with $x = 0$ maintained at zero temperature, radiation in to the medium at zero temperature at $x = L$, and initial temperature $f(x)$.
If $f(x)$ is neither even nor odd, the solution is given by equation (6.2.48), and involves the root of both equations (6.2.53) and (6.2.54). If the initial temperature of the body is T_0, then the solution becomes

$$\frac{T}{T_0} = \sum_{n=1}^{\infty} \frac{2h_s \cos \alpha_n x}{[(\alpha_n^2 + h_s^2)L + h_s] \cos \alpha_n L} e^{-\lambda^2 \alpha t} \tag{6.2.57}$$

If the initial temperature of the body is zero, and it is heated by radiation from a medium at T_R, the solution becomes

$$\frac{T}{T_R} = 1 - \sum_{n=1}^{\infty} \frac{2h_s \cos \alpha_n x}{[(\alpha_n^2 + h_s^2)L + h_s] \cos \alpha_n L} e^{-\lambda^2 \alpha t} \tag{6.2.58}$$

Let

$$\vartheta = T - T_0 \tag{6.2.59}$$

Then equation (6.1.1) becomes

$$\frac{\partial \vartheta}{\partial t} = \alpha \frac{\partial^2 \vartheta}{\partial x^2} \tag{6.2.60}$$

with initial condition

$$\vartheta(x, 0) = 0 \tag{6.2.61}$$

and boundary conditions

$$\frac{\partial \vartheta}{\partial x} = \frac{h_s}{k_p}(\vartheta - \vartheta_R) \text{ at } x = 0 \tag{6.2.62}$$

$$\frac{\partial \vartheta}{\partial x} = 0 \text{ at } x = L \tag{6.2.63}$$

The exposed side is considered to be insulated.

The solution of equation with convective boundary conditions is given by

$$\frac{\vartheta}{T_R} = 1 - \frac{2e^{-E_p} cos(\sqrt{Bi_s}(1 - \frac{X}{L}))}{(2 + Bi_s) cos\sqrt{Bi_s}} - \sum_{n=2}^{\infty} \frac{(-1)^{n+1}(2Bi_s)e^{-\frac{\pi^2(n-1)^2 E_p}{Bi_s}} \cos \frac{(n-1)\pi(L-X)}{L}}{Bi_s^2 + Bi_s + (n-1)^2\pi^2} \tag{6.2.64}$$

where E_p is the exponent given by

$$E_p = \frac{\kappa_p Bi_s t}{C_p W_b L} \tag{6.2.65}$$

where t is the time for which fabric is in contact with the roll, κ_p is thermal conductivity, C_p is specific heat, W_b is the fabric basis weight, Bi_s is the Biot number for contact resistance.

In equation (6.2.64), ϑ is the difference between fabric temperature and initial temperature of fabric given by equation (6.2.59). T_R is the difference between the roll temperature R_T and the initial temperature T_0 i.e. $T_r = R_T - T_0$. Therefore

$$\frac{T - T_0}{R_T - T_0} = 1 - \frac{2e^{-E_p} cos(\sqrt{Bi_s}(1 - \frac{X}{L}))}{(2 + Bi_s) cos\sqrt{Bi_s}} - \sum_{n=2}^{\infty} \frac{(-1)^{n+1}(2Bi_s)e^{-\frac{\pi^2(n-1)^2 E_p}{Bi_s}} \cos \frac{(n-1)\pi(L-X)}{L}}{Bi_s^2 + Bi_s + (n-1)^2\pi^2} \tag{6.2.66}$$

Hence,

$$T = T_0 + (R_T - T_0)\left(1 - \frac{2e^{-E_p}cos(\sqrt{Bi_s}(1-\frac{X}{L}))}{(2+Bi_s)cos\sqrt{Bi_s}} - \sum_{n=2}^{\infty}\frac{(-1)^{n+1}(2Bi_s)e^{-\frac{\pi^2(n-1)^2E_p}{Bi_s}}\cos\frac{(n-1)\pi(L-X)}{L}}{Bi_s^2+Bi_s+(n-1)^2\pi^2}\right) \tag{6.2.67}$$

Equation (6.2.67) is the solution of heat conduction under convective boundary conditions when $E_p < 0.05$.

when $E_p > 0.05$,

$$T = T_0 + (R_T - T_0)\left(1 - \frac{2e^{-E_p}cos(\sqrt{Bi_s}(1-\frac{X}{L}))}{(2+Bi_s)cos\sqrt{Bi_s}}\right) \tag{6.2.68}$$

6.3 Solution of Heat transfer Model using Forward Time Central Space Method

In this section, solution of heat transfer model has been solved using forward time central space method. On applying energy balance for n^{th} node,

$$-kA\frac{\partial T}{\partial x} + hA(T_{inf} - T_{n,0}) = \rho cA\frac{\Delta x}{2}\frac{\partial T}{\partial t} \tag{6.3.1}$$

where T_{inf} is temperature close to node n and $T_{n,0}$ is initial temperature at node n. Using FTCS finite difference approximations,

$$-k\frac{(T_{n,0} - T_{n-1,0})}{\Delta x} + h(T_{inf} - T_{n,0}) = \rho c\frac{\Delta x}{2}\frac{T_{n,1} - T_{n,0}}{\Delta t} \tag{6.3.2}$$

Multiply equation (6.3.2) with $\frac{2\Delta x}{k}$,

$$2(T_{n-1,0} - T_{n,0}) + \frac{2h\Delta x}{k}(T_{inf} - T_{n,0}) = \frac{\rho c\Delta x^2}{k}\left(\frac{T_{n,1} - T_{n,0}}{\Delta t}\right) \tag{6.3.3}$$

$$2T_{n-1,0} - 2T_{n,0} + \left(\frac{2h\Delta x}{k}\right)T_{inf} - \left(\frac{2h\Delta x}{k}\right)T_{n,0} = \frac{\Delta x^2}{\alpha\Delta t}T_{n,1} - \frac{\Delta x^2}{\alpha\Delta t}T_{n,0} \tag{6.3.4}$$

On rearranging,

$$T_{n,1} = \frac{\alpha\Delta t}{\Delta x^2}\left(\frac{2h\Delta x}{k}T_{inf} + 2T_{n-1,0} + (\frac{\Delta x^2}{\alpha\Delta t} - \frac{2h\Delta x}{k} - 2)T_{n,0}\right) \tag{6.3.5}$$

$$T_{n,1} = d\big(2Bi\ T_{inf} + 2T_{n-1,0} + (\frac{1}{d} - 2Bi - 2)T_{n,0}\big) \tag{6.3.6}$$

where d is non dimensional diffusion number given by $d = \frac{\alpha \Delta t}{\Delta x^2}$, Bi is biot number. Discretizing the domain into ten grid spacing and then applying energy balance at first and eleventh node. On applying energy balance for 1^{st} node,

$$-kA\frac{\partial T}{\partial x} + h_1 A(T_{inf1} - T_{1,0}) = \rho c \frac{\Delta x}{2} A \frac{\partial T}{\partial t} \tag{6.3.7}$$

where T_{inf1} is temperature close to node 1 and $T_{1,0}$ is initial temperature at node 1.

$$-k\frac{(T_{1,0} - T_{2,0})}{\Delta x} + h_1(T_{inf1} - T_{1,0}) = \rho c \frac{\Delta x}{2} \frac{T_{1,1} - T_{1,0}}{\Delta t} \tag{6.3.8}$$

Multiply with above equation with $(\frac{2\Delta x}{k})$,

$$2(T_{2,0} - T_{1,0}) + \left(\frac{2h_1 \Delta x}{k}\right) T_{inf1} - T_{1,0} = \frac{\rho c \Delta x^2}{k} \frac{T_{1,1} - T_{1,0}}{\Delta t} \tag{6.3.9}$$

$$2T_{2,0} - 2T_{1,0} + \left(\frac{2h_1 \Delta x}{k}\right) T_{inf1} - \left(\frac{2h_1 \Delta x}{k}\right) T_{1,0} = \frac{\Delta x^2}{\alpha \Delta t} T_{1,1} - \frac{\Delta x^2}{\alpha \Delta t} T_{1,0} \tag{6.3.10}$$

On rearranging,

$$T_{1,1} = \frac{\alpha \Delta t}{\Delta x^2}\left(\frac{2h_1 \Delta x}{k} T_{inf1} + 2T_{2,0} + (\frac{\Delta x^2}{\alpha \Delta t} - \frac{2h\Delta x}{k} - 2)T_{1,0}\right) \tag{6.3.11}$$

$$T_{1,1} = d(2Bi_1 T_{inf1} + 2T_{2,0} + (\frac{1}{d} - 2Bi_1 - 2)T_{1,0}) \tag{6.3.12}$$

where Bi_1 is biot number at first node given by $Bi_1 = \frac{h_1 \Delta x}{k}$.

On applying energy balance for 11^{th} node,

$$-kA\frac{\partial T}{\partial x} + h_2 A(T_{inf2} - T_{11,0}) = \rho c \frac{\Delta x}{2} A \frac{\partial T}{\partial t} \tag{6.3.13}$$

where T_{inf2} is ambient temperature close to node 11 and $T_{11,0}$ is initial temperature at node 11.

$$-k\frac{(T_{11,0} - T_{10,0})}{\Delta x} + h_2(T_{inf2} - T_{11,0}) = \rho c \frac{\Delta x}{2} \frac{T_{11,1} - T_{11,0}}{\Delta t} \tag{6.3.14}$$

Multiply with equation (6.3.14) with $(\frac{2\Delta x}{k})$,

$$2(T_{10,0} - T_{11,0}) + \left(\frac{2h_2 \Delta x}{k}\right)(T_{inf2} - T_{11,0}) = \frac{\rho c \Delta x^2}{k} \frac{T_{11,1} - T_{11,0}}{\Delta t} \tag{6.3.15}$$

$$2T_{10,0} - 2T_{11,0} + \left(\frac{2h_2 \Delta x}{k}\right) T_{inf2} - \left(\frac{2h_2 \Delta x}{k}\right) T_{11,0} = \frac{\Delta x^2}{\alpha \Delta t} T_{11,1} - \frac{\Delta x^2}{\alpha \Delta t} T_{11,0} \tag{6.3.16}$$

On rearranging,

$$T_{11,1} = \frac{\alpha \Delta t}{\Delta x^2}\left(\frac{2h_2 \Delta x}{k} T_{inf2} + 2T_{10,0} + (\frac{\Delta x^2}{\alpha \Delta t} - \frac{2h\Delta x}{k} - 2)T_{11,0}\right) \tag{6.3.17}$$

$$T_{11,1} = d\left(2Bi_2 T_0 + 2T_{10,0} + (\frac{1}{d} - 2Bi_2 - 2)T_{11,0}\right) \tag{6.3.18}$$

where Bi_2 is biot number at eleventh node given by $Bi_2 = \frac{h_2 \Delta x}{k}$.
Substituting the values of diffusion parameter, Biot number in equations (6.3.12) and (6.3.18) and solve these equations for first and eleventh node using MATLAB.

6.4 Simulation of Models

Simulation of heat transfer model when fabric comes out from the calender nip is done for machine and rolling single nip calender using equations (6.2.67), (6.2.68), and (6.3.6). Roll temperature (RT) is taken in the range from 100°C to 210°C for machine calender and from 70°C to 210°C for rolling calender. The initial fabric temperature are taken as 50°C and 70°C. The range of design and process parameters and adopted values for single nip machine calender and rolling calender for simulation purpose are given in table (3.1) of APPENDIX.

6.5 Results and Discussion

6.5.1 Impact of Roll Temperature on Fabric Temperature in Thickness Direction at Various Depths for Machine Calender having Same and Different Roll Temperature

The impact of roll temperature on fabric temperature in thickness direction at various depths with initial temperature 50°C and 70°C has been investigated when fabric comes out from the machine calender nip having same and different roll temperature. The calculated values are given in tables 6.1 to 6.32 of APPENDIX. The results

obtained are shown in figures 6.2 to 6.9.

It clearly shows that when fabric comes out from the machine calender nip having same and different roll temperature, the side of fabric which is in touch with the hot roll gets heated and temperature decreases as depth increases. The other side of fabric which is in contact with air remains nearly at the same average temperature. Also it is found that more heat penetrates into the fabric when $E_p > 0.05$. The results obtained using analytical method are compared with forward time central space method. It is found that there is a significant error in the results obtained using these methods.

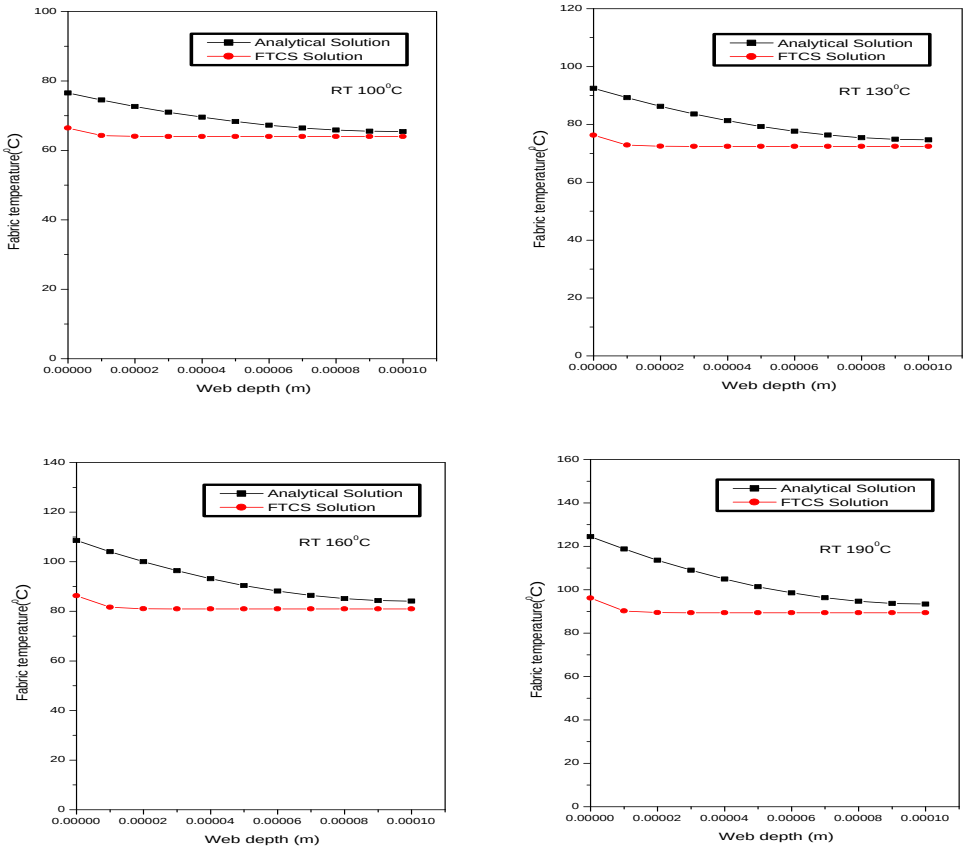

Figure 6.2: Impact of same roll temperature on fabric temperature in thickness direction at various depths with initial temperature 50°C when $E_p < 0.05$ for machine calender

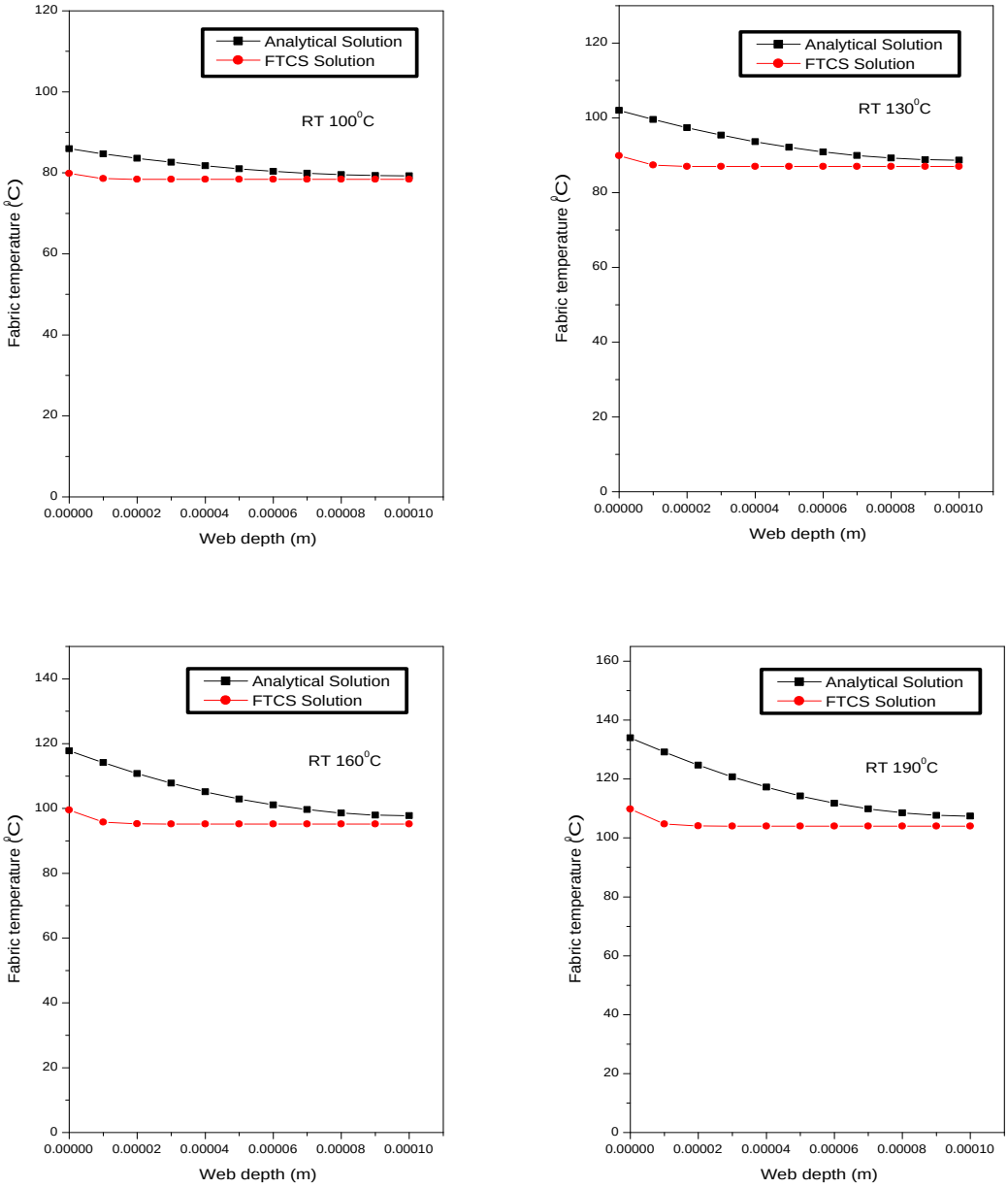

Figure 6.3: Impact of same roll temperature on fabric temperature in thickness direction at various depths with initial temperature 70°C when $E_p < 0.05$ for machine calender

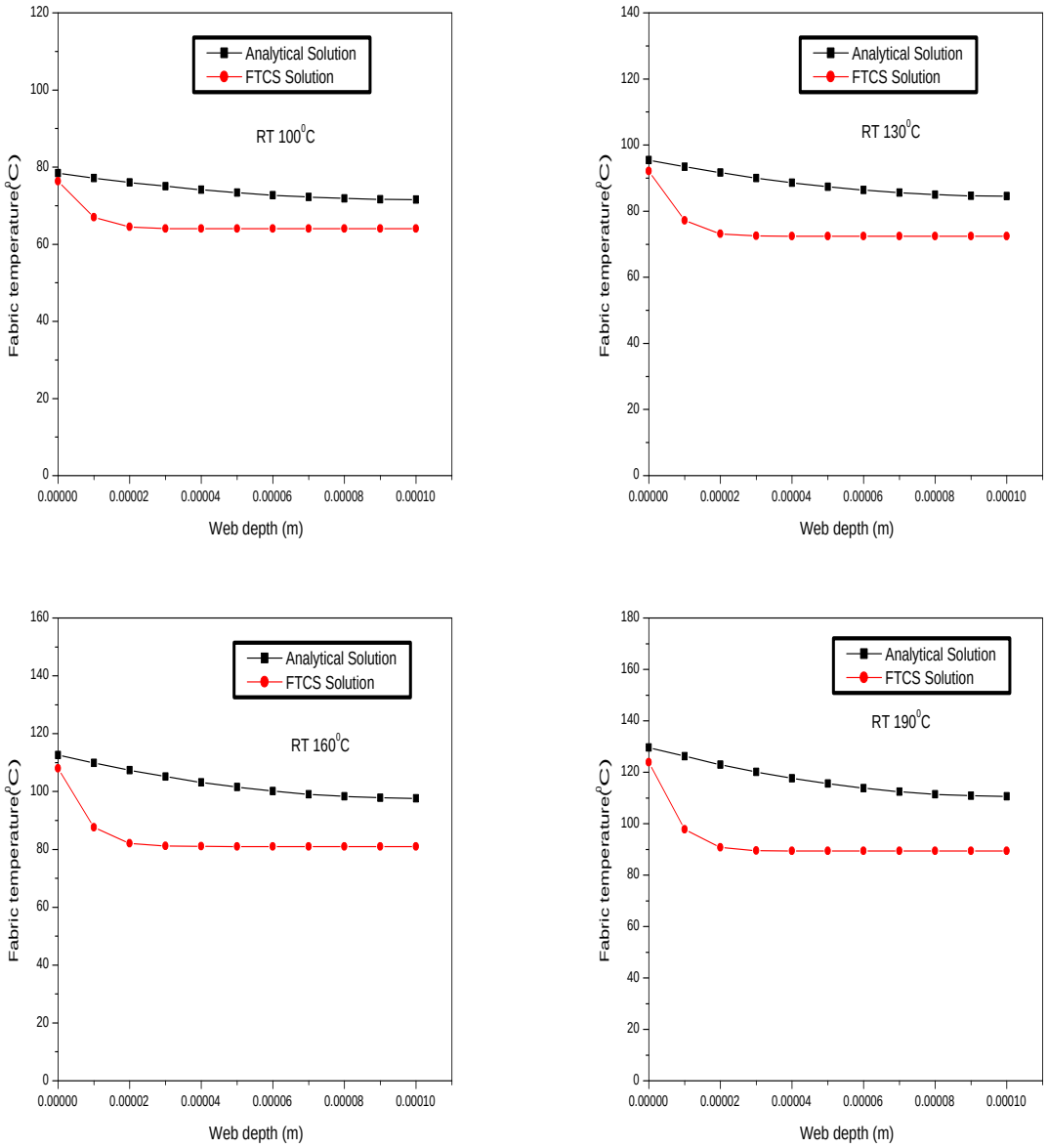

Figure 6.4: Impact of same roll temperature on fabric temperature in thickness direction at various depths with initial temperature 50°C when $E_p > 0.05$ for machine calender

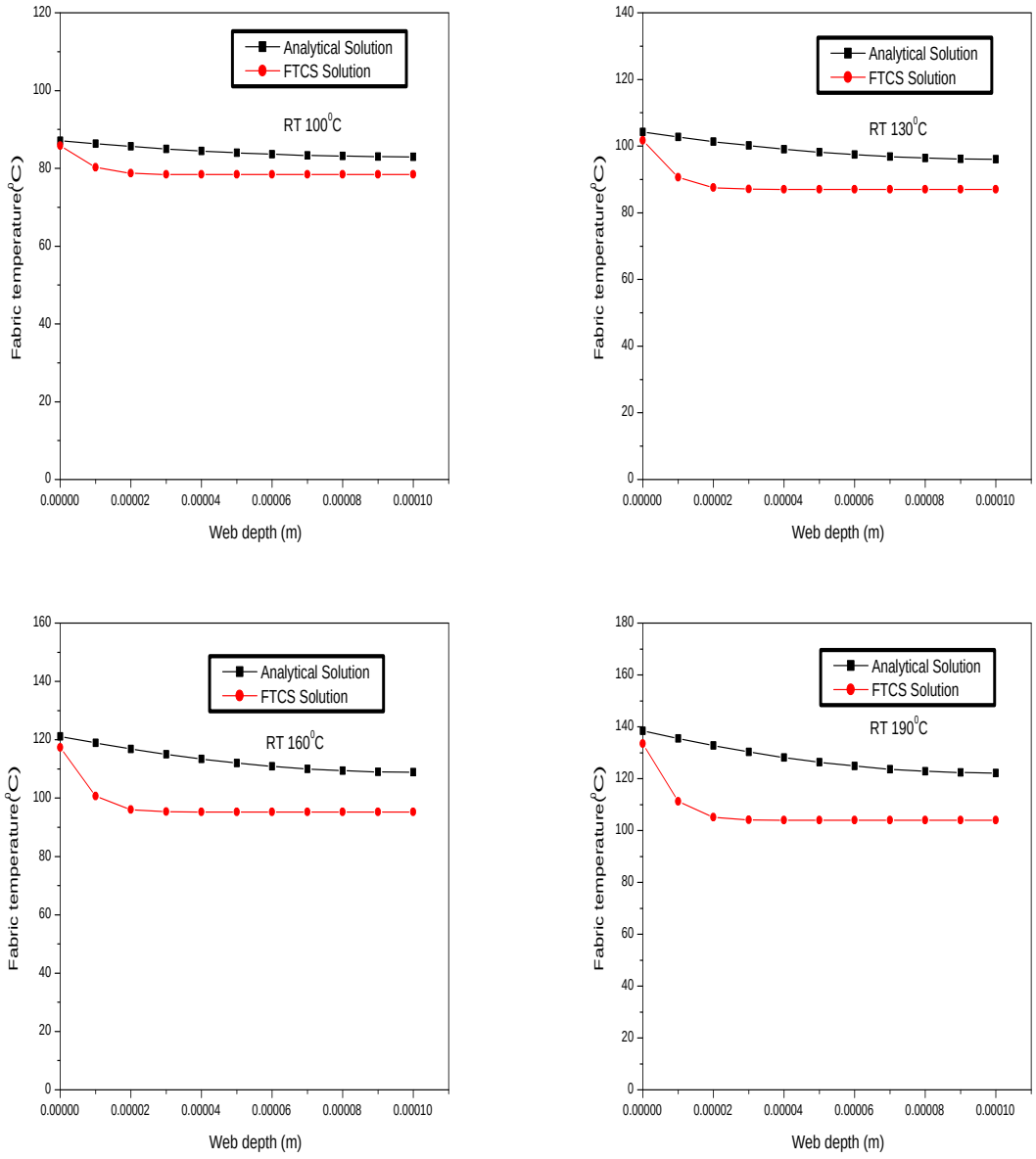

Figure 6.5: Impact of same roll temperature on fabric temperature in thickness direction at various depths with initial temperature 70°C when $E_p > 0.05$ for machine calender

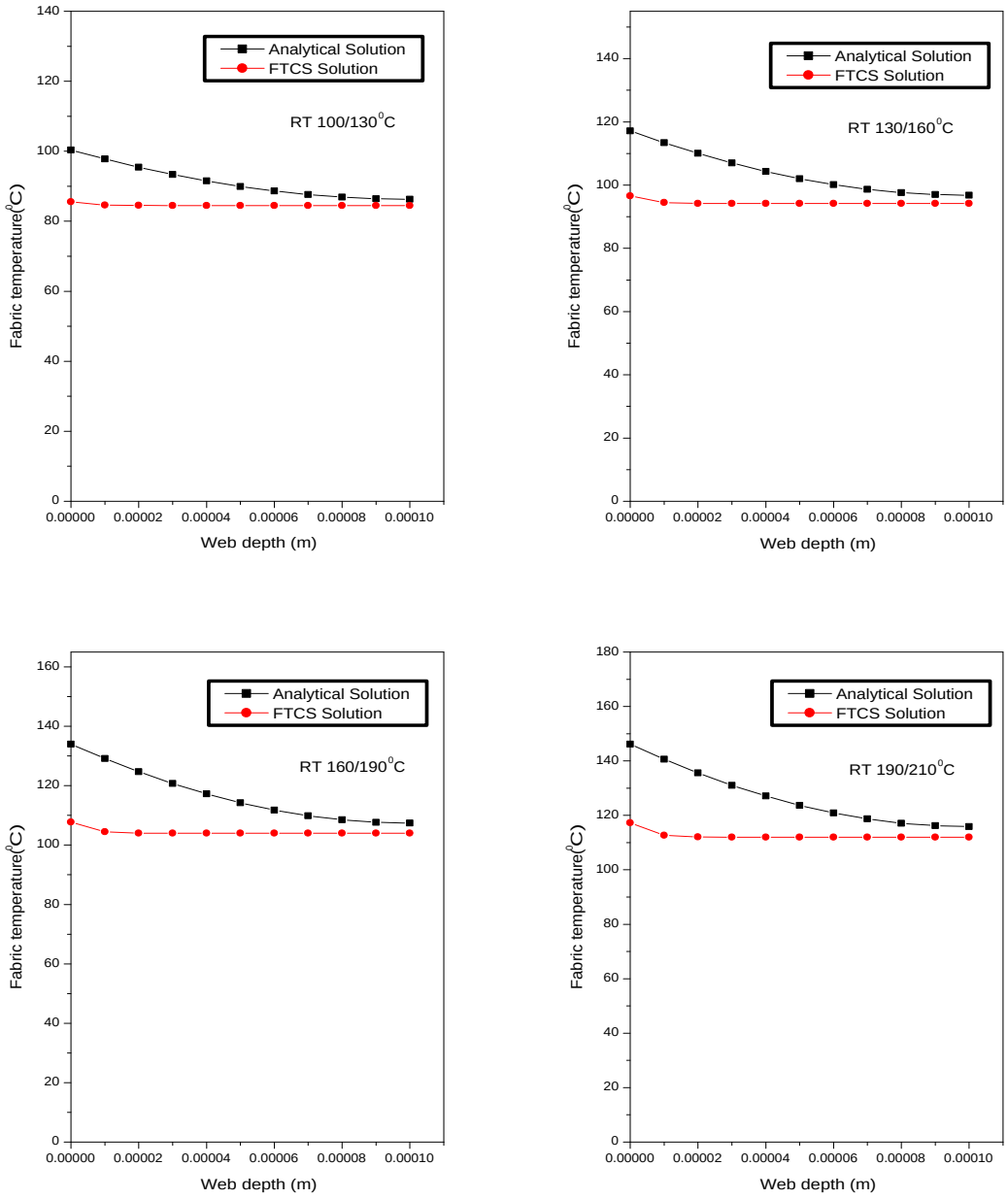

Figure 6.6: Impact of different roll temperature on fabric temperature in thickness direction at various depths with initial temperature 50°C when $E_p < 0.05$ for machine calender

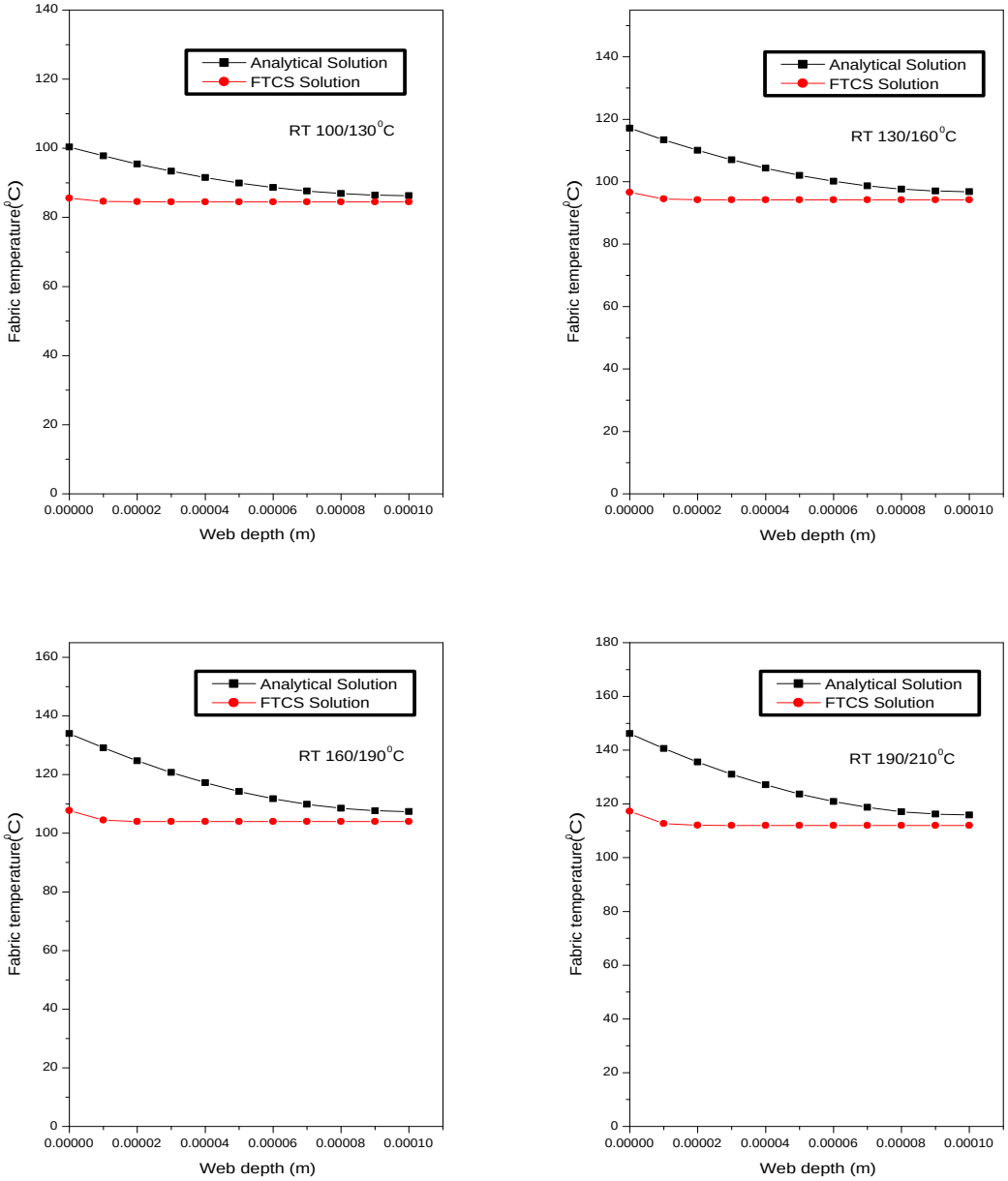

Figure 6.7: Impact of different roll temperature on fabric temperature in thickness direction at various depths with initial temperature 70°C when $E_p < 0.05$ for machine calender

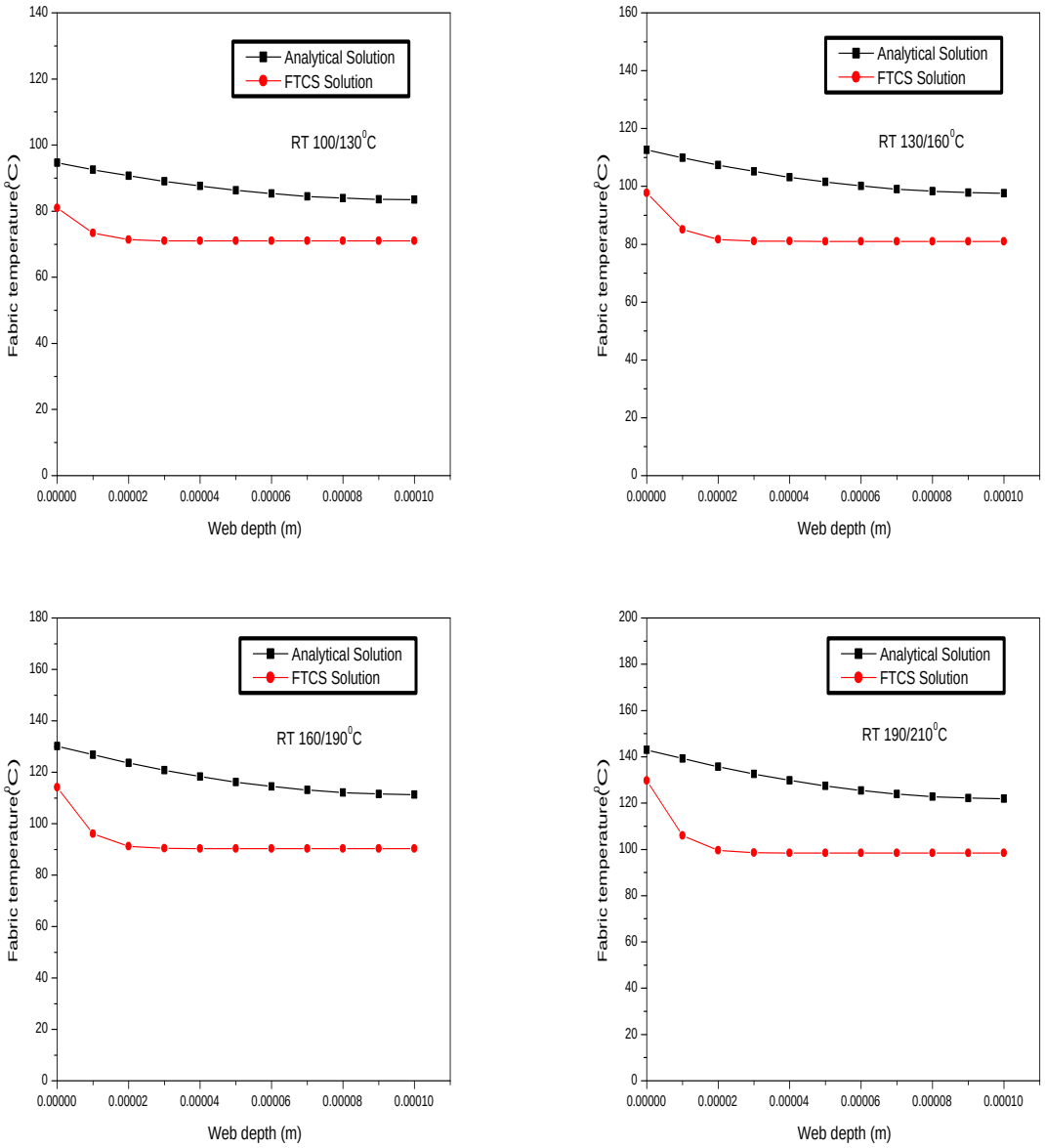

Figure 6.8: Impact of different roll temperature on fabric temperature in thickness direction at various depths with initial temperature 50°C when $E_p > 0.05$ for machine calender

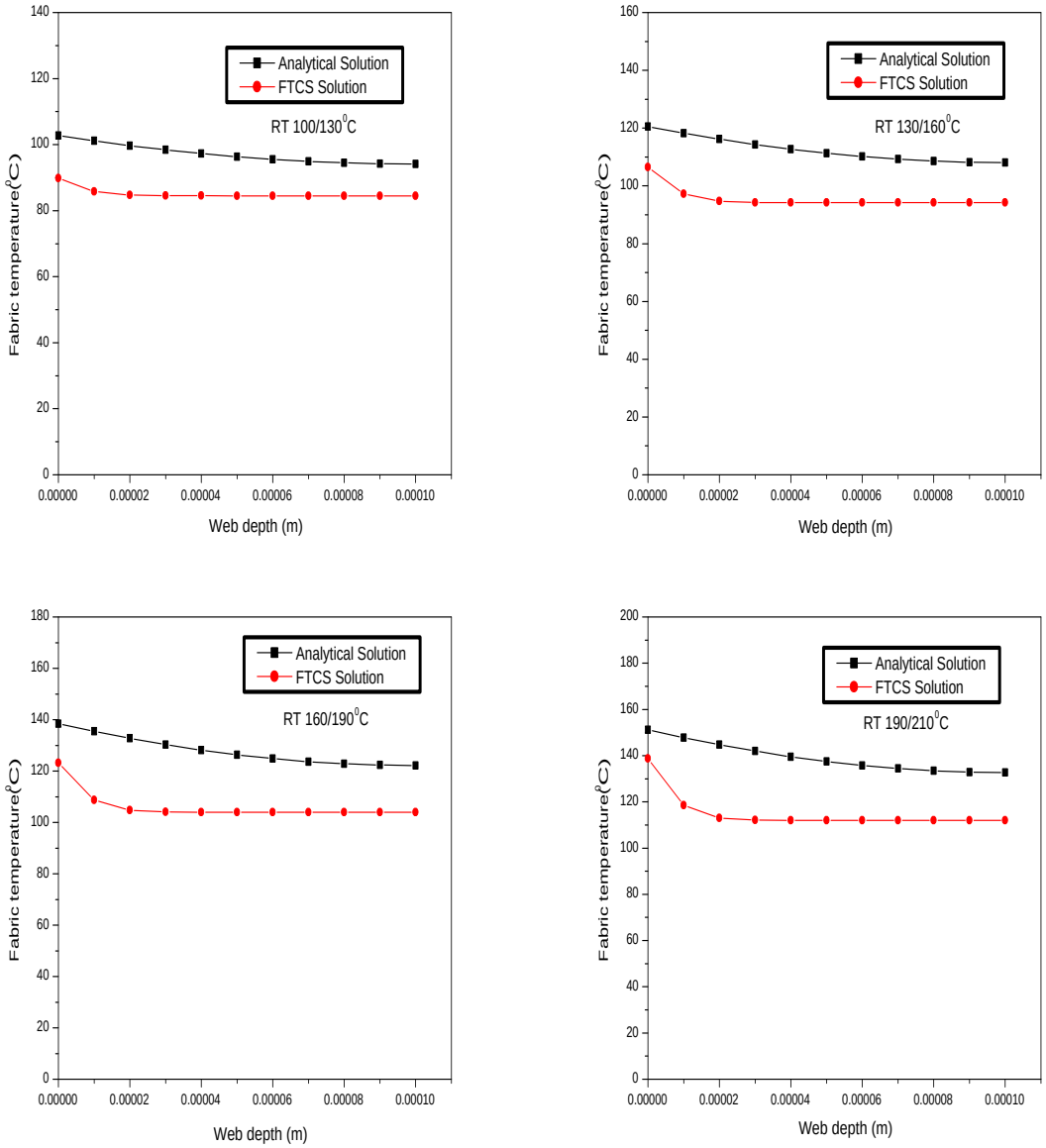

Figure 6.9: Impact of different roll temperature on fabric temperature in thickness direction at various depths with initial temperature 70°C when $E_p > 0.05$ for machine calender

6.5.2 Impact of Roll Temperature on Average Fabric Temperature for Machine Calender having Same and Different Roll Temperature

The impact of roll temperature on average fabric temperature with initial temperature 50°C and 70°C has been investigated when fabric comes out from the machine calender nip having same and different roll temperature. The calculated values are given in tables 6.1 to 6.32 of APPENDIX. The results obtained are shown in figures 6.10 to 6.17.

It clearly indicates that, with increase in roll temperature, average fabric temperature increases linearly. The results obtained using analytical method are compared with forward time central space method. It is found that there is a significant error in the results obtained using these methods. Also for $E_p > 0.05$, more heat penetrates to fabric and thus average fabric temperature increases.

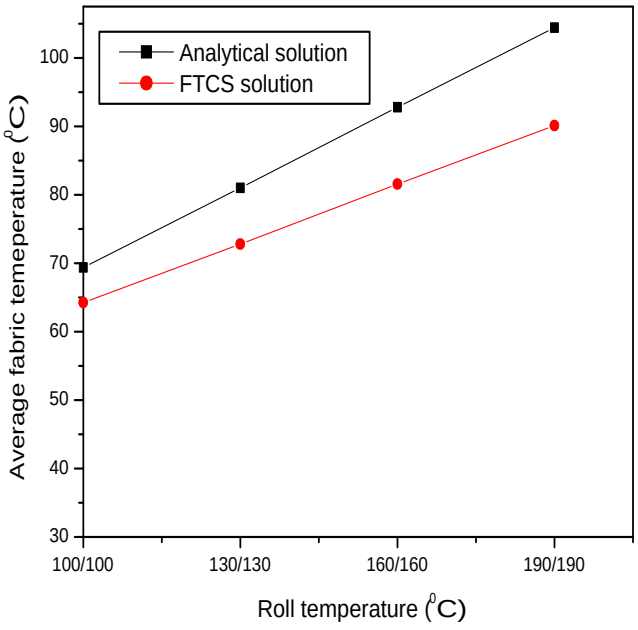

Figure 6.10: Impact of same roll temperature on average fabric temperature with initial temperature 50°C when $E_p < 0.05$ for machine calender

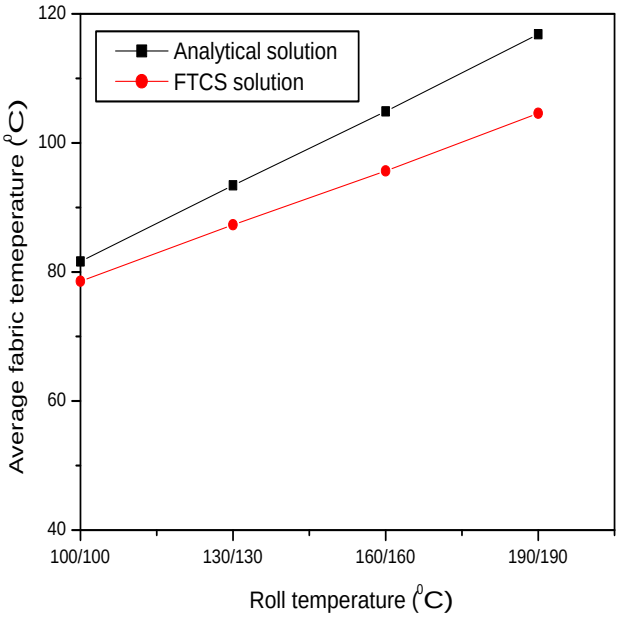

Figure 6.11: Impact of same roll temperature on average fabric temperature with initial temperature 70°C when $E_p < 0.05$ for machine calender

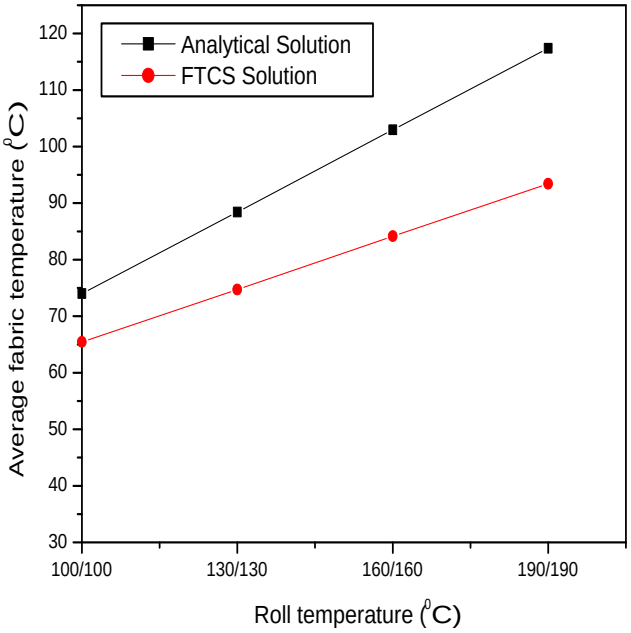

Figure 6.12: Impact of same roll temperature on average fabric temperature with initial temperature 50°C when $E_p > 0.05$ for machine calender

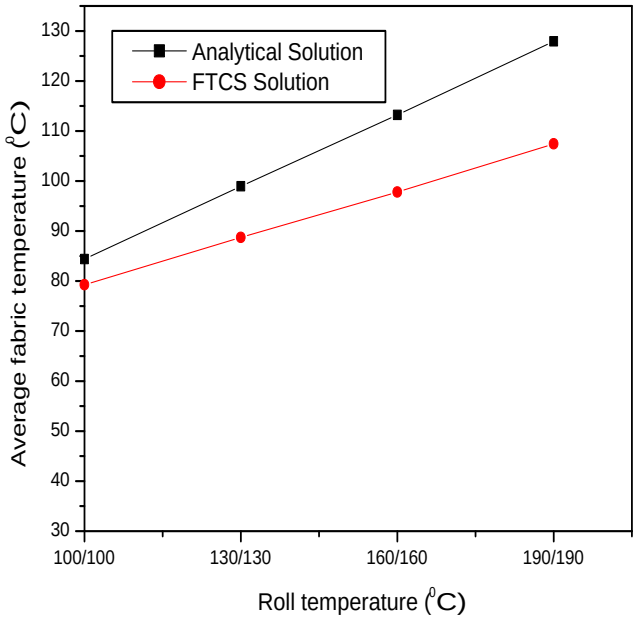

Figure 6.13: Impact of same roll temperature on average fabric temperature with initial temperature 70°C when $E_p > 0.05$ for machine calender

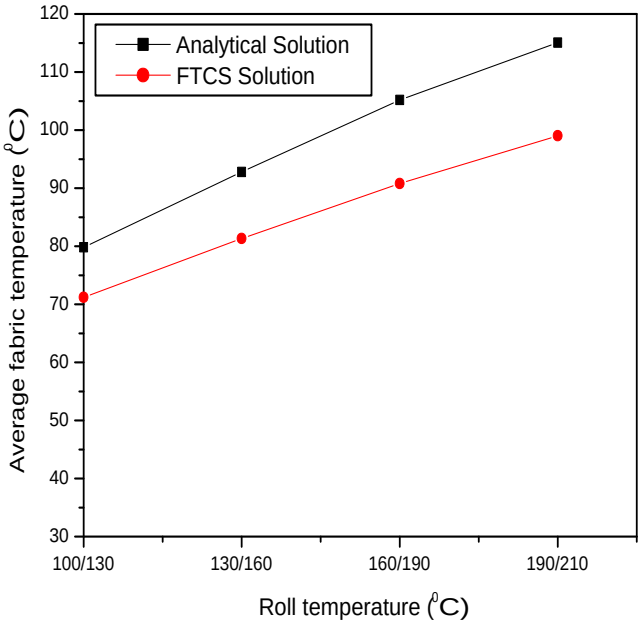

Figure 6.14: Impact of different roll temperature on average fabric temperature with initial temperature 50°C when $E_p < 0.05$ for machine calender

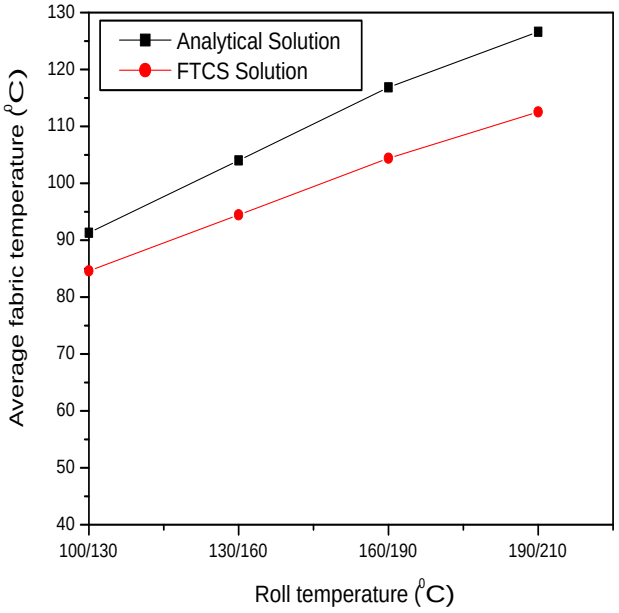

Figure 6.15: Impact of different roll temperature on average fabric temperature with initial temperature 70°C when $E_p < 0.05$ for machine calender

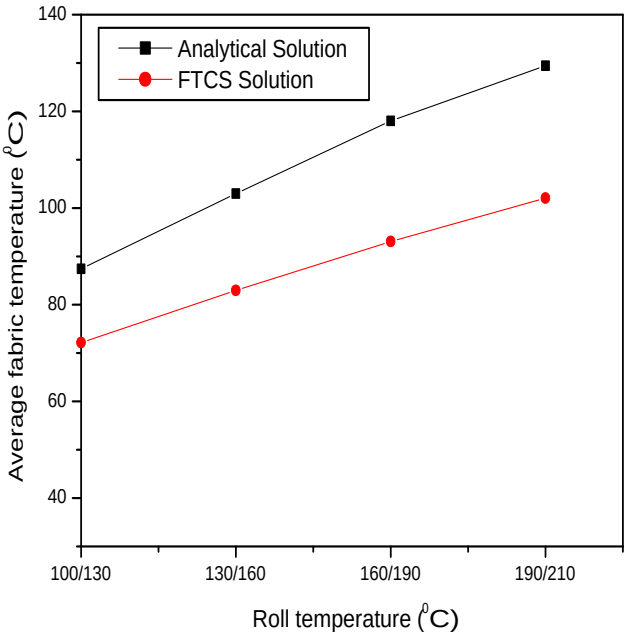

Figure 6.16: Impact of different roll temperature on average fabric temperature with initial temperature 50°C when $E_p > 0.05$ for machine calender

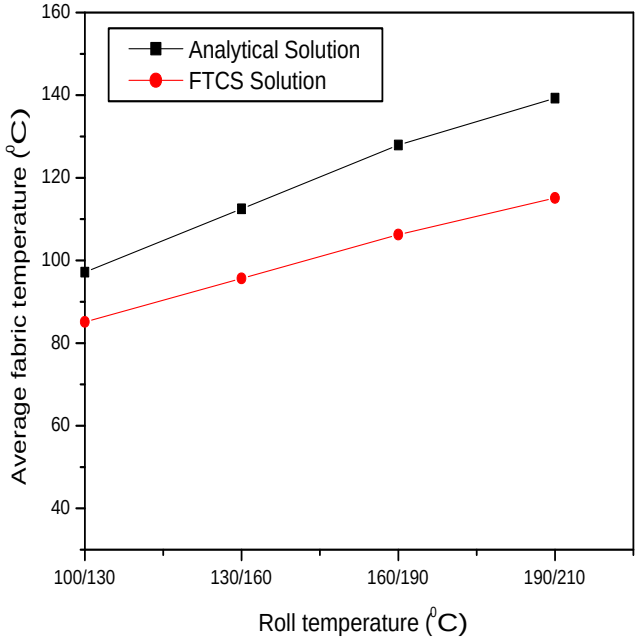

Figure 6.17: Impact of different roll temperature on average fabric temperature with initial temperature 70°C when $E_p > 0.05$ for machine calender

6.5.3 Impact of Roll Temperature on Fabric Temperature in Thickness Direction at Various Depths for Rolling Calender

The impact of roll temperature on fabric temperature in thickness direction at various depths with initial temperature 50°C and 70°C has been investigated when fabric comes out from the rolling calender nip. The calculated values are given in tables 6.33 to 6.48 of APPENDIX. The results obtained are shown in figures 6.18 to 6.21. It clearly shows that when fabric comes out from the the rolling calender nip, the side of fabric which is in touch with the hot roll gets heated and temperature decreases as depth increases. The other side of fabric which is in contact with air remains nearly at the same average temperature. Also it is found that more heat penetrates into the fabric when $E_p > 0.05$. The results obtained using analytical method are compared with forward time central space method. It is found that there is a significant error in the results obtained using these methods.

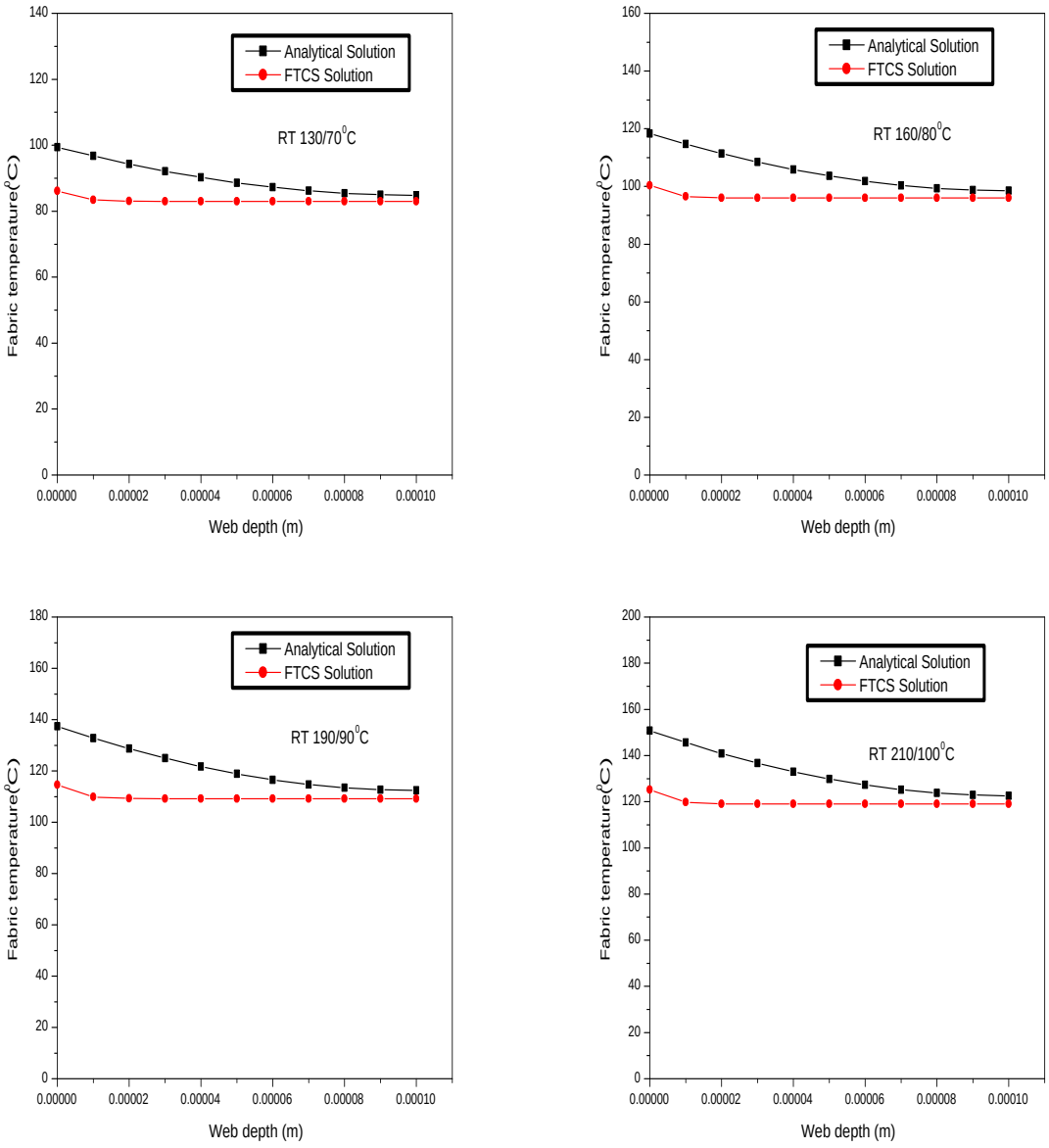

Figure 6.18: Impact of roll temperature on fabric temperature in thickness direction at various depths with initial temperature 50°C when $E_p < 0.05$ for rolling calender

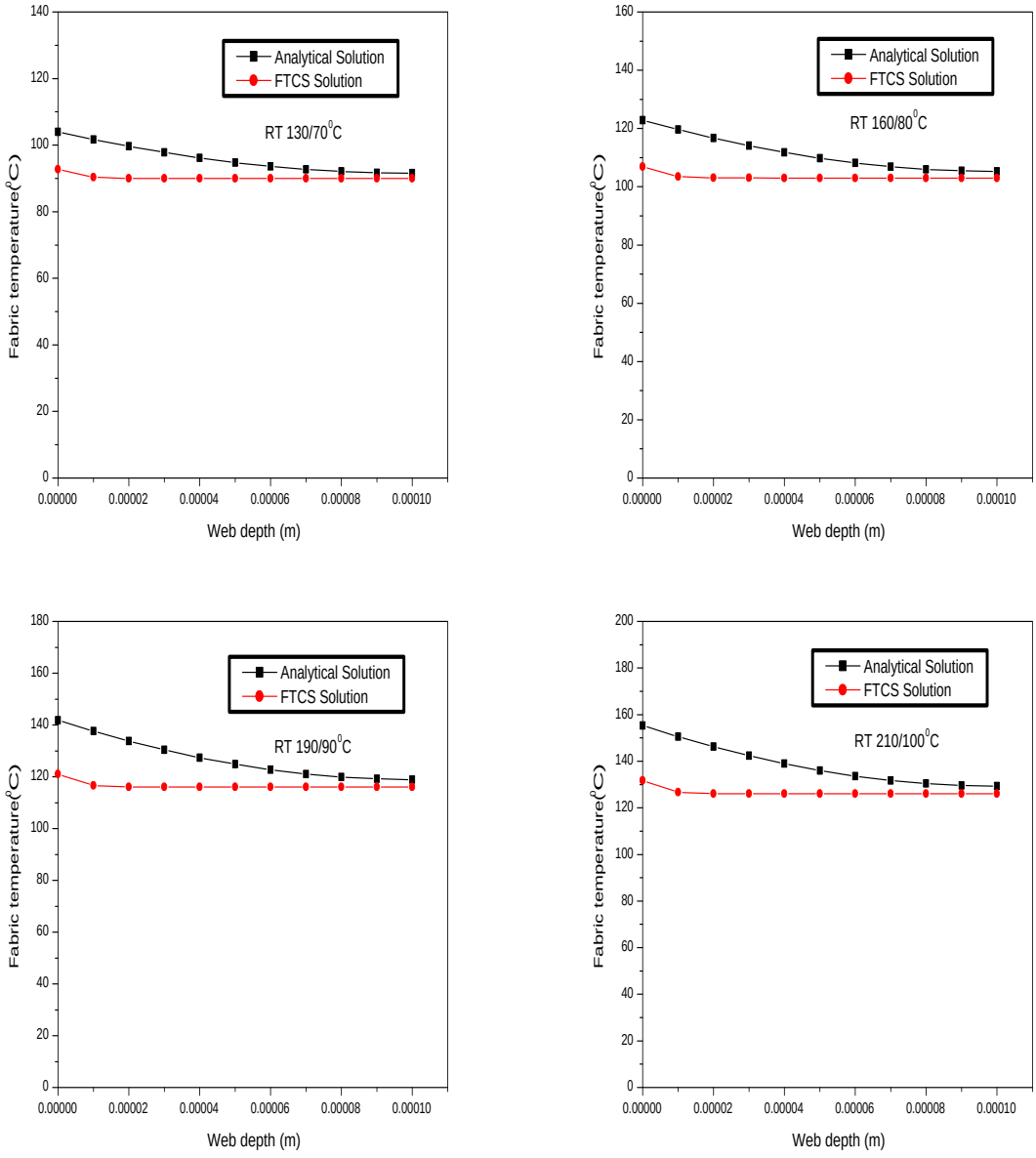

Figure 6.19: Impact of roll temperature on fabric temperature in thickness direction at various depths with initial temperature 70°C when $E_p < 0.05$ for rolling calender

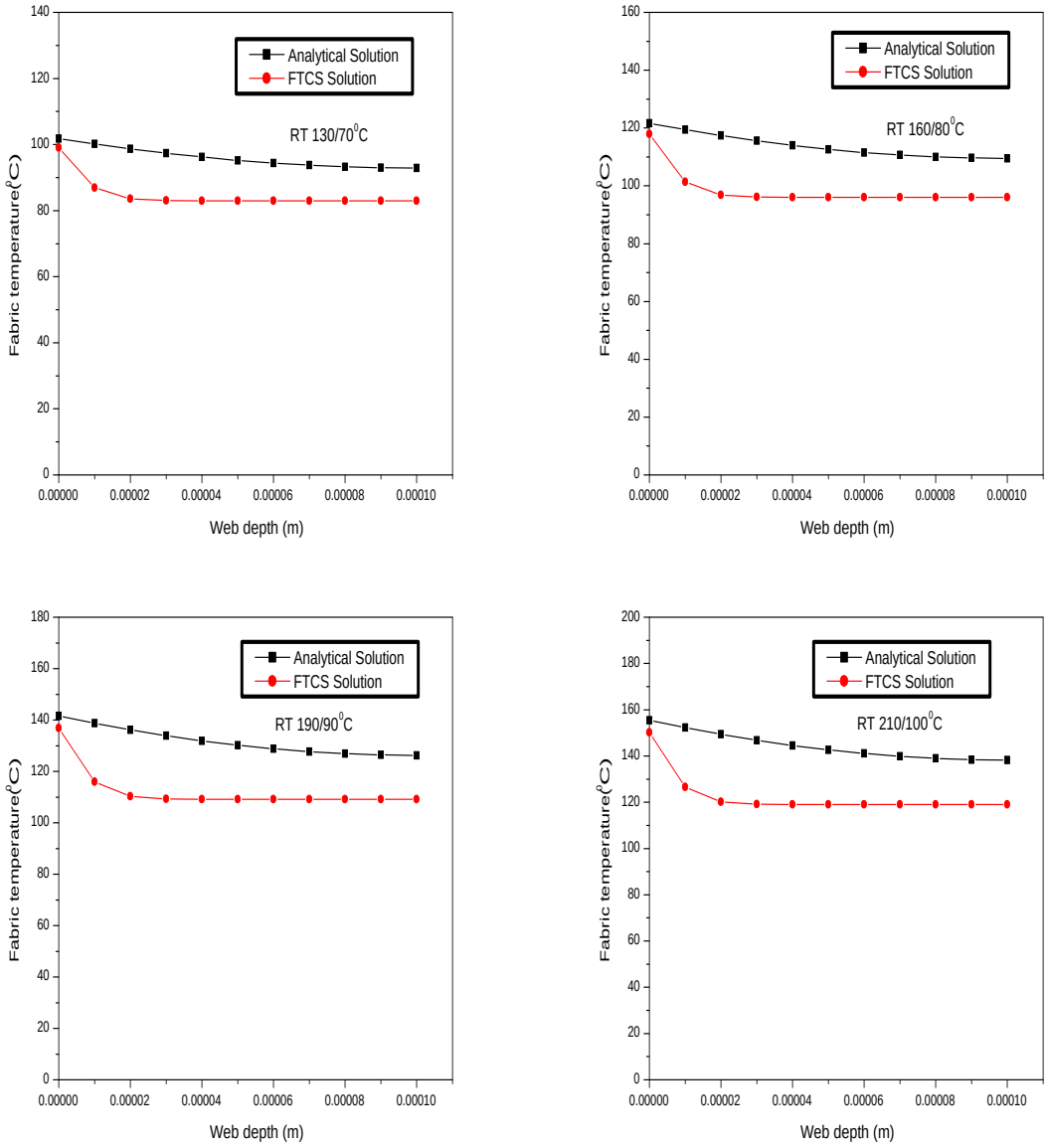

Figure 6.20: Impact of roll temperature on fabric temperature in thickness direction at various depths with initial temperature 50°C when $E_p > 0.05$ for rolling calender

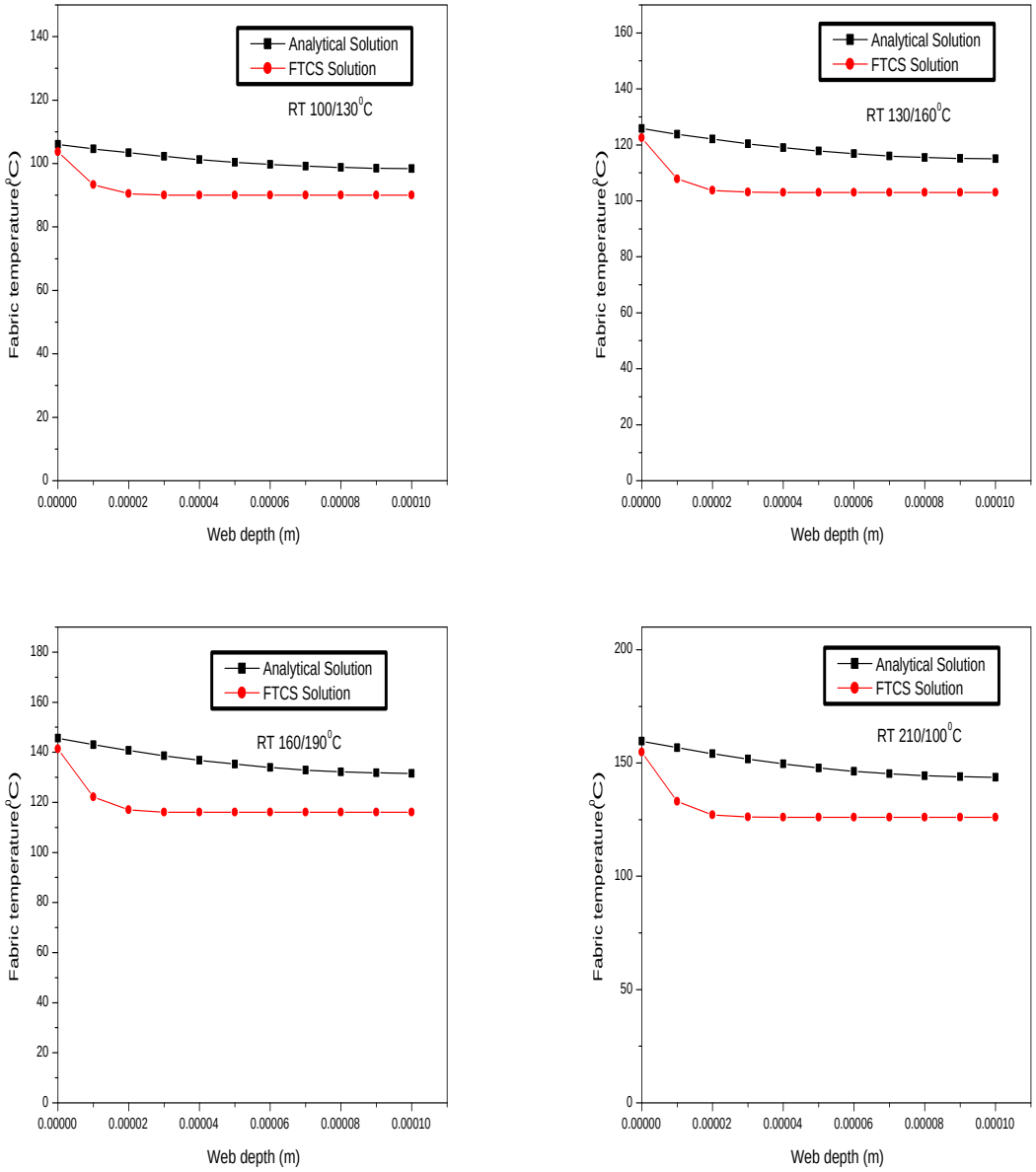

Figure 6.21: Impact of roll temperature on fabric temperature in thickness direction at various depths with initial temperature 70°C when $E_p > 0.05$ for rolling calender

6.5.3.1 Impact of Roll Temperature on Average Fabric Temperature for Rolling Calender

The impact of roll temperature on average fabric temperature with initial temperature 50°C and 70°C has been investigated when fabric comes out from the rolling calender nip. The calculated values are given in tables 6.33 to 6.48 of APPENDIX. The results obtained are shown in figures 6.22 to 6.25.

It clearly indicates that, with increase in roll temperature, average fabric temperature increases linearly. The results obtained using analytical method are compared with forward time central space method. It is found that there is a significant error in the results obtained using these methods. Also for $E_p > 0.05$, more heat penetrates to fabric and thus average fabric temperature increases.

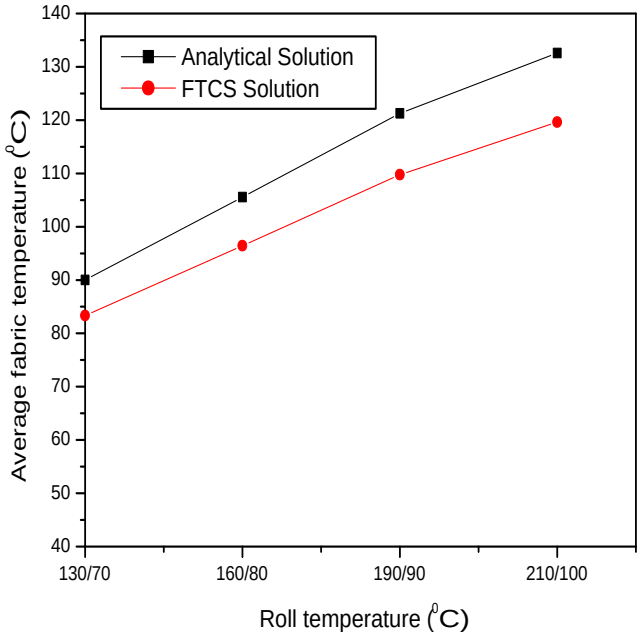

Figure 6.22: Impact of roll temperature on average fabric temperature with initial temperature 50°C when $E_p < 0.05$ for rolling calender

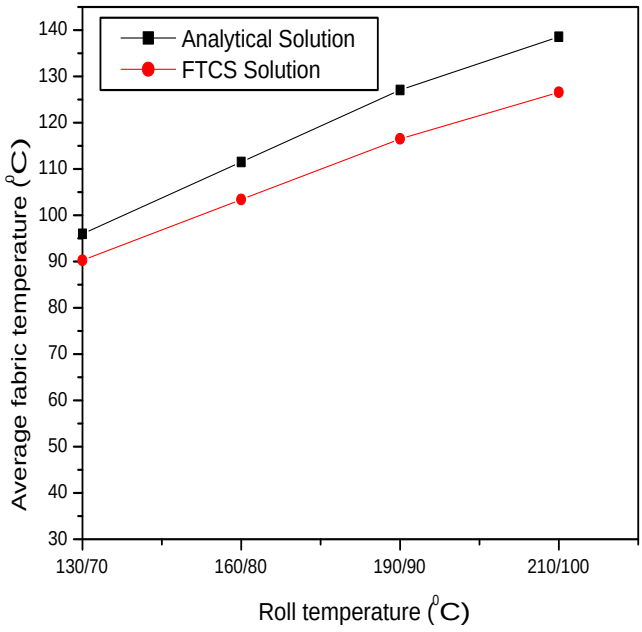

Figure 6.23: Impact of roll temperature on average fabric temperature with initial temperature 70°C when $E_p < 0.05$ for rolling calender

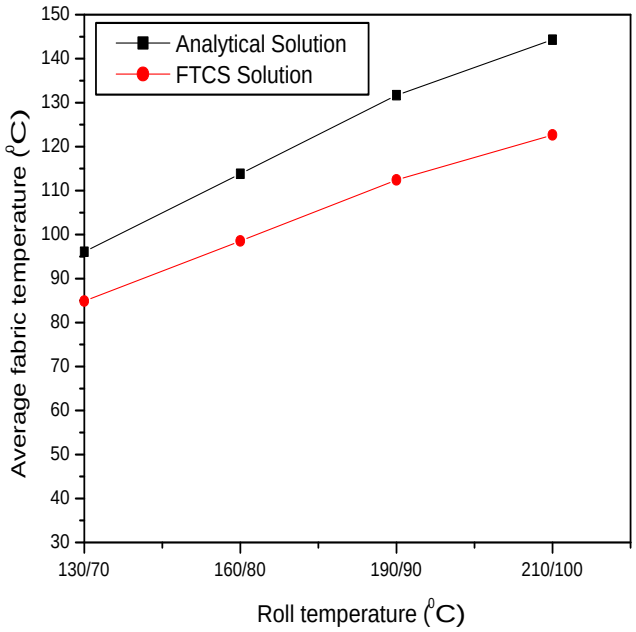

Figure 6.24: Impact of roll temperature on average fabric temperature with initial temperature 50°C when $E_p > 0.05$ for rolling calender

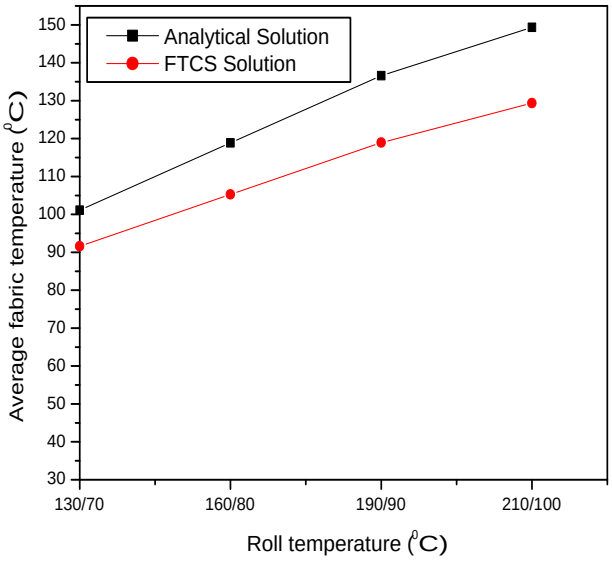

Figure 6.25: Impact of roll temperature on average fabric temperature with initial temperature 70°C when $E_p > 0.05$ for rolling calender

6.6 Conclusion

In this chapter, mathematical model for heat transfer when fabric comes out from the calender nip i.e. one side of fabric is in contact with the roll and other side is in contact with air have been solved using analytical and forward time central space finite difference method for machine calender and rolling calender used in textile industry. Also, comparison of results obtained using explicit FTCS method with results obtained from analytical method reflects the remarkable applicability of numerical and analytical methods in analyzing the temperature profile of the fabric when fabric comes out from the calender nip for same and different roll temperatures. It is found that there is steep temperature gradient at the outer surface contacting the roll. The side of fabric which is in touch with the hot roll gets heated whereas center of fabric remains unheated. For $E_p > 0.05$ more heat penetrates into the fabric due to which fabric temperature increases. It is found that there is remarkable increase in average fabric temperature in the range of 10% to 18% with increase in roll temperature from 70°C to 210°C before entering into the second nip of calendering machine.

Chapter 7

Conclusion

A comprehensive description of finishing process, mathematical modelling and simulation of nip mechanics and heat transfer in calendering system used in textile industry has been done. The design and process parameters such as material composition, temperature, nip load and roll diameter of various types of textile calenders has been analysed which shows the effect of calendering on fabric properties.

7.1 Main Conclusions of Nip Mechanics Model

The developed nip mechanics models are more generalized models which can overcome the difficulties poised by the models of Hertz and Meijers. Hertz had not considered the elastic cover thickness on the cylinder, so this model is not appropriate for to textile calenders. Also, the solution given by Meijers cannot be applied directly for the calendering process because of the results presented are in non dimensional form which making it difficult to extract the needed information. The nip mechanics model for machine calender (NMMM) and nip mechanics model for rolling calender (NMMR) developed in this present investigation are extension of Hertz and modification of Meijers which can be suitably used for textile calenders of any design depending upon composition of material. The impact of load applied, equivalent diameter, equivalent bulk modulus and cover thickness on nip width has been investigated for

machine and rolling calender. Also impact of cover thickness on average pressure has been investigated for both the calenders. The obtained results of the present models are compared with the data obtained from textile mill and with the results obtained by Hertz model. The data obtained from textile mill matches more closely with the NMMM and NMMR solution as compared with the Hertz solution. From NMMM and NMMR models, it is found that nip width increases with increase in line load and equivalent diameter. Nip width increases with decrease in equivalent elastic modulus. With increase in nip width, dwell time increases and hence gloss and smoothness of fabric increases. The equivalent elastic modulus of rolling calender is small as compared to machine calender because machine calender consists of hard rolls and rolling calender consist of alternate hard and soft rolls. Due to which, nip width of rolling calender is greater than nip width of machine calender having same dimensions.

There is no effect of cover thickness on nip width obtained from Hertz solution as Hertz had not considered the elastic cover thickness of the rolls in contact. But NMMM and NMMR solution shows that nip width increases with increase in cover thickness. Also, average pressure remains same in case of Hertz solution, while developed models shows that average pressure decreases with increase in cover thickness. The simulated results shows that there is difference between the results obtained from developed nip mechanics models and Hertz model because of the cover thickness factor which cannot be neglected.

From the analysis of the models it is found that the both the models give better results as compared to conventional models and near to the actual industry data. Hence with the help of these models, designing of calendering machine of any type can be made to obtain desired gloss and smoothness.

7.2 Main Conclusions of Heat Transfer Model when Fabric is Inside the Calender Nip

Simultaneous heat transfer has major impact on the calendering process and on the functioning of calender stack. In the present investigation, heat transfer model has been developed for machine and rolling calender when fabric is inside and outside the nip. The heat transfer model when fabric is inside the calender nip having same and different roll temperature for machine and rolling calender gives an evolutionary advantage that helps in predicting the fabric temperature at various depths in thickness direction which is not possible using temperature measuring instruments as they can only measure temperature on the surface of the fabric.

The impact of roll temperature on fabric temperature in thickness direction at various depths, dwell time, thermal diffusivity, roll temperature on average fabric temperature has also been investigated for machine and rolling calender. Simulated results show that the middle part of fabric remains at initial temperature and temperature of the fabric decreases from outer part to mid part of the fabric from both sides in thickness direction. Also it is found that with increase in roll temperature, dwell time and thermal diffusivity, average fabric temperature increases as more heat is conducted at different layers of the fabric. For machine calender when fabric comes out of the nip, there is remarkable increase in average fabric temperature in the range of 12% to 80% with increase in same roll temperature from 100°C to 190°C and in the range of 20% to 96% with increase in different roll temperature from 100°C to 210°C. For rolling calender when fabric comes out of the nip, there is remarkable increase in average fabric temperature in the range of 29% to 80% with increase in different roll temperature from 70°C to 210°C.

The results obtained using homotopy perturbation method are similar with the exact results while there is a negligible error in the results obtained using finite difference methods such as BTCS, FTCS and CN. It is found that results obtained using BTCS method are very close to results obtained using HPM which reflects the remarkable applicability of numerical methods in analyzing the temperature profile of the fabric

inside the calender nip for same and different roll temperatures. From the simulation of the heat transfer model, it is clear that with increase in roll temperature (and/or) decrease in calender speed, more heat penetrates inside the fabric from both sides in thickness direction which results in increase of average fabric temperature.

With increase in pressure and temperature in calendering system, surface smoothness for the fabric can be improved but with increase in both the factors beyond a certain limit can cause damage to the fibre bond resulting in reduction in the mechanical strength of the fabric. To overcome these undesirable effects, the process of temperature gradient calendering is employed. Temperature gradient calender (TGC) consist of alternating hard and soft rolls in which soft roll at room temperature and hard roll at higher temperature. The mathematical model for TGC has been developed considering incompressible and compressible fabric medium to anticipate the temperature profile of the fabric in thickness direction.

The impact of roll temperature on fabric temperature in thickness direction at various depths, impact of dwell time, thermal diffusivity, roll temperature on average fabric temperature has been investigated when fabric is inside the temperature gradient calender nip. Simulated results show that the side of fabric which is in touch with the heated roll is at higher temperature as compared to the side which is in contact with the non heated roll. With increase in heated roll temperature (and/or) dwell time, more heat is conducted to the fabric, which increases the average temperature of the fabric. It is found that for temperature gradient calender when fabric comes out of the nip, there is remarkable increase in average fabric temperature in the range of 25% to 76% with increase in roll temperature from 200°C to 320°C. In case of TGC, heat is not transformed upto the center of the fabric in thickness direction, thus the fibres which are in direct contact with the heated roll get deformed permanently, while the fibres on the other side and upto the middle of the fabric do not get deformed due to which the surface properties of the fabric are developed while maintaining the bulk and strength properties. Subsequently better gloss and smoothness of the fabric can be accomplished in case of TGC with more than one nip without affecting the bulk and strength properties. Also, neglecting the effect of volume change results, difference in amount of heat conducted at distinct depths and on the average fab-

ric temperature, so volume change during the heat transfer inside the calender nip cannot be neglected.

7.3 Main Conclusions of Heat Transfer Model when Fabric is Outside the Calender Nip

When fabric comes out from the calender nip, one side of the fabric is in contact with the heated roll and other side is exposed to air having convective heat loss. During subsequent contact with the roll, fabric assumes a temperature gradient which diminishes as the fabric heats upto the roll temperature. Mathematical model for heat transfer when one side of fabric is in contact with the roll and other side is in contact with air have been developed and simulation of the model has been done for machine and rolling calender used in textile industry. Simulated results show that the side of fabric which is in touch with the hot roll gets heated and temperature decreases as depth increases. The other side of fabric which is in contact with air remains nearly at the same temperature. Also, comparison of results obtained using explicit FTCS method with results obtained from analytical method reflects the remarkable applicability of numerical methods in analyzing the temperature profile of the fabric. It is found that there is a significant error in the results obtained using these methods. For $E_p > 0.05$ more heat penetrates into the fabric due to which average fabric temperature increases. It is found that there is remarkable increase in average fabric temperature in the range of 10% to 18% with increase in roll temperature from 70°C to 210°C before entering into the second nip of calendering machine.

7.4 Future Work

- To develop nip mechanics and heat transfer model applicable to process industries where there is roll to roll or roll to plate contact such as printing and leather industries.
- To apply Finite element method on nip mechanics and heat transfer models considering the structural inhomogeneities of calendering system.
- To apply artificial neural network technique for modelling the nip mechanics and heat transfer process.
- To apply other finite difference methods for heat conduction under convective boundary conditions.
- To do extensive experimentation on pilot calender for different kind of fabrics.

Bibliography

[1] A. J. Hall, "Textile Finishing, " *Haywood Books, London*, 1996.

[2] M. Jokio, "Papermaking: Finishing, Papermaking Science and Technology series, " *Tappi press and Finish Paper Engineer's Association*, vol. 10, pp.14–141, 1999.

[3] L. Harmuth, "Dictionary of textiles, Harmuth dictionary, " *Fairchild publishing company*, vol. 106, 1915.

[4] L. Cresswell, B. Lawyer, S. Watins, H. Wilson, "Textiles technology, " *Heinemann Educational*, vol. 36, 2002.

[5] M. Paine, "Fabric Magic, " *Frances Lincoln ltd., Knopf Doubleday Publishing Group*, vol.24, 1987.

[6] P. H. Nystrom, "Textiles, " *Appleton's business books, D. Appleton*, pp.274–275, 1916.

[7] V. Litvinov, R. Farnood, "Modeling of the compression of coated papers in a soft rolling nip," *Journal of materials science*, vol. 45(1), pp.216–226, 2010.

[8] G. V. Kuznetsov, M. A. Sheremet, "Mathematical modelling of complex heat transfer in a rectangular enclosure, " *Thermophysics and Aeromechanics*, vol. 16(1), pp.119–128, 2009.

[9] B. Dubey, R. K. Upadhyay, J. Hussain, "Effects of industrialization and pollution on resource biomass: a mathematical model. " *Ecological modelling*, vol. 167(1), pp.83–95, 2003.

[10] R. K. Upadhyay, S. R. Iyengar, "Introduction to mathematical modeling and chaotic dynamics, " *Chapman and Hall/CRC*, pp.1–363, 2013.

[11] N. K. Thakur, S. K. Tiwari, B. Dubey, R. K. Upadhyay, "Diffusive three species plankton model in the presence of toxic prey: application to Sundarban mangrove wetland, " *Journal of Biological Systems*, vol. 25(2), pp.185–206, 2017.

[12] P. Roy, R. K. Upadhyay, J. Caur, "Modeling Zika transmission dynamics: prevention and control, " *Journal of Biological Systems*, vol. 28(3), pp.719–749, 2020.

[13] S. Kumari, R. K. Upadhyay, P. Kumar, V. Rai, "Dynamics and patterns of species abundance in ocean: A mathematical modeling study, " *Nonlinear Analysis: Real World Applications*, vol. 60, pp.103303, 2021.

[14] W. Boscheri, G. Dimarco, L. Pareschi, "Modeling and simulating the spatial spread of an epidemic through multiscale kinetic transport equations, " *Mathematical Models and Methods in Applied Sciences*, pp.1–39, 2021.

[15] G. Albi, L. Pareschi, "Modeling of self-organized systems interacting with a few individuals: from microscopic to macroscopic dynamics, " *Applied Mathematics Letters*, vol. 26(4), pp.397–401, 2013.

[16] N. Kanth, A. K. Ray, R. Dang, "Mathematical model to investigate the effect of design and process parameters on contact width of supercalender, " *International Journal of Modeling, Simulation, and Scientific Computing*, vol. 5(4), pp.1–12, 2014.

[17] N. Kanth, A. K. Ray, R. Dang, "Effect of design and process parameters on nip width of soft calendering," *International Journal for Computational Methods in Engineering Science and Mechanics*, vol. 17(4), pp.247–252, 2016.

[18] R.J. Kerekes, "Newsprint calendering: an experimental comparison of temperature and loading effects, " *Pulp Paper Can*, vol. 75(11), pp.65–72, 1974.

[19] T. Enomae, T. Huang, P. Lepoutre, "Softcalendering: Effect of temperature, pressure and speed on sheet properties, " *Nordic Pulp Paper Research Journal*, vol. 12(1), pp.13–18, 1997.

[20] J. D. Peel, "Supercalendering and soft nip calendering compared, " *Tappi Journal, Technical Association of the Pulp and Paper Industry*, vol. 74(10), pp.179–186, 1991.

[21] J. Rodal, "Soft-nip calendering of paper and paperboard, " *Tappi Journal*, vol. 72(5), pp.177–186, 1989.

[22] N. Kanth, A. K. Ray, "Analysis of heat conduction inside the nip of machine calender for the same and different roll temperatures," *Heat Transfer Asian Research*, vol. 8(8), pp.3557–3573, 2019.

[23] S. Samula, J. A. Katoja, K. Niskanen, "Heat transfer to paper in a hot nip, " *Nordic pulp and paper research journal*, vol. 14(4), pp.273–278, 1999.

[24] P. Gerstner, J. Paltakari, P. A. C. Gani, "Measurement and modelling of heat transfer in paper coating structure, " *Journal of material science*, vol. 44(2), pp.483–491, 2009.

[25] R. H. Hestmo, M. Lamvik, "Heat transfer during calendering of paper," *Journal of pulp and paper science*, vol. 28(4), pp.128–135, 2002.

[26] S. Keller, "Heat transfer in a calender nip, " *Journal of pulp and paper science*, vol. 20(1), pp.J33–J37, 1994.

[27] B. Singh, "Heat Transfer Due to Thermoelastic Wave Propagation in a Porous Rod, " *ASME J. Heat Transfer*, vol. 143(4), pp.042102, 2021.

[28] R. J. Kerekes, "Heat transfer in calendering," *Transactions PPMC*, vol. 5(3), pp.TR66–76, 1979.

[29] H. S. Carslaw, J. C. Jaeger, "Conduction of Heat in Solids, " *Oxford Science Publications*, pp.1–510, 1959.

[30] N. Gupta, N. Kanth, "Study of Heat Conduction inside Rolling Calender Nip for Different Roll Temperatures, " *Journal of Physics Conference Series*, vol. 1276, pp.012044 1-9, 2019.

[31] N. Gupta, N. Kanth, "Analysis of Heat Conduction inside the Calender Nip Used in Textile Industry, " *AIP conference proceedings*, vol. 2214(1), pp. 020008, 2020.

[32] M.F. Gratton, J. Hamel, J. D. McDonald, "Temperature-gradient calendering: From the laboratory to commercial reality, " *Pulp and paper canada ontario*, vol. 98(3), pp.62–71, 1997.

[33] R. Holmstad, K. A. Kure, G. Chinga, Ø.W. Gregersen, "Effect of temperature gradient multi-nip calendering on the structure of SC paper, " *Nordic Pulp & Paper Research Journal*, vol. 19(4), pp.489–494, 2004.

[34] A. Lehtinen, R. Karvinen, "Analytical solution for heat transfer in temperature gradient calendering, " *Paperi ja puu*, vol. 87(8), pp.525–527, 2005.

[35] V. J. Lunardini, "Freezing of a semi-infinite medium with initial temperature gradient," *Journal of Energy Resources Technology*, vol. 106(1), pp.103–106, 1984.

[36] M. F. Gratton, R. S. Seth, R. H. Crotogino, "Temperature-gradient calendering of foodboard, " *TAPPI journal*, vol. 71(1), pp.81–86, 1988.

[37] R. H. Crotogino, "Temperature gradient calendering of newsprint, " *Tappi Journal*, vol. 65(10), pp.97–101, 1982.

[38] K. L. Johnson, "One Hundred Years of Hertz Contact, " *Proc. Instn. Mech. Engrs.*, vol. 196(1), pp.363–378, 1982.

[39] K. L. Johnson, "Contact Mechanics, " *Cambridge Univ. Press, Cambridge, UK*, pp.84–144, 1985.

[40] P. Meijers, "The contact problem of a rigid cylinder on an elastic layer, " *Applied Science Research Journal*, vol. 18, pp.353–383, 1968.

[41] N. V. Deshpande, "Calculation of contact width, penetration, and pressure for contact between cylinders with elastomeric covering, " *Tappi Journal*, vol. 61(10), pp.115–118, 1978.

[42] N. Ahmadi, L. M. Keer, T. Mura, "Non-Hertzian contact stress analysis for an elastic half space-normal and sliding contact, " *International Journal of Solids and Structures*, vol. 19(4), pp.357-373, 1983.

[43] S. Liu, A. Peyronnel, Q. J. Wang, L. M. Keer, "An extension of the Hertz theory for 2D coated components, " *Tribology Letters*, vol. 18(4), pp.505–511, 2005.

[44] S. Liu, A. Peyronnel, Q. J. Wang, L. M. Keer, "An extension of the Hertz theory for 2D coated components, " *Tribology Letters*, vol. 18(4), pp.505–511, 2005.

[45] S. H. Khedkar, S. Chavhan, A. Dhanaskar, S. Kirnapure, P. Rathod, "Case Study on Steam Mechanism in Textile Industry," *International Journal for Scientific Research & Development*, vol. 6(2), pp.1309–1311, 2018.

[46] M. Wikstrom, M. Rigdahl, "Finite element modeling of calendaring-some aspects of the effect of temperature gradients and structure inhomogeneties, " *Journal of material science*, vol. 31, pp.3159–3166, 1996.

[47] J. Hamel, M. Dostie, "Convective heat transfer in calendaring. " *JPPS*, vol. 23(2), pp.J77–J85, 1997.

[48] D. W. Kawka, R. H. Crotogino, W. J. M. Douglas, "Effect of Temperature and moisture Content on paper behaviour in the nip " *Tappi Journal*, vol. 85(12), 2002.

[49] D. Guerin, V. Morin, P. Svenka, "Influence of some parameters on Heat Transfer Calendering:case of a wood free Coated Paper, " *Ippta convension*, pp.17–22, 2003.

[50] B. Vyse, T. Stelle, P. Neill,"Practical Improvements in Paper Calendering and Finishing, " *Ippta convension Issue*, pp.23–30 ,2003.

[51] G. S. Bhat, P. K. Jangala, J. E. Spruiell, "Thermal bonding of polypropylene nonwovens: effect of bonding variables on the structure and properties of the fabrics, " *Journal of Applied Polymer Science*, vol. 92(6), pp.3593–3600, 2004.

[52] N. Fedorova, S. Verenich, B. Pourdeyhimi, "Strength optimization of thermally bonded spunbond nonwovens, " *Journal of Engineered Fibers and Fabrics*, vol. 2(1), pp.38–48, 2007.

[53] A. R. Horrocks, S. C. Anand, "Handbook of technical textiles, " *Woodhead Publishing Elsevier*, vol. 2, pp.1–452, 2000.

[54] M. L. Gulrajani, "Advances in the dyeing and finishing of technical textiles, " *Woodhead Publishing Elsevier*, pp.1–442, 2013.

[55] A. Majumdar, A. Das, R. Alagirusamy, V. K. Kothari, "Process control in textile manufacturing, " *Woodhead Publishing Elsevier*, pp.1–512, 2012.

[56] A. K. Choudhury, "Principles of textile finishing, " *Woodhead Publishing Elsevier*, pp.1–556, 2017.

[57] N. Gupta, "Analysis on the defects in yarn manufacturing process & its prevention in textile industry, " *International journal of Engineering inventions*, vol. 2(7), pp.45–67, 2013.

[58] J. J. B. Perez, A. G. Arrieta, A. H. Encinas, M. A. Q. Dios, "Manufacturing processes in the textile industry, expert systems for fabrics production, " *Adcaij-Advances in Distributed Computing and Artificial Intelligence Journal*, vol. 6(4), pp.15–23, 2017.

[59] D. Chaussy, D. Gurin, "Calendering of Papers and Boards: Processes and Basic Mechanisms, " *Lignocellulosic Fibers and Wood Handbook: Renewable Materials for Today's Environment*, pp.493-529, 2016.

[60] G. S. Bhat, P. Gulgunje, K. Desai, "Development of structure and properties during thermal calendering of polylactic acid (PLA) fiber webs," *Express Polymer Letters*, vol.2(1), pp.49–56, 2008.

[61] J. D. Peel, "Recent developments in the technology and understanding of the calendering processes, " *In Trans. IXth Fundam. Research Symp., London, Mech. Eng. Publ. Ltd.*, pp. 979–1025, 1989.

[62] P. Vernhes, M. Dub, J. F. Bloch, "Effect of calendering on paper surface properties, " *Applied surface science*, vol. 256(22), pp.6923–6927, 2010.

[63] J. V. Poplawski, S. M. Peters, E. V. Zaretsky, "Effect of roller profile on cylindrical roller bearing life prediction-Part I: Comparison of bearing life theories, " *Tribology Transactions*, vol. 44(3), pp.339–350, 2001.

[64] M. Emel, O. Nida, B. Sehrazat, A. Marmarali, "Effects of calendering and milling processes on clothing comfort properties of suit fabrics, " *Textile and Apparel*, vol. 24(2), pp.212–218, 2014.

[65] P. Vernhes, J. F. Bloch, A. Blayo, B. Pineaux, "Effect of calendering on paper surface micro-structure: A multi-scale analysis, " *Journal of materials processing technology*, vol. 209(11), pp.5204–5210, 2009.

[66] N. Gupta, N. Kanth, "Analysis of Nip Mechanics Model for Rolling Calender used in Textile Industry," *Journal of the Serbian Society for Computational Mechanics*, vol. 12(2), pp.39–52, 2018.

[67] G. R. Naghieh, H. Rahnejat, Z. M. Jin, "Charecteristics of frictionless contact of bounded elastic and viscoelastic layered solids, " *Wear, Elsevier*, vol. 232(2), pp.243–249, 1999.

[68] W. D. Callisters, "Material Science and Engineering, " *Wiley, New York*, pp.A6–A10, 2007.

[69] J. Sorvari, M. Parola, "Feeding in rolling contact of layered printing cylinders, " *International Journal of Mechanical Sciences*, vol. 88, pp.82–92, 2014.

[70] J. Margetson, "The indentation of elastic and viscoelastic strips by rigid or elastic cylinders " *Zeitschrift fr angewandte Mathematik und Physik ZAMP*, vol. 21(6), pp.1040–1052, 1970.

[71] M. T. Solanki, D. Vakharia, "A finite element analysis of an elastic contact between a layered cylindrical hollow roller and flat contact, " *Industrial Lubrication and Tribology*, vol. 69(1), pp.30–41, 2017.

[72] M. T. Solanki, D. Vakharia, "Extending hertz equation for an elastic contact between a layered cylindrical hollow roller and flat plate through an experimental technique, " *Industrial Lubrication and Tribology*, vol. 69(2), pp.312–324, 2017.

[73] G. R. Naghieh, H. Rahnejat, Z. M. Jin, "Characteristics of frictionless contact of bonded elastic and viscoelastic layered solids, " *Wear*, vol. 232(2), pp.243–249, 1999.

[74] M. N. Balci, S. Dag, "Solution of the dynamic frictional contact problem between a functionally graded coating and a moving cylindrical punch, " *International Journal of Solids and Structures*, vo. 161, pp.267–281, 2019.

[75] D. R. Roisum, "Nip Impressions, " *Finishing Technologies, Inc*, pp.1–13, 2003.

[76] J. H. He, "Homotopy perturbation method: a new nonlinear analytical technique, " *Applied Mathematics and computation*, vol. 135(1), pp.73–79, 2003.

[77] J. H. He,"Homotopy perturbation method for solving boundary value problems, " *Physics letters A*, vol. 350(1), pp.87–88, 2006.

[78] J. H. He, "Some asymptotic methods for strongly nonlinear equations, " *International journal of Modern physics B*, vol. 20(10), pp.1141–1199, 2006.

[79] A. Demir, S. Erman, B. Ozgur, E. Korkmaz, "Analysis of the new homotopy perturbation method for linear and nonlinear problems, " *Boundary Value Problems*, vol. 2013(1), pp.1–11, 2013.

[80] J. H. He,"A coupling method of a homotopy technique and a perturbation technique for non-linear problems, " *International journal of non-linear mechanics*, vol. 35(1), pp.37–43, 2000.

[81] J. Biazar, M. Eslami, "A new homotopy perturbation method for solving systems of partial differential equations, " *Computers and Mathematics with Applications*, vol. 62(1), pp.225–234, 2011.

[82] M. ELbadri, "A New Homotopy Perturbation Method for Solving Laplace Equation, " *Advances in Theoretical and Applied Mathematics*, vol. 4(3), pp.237–242, 2013.

[83] M. Mirzazadeh, Z. Ayati, "New homotopy perturbation method for system of Burgers equations, " *Alexandria Engineering Journal*, vol. 55(3), pp.1619–1624, 2016.

[84] M. Elbadri, T. M. Elzaki, "New Modification of Homotopy Perturbation Method and the Fourth-Order Parabolic Equations with Variable Coefficients, " *Pure Appl. Math. J.*, vol. 4(6), pp.242–247, 2015.

[85] J. H. He, "Homotopy perturbation technique, " *Computer methods in applied mechanics and engineering*, vol. 178(3), pp.257–262, 1999.

[86] D. Grover, V. Kumar, D. Sharma, "A Comparative Study of Numerical Techniques and Homotopy Perturbation Method for Solving Parabolic Equation and Nonlinear Equations, " *Int. J. Comput. Methods Eng. Sci. Mech*, vol. 13(6), pp.403–407, 2012.

[87] F. Shakeri, M. Dehghan, "Solution of delay differential equations via a homotopy perturbation method, " *Mathematical and computer Modelling*, vol. 48(3), pp.486–498, 2008.

[88] Y. X. Wang, H. Y. Si, L. F. Mo, "Homotopy perturbation method for solving reaction-diffusion equations, " *Mathematical Problems in Engineering*, vol. 2008, pp. 1–6, 2008.

[89] M. Omidvar, A. Barari, G. Domairry, "Solution of Diffusion Equations Using Homotopy Perturbation and Variational Iteration Methods, " *Trakia Journal of Sciences*, vol. 8(3), pp.21–28, 2010.

[90] J. H. He, "Some asymptotic methods for strongly nonlinear equations, " *International journal of Modern physics B*, vol. 20(10), pp.1141–1199, 2006.

[91] J. Biazar, B. Ghanbari, "HAM solution of some initial value problems arising in heat radiation equations," *Journal of King Saud University-Science*, vol. 24(2), pp.161–165, 2012.

[92] D. M. Wang, W. Zhang, M. H. Yao, Y. L. Liu, "A New technique of Initial Boundary Value Problems Using Homotopy Analysis Method, " *In Journal of Physics: Conference Series*, vol. 916(1), pp. 012039, 2017.

[93] V. G. Gupta, S. Gupta, "Applications of homotopy analysis transform method for solving various nonlinear equations, " *World Applied Sciences Journal*, vol. 18(12), pp.1839–1846, 2012.

[94] N. Gupta, N. Kanth, "Application of Perturbation Theory in Heat Flow Analysis, " *A Collection of Papers on Chaos Theory and Its Applications*, vol. 173, 2021.

[95] N. Gupta, N. Kanth, "Study of Heat Flow in a Rod using Homotopy Analysis Method and Homotopy Perturbation Method, " *AIP conference proceedings*, vol. 2061(1), pp.020013 1-8, 2019.

[96] N. Gupta, N. Kanth, "Analytical approximate solution of heat conduction equation using new homotopy perturbation method, " *Matrix Science Mathematic*, vol. 3(2), pp.01-07, 2019.

[97] M. Dehghan, J. Manafian, "The solution of the variable coefficients fourth-order parabolic partial differential equations by the homotopy perturbation method, " *Zeitschrift fr Naturforschung A*, vol. 64(8), pp.420–430, 2009.

[98] F. Shakeri, M. Dehghan, "Inverse problem of diffusion equation by He's homotopy perturbation method, " *Physica Scripta*, vol. 75(4), pp.551, 2007.

[99] B. Gupta, V. K. Kukreja, "Numerical approach for solving diffusion problems using cubic B-spline collocation method, " *Applied Mathematics and Computation*, vol. 219(4), pp.2087–2099, 2012.

[100] B. Gupta, V. K. Kukreja, N. Parumasur, P. Singh, "Numerical study of a nonlinear diffusion model for washing of packed bed of cylindrical fiber particles, " *Arabian Journal for Science and Engineering*, vol. 40(5), pp.1279–1287, 2015.

[101] A. Mohebbi, M. Dehghan, "High-order compact solution of the one-dimensional heat and advection-diffusion equations, " *Applied mathematical modelling*, vol. 34(10), pp.3071–3084, 2010.

[102] W. Liao, M. Dehghan, A. Mohebbi, "Direct numerical method for an inverse problem of a parabolic partial differential equation, " *Journal of Computational and Applied Mathematics*, vol. 232(2), pp.351–360, 2009.

[103] A. Mohebbi, M. Dehghan, "High-order compact solution of the one-dimensional heat and advection-diffusion equations, " *Applied mathematical modelling*, vol. 34(10), pp.3071–3084, 2010.

[104] W. Liao, P. Yong, H. Dastour, J. Huang, "Efficient and accurate numerical simulation of acoustic wave propagation in a 2D heterogeneous media, " *Applied Mathematics and Computation*, vol. 321, pp.385–400, 2018.

[105] M. Abbaszadeh, M. Dehghan, "Numerical and analytical investigations for solving the inverse tempered fractional diffusion equation via interpolating element-free Galerkin (IEFG) method, " *Journal of Thermal Analysis and Calorimetry*, vol. 143(3), pp.1917–1933, 2021.

[106] N. Gupta, N. Kanth, "Numerical solution of diffusion equation using method of lines, " *Indian Journal of Industrial and Applied Mathematics*, vol. 10(2), pp.194–203, 2019.

[107] J. Biazar and R. Asayesh, "A new finite difference scheme for parabolic equations, " *The 50th Annual Iranian Mathematics Conference*, pp.1–4, 2019.

[108] S. E. Fadugba, O. H. Edogbanya, S. C. Zelibe, "Crank Nicolson methof for solving parabolic partial differential equations, " *International journal of Applied Mathematics and Modeling*, vol. 1(3), pp.8–23, 2013.

[109] M. Dehghan, "Finite difference procedures for solving a problem arising in modeling and design of certain optoelectronic devices, " *Mathematics and Computers in Simulation*, vol. 71(1), pp.16–30, 2006.

[110] W. Liao, "An implicit fourth-order compact finite difference scheme for one-dimensional Burgers equation, " *Applied Mathematics and Computation*, vol.206(2), pp.755-764, 2008.

[111] H. Dastour, W. Liao, "An optimal 13-point finite difference scheme for a 2D Helmholtz equation with a perfectly matched layer boundary condition, " *Numerical Algorithms*, vol. 86(3), pp.1109–1141, 2021.

[112] D. Li, K. Li, W. Liao, "Efficient and stable finite difference modelling of acoustic wave propagation in variable-density media, " *arXiv preprint arXiv*, vol. 2003, pp.09812, 2020.

[113] H. Dastour, W. Liao, "A fourth-order optimal finite difference scheme for the Helmholtz equation with PML, " *Computers and Mathematics with Applications*, vol. 78(6), pp.2147–2165, 2019.

[114] I. Miroshnichenko, M. Sheremet, "Numerical Simulation of Heat Transfer in an Enclosure with Time-Periodic Heat Generation Using Finite-Difference Method, " *International Conference on Computational Science, Springer, Cham*, pp.149–162 2020.

[115] M. Abbaszadeh, M. Dehghan, Y. Zhou, "Crank-Nicolson/Galerkin spectral method for solving two-dimensional time-space distributed-order weakly singular integro-partial differential equation, " *Journal of Computational and Applied Mathematics*, vol. 374, pp.112739, 2020.

[116] G. Dimarco, L. Pareschi, "Implicit-explicit linear multistep methods for stiff kinetic equations, " *SIAM Journal on Numerical Analysis*, vol. 55(2), pp.664–690, 2017.

[117] A. Mohebbi, "Finite difference and spectral collocation methods for the solution of semilinear time fractional convection-reaction-diffusion equations with time delay, " *Journal of Applied Mathematics and Computing*, vol. 61(1), pp.635–656, 2019.

[118] A. Mohebbi, "Crank-Nicolson and Legendre spectral collocation methods for a partial integro-differential equation with a singular kernel. " *Journal of Computational and Applied Mathematics*, vol. 349, pp.197–206, 2019.

[119] A. Mohebbi, "Compact finite difference scheme for the solution of a time fractional partial integro- differential equation with a weakly singular kernel, " *Mathematical Methods in the Applied Sciences*, vol. 40(18), pp.7627–7639, 2017.

[120] A. Mohebbi, M. Abbaszadeh, M. Dehghan, "Compact finite difference scheme and RBF meshless approach for solving 2D Rayleigh-Stokes problem for a heated generalized second grade fluid with fractional derivatives, " *Computer Methods in Applied Mechanics and Engineering*, vol. 264, pp.163–177, 2013.

[121] M. Haghi, M. Ilati, M. Dehghan, "A fourth-order compact difference method for the nonlinear time-fractional fourth-order reaction-diffusion equation. " *Engineering with Computers*, pp.1–12, 2021.

[122] L. Pareschi, G. Russo, "Implicit-explicit Runge-Kutta schemes for stiff systems of differential equations. " *Recent trends in numerical analysis*, vol. 3, pp.269–289, 2000.

[123] G. W. Bluman, S. C. Anco, "Symmetry and integration methods for differential equations, " *Springer Science & Business Media*, vol. 154, pp.1–419, 2004.

[124] V. Kumar, R. K. Gupta, R. Jiwari, "Lie group analysis, numerical and non-traveling wave solutions for the (2+ 1)-dimensional diffusion-advection equation with variable coefficients, " *Chinese Physics B*, vol. 23(3), pp.030201, 2014.

[125] S. L. Mitchell, T. G. Myers, "Application of heat balance integral methods to one dimensional phase change problems, " *International Journal of Differential Equations*, vol. 2012, pp.1–22 2012.

[126] D. Langford, "The heat balance integral method, " *International Journal of Heat and Mass Transfer*, vol. 16(12), pp.2424–2428, 1973.

[127] B. Baudouy, "Integral method for transient He II heat transfer in a semi-infinite domain, " *AIP Conference Proceedings*, vol. 613(1), pp.1349–1355, 2002.

[128] V. A. Kot, "Integral method of boundary characteristics: The Dirichlet condition. Principles, " *Heat Transfer Research*, vol. 47(10), pp.927–944, 2016.

[129] M. Guellal, H. Sadat, C. Prax, "A simple model for transient heat conduction in an infinite cylinder with convective boundary conditions, " *Journal of heat transfer*, vol. 131(5), pp. 054501, 2009.

[130] M. A. Sheremet, I. Pop, "Natural convection in a square porous cavity with sinusoidal temperature distributions on both side walls filled with a nanofluid: Buongiorno's mathematical model," *Transport in Porous Media*, vol. 105(2), pp.411–429, 2014.

[131] A. J. Chamkha, I. V. Miroshnichenko, M. A. Sheremet, "Numerical analysis of unsteady conjugate natural convection of hybrid water-based nanofluid in a semicircular cavity," *Journal of Thermal Science and Engineering Applications*, vol. 9(4), pp.041004, 2017.

[132] G. V. Kuznetsov, M. A. Sheremet, "Numerical simulation of turbulent natural convection in a rectangular enclosure having finite thickness walls, " *International Journal of Heat and Mass Transfer*, vol. 53(1), pp.163–177, 2010.

[133] M. A. Sheremet, "The influence of cross effects on the characteristics of heat and mass transfer in the conditions of conjugate natural convection, " *Journal of Engineering Thermophysics*, vol. 19(3), pp.119–127, 2010.

[134] J. Prakash, R. Bala, K. Vaid, "On the characterization of magnetohydrodynamic triply diffusive convection, " *J. Magn. Magn. Mater.*, vol. 377, pp.378-385, 2015.

[135] M. B. Banerjee, J. R. Gupta, R. G. Shandil, J. Prakash, "On Thermohaline Convection of Veronis Type, " *J. Math. Anal. and Appl.*, vol. 179, pp.327–334, 1993.

[136] J. Prakash, S. K. Gupta, "On arresting the complex growth rates in ferromagnetic convection with magnetic field dependent viscosity in a rotating ferrofluid layer, " *J. Magnetism and Magnetic Materials*, vol. 345, pp.201-207, 2013.

APPENDIX

Table 2.1: Design and process variables of three different principal types of calenders

Hard Nip Calender	Soft Nip Calender	Temperature Gradient Calender
Linear load	Linear load	Linear load in the bottom nip
Nip dwell time	Running speed	Surface temperature of heated rolls
Number of Nips	Hot roll temperature	Hardness and material of filled roll
Machine speed	Soft roll cover material	Calender speed
Roll diameter		
Roll Surface Smoothness	Soft roll position(against top side of the web)	

Table 2.2: Design and process parameters of various types of textile calenders

Calender parameters	Rolling calender	Silk finishing calender	Friction calender	Embossing Calender	Cire Calender
Rolls	Alternate hard and soft rolls	Top and bottom filled roll, steel middle roll	Top and bottom heated rolls, filled middle roll	Forged top Steel roll and filled bottom roll	Top and bottom heated rolls, filled middle roll
Speed(m/s)	2	1.5	0.46	0.76	0.48-0.53
No. of rolls	2-6	3	3	2	2-3
No. of Nips	1-4	2	2	1	1-2
Nip load(kN/m)	85-435	70-122	262-437	Upto 265	262-525
Heated roll(°C)	150-210	150-180	60-220	180-240	150-260

Table 3.1: Design and process parameters

Parameters	Machine Calender	Soft Calender	Temperature Gradient Calender
Composition	Hard rolls	Alternate hard and soft rolls	Alternate hard and soft rolls
Hard roll material	Steel cylinders having covering of chilled cast iron	Steel cylinders having covering of chilled cast iron	Steel cylinders having covering of chilled cast iron
Soft roll material	Nil	Steel cylinders having covering of soft material like cotton, rubber and polymer etc	Steel cylinders having covering of soft material like cotton, rubber and polymer etc
Nip width(mm)	$1-5$	$5-15$	$5-25$
Cover thickness(mm)	$8-18$	$8-18$	$8-18$
Thickness of soft cover(mm)	Nil	$5-50$	$5-50$
Diameter of rolls(mm)	$300-1200$	$300-1200$	$300-1200$
Speed(m/min)	$150-400$	$30-70$	$400-900$
Linear load(kN/m)	$90-550$	$120-480$	$120-480$
Hot roll temperature(°C)	$100-250$	$60-240$	$180-420$
Specific heat($J/Kg.K$)	$1400-1900$	$1500-1900$	$1500-2200$
Thermal conductivity($W/m.K$)	$0.17-0.22$	$0.17-0.22$	$0.17-0.22$
Density of fiber(Kg/m^3)	$895-920$	$895-920$	$895-920$
Dwell time(sec)	$0.0001-0.0009$	$0.0001-0.0009$	$0.0001-0.0009$
Thermal diffusivity(m^2/sec)	$9.1-11.6\times10^{-8}$	$9.1-11.6\times10^{-8}$	$9.1-11.6\times10^{-8}$
Thickness of the web at entering the nip (m)			100×10^{-6}
Minimum thickness of the web (m)			60×10^{-6}

Table 3.2: Impact of load applied on nip width for machine calender

Load applied (kN/mm)	Nip width (mm) NMMM	Nip width (mm) Hertz model	Textile mill data (mm)
0.2	1.255	1.2609	1.253
0.25	1.4053	1.4097	1.4
0.3	1.5411	1.5443	1.54
0.35	1.666	1.668	1.66
0.4	1.7819	1.7832	1.78
0.45	1.8906	1.8913	1.89
0.5	1.9937	1.9932	1.993
0.55	2.092	2.0909	2.091
0.6	2.1794	2.1839	2.179

Table 3.3: Impact of equivalent diameter on nip width for machine calender

Equivalent Diameter(mm)	Nip width (mm) NMMM	Nip width (mm) Hertz model
200	1.3228	1.296
250	1.4747	1.449
300	1.6124	1.5875
350	1.7464	1.7146
400	1.8641	1.833
450	1.9748	1.9442
500	2.0856	2.049

Table 3.4: Impact of equivalent bulk modulus on nip width for machine calender

Equivalent Bulk Modulus (kN/mm^2)	Nip width (mm)NMMM	Nip width (mm) Hertz model
76	1.4577	1.4545
79	1.423	1.4267
82	1.3964	1.4003
85	1.3784	1.3754
88	1.3509	1.3517

Table 3.5: Impact of cover thickness on nip width for machine calender

Cover thickness(mm)	Nip width (mm)NMMM	Nip width (mm) Hertz model
10	0.288	1.4458
11	0.3168	1.4458
12	0.3456	1.4458
13	0.3744	1.4458
14	0.4032	1.4458
15	0.432	1.4458

Table 3.6: Impact of average pressure at various cover thickness for machine calender

Cover thickness(mm)	Average Pressure NMMM	Average pressure Hertz model
10	0.9132	0.1819
11	0.83018	0.1819
12	0.761	0.1819
13	0.7025	0.1819
14	0.6523	0.1819
15	0.6088	0.1819

Table 3.7: Impact of load applied on nip width for rolling calender

Load applied (kN/mm)	Nip width (mm) NMMM	Nip width (mm) Hertz model	Textile mill data (mm)
0.2	5.765	5.845	5.75
0.25	6.4226	6.535	6.4
0.3	7.0132	7.1588	7
0.35	7.5516	7.7324	7.6
0.4	8.0483	8.2662	8.15
0.45	8.511	8.7677	8.55
0.5	8.945	9.242	9

Table 3.8: Impact of equivalent diameter on nip width for rolling calender

Equivalent Diameter(mm)	Nip width (mm) NMMR	Nip width (mm) Hertz model
200	6.4584	6.5413
250	7.1924	7.3134
300	7.8477	8.0114
350	8.4437	8.6533
400	8.994	9.2508
450	9.5048	9.812
500	9.9838	10.3427

Table 3.9: Impact of equivalent bulk modulus on nip width for rolling calender

Equivalent Bulk Modulus (kN/mm^2)	Nip width (mm)NMMR	Nip width (mm) Hertz model
3	5.9192	6.8486
4	5.1442	5.9311
5	4.6109	5.305
6	4.2152	4.8428
7	3.9066	4.4835

Table 3.10: Impact of cover thickness on nip width for rolling calender

Cover thickness(mm)	Nip width (mm)NMMR	Nip width (mm) Hertz model
10	6.3943	6.7028
11	6.4403	6.7028
12	6.477	6.7028
13	6.5065	6.7028
14	6.531	6.7028
15	6.5511	6.7028

Table 3.11: Impact of average pressure at various cover thickness for rolling calender

Cover thickness(mm)	Average pressure NMMR	Average pressure Hertz model
10	0.0411	0.0392
11	0.0408	0.0392
12	0.0406	0.0392
13	0.0404	0.0392
14	0.0402	0.0392
15	0.0401	0.0392

Table 4.1: Impact of same roll temperature 100/100(°C) on fabric layer temperature in thickness direction at various depths with initial temperature 50°C for machine calender

Web Depth (m)	RT 100/100(°C)			
	Fabric Layer Temperature (°C)			
	HPM Solution	BTCS Solution	CN Solution	FTCS Solution
0	100	100	100	100
0.00001	70.987	70.29011	70.96644	71.65624
0.00002	55.3292	56.07179	56.13636	56.23085
0.00003	50.7747	51.47399	51.34926	51.20425
0.00004	50.0625	50.31647	50.24073	50.15815
0.00005	50.0055	50.114	50.06913	50.02751
0.00006	50.0625	50.31647	50.24073	50.15815
0.00007	50.7747	51.47399	51.34926	51.20425
0.00008	55.3292	56.07179	56.13636	56.23085
0.00009	70.987	70.29011	70.96644	71.65624
0.0001	100	100	100	100
Average temperature	64.0284	64.2199	64.3141	64.4115

Table 4.2: Impact of same roll temperature 130/130(°C) on fabric layer temperature in thickness direction with initial temperature 50°C for machine calender

Web Depth (m)	RT 130/130(°C)			
	Fabric Layer Temperature (°C)			
	HPM Solution	BTCS Solution	CN Solution	FTCS Solution
0	130	130	130	130
0.00001	83.5792	82.46418	83.5463	84.64998
0.00002	58.5267	59.71486	59.81817	59.96937
0.00003	51.2395	52.35838	52.15881	51.9268
0.00004	50.1	50.50636	50.38516	50.25305
0.00005	50.0088	50.18241	50.11061	50.04401
0.00006	50.1	50.50636	50.38516	50.25305
0.00007	51.2395	52.35838	52.15881	51.9268
0.00008	58.5267	59.71486	59.81817	59.96937
0.00009	83.5792	82.46418	83.5463	84.64998
0.0001	130	130	130	130
Average temperature	72.4454	72.7518	72.9025	73.0584

Table 4.3: Impact of same roll temperature 160/160(°C) on fabric layer temperature in thickness direction with initial temperature 50°C for machine calender

Web Depth (m)	RT 160/160(°C)			
	Fabric Layer Temperature (°C)			
	HPM Solution	BTCS Solution	CN Solution	FTCS Solution
0	160	160	160	160
0.00001	96.1715	94.63825	96.12617	97.64373
0.00002	61.7241	63.35793	63.49999	63.70788
0.00003	51.7044	53.24277	52.96837	52.64934
0.00004	50.1375	50.69624	50.5296	50.34794
0.00005	50.012	50.25081	50.15209	50.06051
0.00006	50.1375	50.69624	50.5296	50.34794
0.00007	51.7044	53.24277	52.96837	52.64934
0.00008	61.7241	63.35793	63.49999	63.70788
0.00009	96.1715	94.63825	96.12617	97.64373
0.0001	160	160	160	160
Average temperature	80.8625	81.2837	81.4909	81.7053

Table 4.4: Impact of same roll temperature 190/190(°C) on fabric layer temperature in thickness direction with initial temperature 50°C for machine calender

Web Depth (m)	RT 190/190(°C)			
	Fabric Layer Temperature (°C)			
	HPM Solution	BTCS Solution	CN Solution	FTCS Solution
0	190	190	190	160
0.00001	108.764	106.81232	108.70603	97.64373
0.00002	64.9216	67.001	67.1818	63.70788
0.00003	52.1692	54.12716	53.77793	52.64934
0.00004	50.175	50.88612	50.67404	50.34794
0.00005	50.0153	50.31921	50.19357	50.06051
0.00006	50.175	50.88612	50.67404	50.34794
0.00007	52.1692	54.12716	53.77793	52.64934
0.00008	64.9216	67.001	67.1818	63.70788
0.00009	108.764	106.81232	108.70603	97.64373
0.0001	190	190	190	160
Average temperature	89.2795	89.8157	90.0794	81.7053

Table 4.5: Impact of same roll temperature 100/100(°C) on fabric layer temperature in thickness direction with initial temperature 70°C for machine calender

Web Depth (m)	RT 100/100(°C)			
	Fabric Layer Temperature (°C)			
	HPM Solution	BTCS Solution	CN Solution	FTCS Solution
0	100	100	100	100
0.00001	82.5922	82.17407	82.57986	82.99374
0.00002	73.1975	73.64307	73.68181	73.73851
0.00003	70.4648	70.88439	70.80956	70.72255
0.00004	70.0375	70.18988	70.14444	70.09489
0.00005	70.0033	70.0684	70.04148	70.0165
0.00006	70.0375	70.18988	70.14444	70.09489
0.00007	70.4648	70.88439	70.80956	70.72255
0.00008	73.1975	73.64307	73.68181	73.73851
0.00009	82.5922	82.17407	82.57986	82.99374
0.0001	100	100	100	100
Average temperature	78.4170	78.5319	78.5884	78.6469

Table 4.6: Impact of same roll temperature 130/130(°C) on fabric layer temperature in thickness direction with initial temperature 70°C for machine calender

Web Depth (m)	RT 130/130(°C)			
	Fabric Layer Temperature (°C)			
	HPM Solution	BTCS Solution	CN Solution	FTCS Solution
0	130	130	130	130
0.00001	95.1844	94.34814	95.15973	95.98749
0.00002	76.395	77.28614	77.36363	77.47702
0.00003	70.9297	71.76878	71.61911	71.4451
0.00004	70.075	70.37977	70.28887	70.18978
0.00005	70.0066	70.1368	70.08296	70.03301
0.00006	70.075	70.37977	70.28887	70.18978
0.00007	70.9297	71.76878	71.61911	71.4451
0.00008	76.395	77.28614	77.36363	77.47702
0.00009	95.1844	94.34814	95.15973	95.98749
0.0001	130	130	130	130
Average temperature	86.8341	87.0639	87.1769	87.2938

Table 4.7: Impact of same roll temperature 160/160(°C) on fabric layer temperature in thickness direction with initial temperature 70°C for machine calender

Web Depth (m)	RT 160/160(°C)			
	Fabric Layer Temperature (°C)			
	HPM Solution	BTCS Solution	CN Solution	FTCS Solution
0	160	160	160	160
0.00001	107.777	106.5222	107.73959	108.98123
0.00002	79.5925	80.92921	81.04544	81.21554
0.00003	71.3945	72.65317	72.42867	72.16765
0.00004	70.1125	70.56965	70.43331	70.28468
0.00005	70.0099	70.20521	70.12444	70.04951
0.00006	70.1125	70.56965	70.43331	70.28468
0.00007	71.3945	72.65317	72.42867	72.16765
0.00008	79.5925	80.92921	81.04544	81.21554
0.00009	107.777	106.5222	107.73959	108.98123
0.0001	160	160	160	160
Average temperature	95.2512	95.5958	95.7653	95.9407

Table 4.8: Impact of same roll temperature 190/190(°C) on fabric layer temperature in thickness direction with initial temperature 70°C for machine calender

Web Depth (m)	RT 190/190(°C)			
	Fabric Layer Temperature (°C)			
	HPM Solution	BTCS Solution	CN Solution	FTCS Solution
0	190	190	190	190
0.00001	120.369	118.69627	120.31946	121.97497
0.00002	82.79	84.57229	84.72726	84.95405
0.00003	71.8593	73.53756	73.23822	72.89019
0.00004	70.15	70.75953	70.57774	70.37957
0.00005	70.0131	70.27361	70.16592	70.06601
0.00006	70.15	70.75953	70.57774	70.37957
0.00007	71.8593	73.53756	73.23822	72.89019
0.00008	82.79	84.57229	84.72726	84.95405
0.00009	120.369	118.69627	120.31946	121.97497
0.0001	190	190	190	190
Average temperature	103.6682	104.1277	104.3538	104.5876

Table 4.9: Impact of dwell time on average fabric temperature with initial temperature 50°C for machine calender having same roll temperature 100/100°C

Dwell time (s)	RT 100/100(°C)			
	Average fabric Temperature (°C)			
	HPM Solution	BTCS Solution	CN Solution	FTCS Solution
0.0002	60.07127	60.63594	60.69091	60.75397
0.0004	61.60851	61.97331	62.05379	62.14195
0.0006	62.90261	63.15582	63.24689	63.34335
0.0008	64.02839	64.21988	64.31406	64.4115

Table 4.10: Impact of dwell time on average fabric temperature with initial temperature 50°C for machine calender having same roll temperature 130/130°C

Dwell time (s)	RT 130/130(°C)			
	Average fabric Temperature (°C)			
	HPM Solution	BTCS Solution	CN Solution	FTCS Solution
0.0002	66.114	67.0175	67.10546	67.20635
0.0004	68.5736	69.1573	69.28607	69.42712
0.0006	70.64417	71.04932	71.19502	71.34935
0.0008	72.44542	72.75181	72.9025	73.0584

Table 4.11: Impact of dwell time on average fabric temperature with initial temperature 50°C for machine calender having same roll temperature 160/160°C

Dwell time (s)	RT 160/160(°C)			
	Average fabric Temperature (°C)			
	HPM Solution	BTCS Solution	CN Solution	FTCS Solution
0.0002	72.15676	73.39907	73.52001	73.65873
0.0004	75.53873	76.34128	76.51835	76.71229
0.0006	78.38574	78.94281	79.14316	79.35536
0.0008	80.86245	81.28374	81.49094	81.7053

Table 4.12: Impact of dwell time on average fabric temperature with initial temperature 50°C for machine calender having same roll temperature 190/190°C

Dwell time (s)	RT 190/190(°C)			
	Average fabric Temperature (°C)			
	HPM Solution	BTCS Solution	CN Solution	FTCS Solution
0.0002	78.19953	79.78063	79.93455	80.11111
0.0004	82.5038	83.52527	83.75062	83.99746
0.0006	86.12732	86.83631	87.09129	87.36137
0.0008	89.27954	89.81567	90.07938	90.3522

Table 4.13: Impact of dwell time on average fabric temperature with initial temperature 70°C for machine calender having same roll temperature 100/100°C

Dwell time (s)	RT 100/100(°C)			
	Average fabric Temperature (°C)			
	HPM Solution	BTCS Solution	CN Solution	FTCS Solution
0.0002	76.04276	76.38156	76.41455	76.45238
0.0004	76.96513	77.18399	77.23228	77.28517
0.0006	77.74156	77.89349	77.94813	78.00601
0.0008	78.41703	78.53193	78.58844	78.6469

Table 4.14: Impact of dwell time on average fabric temperature with initial temperature 70°C for machine calender having same roll temperature 130/130°C

Dwell time (s)	RT 130/130(°C)			
	Average fabric Temperature (°C)			
	HPM Solution	BTCS Solution	CN Solution	FTCS Solution
0.0002	82.08551	82.76313	82.82909	82.90476
0.0004	83.9302	84.36797	84.46455	84.57034
0.0006	85.48313	85.78699	85.89627	86.01201
0.0008	86.83407	87.06386	87.17688	87.2938

Table 4.15: Impact of dwell time on average fabric temperature with initial temperature 70°C for machine calender having same roll temperature 160/160°C

Dwell time (s)	RT 160/160(°C)			
	Average fabric Temperature (°C)			
	HPM Solution	BTCS Solution	CN Solution	FTCS Solution
0.0002	88.12827	89.14469	89.24364	89.35714
0.0004	90.89533	91.55196	91.69683	91.85551
0.0006	93.22464	93.68048	93.8444	94.01802
0.0008	95.25117	95.59579	95.76531	95.9407

Table 4.16: Impact of dwell time on average fabric temperature with initial temperature 70°C for machine calender having same roll temperature 190/190°C

Dwell time (s)	RT 190/190(°C)			
	Average fabric Temperature (°C)			
	HPM Solution	BTCS Solution	CN Solution	FTCS Solution
0.0002	94.17102	95.52626	95.65819	95.80952
0.0004	97.86042	98.73594	98.9291	99.14068
0.0006	100.96622	101.57398	101.79254	102.02403
0.0008	103.66815	104.12772	104.35375	104.5876

Table 4.17: Impact of thermal diffusivity on average fabric temperature with initial temperature 50°C for machine calender having same roll temperature 100/100°C

Thermal diffusivity (m^2/s)	RT 100/100(°C)			
	Average fabric Temperature (°C)			
	HPM Solution	BTCS Solution	CN Solution	FTCS Solution
$9.2x10^{-8}$	63.84998	64.06208	64.15242	64.24605
$9.5x10^{-8}$	63.98411	64.18051	64.27373	64.37022
$9.8x10^{-8}$	64.11635	64.30777	64.40408	64.50362
$10.1x10^{-8}$	64.24689	64.43203	64.53134	64.63383

Table 4.18: Impact of thermal diffusivity on average fabric temperature with initial temperature 50°C for machine calender having same roll temperature 130/130°C

Thermal diffusivity (m^2/s)	RT 130/130(°C)			
	Average fabric Temperature (°C)			
	HPM Solution	BTCS Solution	CN Solution	FTCS Solution
9.2x10^{-8}	72.15996	72.49933	72.64388	72.79368
9.5x10^{-8}	72.37455	72.68881	72.83797	72.99235
9.8x10^{-8}	72.58618	72.89244	73.04653	73.2058
10.1x10^{-8}	72.79498	73.09124	73.25014	73.41413

Table 4.19: Impact of thermal diffusivity on average fabric temperature with initial temperature 50°C for machine calender having same roll temperature 160/160°C

Thermal diffusivity (m^2/s)	RT 160/160(°C)			
	Average fabric Temperature (°C)			
	HPM Solution	BTCS Solution	CN Solution	FTCS Solution
9.2x10^{-8}	80.46997	80.93657	81.13533	81.34132
9.5x10^{-8}	80.76502	81.19711	81.40221	81.61448
9.8x10^{-8}	81.056	81.4771	81.68898	81.90797
10.1x10^{-8}	81.34313	81.75046	81.96894	82.19443

Table 4.20: Impact of thermal diffusivity on average fabric temperature with initial temperature 50°C having same roll temperature 190/190°C for machine calender

Thermal diffusivity (m^2/s)	RT 190/190(°C)			
	Average fabric Temperature (°C)			
	HPM Solution	BTCS Solution	CN Solution	FTCS Solution
9.2x10^{-8}	88.78004	89.37382	89.62679	89.88895
9.5x10^{-8}	89.15553	89.70541	89.96644	90.23661
9.8x10^{-8}	89.52575	90.06177	90.33143	90.61015
10.1x10^{-8}	89.89117	90.40968	90.68774	90.97473

Table 4.21: Impact of thermal diffusivity on average fabric temperature with initial temperature 70°C for machine calender having same roll temperature 100/100°C

Thermal diffusivity (m^2/s)	RT 100/100(°C)			
	Average fabric Temperature (°C)			
	HPM Solution	BTCS Solution	CN Solution	FTCS Solution
$9.2x10^{-8}$	78.30999	78.43725	78.49145	78.54763
$9.5x10^{-8}$	78.39044	78.5083	78.56424	78.62213
$9.8x10^{-8}$	78.46981	78.58466	78.64245	78.70217
$10.1x10^{-8}$	78.54811	78.65922	78.7188	78.7803

Table 4.22: Impact of thermal diffusivity on average fabric temperature with initial temperature 70°C for machine calender having same roll temperature 130/130°C

Thermal diffusivity (m^2/s)	RT 130/130(°C)			
	Average fabric Temperature (°C)			
	HPM Solution	BTCS Solution	CN Solution	FTCS Solution
$9.2x10^{-8}$	86.61997	86.8745	86.98291	87.09526
$9.5x10^{-8}$	86.78091	87.01661	87.12848	87.24426
$9.8x10^{-8}$	86.93965	87.16933	87.2849	87.40435
$10.1x10^{-8}$	87.09626	87.31843	87.4376	87.5606

Table 4.23: Impact of thermal diffusivity on average fabric temperature with initial temperature 70°C for machine calender having same roll temperature 160/160°C

Thermal diffusivity (m^2/s)	RT 160/160(°C)			
	Average fabric Temperature (°C)			
	HPM Solution	BTCS Solution	CN Solution	FTCS Solution
$9.2x10^{-8}$	94.92996	95.31174	95.47436	95.64289
$9.5x10^{-8}$	95.17131	95.52491	95.69271	95.86639
$9.8x10^{-8}$	95.40943	95.75399	95.92735	96.10652
$10.1x10^{-8}$	95.64437	95.97765	96.15641	96.3409

Table 4.24: Impact of thermal diffusivity on average fabric temperature with initial temperature 70°C for machine calender having same roll temperature 190/190°C

Thermal diffusivity (m^2/s)	RT 190/190(°C)			
	Average fabric Temperature (°C)			
	HPM Solution	BTCS Solution	CN Solution	FTCS Solution
9.2x10^{-8}	103.23989	103.74899	103.96582	104.19053
9.5x10^{-8}	103.56175	104.03321	104.25695	104.48853
9.8x10^{-8}	103.87932	104.33866	104.5698	104.8087
10.1x10^{-8}	104.19255	104.63687	104.87521	105.1212

Table 4.25: Impact of different roll temperature 100/130(°C) on fabric layer temperature in thickness direction with initial temperature 50°C for machine calender

Web Depth (m)	RT 100/130(°C)			
	Fabric Layer Temperature (°C)			
	HPM Solution	BTCS Solution	CN Solution	FTCS Solution
0	100	100	100	100
0.00001	83.4373	70.29013	70.96644	71.65624
0.00002	67.6121	56.07192	56.13639	56.23085
0.00003	53.6394	51.4749	51.34955	51.20426
0.00004	43.1805	50.32228	50.24335	50.15862
0.00005	38.2807	50.1482	50.08987	50.03576
0.00006	40.8907	50.50055	50.38254	50.25258
0.00007	52.2262	52.35746	52.15852	51.92678
0.00008	72.1989	59.71472	59.81814	59.96936
0.00009	99.1475	82.46416	83.5463	84.64998
0.0001	130	130	130	130
Average temperature	70.9649	68.4858	68.6083	68.7349

Table 4.26: Impact of different roll temperature 130/160(°C) on fabric layer temperature in thickness direction with initial temperature 50°C for machine calender

Web Depth (m)	RT 130/160(°C)			
	Fabric Layer Temperature (°C)			
	HPM Solution	BTCS Solution	CN Solution	FTCS Solution
0	130	130	130	130
0.00001	102.495	82.4642	83.54631	84.64998
0.00002	76.7993	59.71499	59.8182	59.96937
0.00003	54.993	52.35929	52.15911	51.92681
0.00004	39.5047	50.51217	50.38778	50.25351
0.00005	32.8718	50.21661	50.13135	50.05226
0.00006	37.2148	50.69043	50.52698	50.34748
0.00007	53.5798	53.24185	52.96808	52.64933
0.00008	81.3861	63.35779	63.49996	63.70788
0.00009	118.206	94.63823	96.12617	97.64373
0.0001	160	160	160	160
Average temperature	80.641	77.0178	77.1967	77.3819

Table 4.27: Impact of different roll temperature 160/190(°C) on fabric layer temperature in thickness direction with initial temperature 50°C for machine calender

Web Depth (m)	RT 160/190(°C)			
	Fabric Layer Temperature (°C)			
	HPM Solution	BTCS Solution	CN Solution	FTCS Solution
0	160	160	160	160
0.00001	121.553	94.63827	96.12617	97.64373
0.00002	85.9865	63.35807	63.50002	63.70788
0.00003	56.3466	53.24369	52.96866	52.64936
0.00004	35.8288	50.70205	50.53222	50.3484
0.00005	27.4629	50.28501	50.17283	50.06877
0.00006	33.539	50.88031	50.67141	50.44237
0.00007	54.9334	54.12624	53.77763	53.37188
0.00008	90.5733	67.00086	67.18177	67.44639
0.00009	137.264	106.8123	108.70603	110.63747
0.0001	190	190	190	190
Average temperature	90.3171	85.5497	85.7852	86.0288

Table 4.28: Impact of different roll temperature 190/210(°C) on fabric layer temperature in thickness direction with initial temperature 50°C for machine calender

Web Depth (m)	RT 190/210(°C)			
	Fabric Layer Temperature (°C)			
	HPM Solution	BTCS Solution	CN Solution	FTCS Solution
0	190	190	190	190
0.00001	140.054	106.81233	108.70603	110.63747
0.00002	94.4069	67.00109	67.18182	67.44639
0.00003	57.239	54.12777	53.77812	53.3719
0.00004	32.3839	50.89	50.67578	50.44314
0.00005	22.9555	50.34201	50.2074	50.08252
0.00006	30.8574	51.00884	50.76858	50.50578
0.00007	56.2969	54.71614	54.31743	53.85358
0.00008	97.4648	69.42962	69.63632	69.93873
0.00009	150.527	114.92835	117.09261	119.29996
0.0001	210	210	210	210
Average temperature	98.3805	92.6597	92.9422	93.2345

Table 4.29: Impact of different roll temperature 100/130(°C) on fabric layer temperature in thickness direction with initial temperature 70°C for machine calender

Web Depth (m)	RT 100/130(°C)			
	Fabric Layer Temperature (°C)			
	HPM Solution	BTCS Solution	CN Solution	FTCS Solution
0	100	100	100	100
0.00001	90.732	82.17409	82.57987	82.99374
0.00002	81.4873	73.64321	73.68184	73.73851
0.00003	72.737	70.88531	70.80985	70.72256
0.00004	65.6311	70.19569	70.14706	70.09536
0.00005	61.8866	70.1026	70.06222	70.02476
0.00006	63.3413	70.37396	70.28625	70.18932
0.00007	71.3238	71.76786	71.61882	71.44508
0.00008	86.0742	77.28601	77.3636	77.47702
0.00009	106.442	94.34812	95.15973	95.98749
0.0001	130	130	130	130
Average temperature	84.5141	82.7979	82.8827	82.9703

Table 4.30: Impact of different roll temperature 130/160(°C) on fabric layer temperature in thickness direction with initial temperature 70°C for machine calender

Web Depth (m)	RT 130/160(°C)			
	Fabric Layer Temperature (°C)			
	HPM Solution	BTCS Solution	CN Solution	FTCS Solution
0	130	130	130	130
0.00001	109.79	94.34816	95.15973	95.98749
0.00002	90.6745	77.28628	77.36366	77.47702
0.00003	74.0906	71.7697	71.61941	71.44511
0.00004	61.9552	70.38558	70.29149	70.19025
0.00005	56.4777	70.171	70.1037	70.04126
0.00006	59.6654	70.56384	70.43069	70.28421
0.00007	72.6774	72.65225	72.42837	72.16763
0.00008	95.2613	80.92908	81.04541	81.21554
0.00009	125.5	106.52218	107.73959	108.98123
0.0001	160	160	160	160
Average temperature	94.1902	91.3298	91.4711	91.6172

Table 4.31: Impact of different roll temperature 160/190(°C) on fabric layer temperature in thickness direction with initial temperature 70°C for machine calender

Web Depth (m)	RT 160/190(°C)			
	Fabric Layer Temperature (°C)			
	HPM Solution	BTCS Solution	CN Solution	FTCS Solution
0	160	160	160	160
0.00001	128.848	106.52222	107.73959	108.98123
0.00002	99.8617	80.92935	81.04547	81.21554
0.00003	75.4442	72.65409	72.42896	72.16766
0.00004	58.2794	70.57546	70.43593	70.28514
0.00005	51.0688	70.23941	70.14518	70.05776
0.00006	55.9896	70.75372	70.57512	70.37911
0.00007	74.031	73.53665	73.23793	72.89018
0.00008	104.448	84.57215	84.72723	84.95405
0.00009	144.558	118.69625	120.31945	121.97497
0.0001	190	190	190	190
Average temperature	103.8662	99.86175	100.0595	100.2641

Table 4.32: Impact of different roll temperature 190/210(°C) on fabric layer temperature in thickness direction with initial temperature 70°C for machine calender

Web Depth (m)	RT 190/210(°C)			
	Fabric Layer Temperature (°C)			
	HPM Solution	BTCS Solution	CN Solution	FTCS Solution
0	190	190	190	190
0.00001	147.348	118.69628	120.31946	121.97497
0.00002	108.282	84.57238	84.72728	84.95405
0.00003	76.3366	73.53818	73.23842	72.8902
0.00004	54.8345	70.76341	70.57949	70.37988
0.00005	46.5614	70.29641	70.17975	70.07152
0.00006	53.308	70.88225	70.67229	70.44252
0.00007	75.3945	74.12655	73.77773	73.37188
0.00008	111.34	87.00091	87.18178	87.44639
0.00009	157.822	126.8123	128.70603	130.63747
0.0001	210	210	210	210
Average temperature	111.9297	106.9717	107.2166	107.4699

Table 4.33: Impact of dwell time on average fabric temperature with initial temperature 50°C for machine calender having different roll temperature 100/130°C

Dwell time (s)	RT 100/130(°C)			
	Average fabric Temperature (°C)			
	HPM Solution	BTCS Solution	CN Solution	FTCS Solution
0.0002	68.38897	63.82672	63.89819	63.98016
0.0004	69.26394	65.5653	65.66993	65.78453
0.0006	70.12245	67.10257	67.22096	67.34635
0.0008	70.96485	68.48585	68.60828	68.73495

Table 4.34: Impact of dwell time on average fabric temperature with initial temperature 50°C for machine calender having different roll temperature 130/160°C

Dwell time (s)	RT 130/160(°C)			
	Average fabric Temperature (°C)			
	HPM Solution	BTCS Solution	CN Solution	FTCS Solution
0.0002	76.87618	70.20829	70.31273	70.43254
0.0004	78.15495	72.74929	72.90221	73.0697
0.0006	79.40973	74.99607	75.16909	75.35236
0.0008	80.64095	77.01778	77.19672	77.38185

Table 4.35: Impact of dwell time on average fabric temperature with initial temperature 50°C for machine calender having different roll temperature 160/190°C

Dwell time (s)	RT 160/190(°C)			
	Average fabric Temperature (°C)			
	HPM Solution	BTCS Solution	CN Solution	FTCS Solution
0.0002	85.36342	76.58985	76.72728	76.88492
0.0004	87.04603	79.93327	80.13448	80.35487
0.0006	88.69706	82.88956	83.11723	83.35836
0.0008	90.31705	85.54971	85.78516	86.02875

Table 4.36: Impact of dwell time on average fabric temperature with initial temperature 50°C for machine calender having different roll temperature 190/210°C

Dwell time (s)	RT 190/210(°C)			
	Average fabric Temperature (°C)			
	HPM Solution	BTCS Solution	CN Solution	FTCS Solution
0.0002	92.43614	81.90782	82.07274	82.2619
0.0004	94.45523	85.91993	86.16138	86.42585
0.0006	96.43641	89.46747	89.74067	90.03004
0.0008	98.38045	92.65965	92.94219	93.2345

Table 4.37: Impact of dwell time on average fabric temperature with initial temperature 70°C for machine calender having different roll temperature 100/130°C

Dwell time (s)	RT 100/130(°C)			
	Average fabric Temperature (°C)			
	HPM Solution	BTCS Solution	CN Solution	FTCS Solution
0.0002	82.73085	79.57235	79.62182	79.67857
0.0004	83.3366	80.77598	80.84841	80.92775
0.0006	83.93095	81.84024	81.9222	82.00901
0.0008	84.51412	82.79789	82.88266	82.97035

Table 4.38: Impact of dwell time on average fabric temperature with initial temperature 70°C for machine calender having different roll temperature 130/160°C

Dwell time (s)	RT 130/160(°C)			
	Average fabric Temperature (°C)			
	HPM Solution	BTCS Solution	CN Solution	FTCS Solution
0.0002	91.21807	85.95391	86.03637	86.13095
0.0004	92.22762	87.95996	88.08069	88.21292
0.0006	93.21825	89.73374	89.87034	90.01502
0.0008	94.19019	91.32982	91.4711	91.61725

Table 4.39: Impact of dwell time on average fabric temperature with initial temperature 70°C for machine calender having different roll temperature 160/190°C

Dwell time (s)	RT 160/190(°C)			
	Average fabric Temperature (°C)			
	HPM Solution	BTCS Solution	CN Solution	FTCS Solution
0.0002	99.70529	92.33547	92.45092	92.58333
0.0004	101.11859	95.14395	95.31297	95.49809
0.0006	102.50552	97.62723	97.81847	98.02102
0.0008	103.86625	99.86175	100.05953	100.26415

Table 4.40: Impact of dwell time on average fabric temperature having different roll temperature 190/210°C for machine calender with initial temperature 70°C

Dwell time (s)	RT 190/210(°C)			
	Average fabric Temperature (°C)			
	HPM Solution	BTCS Solution	CN Solution	FTCS Solution
0.0002	106.77795	97.65344	97.79637	97.96031
0.0004	108.52781	101.13061	101.33986	101.56907
0.0006	110.24499	104.20514	104.44191	104.6927
0.0008	111.92973	106.9717	107.21657	107.4699

Table 4.41: Impact of thermal diffusivity on average fabric temperature with initial temperature 50°C for machine calender having different roll temperature 100/130°C

Thermal diffusivity (m^2/s)	RT 100/130(°C)			
	Average fabric Temperature (°C)			
	HPM Solution	BTCS Solution	CN Solution	FTCS Solution
$9.2x10^{-8}$	70.82555	68.2807	68.39815	68.51987
$9.5x10^{-8}$	70.93008	68.43466	68.55585	68.68128
$9.8x10^{-8}$	71.03435	68.60011	68.72531	68.85471
$10.1x10^{-8}$	71.13836	68.76164	68.89074	69.02398

Table 4.42: Impact of thermal diffusivity on average fabric temperature with initial temperature 50°C for machine calender having different roll temperature 130/160°C

Thermal diffusivity (m^2/s)	RT 130/160(°C)			
	Average fabric Temperature (°C)			
	HPM Solution	BTCS Solution	CN Solution	FTCS Solution
9.2x10^{-8}	80.4373	76.71795	76.88961	77.0675
9.5x10^{-8}	80.59008	76.94296	77.12009	77.30342
9.8x10^{-8}	80.74247	77.18477	77.36776	77.55689
10.1x10^{-8}	80.89454	77.42085	77.60954	77.80428

Table 4.43: Impact of thermal diffusivity on average fabric temperature with initial temperature 50°C for machine calender having different roll temperature 160/190°C

Thermal diffusivity (m^2/s)	RT 160/190(°C)			
	Average fabric Temperature (°C)			
	HPM Solution	BTCS Solution	CN Solution	FTCS Solution
9.2x10^{-8}	90.0492	85.1552	85.38106	85.61513
9.5x10^{-8}	90.25025	85.45126	85.68432	85.92555
9.8x10^{-8}	90.45067	85.76944	86.01021	86.25906
10.1x10^{-8}	90.65066	86.08007	86.32834	86.58458

Table 4.44: Impact of thermal diffusivity on average fabric temperature with initial temperature 50°C for machine calender having different roll temperature 190/210°C

Thermal diffusivity (m^2/s)	RT 190/210(°C)			
	Average fabric Temperature (°C)			
	HPM Solution	BTCS Solution	CN Solution	FTCS Solution
9.2x10^{-8}	98.05905	92.18624	92.45727	92.73816
9.5x10^{-8}	98.30016	92.54152	92.82119	93.11066
9.8x10^{-8}	98.54078	92.92332	93.21225	93.51087
10.1x10^{-8}	98.78086	93.29608	93.59401	93.90149

Table 4.45: Impact of thermal diffusivity on average fabric temperature with initial temperature 70°C for machine calender having different roll temperature 100/130°C

Thermal diffusivity (m^2/s)	RT 100/130(°C)			
	Average fabric Temperature (°C)			
	HPM Solution	BTCS Solution	CN Solution	FTCS Solution
9.2x10^{-8}	84.41774	82.65587	82.73718	82.82145
9.5x10^{-8}	84.49005	82.76245	82.84636	82.9332
9.8x10^{-8}	84.56223	82.877	82.96368	83.05326
10.1x10^{-8}	84.63427	82.98882	83.0782	83.17045

Table 4.46: Impact of thermal diffusivity on average fabric temperature with initial temperature 70°C for machine calender having different roll temperature 130/160°C

Thermal diffusivity (m^2/s)	RT 130/160(°C)			
	Average fabric Temperature (°C)			
	HPM Solution	BTCS Solution	CN Solution	FTCS Solution
9.2x10^{-8}	94.02948	91.09312	91.22864	91.36908
9.5x10^{-8}	94.15007	91.27076	91.41059	91.55533
9.8x10^{-8}	94.27035	91.46166	91.60613	91.75544
10.1x10^{-8}	94.39044	91.64804	91.79701	91.95075

Table 4.47: Impact of thermal diffusivity on average fabric temperature with initial temperature 70°C for machine calender having different roll temperature 160/190°C

Thermal diffusivity (m^2/s)	RT 160/190(°C)			
	Average fabric Temperature (°C)			
	HPM Solution	BTCS Solution	CN Solution	FTCS Solution
9.2x10^{-8}	103.64131	99.53037	99.72009	99.91671
9.5x10^{-8}	103.81016	99.77906	99.97483	100.17746
9.8x10^{-8}	103.97856	100.04633	100.24858	100.45761
10.1x10^{-8}	104.14664	100.30726	100.51581	100.73105

Table 4.48: Impact of thermal diffusivity on average fabric temperature with initial temperature 70°C for machine calender having different roll temperature 190/210°C

Thermal diffusivity (m^2/s)	RT 190/210(°C)			
	Average fabric Temperature (°C)			
	HPM Solution	BTCS Solution	CN Solution	FTCS Solution
9.2x10^{-8}	111.6511	106.56141	106.7963	107.03974
9.5x10^{-8}	111.86011	106.86931	107.1117	107.36257
9.8x10^{-8}	112.06867	107.20021	107.45062	107.70942
10.1x10^{-8}	112.27671	107.52327	107.78148	108.04796

Table 4.49: Impact of roll temperature 130/70(°C) on fabric layer temperature in thickness direction with initial temperature 50°C for rolling calender

Web Depth (m)	RT 130/70(°C)			
	Fabric Layer Temperature (°C)			
	HPM Solution	BTCS Solution	CN Solution	FTCS Solution
0	130	130	130	130
0.00001	114.24	113.83579	114.21027	114.47772
0.00002	99.5889	98.9334	99.56004	100.26172
0.00003	86.989	86.30103	86.99959	87.51419
0.00004	77.0862	76.53995	77.15602	77.98239
0.00005	70.1674	69.8276	70.28442	70.60742
0.00006	66.1688	66.00065	66.2984	66.81157
0.00007	64.7408	64.66899	64.84826	64.91349
0.00008	65.3407	65.30698	65.40902	65.60337
0.00009	67.3226	67.30559	67.35316	67.34254
0.0001	70	70	70	70
Average temperature	82.8768	82.6109	82.9199	83.2286

Table 4.50: Impact of roll temperature 160/80(°C) on fabric layer temperature in thickness direction with initial temperature 50°C for rolling calender

Web Depth (m)	RT 160/80(°C)			
	Fabric Layer Temperature (°C)			
	HPM Solution	BTCS Solution	CN Solution	FTCS Solution
0	160	160	160	160
0.00001	138.372	137.8191	138.33248	138.69764
0.00002	118.283	117.38588	118.24569	119.21113
0.00003	101.043	100.10038	101.06105	101.76651
0.00004	87.5567	86.80462	87.65651	88.80298
0.00005	78.2344	77.75864	78.39818	78.85039
0.00006	73.0003	72.75222	73.17969	73.90856
0.00007	71.3787	71.25766	71.52594	71.63224
0.00008	72.6186	72.55066	72.71099	73
0.00009	75.8155	75.77883	75.85632	75.85072
0.0001	80	80	80	80
Average temperature	96.0275	95.6553	96.0879	96.52

Table 4.51: Impact of roll temperature 190/90(°C) on fabric layer temperature in thickness direction with initial temperature 50°C for rolling calender

Web Depth (m)	RT 190/90(°C)			
	Fabric Layer Temperature (°C)			
	HPM Solution	BTCS Solution	CN Solution	FTCS Solution
0	190	190	190	190
0.00001	162.504	161.80241	162.45468	162.91755
0.00002	136.977	135.83836	136.93134	138.16054
0.00003	115.097	113.89972	115.12251	116.01883
0.00004	98.0273	97.0693	98.157	99.62358
0.00005	86.3013	85.68968	86.51195	87.09336
0.00006	79.8317	79.50378	80.06097	81.00555
0.00007	78.0167	77.84633	78.20362	78.351
0.00008	79.8965	79.79433	80.01297	80.39662
0.00009	84.3084	84.25207	84.35949	84.35891
0.0001	90	90	90	90
Average temperature	109.1782	108.6996	109.2559	109.8114

Table 4.52: Impact of roll temperature 210/100(°C) on fabric layer temperature in thickness direction with initial temperature 50°C for rolling calender

Web Depth (m)	RT 210/100(°C)			
	Fabric Layer Temperature (°C)			
	HPM Solution	BTCS Solution	CN Solution	FTCS Solution
0	210	210	210	210
0.00001	178.648	177.85114	178.59396	179.11852
0.00002	149.57	148.27661	149.52262	150.9285
0.00003	124.711	123.3479	124.74563	125.76637
0.00004	105.425	104.32866	105.57997	107.27357
0.00005	92.3515	91.63796	92.59728	93.27559
0.00006	85.4102	85.0066	85.67433	86.79374
0.00007	83.9221	83.68916	84.13485	84.33176
0.00008	86.782	86.62819	86.91241	87.38819
0.00009	92.633	92.54576	92.68925	92.70402
0.0001	100	100	100	100
Average temperature	119.0412	118.4829	119.1318	119.78

Table 4.53: Impact of roll temperature 130/70(°C) on fabric layer temperature in thickness direction with initial temperature 70°C for rolling calender

Web Depth (m)	RT 130/70(°C)			
	Fabric Layer Temperature (°C)			
	HPM Solution	BTCS Solution	CN Solution	FTCS Solution
0	130	130	130	130
0.00001	117.927	117.60752	117.89759	118.11367
0.00002	106.603	106.08532	106.56623	107.0887
0.00003	96.6431	96.10703	96.63002	97.02865
0.00004	88.4352	88.03183	88.46514	89.0236
0.00005	82.1004	81.89656	82.17065	82.36445
0.00006	77.5178	77.49253	77.60752	77.85278
0.00007	74.3948	74.47499	74.47869	74.42795
0.00008	72.3548	72.45891	72.41521	72.43035
0.00009	71.0101	71.07731	71.04047	70.97849
0.0001	70	70	70	70
Average temperature	89.726	89.5665	89.752	89.9372

Table 4.54: Impact of roll temperature 160/80(°C) on fabric layer temperature in thickness direction with initial temperature 70°C for rolling calender

Web Depth (m)	RT 160/80(°C)			
	Fabric Layer Temperature (°C)			
	HPM Solution	BTCS Solution	CN Solution	FTCS Solution
0	160	160	160	160
0.00001	142.059	141.59083	142.01979	142.33359
0.00002	125.297	124.5378	125.25188	126.03811
0.00003	110.697	109.90637	110.69148	111.28097
0.00004	98.9057	98.2965	98.96563	99.84419
0.00005	90.1674	89.8276	90.28442	90.60742
0.00006	84.3493	84.2441	84.4888	84.94977
0.00007	81.0328	81.06365	81.15637	81.14671
0.00008	79.6327	79.70258	79.71718	79.82698
0.00009	79.503	79.55055	79.54364	79.48667
0.0001	80	80	80	80
Average temperature	102.8767	102.6109	102.9199	103.2286

Table 4.55: Impact of roll temperature 190/90(°C) on fabric layer temperature in thickness direction with initial temperature 70°C for rolling calender

Web Depth (m)	RT 190/90(°C)			
	Fabric Layer Temperature (°C)			
	HPM Solution	BTCS Solution	CN Solution	FTCS Solution
0	190	190	190	190
0.00001	166.191	165.57414	166.142	166.5535
0.00002	143.991	142.99028	143.93753	144.98752
0.00003	124.751	123.70572	124.75294	125.53329
0.00004	109.376	108.56118	109.46611	110.66478
0.00005	98.2344	97.75864	98.39818	98.85039
0.00006	91.1807	90.99566	91.37008	92.04676
0.00007	87.6707	87.65232	87.83405	87.86546
0.00008	86.9106	86.94625	87.01915	87.2236
0.00009	87.9959	88.02379	88.0468	87.99486
0.0001	90	90	90	90
Average temperature	116.0274	115.6553	116.0879	116.52

Table 4.56: Impact of roll temperature 210/100(°C) on fabric layer temperature in thickness direction with initial temperature 70°C for rolling calender

Web Depth (m)	RT 210/100(°C)			
	Fabric Layer Temperature (°C)			
	HPM Solution	BTCS Solution	CN Solution	FTCS Solution
0	210	210	210	210
0.00001	182.336	181.62286	182.28127	182.75447
0.00002	156.584	155.42854	156.52881	157.75548
0.00003	134.365	133.15389	134.37606	135.28084
0.00004	116.774	115.82054	116.88908	118.31478
0.00005	104.285	103.70692	104.48351	105.03262
0.00006	96.7592	96.49848	96.98345	97.83495
0.00007	93.5762	93.49515	93.76528	93.84622
0.00008	93.796	93.78011	93.91859	94.21517
0.00009	96.3205	96.31748	96.37656	96.33997
0.0001	100	100	100	100
Average temperature	125.8905	125.4385	125.9639	126.4889

Table 4.57: Impact of dwell time on average fabric temperature with initial temperature 50°C for rolling calender having different roll temperature 130/70°C

Dwell time (s)	RT 130/70(°C)			
	Average fabric Temperature (°C)			
	HPM Solution	BTCS Solution	CN Solution	FTCS Solution
0.002	69.76725	68.85615	69.25873	69.61429
0.004	74.98617	74.66195	74.98359	75.27827
0.006	79.30418	79.05789	79.36277	79.65651
0.008	82.87676	82.61091	82.91993	83.22858

Table 4.58: Impact of dwell time on average fabric temperature with initial temperature 50°C for rolling calender having different roll temperature 160/80°C

Dwell time (s)	RT 160/80(°C)			
	Average fabric Temperature (°C)			
	HPM Solution	BTCS Solution	CN Solution	FTCS Solution
0.002	77.67417	76.39862	76.96222	77.46
0.004	84.98058	84.52673	84.97702	85.38958
0.006	91.02587	90.68104	91.10788	91.51912
0.008	96.02747	95.65527	96.0879	96.52002

Table 4.59: Impact of dwell time on average fabric temperature with initial temperature 50°C for rolling calender having different roll temperature 190/90°C

Dwell time (s)	RT 190/90(°C)			
	Average fabric Temperature (°C)			
	HPM Solution	BTCS Solution	CN Solution	FTCS Solution
0.002	85.58104	83.94108	84.66572	85.30571
0.004	94.97507	94.39151	94.97046	95.50089
0.006	102.74753	102.3042	102.85299	103.38173
0.008	109.17817	108.69963	109.25587	109.81145

Table 4.60: Impact of dwell time on average fabric temperature with initial temperature 50°C for rolling calender having different roll temperature 210/100°C

Dwell time (s)	RT 210/100(°C)			
	Average fabric Temperature (°C)			
	HPM Solution	BTCS Solution	CN Solution	FTCS Solution
0.002	91.51125	89.59792	90.44334	91.19
0.004	102.47095	101.7901	102.46553	103.08437
0.006	111.53872	111.02157	111.66183	112.27868
0.008	119.04116	118.48291	119.13184	119.78002

Table 4.61: Impact of dwell time on average fabric temperature with initial temperature 70°C for rolling calender having different roll temperature 130/70°C

Dwell time (s)	RT 130/70(°C)			
	Average fabric Temperature (°C)			
	HPM Solution	BTCS Solution	CN Solution	FTCS Solution
0.002	81.8603	81.31369	81.55524	81.76857
0.004	84.99172	84.79717	84.99015	85.16696
0.006	87.58248	87.43473	87.61766	87.79391
0.008	89.72602	89.56654	89.75196	89.93715

Table 4.62: Impact of dwell time on average fabric temperature with initial temperature 70°C for rolling calender having different roll temperature 160/80°C

Dwell time (s)	RT 160/80(°C)			
	Average fabric Temperature (°C)			
	HPM Solution	BTCS Solution	CN Solution	FTCS Solution
0.002	89.76724	88.85615	89.25873	89.61429
0.004	94.98613	94.66195	94.98359	95.27827
0.006	99.30417	99.05789	99.36277	99.65651
0.008	102.87672	102.61091	102.91993	103.22858

Table 4.63: Impact of dwell time on average fabric temperature with initial temperature 70°C for rolling calender having different roll temperature 190/90°C

Dwell time (s)	RT 190/90(°C)			
	Average fabric Temperature (°C)			
	HPM Solution	BTCS Solution	CN Solution	FTCS Solution
0.002	97.67418	96.39862	96.96222	97.46
0.004	104.98064	104.52673	104.97702	105.38958
0.006	111.02592	110.68104	111.10788	111.51912
0.008	116.02739	115.65527	116.0879	116.52002

Table 4.64: Impact of dwell time on average fabric temperature with initial temperature 70°C for rolling calender having different roll temperature 210/100°C

Dwell time (s)	RT 210/100(°C)			
	Average fabric Temperature (°C)			
	HPM Solution	BTCS Solution	CN Solution	FTCS Solution
0.002	103.60429	102.05546	102.73984	103.34429
0.004	112.47652	111.92532	112.4721	112.97306
0.006	119.81697	119.39841	119.91672	120.41607
0.008	125.89054	125.43854	125.96387	126.48859

Table 4.65: Impact of thermal diffusivity on average fabric temperature with initial temperature 50°C for rolling calender having different roll temperature 130/70°C

Thermal diffusivity (m^2/s)	RT 130/70(°C)			
	Average fabric Temperature (°C)			
	HPM Solution	BTCS Solution	CN Solution	FTCS Solution
9.2x10^{-8}	82.32731	82.1072	82.40315	82.69969
9.5x10^{-8}	82.74097	82.48598	82.79172	83.0976
9.8x10^{-8}	83.14498	82.88789	83.20427	83.51793
10.1x10^{-8}	83.53963	83.27509	83.60196	83.91712

Table 4.66: Impact of thermal diffusivity on average fabric temperature with initial temperature 50°C for rolling calender having different roll temperature 160/80°C

Thermal diffusivity (m^2/s)	RT 160/80(°C)			
	Average fabric Temperature (°C)			
	HPM Solution	BTCS Solution	CN Solution	FTCS Solution
9.2x10^{-8}	95.2583	94.95009	95.36441	95.77957
9.5x10^{-8}	95.83744	95.48038	95.90841	96.33665
9.8x10^{-8}	96.40302	96.04305	96.48598	96.9251
10.1x10^{-8}	96.95548	96.58512	97.04274	97.48397

Table 4.67: Impact of thermal diffusivity on average fabric temperature with initial temperature 50°C for rolling calender having different roll temperature 190/90°C

Thermal diffusivity (m^2/s)	RT 190/90(°C)			
	Average fabric Temperature (°C)			
	HPM Solution	BTCS Solution	CN Solution	FTCS Solution
9.2x10^{-8}	108.18927	107.79297	108.32568	108.85944
9.5x10^{-8}	108.93383	108.47477	109.0251	109.57569
9.8x10^{-8}	109.66107	109.1982	109.76769	110.33227
10.1x10^{-8}	110.37127	109.89516	110.48353	111.05081

Table 4.68: Impact of thermal diffusivity on average fabric temperature with initial temperature 50°C for rolling calender having different roll temperature 210/100°C

Thermal diffusivity (m^2/s)	RT 210/100(°C)			
	Average fabric Temperature (°C)			
	HPM Solution	BTCS Solution	CN Solution	FTCS Solution
9.2x10^{-8}	117.88741	117.42513	118.04662	118.66935
9.5x10^{-8}	118.75615	118.22056	118.86261	119.50497
9.8x10^{-8}	119.60465	119.06457	119.72897	120.38765
10.1x10^{-8}	120.43308	119.87768	120.56412	121.22595

Table 4.69: Impact of thermal diffusivity on average fabric temperature with initial temperature 70°C for rolling calender having different roll temperature 130/70°C

Thermal diffusivity (m^2/s)	RT 130/70(°C)			
	Average fabric Temperature (°C)			
	HPM Solution	BTCS Solution	CN Solution	FTCS Solution
9.2x10^{-8}	89.39635	89.26432	89.44189	89.61981
9.5x10^{-8}	89.64465	89.49159	89.67503	89.85856
9.8x10^{-8}	89.88696	89.73273	89.92256	90.11076
10.1x10^{-8}	90.12376	89.96505	90.16118	90.35027

Table 4.70: Impact of thermal diffusivity on average fabric temperature with initial temperature 70°C for rolling calender having different roll temperature 160/80°C

Thermal diffusivity (m^2/s)	RT 160/80(°C)			
	Average fabric Temperature (°C)			
	HPM Solution	BTCS Solution	CN Solution	FTCS Solution
9.2x10^{-8}	102.32725	102.1072	102.40315	102.69969
9.5x10^{-8}	102.74103	102.48598	102.79172	103.0976
9.8x10^{-8}	103.14503	102.88789	103.20427	103.51793
10.1x10^{-8}	103.53955	103.27509	103.60196	103.91712

Table 4.71: Impact of thermal diffusivity on average fabric temperature with initial temperature 70°C for rolling calender having different roll temperature 190/90°C

Thermal diffusivity (m^2/s)	RT 190/90(°C)			
	Average fabric Temperature (°C)			
	HPM Solution	BTCS Solution	CN Solution	FTCS Solution
9.2x10^{-8}	115.25825	114.95009	115.36441	115.77957
9.5x10^{-8}	115.83738	115.48038	115.90841	116.33665
9.8x10^{-8}	116.40309	116.04305	116.48598	116.9251
10.1x10^{-8}	116.95539	116.58512	117.04274	117.48397

Table 4.72: Impact of thermal diffusivity on average fabric temperature with initial temperature 70°C for rolling calender having different roll temperature 210/100°C

Thermal diffusivity (m^2/s)	RT 210/100(°C)			
	Average fabric Temperature (°C)			
	HPM Solution	BTCS Solution	CN Solution	FTCS Solution
9.2x10^{-8}	124.95647	124.58225	125.08536	125.58947
9.5x10^{-8}	125.65987	125.22617	125.74592	126.26593
9.8x10^{-8}	126.34663	125.90941	126.44726	126.98048
10.1x10^{-8}	127.01725	126.56765	127.12333	127.6591

Table 5.1: Impact of roll temperature 200°C on fabric layer temperature at various depths in thickness direction with initial temperature 50°C

Web Depth (m)	Heated Roll Temperature	
	RT 200°C (Lie Method)	RT 200°C (Integral Method)
0	200	200
0.00001	112.961	117.492
0.00002	65.9875	77.3954
0.00003	52.3241	59.7299
0.00004	50.1873	52.8862
0.00005	50.0082	50.6626
0.00006	50.0002	50.1026
0.00007	50	50.008
0.00008	50	50.0001
0.00009	50	50
0.0001	50	50
Average Temperature	71.0426	73.4797

Table 5.2: Impact of roll temperature 240°C on fabric layer temperature at various depths in thickness direction with initial temperature 50°C

Web Depth (m)	Heated Roll Temperature	
	RT 240°C (Lie Method)	RT 240°C (Integral Method)
0	240	240
0.00001	129.751	135.489
0.00002	70.2508	84.7009
0.00003	52.9439	62.3245
0.00004	50.2373	53.6558
0.00005	50.0104	50.8393
0.00006	50.0002	50.1299
0.00007	50	50.0101
0.00008	50	50.002
0.00009	50	50
0.0001	50	50
Average Temperature	76.6539	79.741

Table 5.3: Impact of roll temperature 280°C on fabric layer temperature at various depths in thickness direction with initial temperature 50°C

Web Depth (m)	Heated Roll Temperature	
	RT 280°C (Lie Method)	RT 280°C (Integral Method)
0	280	280
0.00001	146.54	153.487
0.00002	74.5141	92.0063
0.00003	53.5637	64.9192
0.00004	50.2872	54.4255
0.00005	50.0126	51.016
0.00006	50.0003	50.1573
0.00007	50	50.0123
0.00008	50	50.0002
0.00009	50	50
0.0001	50	50
Average Temperature	82.2653	86.0022

Table 5.4: Impact of roll temperature 320°C on fabric layer temperature at various depths in thickness direction with initial temperature 50°C

Web Depth (m)	Heated Roll Temperature	
	RT 320°C (Lie Method)	RT 320°C (Integral Method)
0	320	320
0.00001	163.33	171.485
0.00002	78.7775	99.3118
0.00003	54.1835	67.5138
0.00004	50.3372	55.1951
0.00005	50.0148	51.1927
0.00006	50.0003	50.1846
0.00007	50	50.0144
0.00008	50	50.0002
0.00009	50	50
0.0001	50	50
Average Temperature	87.8767	92.2634

Table 5.5: Impact of roll temperature 200°C on fabric layer temperature at various depths in thickness direction with initial temperature 70°C

Web Depth (m)	Heated Roll Temperature	
	RT 200°C (Lie Method)	RT 200°C (Integral Method)
0	200	200
0.00001	124.566	128.493
0.00002	83.8558	93.7427
0.00003	72.0143	78.4326
0.00004	70.1623	72.5013
0.00005	70.0071	70.5742
0.00006	70.0002	70.0889
0.00007	70	70.0069
0.00008	70	70.0001
0.00009	70	70
0.0001	70	70
Average Temperature	88.2369	90.3491

Table 5.6: Impact of roll temperature 240°C on fabric layer temperature at various depths in thickness direction with initial temperature 70°C

Web Depth (m)	Heated Roll Temperature	
	RT 240°C (Lie Method)	RT 240°C (Integral Method)
0	240	240
0.00001	141.356	146.49
0.00002	88.1191	101.048
0.00003	72.634	81.0272
0.00004	70.2123	73.271
0.00005	70.0043	70.7509
0.00006	70.0002	70.1163
0.00007	70	70.0091
0.00008	70	70.0002
0.00009	70	70
0.0001	70	70
Average Temperature	93.8478	96.6103

Table 5.7: Impact of roll temperature 280°C on fabric layer temperature at various depths in thickness direction with initial temperature 70°C

Web Depth (m)	Heated Roll Temperature	
	RT 280°C (Lie Method)	RT 280°C (Integral Method)
0	280	280
0.00001	158.146	164.488
0.00002	92.3825	108.354
0.00003	73.2538	83.6219
0.00004	70.2623	74.0406
0.00005	70.0115	70.9276
0.00006	70.0003	70.1436
0.00007	70	70.0112
0.00008	70	70.0002
0.00009	70	70
0.0001	70	70
Average Temperature	99.4597	102.8716

Table 5.8: Impact of roll temperature 320°C on fabric layer temperature at various depths in thickness direction with initial temperature 70°C

Web Depth (m)	Heated Roll Temperature	
	RT 320°C (Lie Method)	RT 320°C (Integral Method)
0	320	320
0.00001	174.935	182.486
0.00002	96.6458	115.659
0.00003	73.8736	86.2165
0.00004	70.3122	74.8103
0.00005	70.0137	71.1043
0.00006	70.0003	70.171
0.00007	70	70.0133
0.00008	70	70.0002
0.00009	70	70
0.0001	70	70
Average Temperature	105.071	109.1328

Table 5.9: Impact of dwell time on average fabric temperature with initial temperature 50°C at roll temperature 200°C for incompressible semi infinite medium

Dwell time (s)	Heated Roll Temperature	
	RT 200°C (Lie Method)	RT 200°C (Integral Method)
0.0002	65.1068	66.3986
0.0004	67.4128	69.1956
0.0006	69.3539	71.4917
0.0008	71.0426	73.4797

Table 5.10: Impact of dwell time on average fabric temperature with initial temperature 50°C at roll temperature 240°C for incompressible semi infinite medium

Dwell time (s)	Heated Roll Temperature	
	RT 240°C (Lie Method)	RT 240°C (Integral Method)
0.0002	69.1353	70.7715
0.0004	72.0562	74.3144
0.0006	74.515	77.2228
0.0008	76.6994	79.7409

Table 5.11: Impact of dwell time on average fabric temperature with initial temperature 50°C at roll temperature 280°C for incompressible semi infinite medium

Dwell time (s)	Heated Roll Temperature	
	RT 280°C (Lie Method)	RT 280°C (Integral Method)
0.0002	73.1638	75.1445
0.0004	76.6996	79.4332
0.0006	79.676	82.954
0.0008	82.2653	86.0022

Table 5.12: Impact of dwell time on average fabric temperature with initial temperature 50°C at roll temperature 320°C for incompressible semi infinite medium

Dwell time (s)	Heated Roll Temperature	
	RT 320°C (Lie Method)	RT 320°C (Integral Method)
0.0002	77.1923	79.5174
0.0004	81.343	84.5521
0.0006	84.837	88.1396
0.0008	87.8767	92.2634

Table 5.13: Impact of dwell time on average fabric temperature with initial temperature 70°C at roll temperature 200°C for incompressible semi infinite medium

Dwell time (s)	Heated Roll Temperature	
	RT 200°C (Lie Method)	RT 200°C (Integral Method)
0.0002	83.0926	84.2121
0.0004	85.0911	86.6362
0.0006	86.7734	88.6262
0.0008	88.2369	90.3491

Table 5.14: Impact of dwell time on average fabric temperature with initial temperature 70°C at roll temperature 240°C for incompressible semi infinite medium

Dwell time (s)	Heated Roll Temperature	
	RT 240°C (Lie Method)	RT 240°C (Integral Method)
0.0002	87.1211	88.5851
0.0004	89.7345	91.7551
0.0006	91.9345	94.3573
0.0008	93.8483	96.6103

Table 5.15: Impact of dwell time on average fabric temperature with initial temperature 70°C at roll temperature 280°C for incompressible semi infinite medium

Dwell time (s)	Heated Roll Temperature	
	RT 280°C (Lie Method)	RT 280°C (Integral Method)
0.0002	91.1496	92.958
0.0004	94.5597	96.8739
0.0006	97.0955	100.0884
0.0008	99.4597	102.8716

Table 5.16: Impact of dwell time on average fabric temperature with initial temperature 70°C at roll temperature 320°C for incompressible semi infinite medium

Dwell time (s)	Heated Roll Temperature	
	RT 320°C (Lie Method)	RT 320°C (Integral Method)
0.0002	95.1781	97.331
0.0004	99.0213	101.9927
0.0006	102.2567	105.8195
0.0008	105.071	109.1328

Table 5.17: Impact of thermal diffusivity on average fabric temperature with initial temperature 50°C at roll temperature 200°C for incompressible semi infinite medium

Thermal diffusivity (m^2/s)	Heated Roll Temperature	
	RT 200°C (Lie Method)	RT 200°C (Integral Method)
$9.2x10^{-8}$	70.775	72.3468
$9.5x10^{-8}$	70.9762	73.4015
$9.8x10^{-8}$	71.1746	73.6348
$10.1x10^{-8}$	71.3703	73.865

Table 5.18: Impact of thermal diffusivity on average fabric temperature with initial temperature 50°C at roll temperature 240°C for incompressible semi infinite medium

Thermal diffusivity (m^2/s)	Heated Roll Temperature	
	RT 240°C (Lie Method)	RT 240°C (Integral Method)
$9.2x10^{-8}$	76.315	79.3423
$9.5x10^{-8}$	76.5698	79.6419
$9.8x10^{-8}$	76.8211	79.9375
$10.1x10^{-8}$	77.0691	80.229

Table 5.19: Impact of thermal diffusivity on average fabric temperature with initial temperature 50°C at roll temperature 280°C for incompressible semi infinite medium

Thermal diffusivity (m^2/s)	Heated Roll Temperature	
	RT 280°C (Lie Method)	RT 280°C (Integral Method)
$9.2x10^{-8}$	81.855	85.5196
$9.5x10^{-8}$	82.1634	85.8823
$9.8x10^{-8}$	82.4677	86.2401
$10.1x10^{-8}$	82.7679	86.5931

Table 5.20: Impact of thermal diffusivity on average fabric temperature with initial temperature 50°C at roll temperature 320°C for incompressible semi infinite medium

Thermal diffusivity (m^2/s)	Heated Roll Temperature	
	RT 320°C (Lie Method)	RT 320°C (Integral Method)
$9.2x10^{-8}$	87.3949	91.6968
$9.5x10^{-8}$	87.7571	92.1209
$9.8x10^{-8}$	88.1142	92.5427
$10.1x10^{-8}$	88.4666	92.9569

Table 5.21: Impact of thermal diffusivity on average fabric temperature with initial temperature 70°C at roll temperature 200°C for incompressible semi infinite medium

Thermal diffusivity (m^2/s)	Heated Roll Temperature	
	RT 200°C (Lie Method)	RT 200°C (Integral Method)
9.2x10^{-8}	88.0049	90.0763
9.5x10^{-8}	88.1794	90.2813
9.8x10^{-8}	88.3513	90.4835
10.1x10^{-8}	88.521	90.683

Table 5.22: Impact of thermal diffusivity on average fabric temperature with initial temperature 70°C at roll temperature 240°C for incompressible semi infinite medium

Thermal diffusivity (m^2/s)	Heated Roll Temperature	
	RT 240°C (Lie Method)	RT 240°C (Integral Method)
9.2x10^{-8}	93.55	96.2536
9.5x10^{-8}	93.773	96.5217
9.8x10^{-8}	93.9978	96.7818
10.1x10^{-8}	94.2197	97.047

Table 5.23: Impact of thermal diffusivity on average fabric temperature with initial temperature 70°C at roll temperature 280°C for incompressible semi infinite medium

Thermal diffusivity (m^2/s)	Heated Roll Temperature	
	RT 280°C (Lie Method)	RT 280°C (Integral Method)
9.2x10^{-8}	99.0849	102.4309
9.5x10^{-8}	99.3666	102.762
9.8x10^{-8}	99.6398	103.089
10.1x10^{-8}	99.9185	103.411

Table 5.24: Impact of thermal diffusivity on average fabric temperature with initial temperature 70°C at roll temperature 320°C for incompressible semi infinite medium

Thermal diffusivity (m^2/s)	Heated Roll Temperature	
	RT 320°C (Lie Method)	RT 320°C (Integral Method)
$9.2x10^{-8}$	104.625	108.6082
$9.5x10^{-8}$	104.96	109.0935
$9.8x10^{-8}$	105.2909	109.3915
$10.1x10^{-8}$	105.6172	118.8659

Table 5.25: Impact of roll temperature 200°C on fabric layer temperature at various depths in thickness direction with initial temperature 50°C

Web Depth (m)	Heated Roll Temperature	
	RT 200°C (Without Volume Change)	RT 200°C (With Volume Change)
0	200	200
0.00001	117.954	136.704
0.00002	70.013	89.8858
0.00003	53.6566	64.2731
0.00004	50.403	53.9113
0.00005	50.0263	50.812
0.00006	50.001	50.1267
0.00007	50	50.0148
0.00008	50	50.0013
0.00009	50	50.0001
0.0001	50	50
Average Temperature	72.0049	76.8845

Table 5.26: Impact of roll temperature 240°C on fabric layer temperature at various depths in thickness direction with initial temperature 50°C

Web Depth (m)	Heated Roll Temperature	
	RT 240°C (Without Volume Change)	RT 240°C (With Volume Change)
0	240	240
0.00001	136.075	159.825
0.00002	75.3498	100.522
0.00003	54.6317	68.0793
0.00004	50.5104	54.9544
0.00005	50.0333	51.0285
0.00006	50.0013	50.1605
0.00007	50	50.0187
0.00008	50	50.0016
0.00009	50	50.0001
0.0001	50	50
Average Temperature	77.8729	84.0536

Table 5.27: Impact of roll temperature 280°C on the fabric layer temperature at various depths in thickness direction with initial temperature 50°C

Web Depth (m)	Heated Roll Temperature	
	RT 280°C (Without Volume Change)	RT 280°C (With Volume Change)
0	280	280
0.00001	154.197	182.946
0.00002	80.6866	111.158
0.00003	55.6068	71.8855
0.00004	50.6179	55.9974
0.00005	50.0404	51.245
0.00006	50.0015	50.1943
0.00007	50	50.0227
0.00008	50	50.002
0.00009	50	50.0001
0.0001	50	50
Average Temperature	83.7409	91.2228

Table 5.28: Impact of roll temperature 320°C on fabric layer temperature at various depths in thickness direction with initial temperature 50°C

Web Depth (m)	Heated Roll Temperature	
	RT 320°C (Without Volume Change)	RT 320°C (With Volume Change)
0	320	320
0.00001	172.318	206.067
0.00002	86.0234	121.794
0.00003	56.5819	75.6917
0.00004	50.7234	57.0404
0.00005	50.0474	51.4616
0.00006	50.0018	50.2281
0.00007	50	50.0266
0.00008	50	50.0023
0.00009	50	50.0001
0.0001	50	50
Average Temperature	89.6087	98.392

Table 5.29: Impact of roll temperature 200°C on fabric layer temperature at various depths in thickness direction with initial temperature 70°C

Web Depth (m)	Heated Roll Temperature	
	RT 200°C (Without Volume Change)	RT 200°C (With Volume Change)
0	200	200
0.00001	124.566	141.466
0.00002	83.8558	100.105
0.00003	72.0143	79.4562
0.00004	70.1623	72.1748
0.00005	70.0071	70.3618
0.00006	70.0002	70.0432
0.00007	70	70.0037
0.00008	70	70.0002
0.00009	70	70
0.0001	70	70
Average Temperature	88.2369	92.1465

Table 5.30: Impact of roll temperature 240°C on fabric layer temperature at various depths in thickness direction with initial temperature 70°C

Web Depth (m)	Heated Roll Temperature	
	RT 240°C (Without Volume Change)	RT 240°C (With Volume Change)
0	240	240
0.00001	141.356	163.455
0.00002	88.1191	109.368
0.00003	72.634	82.3658
0.00004	70.2123	72.8439
0.00005	70.0093	70.4731
0.00006	70.0002	70.0564
0.00007	70	70.0048
0.00008	70	70.0003
0.00009	70	70
0.0001	70	70
Average Temperature	93.8483	98.9607

Table 5.31: Impact of roll temperature 280°C on fabric layer temperature at various depths in thickness direction with initial temperature 70°C

Web Depth (m)	Heated Roll Temperature	
	RT 280°C (Without Volume Change)	RT 280°C (With Volume Change)
0	280	280
0.00001	158.146	185.445
0.00002	92.3825	118.631
0.00003	73.2538	85.2754
0.00004	70.2623	73.5131
0.00005	70.0115	70.5844
0.00006	70.0003	70.0697
0.00007	70	70.0059
0.00008	70	70.0004
0.00009	70	70
0.0001	70	70
Average Temperature	99.4597	105.775

Table 5.32: Impact of roll temperature 320°C on fabric layer temperature at various depths in thickness direction with initial temperature 70°C

Web Depth (m)	Heated Roll Temperature	
	RT 320°C (Without Volume Change)	RT 320°C (With Volume Change)
0	320	320
0.00001	174.935	207.434
0.00002	96.6458	127.894
0.00003	73.8736	88.185
0.00004	70.3122	74.1822
0.00005	70.0137	70.6957
0.00006	70.0003	70.083
0.00007	70	70.0071
0.00008	70	70.0004
0.00009	70	70
0.0001	70	70
Average Temperature	105.071	112.5892

Table 5.33: Impact of dwell time at roll temperature 200°C on average fabric temperature with initial temperature 50°C

Dwell time (s)	Heated Roll Temperature	
	RT 200°C (Without Volume Change)	RT 200°C (With Volume Change)
0.0002	65.1068	67.0269
0.0004	67.4128	70.4569
0.0006	69.3539	73.2023
0.0008	71.0425	75.5536

Table 5.34: Impact of dwell time at roll temperature 240°C on average fabric temperature with initial temperature 50°C

Dwell time (s)	Heated Roll Temperature	
	RT 240°C (Without Volume Change)	RT 240°C (With Volume Change)
0.0002	69.1353	71.5674
0.0004	72.5617	75.9121
0.0006	74.715	79.3897
0.0008	76.6994	82.3678

Table 5.35: Impact of dwell time at roll temperature 280°C on average fabric temperature with initial temperature 50°C

Dwell time (s)	Heated Roll Temperature	
	RT 280°C (Without Volume Change)	RT 280°C (With Volume Change)
0.0002	73.1638	76.1079
0.0004	76.6996	81.3673
0.0006	79.676	85.5769
0.0008	82.2653	89.1822

Table 5.36: Impact of dwell time at roll temperature 320°C on average fabric temperature with initial temperature 50°C

Dwell time (s)	Heated Roll Temperature	
	RT 320°C (Without Volume Change)	RT 320°C (With Volume Change)
0.0002	77.1923	80.6481
0.0004	81.343	86.8224
0.0006	84.837	91.7645
0.0008	87.8767	95.9964

Table 5.37: Impact of dwell time at roll temperature 200°C on average fabric temperature with initial temperature 70°C

Dwell time (s)	Heated Roll Temperature	
	RT 200°C (Without Volume Change)	RT 200°C (With Volume Change)
0.0002	83.0926	84.7567
0.0004	85.091	87.7293
0.0006	86.7734	90.1087
0.0008	88.2389	92.1465

Table 5.38: Impact of dwell time at roll temperature 240°C on average fabric temperature with initial temperature 70°C

Dwell time (s)	Heated Roll Temperature	
	RT 240°C (Without Volume Change)	RT 240°C (With Volume Change)
0.0002	87.1211	89.2972
0.0004	89.7345	93.1845
0.0006	91.9345	96.296
0.0008	93.8483	98.9607

Table 5.39: Impact of dwell time at roll temperature 280°C on average fabric temperature with initial temperature 70°C

Dwell time (s)	Heated Roll Temperature	
	RT 280°C (Without Volume Change)	RT 280°C (With Volume Change)
0.0002	91.1496	93.8377
0.0004	94.5597	98.7306
0.0006	97.0955	102.4833
0.0008	99.4597	105.775

Table 5.40: Impact of dwell time at roll temperature 320°C on average fabric temperature with initial temperature 70°C

Dwell time (s)	Heated Roll Temperature	
	RT 320°C (Without Volume Change)	RT 320°C (With Volume Change)
0.0002	95.178	98.3782
0.0004	99.0213	104.0949
0.0006	102.2566	108.6705
0.0008	105.071	112.5892

Table 5.41: Impact of thermal diffusivity at roll temperature 200°C on average fabric temperature with initial temperature 50°C

Thermal diffusivity (m^2/s)	Heated Roll Temperature	
	RT 200°C (Without Volume Change)	RT 200°C (With Volume Change)
$9.2x10^{-8}$	70.775	75.1825
$9.5x10^{-8}$	70.9762	75.4615
$9.8x10^{-8}$	71.1746	75.7364
$10.1x10^{-8}$	71.3703	76.0074

Table 5.42: Impact of thermal diffusivity at roll temperature 240°C on average fabric temperature with initial temperature 50°C

Thermal diffusivity (m^2/s)	Heated Roll Temperature	
	RT 240°C (Without Volume Change)	RT 240°C (With Volume Change)
$9.2x10^{-8}$	76.315	81.8978
$9.5x10^{-8}$	76.5698	82.2513
$9.8x10^{-8}$	76.8211	82.5994
$10.1x10^{-8}$	77.0691	82.9427

Table 5.43: Impact of thermal diffusivity at roll temperature 280°C on average fabric temperature with initial temperature 50°C

Thermal diffusivity (m^2/s)	Heated Roll Temperature	
	RT 280°C (Without Volume Change)	RT 280°C (With Volume Change)
9.2x10^{-8}	81.8549	88.6132
9.5x10^{-8}	82.1634	89.0409
9.8x10^{-8}	82.4677	89.4625
10.1x10^{-8}	82.7679	89.8781

Table 5.44: Impact of thermal diffusivity at roll temperature 320°C on average fabric temperature with initial temperature 50°C

Thermal diffusivity (m^2/s)	Heated Roll Temperature	
	RT 320°C (Without Volume Change)	RT 320°C (With Volume Change)
9.2x10^{-8}	87.3949	95.3285
9.5x10^{-8}	87.7571	95.8307
9.8x10^{-8}	88.1142	96.3255
10.1x10^{-8}	88.4666	96.8133

Table 5.45: Impact of thermal diffusivity at roll temperature 200°C on average fabric temperature with initial temperature 70°C

Thermal diffusivity (m^2/s)	Heated Roll Temperature	
	RT 200°C (Without Volume Change)	RT 200°C (With Volume Change)
9.2x10^{-8}	88.0049	91.8248
9.5x10^{-8}	88.1794	92.0667
9.8x10^{-8}	88.3513	92.3049
10.1x10^{-8}	88.521	92.5397

Table 5.46: Impact of thermal diffusivity at roll temperature 240°C on average fabric temperature with initial temperature 70°C

Thermal diffusivity (m^2/s)	Heated Roll Temperature	
	RT 240°C (Without Volume Change)	RT 240°C (With Volume Change)
9.2x10^{-8}	93.55	98.5402
9.5x10^{-8}	93.773	98.8564
9.8x10^{-8}	93.9978	99.168
10.1x10^{-8}	94.2197	99.4751

Table 5.47: Impact of thermal diffusivity at roll temperature 280°C on average fabric temperature with initial temperature 70°C

Thermal diffusivity (m^2/s)	Heated Roll Temperature	
	RT 280°C (Without Volume Change)	RT 280°C (With Volume Change)
9.2x10^{-8}	99.0849	105.2554
9.5x10^{-8}	99.3666	105.6461
9.8x10^{-8}	99.6398	106.031
10.1x10^{-8}	99.9185	106.4104

Table 5.48: Impact of thermal diffusivity at roll temperature 320°C on average fabric temperature with initial temperature 70°C

Thermal diffusivity (m^2/s)	Heated Roll Temperature	
	RT 320°C (Without Volume Change)	RT 320°C (With Volume Change)
9.2x10^{-8}	104.625	111.9708
9.5x10^{-8}	104.96	112.4358
9.8x10^{-8}	105.2909	112.8941
10.1x10^{-8}	105.6172	113.3456

Table 6.1: Impact of same roll temperature 100/100(°C) on fabric temperature in thickness direction at various depths with initial temperature 50°C when $E_p < 0.05$

Web Depth (m)	RT 100/100(°C)	
	Fabric Layer Temperature (°C)	
	Analytical Solution	FTCS Solution
0	76.5552	66.4187
0.00001	74.5194	64.2987
0.00002	72.6644	64.023
0.00003	71.0024	64.0012
0.00004	69.5434	64
0.00005	68.2959	64
0.00006	67.2667	64
0.00007	66.461	64
0.00008	65.8828	64
0.00009	65.5349	64
0.0001	65.4188	64
Average Temperature	69.3768	64.2492

Table 6.2: Impact of same roll temperature 130/130(°C) on fabric temperature in thickness direction at various depths with initial temperature 50°C when $E_p < 0.05$

Web Depth (m)	RT 130/130(°C)	
	Fabric Layer Temperature (°C)	
	Analytical Solution	FTCS Solution
0	92.4884	76.27
0.00001	89.231	72.878
0.00002	86.2631	72.4369
0.00003	83.6038	72.4019
0.00004	81.2694	72.4001
0.00005	79.2734	72.4
0.00006	77.6266	72.4
0.00007	76.3376	72.4
0.00008	75.4126	72.4
0.00009	74.8559	72.4
0.0001	74.67	72.4
Average Temperature	81.0029	72.7988

Table 6.3: Impact of same roll temperature 160/160(°C) on fabric temperature in thickness direction at various depths with initial temperature 50°C when $E_p < 0.05$

Web Depth (m)	RT 160/160(°C)	
	Fabric Layer Temperature (°C)	
	Analytical Solution	FTCS Solution
0	108.552	86.3078
0.00001	104.084	81.6556
0.00002	100.014	81.0506
0.00003	96.3664	81.0026
0.00004	93.1647	81.0001
0.00005	90.4271	81
0.00006	88.1685	81
0.00007	86.4005	81
0.00008	85.1318	81
0.00009	84.3683	81
0.0001	84.1134	81
Average Temperature	92.792	81.547

Table 6.4: Impact of same roll temperature 190/190(°C) on fabric temperature in thickness direction at various depths with initial temperature 50°C when $E_p < 0.05$

Web Depth (m)	RT 190/190(°C)	
	Fabric Layer Temperature (°C)	
	Analytical Solution	FTCS Solution
0	124.485	96.159
0.00001	118.796	90.2348
0.00002	113.612	89.4644
0.00003	108.968	89.4033
0.00004	104.891	89.4001
0.00005	101.405	89.4
0.00006	98.5285	89.4
0.00007	96.2771	89.4
0.00008	94.6615	89.4
0.00009	93.6892	89.4
0.0001	93.3646	89.4
Average Temperature	104.4253	90.0965

Table 6.5: Impact of same roll temperature 100/100(°C) on fabric temperature in thickness direction at various depths with initial temperature 70°C when $E_p < 0.05$

Web Depth (m)	RT 100/100(°C)	
	Fabric Layer Temperature (°C)	
	Analytical Solution	FTCS Solution
0	85.9331	79.8512
0.00001	84.7116	78.5792
0.00002	83.5987	78.4138
0.00003	82.6014	78.4007
0.00004	81.726	78.4
0.00005	80.9775	78.4
0.00006	80.36	78.4
0.00007	79.8766	78.4
0.00008	79.5297	78.4
0.00009	79.3209	78.4
0.0001	79.2513	78.4
Average Temperature	81.6261	78.5495

Table 6.6: Impact of same roll temperature 130/130(°C) on fabric temperature in thickness direction at various depths with initial temperature 70°C when $E_p < 0.05$

Web Depth (m)	RT 130/130(°C)	
	Fabric Layer Temperature (°C)	
	Analytical Solution	FTCS Solution
0	101.997	89.889
0.00001	99.5648	87.3568
0.00002	97.3492	87.0275
0.00003	95.364	87.0014
0.00004	93.6213	87.0001
0.00005	92.1312	87
0.00006	90.9018	87
0.00007	89.9395	87
0.00008	89.249	87
0.00009	88.8334	87
0.0001	88.6946	87
Average Temperature	93.4223	87.2977

Table 6.7: Impact of same roll temperature 160/160(°C) on fabric temperature in thickness direction at various depths with initial temperature 70°C when $E_p < 0.05$

Web Depth (m)	RT 160/160(°C)	
	Fabric Layer Temperature (°C)	
	Analytical Solution	FTCS Solution
0	117.799	99.5537
0.00001	114.135	95.7377
0.00002	110.796	95.2415
0.00003	107.804	95.2021
0.00004	105.178	95.2001
0.00005	102.933	95.2
0.00006	101.08	95.2
0.00007	99.6298	95.2
0.00008	98.5891	95.2
0.00009	97.9628	95.2
0.0001	97.7538	95.2
Average Temperature	104.8782	95.6486

Table 6.8: Impact of same roll temperature 190/190(°C) on fabric temperature in thickness direction at various depths with initial temperature 70°C when $E_p < 0.05$

Web Depth (m)	RT 190/190(°C)	
	Fabric Layer Temperature (°C)	
	Analytical Solution	FTCS Solution
0	133.993	107.7625
0.00001	129.13	104.4647
0.00002	124.698	104.0359
0.00003	120.728	104.0019
0.00004	117.243	104.0001
0.00005	114.262	104
0.00006	111.804	104
0.00007	109.879	104
0.00008	108.498	104
0.00009	107.667	104
0.0001	107.389	104
Average Temperature	116.8446	104.3877

Table 6.9: Impact of same roll temperature 100/100(°C) on fabric temperature in thickness direction at various depths with initial temperature 50°C when $E_p > 0.05$

Web Depth (m)	RT 100/100(°C)	
	Fabric Layer Temperature (°C)	
	Analytical Solution	FTCS Solution
0	78.4069	76.3099
0.00001	77.1572	66.9958
0.00002	76.0217	64.474
0.00003	75.006	64.0512
0.00004	74.1153	64.0039
0.00005	73.3539	64.0002
0.00006	72.7257	64
0.00007	72.2338	64
0.00008	71.8807	64
0.00009	71.6681	64
0.0001	71.5971	64
Average Temperature	74.0151	65.4395

Table 6.10: Impact of same roll temperature 130/130(°C) on fabric temperature in thickness direction at various depths with initial temperature 50°C when $E_p > 0.05$

Web Depth (m)	RT 130/130(°C)	
	Fabric Layer Temperature (°C)	
	Analytical Solution	FTCS Solution
0	95.451	92.0959
0.00001	93.4515	77.1933
0.00002	91.6347	73.1583
0.00003	90.0096	72.4819
0.00004	88.5844	72.4062
0.00005	87.3662	72.4003
0.00006	86.3611	72.4
0.00007	85.5741	72.4
0.00008	85.0091	72.4
0.00009	84.669	72.4
0.0001	84.5554	72.4
Average Temperature	88.4242	74.7033

Table 6.11: Impact of same roll temperature 160/160(°C) on fabric temperature in thickness direction at various depths with initial temperature 50°C when $E_p > 0.05$

Web Depth (m)	RT 160/160(°C)	
	Fabric Layer Temperature (°C)	
	Analytical Solution	FTCS Solution
0	112.615	108.0134
0.00001	109.873	87.5742
0.00002	107.381	82.0401
0.00003	105.152	81.1123
0.00004	103.197	81.0085
0.00005	101.527	81.0004
0.00006	100.148	81
0.00007	99.0686	81
0.00008	98.2937	81
0.00009	97.8272	81
0.0001	97.6715	81
Average Temperature	102.9776	84.1590

Table 6.12: Impact of same roll temperature 190/190(°C) on fabric temperature in thickness direction at various depths with initial temperature 50°C when $E_p > 0.05$

Web Depth (m)	RT 190/190(°C)	
	Fabric Layer Temperature (°C)	
	Analytical Solution	FTCS Solution
0	129.659	123.7994
0.00001	126.167	97.7717
0.00002	122.994	90.7244
0.00003	120.156	89.543
0.00004	117.667	89.4108
0.00005	115.539	89.4006
0.00006	113.783	89.4
0.00007	112.409	89.4
0.00008	111.422	89.4
0.00009	110.828	89.4
0.0001	110.63	89.4
Average Temperature	117.3867	93.4227

Table 6.13: Impact of same roll temperature 100/100(°C) on fabric temperature in thickness direction at various depths with initial temperature 70°C when $E_p > 0.05$

Web Depth (m)	RT 100/100(°C)	
	Fabric Layer Temperature (°C)	
	Analytical Solution	FTCS Solution
0	87.0441	85.7859
0.00001	86.2943	80.1975
0.00002	85.613	78.6844
0.00003	85.0036	78.4307
0.00004	84.4692	78.4023
0.00005	84.0123	78.4001
0.00006	83.6354	78.4
0.00007	83.3403	78.4
0.00008	83.1284	78.4
0.00009	83.0009	78.4
0.0001	82.9583	78.4
Average Temperature	84.4091	79.2637

Table 6.14: Impact of same roll temperature 130/130(°C) on fabric temperature in thickness direction at various depths with initial temperature 70°C when $E_p > 0.05$

Web Depth (m)	RT 130/130(°C)	
	Fabric Layer Temperature (°C)	
	Analytical Solution	FTCS Solution
0	104.208	101.7035
0.00001	102.716	90.5783
0.00002	101.359	87.5661
0.00003	100.146	87.0611
0.00004	99.0821	87.0046
0.00005	98.1727	87.0002
0.00006	97.4223	87
0.00007	96.8348	87
0.00008	96.413	87
0.00009	96.1591	87
0.0001	96.0743	87
Average Temperature	98.9625	88.7194

Table 6.15: Impact of same roll temperature 160/160(°C) on fabric temperature in thickness direction at various depths with initial temperature 70°C when $E_p > 0.05$

Web Depth (m)	RT 160/160(°C)	
	Fabric Layer Temperature (°C)	
	Analytical Solution	FTCS Solution
0	121.132	117.3578
0.00001	118.883	100.5925
0.00002	116.839	96.0531
0.00003	115.011	95.2921
0.00004	113.407	95.207
0.00005	112.037	95.2004
0.00006	110.906	95.2
0.00007	110.021	95.2
0.00008	109.385	95.2
0.00009	109.003	95.2
0.0001	108.875	95.2
Average Temperature	113.2272	97.7912

Table 6.16: Impact of same roll temperature 190/190(°C) on fabric temperature in thickness direction at various depths with initial temperature 70°C when $E_p > 0.05$

Web Depth (m)	RT 190/190(°C)	
	Fabric Layer Temperature (°C)	
	Analytical Solution	FTCS Solution
0	138.416	133.407
0.00001	135.431	111.1567
0.00002	132.718	105.1322
0.00003	130.292	104.1223
0.00004	128.164	104.0092
0.00005	126.345	104.0005
0.00006	124.845	104
0.00007	123.67	104
0.00008	122.826	104
0.00009	122.318	104
0.0001	122.149	104
Average Temperature	127.9249	107.4389

Table 6.17: Impact of different roll temperature 100/130(°C) on fabric temperature in thickness direction at various depths with initial temperature 50°C when $E_p < 0.05$

Web Depth (m)	RT 100/130(°C)	
	Fabric Layer Temperature (°C)	
	Analytical Solution	FTCS Solution
0	91.5766	72.9484
0.00001	88.2401	71.2406
0.00002	85.2	71.0186
0.00003	82.4761	71.001
0.00004	80.085	71
0.00005	78.0405	71
0.00006	76.3537	71
0.00007	75.0333	71
0.00008	74.0858	71
0.00009	73.5155	71
0.0001	73.3252	71
Average Temperature	79.812	71.2008

Table 6.18: Impact of different roll temperature 130/160(°C) on fabric temperature in thickness direction at various depths with initial temperature 50°C when $E_p < 0.05$

Web Depth (m)	RT 130/160(°C)	
	Fabric Layer Temperature (°C)	
	Analytical Solution	FTCS Solution
0	108.552	84.2922
0.00001	104.084	81.4066
0.00002	100.014	81.0314
0.00003	96.3664	81.0016
0.00004	93.1647	81.0001
0.00005	90.4271	81
0.00006	88.1685	81
0.00007	86.4005	81
0.00008	85.1318	81
0.00009	84.3683	81
0.0001	84.1134	81
Average Temperature	92.7992	81.3393

Table 6.19: Impact of different roll temperature 160/190(°C) on fabric temperature in thickness direction at various depths with initial temperature 50°C when $E_p < 0.05$

Web Depth (m)	RT 160/190(°C)	
	Fabric Layer Temperature (°C)	
	Analytical Solution	FTCS Solution
0	125.071	94.9829
0.00001	119.433	90.8784
0.00002	114.296	90.3446
0.00003	109.693	90.3023
0.00004	105.652	90.3001
0.00005	102.197	90.3
0.00006	99.3468	90.3
0.00007	97.1156	90.3
0.00008	95.5144	90.3
0.00009	94.5508	90.3
0.0001	94.2292	90.3
Average Temperature	105.1908	90.7826

Table 6.20: Impact of different roll temperature 190/210(°C) on fabric temperature in thickness direction at various depths with initial temperature 50°C when $E_p < 0.05$

Web Depth (m)	RT 190/210(°C)	
	Fabric Layer Temperature (°C)	
	Analytical Solution	FTCS Solution
0	137.321	104.5543
0.00001	131.01	99.1601
0.00002	125.26	98.4586
0.00003	120.107	98.403
0.00004	115.585	98.4001
0.00005	111.717	98.4
0.00006	108.527	98.4
0.00007	106.029	98.4
0.00008	104.237	98.4
0.00009	103.158	98.4
0.0001	102.798	98.4
Average Temperature	115.0681	99.0342

Table 6.21: Impact of different roll temperature 100/130(°C) on fabric temperature in thickness direction at various depths with initial temperature 70°C when $E_p < 0.05$

Web Depth (m)	RT 100/130(°C)	
	Fabric Layer Temperature (°C)	
	Analytical Solution	FTCS Solution
0	100.368	85.5414
0.00001	97.7953	84.6286
0.00002	95.4509	84.5099
0.00003	93.3502	84.5005
0.00004	91.5062	84.5
0.00005	89.9295	84.5
0.00006	88.6287	84.5
0.00007	87.6104	84.5
0.00008	86.8797	84.5
0.00009	86.44	84.5
0.0001	86.2932	84.5
Average Temperature	91.2956	84.6073

Table 6.22: Impact of different roll temperature 130/160(°C) on fabric temperature in thickness direction at various depths with initial temperature 70°C when $E_p < 0.05$

Web Depth (m)	RT 130/160(°C)	
	Fabric Layer Temperature (°C)	
	Analytical Solution	FTCS Solution
0	117.148	96.6053
0.00001	113.427	94.4971
0.00002	110.037	94.2229
0.00003	106.999	94.2012
0.00004	104.332	94.2
0.00005	102.052	94.2
0.00006	100.171	94.2
0.00007	98.6981	94.2
0.00008	97.6414	94.2
0.00009	97.0055	94.2
0.0001	96.7932	94.2
Average Temperature	104.0277	94.4479

Table 6.23: Impact of different roll temperature 160/190(°C) on fabric temperature in thickness direction at various depths with initial temperature 70°C when $E_p < 0.05$

Web Depth (m)	RT 160/190(°C)	
	Fabric Layer Temperature (°C)	
	Analytical Solution	FTCS Solution
0	133.993	107.7625
0.00001	129.13	104.4647
0.00002	124.698	104.0359
0.00003	120.728	104.0019
0.00004	117.243	104.0001
0.00005	114.262	104
0.00006	111.804	104
0.00007	109.879	104
0.00008	108.498	104
0.00009	107.667	104
0.0001	107.389	104
Average Temperature	116.8446	104.3877

Table 6.24: Impact of different roll temperature 190/210(°C) on fabric temperature in thickness direction at various depths with initial temperature 70°C when $E_p < 0.05$

Web Depth (m)	RT 190/210(°C)	
	Fabric Layer Temperature (°C)	
	Analytical Solution	FTCS Solution
0	146.178	117.2406
0.00001	140.636	112.6473
0.00002	135.587	112.0499
0.00003	131.062	112.0026
0.00004	127.09	112.0001
0.00005	123.694	112
0.00006	120.893	112
0.00007	118.699	112
0.00008	117.126	112
0.00009	116.178	112
0.0001	115.862	112
Average Temperature	126.6368	112.54

Table 6.25: Impact of different roll temperature 100/130(°C) on fabric temperature in thickness direction at various depths with initial temperature 50°C when $E_p > 0.05$

Web Depth (m)	RT 100/130(°C)	
	Fabric Layer Temperature (°C)	
	Analytical Solution	FTCS Solution
0	94.6113	80.9163
0.00001	92.5632	73.4133
0.00002	90.7022	71.3818
0.00003	89.0376	71.0412
0.00004	87.5778	71.0031
0.00005	86.33	71.0002
0.00006	85.3004	71
0.00007	84.4943	71
0.00008	83.9156	71
0.00009	83.5672	71
0.0001	83.4508	71
Average Temperature	87.4137	72.1596

Table 6.26: Impact of different roll temperature 130/160(°C) on fabric temperature in thickness direction at various depths with initial temperature 50°C when $E_p > 0.05$

Web Depth (m)	RT 130/160(°C)	
	Fabric Layer Temperature (°C)	
	Analytical Solution	FTCS Solution
0	112.615	97.7552
0.00001	109.873	85.0777
0.00002	107.381	81.6451
0.00003	105.152	81.0697
0.00004	103.197	81.0053
0.00005	101.527	81.0003
0.00006	100.148	81
0.00007	99.0686	81
0.00008	98.2937	81
0.00009	97.8272	81
0.0001	97.6715	81
Average Temperature	102.9776	82.9594

Table 6.27: Impact of different roll temperature 160/190(°C) on fabric temperature in thickness direction at various depths with initial temperature 50°C when $E_p > 0.05$

Web Depth (m)	RT 160/190(°C)	
	Fabric Layer Temperature (°C)	
	Analytical Solution	FTCS Solution
0	130.199	114.1334
0.00001	126.738	96.1003
0.00002	123.593	91.2176
0.00003	120.781	90.3991
0.00004	118.314	90.3075
0.00005	116.205	90.3004
0.00006	114.465	90.3
0.00007	113.103	90.3
0.00008	112.125	90.3
0.00009	111.536	90.3
0.0001	111.34	90.3
Average Temperature	118.0363	93.0871

Table 6.28: Impact of different roll temperature 190/210(°C) on fabric temperature in thickness direction at various depths with initial temperature 50°C when $E_p > 0.05$

Web Depth (m)	RT 190/210(°C)	
	Fabric Layer Temperature (°C)	
	Analytical Solution	FTCS Solution
0	143.061	129.7219
0.00001	139.187	106.0227
0.00002	135.667	99.6059
0.00003	132.519	98.5302
0.00004	129.757	98.4098
0.00005	127.397	98.4005
0.00006	125.45	98.4
0.00007	123.925	98.4
0.00008	122.83	98.4
0.00009	122.171	98.4
0.0001	121.951	98.4
Average Temperature	129.4468	102.0628

Table 6.29: Impact of different roll temperature 100/130(°C) on fabric temperature in thickness direction at various depths with initial temperature 70°C when $E_p > 0.05$

Web Depth (m)	RT 100/130(°C)	
	Fabric Layer Temperature (°C)	
	Analytical Solution	FTCS Solution
0	102.709	89.8001
0.00001	101.129	85.7899
0.00002	99.6941	84.7041
0.00003	98.4104	84.522
0.00004	97.2846	84.5017
0.00005	96.3223	84.5001
0.00006	95.5283	84.5
0.00007	94.9066	84.5
0.00008	94.4603	84.5
0.00009	94.1916	84.5
0.0001	94.1019	84.5
Average Temperature	97.158	85.1198

Table 6.30: Impact of different roll temperature 130/160(°C) on fabric temperature in thickness direction at various depths with initial temperature 70°C when $E_p > 0.05$

Web Depth (m)	RT 130/160(°C)	
	Fabric Layer Temperature (°C)	
	Analytical Solution	FTCS Solution
0	120.533	106.4415
0.00001	118.248	97.1792
0.00002	116.173	94.6713
0.00003	114.317	94.2509
0.00004	112.688	94.2038
0.00005	111.297	94.2002
0.00006	110.149	94.2
0.00007	109.25	94.2
0.00008	108.604	94.2
0.00009	108.216	94.2
0.0001	108.086	94.2
Average Temperature	112.5056	95.6315

Table 6.31: Impact of different roll temperature 160/190(°C) on fabric temperature in thickness direction at various depths with initial temperature 70°C when $E_p > 0.05$

Web Depth (m)	RT 160/190(°C)	
	Fabric Layer Temperature (°C)	
	Analytical Solution	FTCS Solution
0	138.416	123.1488
0.00001	135.431	108.6602
0.00002	132.718	104.7373
0.00003	130.292	104.0796
0.00004	128.164	104.006
0.00005	126.345	104.0003
0.00006	124.845	104
0.00007	123.67	104
0.00008	122.826	104
0.00009	122.318	104
0.0001	122.149	104
Average Temperature	127.9249	106.2393

Table 6.32: Impact of different roll temperature 190/210(°C) on fabric temperature in thickness direction at various depths with initial temperature 70°C when $E_p > 0.05$

Web Depth (m)	RT 190/210(°C)	
	Fabric Layer Temperature (°C)	
	Analytical Solution	FTCS Solution
0	151.219	138.6715
0.00001	147.817	118.491
0.00002	144.726	113.0269
0.00003	141.961	112.1109
0.00004	139.536	112.0084
0.00005	137.463	112.0004
0.00006	135.753	112
0.00007	134.414	112
0.00008	133.453	112
0.00009	132.874	112
0.0001	132.681	112
Average Temperature	139.2634	115.119

Table 6.33: Impact of roll temperature 130/70(°C) on fabric temperature in thickness direction at various depths with initial temperature 50°C when $E_p < 0.05$

Web Depth (m)	RT 130/70(°C)	
	Fabric Layer Temperature (°C)	
	Analytical Solution	FTCS Solution
0	99.3916	86.1578
0.00001	96.7336	83.39
0.00002	94.3119	83.0301
0.00003	92.142	83.0016
0.00004	90.2372	83.0001
0.00005	88.6085	83
0.00006	87.2648	83
0.00007	86.213	83
0.00008	85.4582	83
0.00009	85.0039	83
0.0001	84.8523	83
Average Temperature	90.0197	83.3254

Table 6.34: Impact of roll temperature 160/80(°C) on fabric temperature in thickness direction at various depths with initial temperature 50°C when $E_p < 0.05$

Web Depth (m)	RT 160/80(°C)	
	Fabric Layer Temperature (°C)	
	Analytical Solution	FTCS Solution
0	118.32	100.3
0.00001	114.701	96.5311
0.00002	111.403	96.041
0.00003	108.449	96.0021
0.00004	105.855	96.0001
0.00005	103.637	96
0.00006	101.807	96
0.00007	100.375	96
0.00008	99.3473	96
0.00009	98.7287	96
0.0001	98.5222	96
Average Temperature	105.5587	96.443

Table 6.35: Impact of roll temperature 190/90(°C) on fabric temperature in thickness direction at various depths with initial temperature 50°C when $E_p < 0.05$

Web Depth (m)	RT 190/90(°C)	
	Fabric Layer Temperature (°C)	
	Analytical Solution	FTCS Solution
0	137.38	114.6287
0.00001	132.81	109.8705
0.00002	128.647	109.2517
0.00003	124.916	109.2027
0.00004	121.642	109.2001
0.00005	118.842	109.2
0.00006	116.532	109.2
0.00007	114.724	109.2
0.00008	113.426	109.2
0.00009	112.645	109.2
0.0001	112.384	109.2
Average Temperature	121.268	109.7594

Table 6.36: Impact of roll temperature 210/100(°C) on fabric temperature in thickness direction at various depths with initial temperature 50°C when $E_p < 0.05$

Web Depth (m)	RT 210/100(°C)	
	Fabric Layer Temperature (°C)	
	Analytical Solution	FTCS Solution
0	150.737	125.114
0.00001	145.591	119.7551
0.00002	140.902	119.0583
0.00003	136.7	119.003
0.00004	133.012	119.0001
0.00005	129.859	119
0.00006	127.257	119
0.00007	125.221	119
0.00008	123.759	119
0.00009	122.88	119
0.0001	122.586	119
Average Temperature	132.591	119.63

Table 6.37: Impact of roll temperature 130/70(°C) on fabric temperature in thickness direction at various depths with initial temperature 70°C when $E_p < 0.05$

Web Depth (m)	RT 130/70(°C)	
	Fabric Layer Temperature (°C)	
	Analytical Solution	FTCS Solution
0	103.95	92.6875
0.00001	101.688	90.3319
0.00002	99.6271	90.0256
0.00003	97.7804	90.0013
0.00004	96.1593	90
0.00005	94.7732	90
0.00006	93.6296	90
0.00007	92.7344	90
0.00008	92.092	90
0.00009	91.7055	90
0.0001	91.5764	90
Average Temperature	95.97418	90.277

Table 6.38: Impact of roll temperature 160/80(°C) on fabric temperature in thickness direction at various depths with initial temperature 70°C when $E_p < 0.05$

Web Depth (m)	RT 160/80(°C)	
	Fabric Layer Temperature (°C)	
	Analytical Solution	FTCS Solution
0	122.879	106.8297
0.00001	119.656	103.473
0.00002	116.719	103.0365
0.00003	114.087	103.0019
0.00004	111.777	103.0001
0.00005	109.802	103
0.00006	108.172	103
0.00007	106.897	103
0.00008	105.981	103
0.00009	105.43	103
0.0001	105.246	103
Average Temperature	111.5133	103.3947

Table 6.39: Impact of roll temperature 190/90(°C) on fabric temperature in thickness direction at various depths with initial temperature 70°C when $E_p < 0.05$

Web Depth (m)	RT 190/90(°C)	
	Fabric Layer Temperature (°C)	
	Analytical Solution	FTCS Solution
0	141.808	120.9718
0.00001	137.623	116.6141
0.00002	133.81	116.0474
0.00003	130.394	116.0025
0.00004	127.395	116.0001
0.00005	124.83	116
0.00006	122.715	116
0.00007	121.059	116
0.00008	119.87	116
0.00009	119.155	116
0.0001	118.916	116
Average Temperature	127.0523	116.512

Table 6.40: Impact of roll temperature 210/100(°C) on fabric temperature in thickness direction at various depths with initial temperature 70°C when $E_p < 0.05$

Web Depth (m)	RT 210/100(°C)	
	Fabric Layer Temperature (°C)	
	Analytical Solution	FTCS Solution
0	155.296	131.6437
0.00001	150.545	126.697
0.00002	146.217	126.0538
0.00003	142.339	126.0028
0.00004	138.935	126.0001
0.00005	136.024	126
0.00006	133.622	126
0.00007	131.742	126
0.00008	130.393	126
0.00009	129.581	126
0.0001	129.31	126
Average Temperature	138.5458	126.5816

Table 6.41: Impact of roll temperature 130/70(°C) on fabric temperature in thickness direction at various depths with initial temperature 50°C when $E_p > 0.05$

Web Depth (m)	RT 130/70(°C)	
	Fabric Layer Temperature (°C)	
	Analytical Solution	FTCS Solution
0	101.809	99.0713
0.00001	100.177	86.9112
0.00002	98.695	83.6188
0.00003	97.369	83.0668
0.00004	96.206	83.005
0.00005	95.212	83.0003
0.00006	94.3919	83
0.00007	93.7497	83
0.00008	93.2887	83
0.00009	93.0111	83
0.0001	92.9185	83
Average Temperature	96.0753	84.8794

Table 6.42: Impact of roll temperature 160/80(°C) on fabric temperature in thickness direction at various depths with initial temperature 50°C when $E_p > 0.05$

Web Depth (m)	RT 160/80(°C)	
	Fabric Layer Temperature (°C)	
	Analytical Solution	FTCS Solution
0	121.612	117.8843
0.00001	119.391	101.3259
0.00002	117.372	96.8426
0.00003	115.566	96.091
0.00004	113.983	96.0069
0.00005	112.629	96.0004
0.00006	111.512	96
0.00007	110.638	96
0.00008	110.01	96
0.00009	109.632	96
0.0001	109.506	96
Average Temperature	113.8046	98.5592

Table 6.43: Impact of roll temperature 190/90(°C) on fabric temperature in thickness direction at various depths with initial temperature 50°C when $E_p > 0.05$

Web Depth (m)	RT 190/90(°C)	
	Fabric Layer Temperature (°C)	
	Analytical Solution	FTCS Solution
0	141.535	136.8289
0.00001	138.731	115.924
0.00002	136.182	110.2638
0.00003	133.902	109.3149
0.00004	131.903	109.2087
0.00005	130.194	109.2005
0.00006	128.784	109.2
0.00007	127.68	109.2
0.00008	126.888	109.2
0.00009	126.411	109.2
0.0001	126.251	109.2
Average Temperature	131.6783	112.431

Table 6.44: Impact of roll temperature 210/100(°C) on fabric temperature in thickness direction at various depths with initial temperature 50°C when $E_p > 0.05$

Web Depth (m)	RT 210/100(°C)	
	Fabric Layer Temperature (°C)	
	Analytical Solution	FTCS Solution
0	155.417	150.1167
0.00001	152.258	126.5728
0.00002	149.388	120.198
0.00003	146.821	119.1294
0.00004	144.569	119.0098
0.00005	142.645	119.0005
0.00006	141.057	119
0.00007	139.813	119
0.00008	138.921	119
0.00009	138.383	119
0.0001	138.204	119
Average Temperature	144.316	122.6389

Table 6.45: Impact of roll temperature 130/70(°C) on fabric temperature in thickness direction at various depths with initial temperature 70°C when $E_p > 0.05$

Web Depth (m)	RT 130/70(°C)	
	Fabric Layer Temperature (°C)	
	Analytical Solution	FTCS Solution
0	106.008	103.6777
0.00001	104.619	93.3287
0.00002	103.357	90.5266
0.00003	102.229	90.0569
0.00004	101.239	90.0043
0.00005	100.393	90.0002
0.00006	99.6952	90
0.00007	99.1487	90
0.00008	98.7563	90
0.00009	98.5201	90
0.0001	98.4412	90
Average Temperature	101.1279	91.5995

Table 6.46: Impact of roll temperature 160/80(°C) on fabric temperature in thickness direction at various depths with initial temperature 70°C when $E_p > 0.05$

Web Depth (m)	RT 160/80(°C)	
	Fabric Layer Temperature (°C)	
	Analytical Solution	FTCS Solution
0	125.811	122.4907
0.00001	123.832	107.7434
0.00002	122.034	103.7504
0.00003	120.426	103.081
0.00004	119.016	103.0061
0.00005	117.81	103.0003
0.00006	116.816	103
0.00007	116.037	103
0.00008	115.478	103
0.00009	115.141	103
0.0001	115.029	103
Average Temperature	118.8573	105.2793

Table 6.47: Impact of roll temperature 190/90(°C) on fabric temperature in thickness direction at various depths with initial temperature 70°C when $E_p > 0.05$

Web Depth (m)	RT 190/90(°C)	
	Fabric Layer Temperature (°C)	
	Analytical Solution	FTCS Solution
0	145.614	141.3037
0.00001	143.045	122.1581
0.00002	140.711	116.9742
0.00003	138.623	116.1052
0.00004	136.792	116.0079
0.00005	135.227	116.0004
0.00006	133.936	116
0.00007	132.925	116
0.00008	132.199	116
0.00009	131.762	116
0.0001	131.616	116
Average Temperature	136.5864	118.959

Table 6.48: Impact of roll temperature 210/100(°C) on fabric temperature in thickness direction at various depths with initial temperature 70°C when $E_p > 0.05$

Web Depth (m)	RT 210/100(°C)	
	Fabric Layer Temperature (°C)	
	Analytical Solution	FTCS Solution
0	159.616	154.7231
0.00001	156.7	132.9903
0.00002	154.051	127.1059
0.00003	151.681	126.1194
0.00004	149.602	126.009
0.00005	147.826	126.0005
0.00006	146.36	126
0.00007	145.212	126
0.00008	144.388	126
0.00009	143.892	126
0.0001	143.727	126
Average Temperature	149.3686	129.3589